

THE STRUCTURAL BEHAVIOUR OF BOLTED CONNECTIONS
UNDER SHEARING AND ROTATIONAL LOADING.

by KENNETH

IN PARTIAL FULFILLMENT OF THE REQUIREMENTS
FOR A MASTER OF SCIENCE DEGREE IN STRUCTURAL
ENGINEERING OF THE UNIVERSITY OF NAIROBI.

Robert Keya Malaba

This thesis submitted in partial fulfillment
of the requirements for a Master of
Science degree in Structural Engineering
of the University of Nairobi.

DECLARATION

This Thesis is my own original work und has not been presented for a degree in any other IJniversiLy.


CANDIDATE: MAI.AHA ROBERT KEYA

Malabar Keya.

This Thesis has been submitted for examination with _{my} approval as university supervisor .

Mr. S.S. MIRING'U

SiCNKD :



MARCH 1992

LIST OF CONTENTS

CONTENTS	PAGE
Declaration	(i)
List of Contents	(ii)
Abstract	1
Acknowledgement	2
CHAPTER ONE	
1.0 INTRODUCTION	3
1.1 General	4
1.2 Effects of Connections on Structural behaviour	5
1.3 Need for further Research	7
1.3.1 Load-deformation behaviour.	7
1.3.2 Non-linear mathematical modelling	7
1.3.3 Analysis and design	8
1.4 Objectives.	8
1.5. Relevance of Research to Structural Engineering	9
1.6 Summary of Results.	9
CHAPTER TWO	
2.0 STEEL AS A CONSTRUCTION MATERIAL	11
2.1 Introduction	12
2.2. Choice of Material.	12
2.2.1 Mechanical properties.	13
2.2.2 Manufacturing process.	14

2.2.3	Cost and Availability.	14
2.2.4	The Construction Programme.	15
2.3	Factors affecting mechanical properties of steel	15
2.3.1	Chemical Composition	15
2.3.2	geometry, Temperature and strain	15
2.3.3	Fabrication Effects.	16
2.3.4	Erection effect.	16
2.3.5	Imperfection effects.	17
2.4	Steel construction in developing countries	18
2.5	Structural components.	18
2.5.1	Structural requirements.	19
2.5.2	Floor Systems.	20
2.5.3	Hoof Systems.	21
2.5.4	Bridges.	21
2.5.5	Special Structures.	22
2.5.5.1	Towers and Pylons.	22
2.5.5.2	Stressed stein Structure.	22
2.5.5.3	Cranes.	23
2.5.6	Connections.	23

CHAPTER THREE

3.0	LITERATURE	25
3.1	Introduction	26
3.2	Loading Effect on Semi-rigidly connected Systems	27
3.2.1	Moment-Rotation characteristic of semi-rigid connections	28
3.2.2	Moment-rotation relation for dynamic loading . . .	39
3.3	Load transfer modes.	42

3.3.1	Failure modes	43
3.3.2	Stress distribution in bolted connections	49
3.3.3	Residual stress	50
3.3.3.1	Residual stress effects on stress-strain relations	55
3.3.3.2	Effects on load capacity and yield	55
3.3.3.3	Effects on moment-curvature.	58
3.3.3.4	Effects on deflections.	58
3.3.3.5	Effects on plastic collapse load	61
3.3.3.6	Effects on shakedown loads.	65
3.3.3.7	Effects on buckling	65
3.3.4	Effects on Strain-hardening on behaviour of Structural Systems.	66
3.4	Design Consideration	68
3.4.1	Bolt types and sizes.	68
3.4.1.1	American classification system	69
3.4.1.2	British classification	72
3.4.2	Behaviour of individual fasteners.	74
3.4.2.1	Bolts subjected to tension	74
3.4.2.2	Bolts subjected to shear.	76
3.4.2.3	Bearing properties	81
3.4.3	Spacing of bolts.	81
3.4.4	Use of washers.	85

CHAPTER FOUR

4.0	MATHEMATICAL MODELLING OR SEMI-RIGID CONNECTIONS	87
4.1	Introduction	88
4.2	Behaviour of Structural Systems « »	88
4.2.1	Behaviour of bolted connections.	89

4.3	Analysis of Structural Systems	90
4.3.1	Analysis of elastic framed structures.	90
4.3.2	Analysis of semi-rigid connections.	94
4.3.2.1	The Slope deflection method	94
4.3.2.2	The cross methods.	100
4.4	Analysis of Load-deformation curves.	102
4.4.1	Linear elastic analysis.	102
4.4.2	Non-Linear elastic analysis.	104
4.5	Modelling of semi-rigid bolted connections	110
4.6	Development of a non-linear mathematical model for bolted connections.	114
4.6.1	Non-linear mathematical model requirements	114
4.6.2	Exponential model for load deformation curves	115
4.6.2.1	Evaluation of model parameters.	116
4.6.2.1.1	Evaluation of R_q and M_q	117
4.6.2.1.2	Evaluation of K_c	117
4.6.2.1.3	Evaluation of C	117
4.6.3	inverse Ramberg-Osgood model for load-deformation curves.	118
4.6.3.1	Evaluation of model parameters.	119
CHAPTER FIVE		
5.0	EXPERIMENTAL DESIGN AND INVESTIGATION	121
5.1	Introduction	122
5.2	Material testing	122
5.2.1	Scope and applicability of material tests	123
5.3	Loaded joint behaviour test.	124
5.3.1	Scope and applicability of tests.	124

5.3.2	Pure shearing tests.124
5.3.3	Pure rotation tests.125
5.4	Materials.126
5.4.1	Bolts and Washers.126
5.4.2	Steel plates and rectangular hollow sections126
5.5	Conduct of tests.127
5.5.1	Material tests.127
5.5.1.1	Tensile tests.127
5.5.1.2	Requirements for specimens.127
5.5.1.3	Testing procedure.128
5.5.2	Loaded joint behaviour test.129
5.5.2.1	Pure shear tests.129
5.5.2.1.1	Specimen dimensions and test joint assembly130
5.5.2.1.2	Pure shear testing rig.130
5.5.2.2	Pure rotation tests.135
5.5.2.2.1	Measurement of joint rotation135
5.5.2.2.2	Specimen dimensions141
5.5.2.3.3	Procedures for rotational tests.141
5.6	Load-deformation curve components.150

CHAPTER SIX

6.0	ANALYSIS OR EXPERIMENTAL DATA151
6.1.	Introduction152
6.2	Schemes of analysis of experimental data152
6.3	Failure modes in pure test joints.153
6.4	Comparisons of predictive model data and experimental data153

CHAPTER SEVEN

7.0	DISCUSSION	170
7.1	Introduction	171
7.2	Basics for selecting mathematical model	171
7.3	Material stress-strain characteristics.	172
7.3.1	Bolts	172
7.3.2	Joint material (RHS).	177
7.4	Pure shear load-deformation curves.	177
7.4.1	Connector load-deformation curves.	177
7.4.1.1	Initial slip	177
7.4.1.2	Failure loads.	1B3
7.4.1.3	Modelling of experimental data	1B4
7.4.1.3.1	Exponential model.	184
7.4.1.3.2	Inverse Ramberg-Osgood model.	185
7.4.2	Joint load-deformation curves.	187
7.4.2.1	Initial slip	188
7.4.2.2	Failure loads	188
7.4.2.3	Modelling experimental data	189
7.4.2.3.1	Exponential model.	189
7.4.2.3.2	The inverse Ramberg-Osgood model.	190
7.5	Pure rotation moment-rotation curves.	191
7.5.1	Connects moment rotation curves.	191
7.5.1.1	Failure moments.	192
7.5.1.2.1	Exponential model.	201
7.5.1.2.2	Inverse Ramberg-Osgood model.	201
7.5.2	Joint moment-rotation curves.	202
7.5.2.1	Failure moments.	207
7.5.2.2	Modelling of experimental data	208

7.5.2.2.1	Exponential model.	208
7.5.2.2.2	Inverse Ramberg-Osgood model.	209
7.6	Failure of test pieces.	209
7.6.1	Shearing of the bolts.	210
7.6.2	Bearing failure.	210
7.6.3	Tearing out of connected material.	211
7.7	Effects of initial bolt pre-load	211
7.8	Location of shear planes and faying surface condition	212
7.9	imperfection effects.	215
7.10	Applicability of superposition to test data . . .	215
7.11	Ranking of the mathematical models.	216
CHAPTER EIGHT.		
8.0	Conclusions and recommendations.	218
8.1	Conclusions.	219
8.2	Recommendations.	220
REFERENCES.		221
APPENDICES.		227
Appendix A	Material requirements for pure shear tests	228
Appendix B	Material requirements for pure rotation tests.	229
Appendix C	Calculation of joint rotation	230
Appendix D	Analysis of data for joints tested in pure shear.	232
Appendix E	Analysis of test data for joints tested in pure rotation	239

Appendix F	Absolute error comparison by the averaging technique	249
Appendix G	Material stress-strain test data	254
Appendix H	Applicability of superposition to test data	259

LIST OF FIGURES.

1.1	Typical moment rotation curves for conventional connection types.	6
2.1	Typical stress-strain diagram for ductile material (e.g mild steel).	13
3.1	Fully pinned connection	30
3.2	Semi-rigid connection	31
3.3	Fully rigid connection	32
3.4	Moment-redistribution in semi-rigid joints	33
3.5	Typical moment-rotation relationships.	35
3.6	Computer model for semi-rigid joints.	36
3.7	Moment rotation demand	37
3.8	Moment-rotation curves for semi-rigid connections.	37
3.9	Typical load deformation curves in semi-rigid connections.	40
3.10	Analytical model for non-rigidly connected frames.	41
3.11	Actual M-0 curve for non-rigid connection	41
3.12	Bolt forces for butt splice joints.	45
3.13	Bolt load distribution model in bending	46
3.14	Types of connection failure.	47
3.15	Staggered fastener pattern	48

3.16	Possible failure paths for different holes patterns.	51
3.17	Bearing stresses.	52
3.18	Failure modes in bearing.	53
3.19	Typical residual stress patterns.	54
3.20	Influence of residual stresses in the stress-strain curve.	56
3.21	Representation of residual stress effects upon the M-0 relationship of a beam.	57
3.22	Residual stress distribution giving greatest elastic range in bending for a rectangular beam	59
3.23	Idealized stress-strain curve for mild steel . . .	60
3.24	Development of plastic zones during the bending of all I-beam with residual stresses.	63
3.25	Total deformation of a simply supported beam . . .	64
3.26	Typical bolt assembly.	71
3.27	High tensile swedge bolt.	72
3.28	Load-elongation curves for bolts tested in tension	75
3.29	Reserve tensile strength torqued bolts.	76
3.30	Typical shear deformation curves for bolts	77
3.31	Typical shear deformation curves for bolts	79
3.32	Shear deformation curves for different failure planes.	80
3.33	Relationship between bearing stress and deformation for tensile type shear.	83
3.34	Bolt spacing patterns.	84
3' 35	Edge distance to prevent shear tear-out.	85

4	Member stiffness matrix for beam element	92
4	Semi-rigid joint element.	93
4	Functional relationship for connection factor Z .	96
4	M-0 curves for semi-rigid connections.	97
4	Conjugate beam method for semi-rigid connections.	98
4	Relative distribution for rigid and semi-rigid connections.	102
4	Non-linear deformation and its approximation by tangent.	103
4	Incremental(secant) method for non-linear analysis.	105
4	Flow chart for incremental method	106
4	Newton-Raphson method	107
4	Newton-Raphson method flow chart	108
4	Mechanically fastened steel joints under actions	109
4	Idealized elastic restraint modelling for a joint.	112
4	Graphical determination of model parameters . . .	113
5	Typical tension specimen	129
5	Dimensions of pure shear rig for connector property tests.	132
5	Dimensions of pure shear rig for joint property tests.	133
5	Load application to pure shear specimen	134
5	Application of pure couple to bolted connections.	138

5.6	Measurement of joint rotation in	140
5.7	Geometric construction showing joint	140
5.8	Bolt arrangement on test specimen...	142
5.9	Forces acting on 6mm diameter bolts...	143
5.10	Forces acting on 8mm diameter bolts...	144
5.11	Forces acting on 10mm diameter bolts	145
5.12	Multiple bolt specimen for connector properties	146
5.13	General test set up for pure relational tests .	147
5.14	Detailed testing set up for relational tests .	148
5.15	Load-deformation curve components...	149
6.1	Schematic representation of errors between experimental and predicted data...	158
6.2	Average cumulative errors, E_c , for connectors loaded in pure shear	162
6.3	Average cumulative errors, E_c , for connectors loaded in pure rotation	164
6.4	Average cumulative errors, E_c , for connection loaded in pure shear	166
6.5	Average cumulative errors, E_c , for connection loaded in pure rotation	168
7.1	Stress-strain curve for 6mm bolt... .	174
7.2	Stress-strain curve for 8mm bolt .	175
7.3	Stress-strain curve for 10mm bolt... .	176
7.4	Stress-strain curve for RHS coupon...	179
7.5	Load-deformation curves for 6mm bolts tested	180

7.6	Load-deformation curves for 8mm bolt tested in pure shear.	181
7.7	Load-deformation curves for 10mm bolt tested in pure shear.	182
7.8	Comparative load-deformation curves for bolts tested in pure shear.	187
7.9	Load-deformation curves for 6mm joints tested in pure shear.	193
7.10	Load-deformation curves for 8mm joints tested in pure shear.	194
7.11	Load-deformation curves for 10mm joints tested in pure shear.	195
7.12	Comparative load-deformation curves for joints tested in pure shear.	196
7.13	Moment rotation curves for 6mm bolts tested in pure shear.	197
7.14	Moment-rotation curves for 8mm bolts in pure rotation.	198
7.15	Moment-rotation curves for 10mm bolts in pure rotation.	199
7.16	Comparative moment-rotation curves for bolts in pure rotation.	200
7.17	Moment-rotation curves for 6mm bolt joints in pure rotation.	203
7.18	Moment-rotation curves for 8mm bolt joints in pure rotation.	204
7.19	Moment-rotation curves for 10mm bolt joints in pure rotation.	205

7.20	Comparative moment-rotation curves in pure rotation	206
7.21	Bearing failure in connected material	213
7.22	Failure by tension tear-out of connected material	214

LIST OF TABLES

3.1	Grade 4.6 blade mild steel and grade 8.8 high tensile	74
3.2	Structural end-distance for various hole sizes.	82
6.1	Load-errors, E_c , kn, in fitting models to data for connectors loaded in pure shear.	161
6.2	Moment errors, E_c , knm in fitting models to data for connections loaded in pure rotation.	163
6.3	Load errors, E_c , kn in fitting models to data for connections loaded in pure shear.	165
6.4	Moment errors, E_c , knm in fitting models to data for connections loaded in pure rotation.	167
7.1	Characteristic values from stress-strain curves for 6, 8 and 10mm bolts	173
7.2	Initial slip values for 6,8, and 10mm in pure shear.	178
7.3	Ultimate shear loads/stresses for the bolts	183
7.4	Ultimate joint failure loads in Pure shear	188
7.5	Ultimate moment and bolt load resistance values (connectors).	192
7-6	Ultimate moment and bolt load resistance values (joints).	207
7.7	Model Ranking for pure shear loading.	216
7-H	Ranking of models for pure rotation	217

LIST OF ILLUSTRATIONS

Plate 5.1	Shear test specimen showing part of the Roell + Korkthus K6 OTM Machine	131
Plate 5.2	Pure Rotation test set up showing loading beam and test specimens.	137
Plate 5.3	Pure Shear test rig for connector property tests.	139
Plate 5.4	Pure Shear test rig for joint property tests.	139
Plate 6.1	Bolt failure in tests on connectors	155
Plate 6.2	Typical bolt deformation for joints in pure shear.	156
Plate 6.3	Side view of pure shear test rig showing location of shear planes and roller guide location	156
Plate 6.4	Pure shear test rig showing of test bolt on rig	157
Plate 6.5	Pure rotation test rig showing pulley and cable system location	157
Plate 6.6.	Pure shear test set up showing pulling system attachment.	160

ABSTRACT.

This research aimed at initiating a consistent accumulation of data on the load-deformation behaviour of both the connections and joints under pure shearing and pure rotational loading that will be useful to engineers and other researchers in future. The experiments were designed to provide data for the bolts as well as the joints and use non-linear mathematical models to describe this behaviour. The principle of superposition was also applied to the experimental data obtained to determine the relative contribution of the bolt and connected material to the overall joint deformation.

The non-linear mathematical models used to model the joint behaviour and experimental loads were:

- (i) the exponential model, and
- (ii) the inverse Ramberg-Osgood model.

These models, which have been used in other related research work, were modified for use during this research. The predictive load-deformation curve obtained by use of these models were compared to the experimental data by use of load-error analysis averaging techniques from the comparative studies of these two sets of data. The Inverse Ramberg-Osgood model was found to describe the load-deformation and moment-rotation of both the connectors and joints loaded in pure shear and pure rotation respectively better. The joint behaviour was also found to be semi-rigid as opposed to the fully rigid assumptions used in design codes.

The information using principle of superposition was not conclusive in that not enough data on the relationship between bolt and joint material load-deformation behaviour was available.

ACKNOWLEDGEMENT.

I wish to register my gratitude to all the people who made this research possible. I wish to thank the University of Nairobi for having awarded me a scholarship to pursue this course.

I am greatly indebted to my supervisor Mr. Miringu whose guidance, resourcefulness and patience in moderating the manuscript was of great help to me. I also wish to thank the Technical staff of the Department of Civil Engineering metal workshop for the time they put in the test assembly fabrication. A word of thanks to the Kenya Bureau of Standards for having allowed me to use the facilities in the materials laboratory during the research.

Finally, I wish to thank my family members for the keen interest they have shown and their support during my schooling, especially my wife, Margaret, who urged me on during the difficult times of the research.

Malaba R. Keya

Nairobi. November 1989.

CHAPTER ONE.
INTRODUCTION.

1.1 GENERAL

With advances in technology over the years, the performance of structural systems in their service states has received increasing attention. In particular, the advent of complex functional aspects of structural systems has led to the adoption of the concept of optimization in structural design. This means that among other factors to be considered, cost is one of the major criterion in most of the designs. However, one does not optimize cost to strength

alone, because aesthetic and in-service deflection must be considered in so far as these important characteristics may be influenced by the structural framework. Optimization also cannot be achieved without consideration of certain aspects of fabrication and erection such as simplicity of joints and importance of shop-fabricated assemblies as a means of speeding up erection, to reduce the cost of field labour.

Foundations, mechanical and electrical systems, and non-structural elements have to be considered when optimising the design of a structural system. Thus optimising design includes consideration of structural components.

The structural components so designed are joined together by connections of a suitable nature to produce a coherent structural system. The quantification of the behaviour of the connection is a pre-requisite in order to employ the analytical tools of structural analyses and designs. These connections might be welded, rivetted, bolted, nailed, glued etc.

The choice of the connection type depends upon the consideration that some particular connection assembly used is more economical than others in satisfying basic requirements for effective performance. These requirements are usually sufficient strength, adequate rotational capacity and connection stiffness. (1) Conventional procedures for the analysis and design of frame structures depends on the basic assumptions that the member end-connections are either fully pinned or fully rigid. This is done despite the knowledge that few connections, if any, behave in either fashion and that significant material savings may be obtained if the true connection behaviour is represented. The primary reason these assumptions have been adopted (2) are that information concerning actual connection behaviour (both analytical and experimental) is limited and the analytical methods developed to incorporate semi-rigid behaviour are cumbersome and often complex.

Connections play an important role in structural systems as they constitute one of the most important components in the overall economics of the structure. The performance of every structural arrangement is dependent as much on the connections as on the physical size and shape of the structural members. Other factors affecting the performance of structural systems are the material properties, climatic conditions and the intended functions. Bolted connections are complex in their behaviour (1) in both the elastic and post-elastic conditions. Their economy and simplicity makes them popular in structural steelwork. This aspect hence would require that the structural behaviour of bolted connections be well understood.

1.2 Effects of connections on structural behaviour

The economics of structural steelwork frame construction are strongly influenced by the forms of joints selected because the response under load of the resulting structure is crucially affected by the behaviour of the joints. The particular aspect of connection behaviour that is of interest in the context of the performance of the structural frame is the rotational stiffness.

This is most conveniently discussed in terms of the relationship between the moment transmitted by the connection, M , and the angular in-plane rotation of the connection, θ . Typical $M-\theta$ curves signifying the three conventional connection types are shown in Figure 1.1. In the figure, the moment rotation curve for a hypothetically fully rigid connection would coincide with the vertical axis while for a hypothetically fully pinned connection would coincide with the horizontal axis. The moment-rotation behaviour of any real connection is intermediate between the two extremes and every connection is capable of developing at least some moment resistance.

Connection moment resistance does affect the beam fixed-end moments which in turn affects the beam weight. This also affects the effective length and the load-carrying capacity of the columns as both factors are dependent on the amount of end restraint provided by the beams framing into the column ends. Also in moment-resistant unbraced frames, connection deformation can contribute substantially to the horizontal drift of the structure under lateral load. The P-D effect in such frameworks tends to amplify the connection moments and lateral displacements. (4) Although each particular type of joint exhibits certain special features, the general picture is as summarised in figure 1.1. Moment rotation curves are typically non-linear, as

are the load-deformation curves. From figure 1.1. it is seen that, all practical moment resisting connections do possess some rotational stiffness. Thus all connection behaviour would more properly be described as semi-rigid. Thus in order to determine the effect a connection would have on a structural system, the correct modelling of the connection should be carried out.

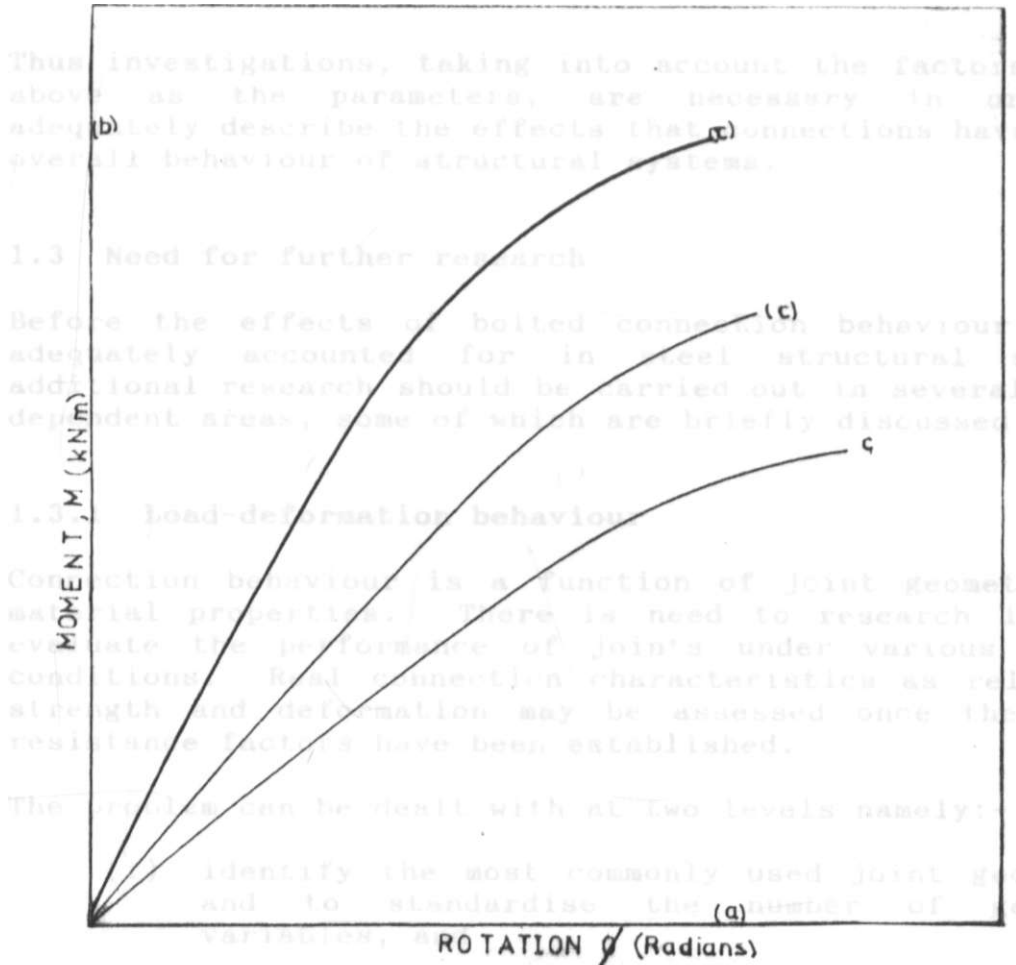


FIGURE 1.1 Typical moment-rotation curves (3.4.5) (a) conventional connection types (b) ideally pinned connection. (c) fully rigid connection. (c) varying degrees of partial connection rigidity.

In general, the force-deformation behaviour of connections depends upon the following factors, (6,7):-

- (i) type and size of fasteners
- (ii) Size, shape and type of connected elements

(iii) material properties of connectors and connection materials

(iv) fastener arrangements

(v) type and magnitude of load transmitted at the connection.

Thus investigations, taking into account the factors listed above as the parameters, are necessary in order to adequately describe the effects that connections have on the overall behaviour of structural systems.

1.3 Need for further research

Before the effects of bolted connection behaviour can be adequately accounted for in steel structural systems, additional research should be carried out in several inter-dependent areas, some of which are briefly discussed below.

1.3.1 Load-deformation behaviour

Connection behaviour is a function of joint geometric and material properties. There is need to research into and evaluate the performance of joints under various loading conditions. Real connection characteristics as relates to strength and deformation may be assessed once the actual resistance factors have been established.

The problem can be dealt with at two levels namely;-

(i) identify the most commonly used joint geometries and to standardise the number of geometric variables, and

(ii) model and test the joint components.

1.3.2 Non-linear mathematical modelling

Semi-rigid connection behaviour is complex and non-linear right from the onset of loading. Most of the mathematical modelling techniques that have been used are based on elasto-plastic analysis of connections, which are either bilinear or approximately so. But due to the non-linear behaviour of the connections from the early loading stages, the models have been incapable of providing realistic representation of connection behaviour. Thus mathematical models based on curve fitting techniques should be researched upon more in order to properly analyse the non-linear behaviour of these connections.

1.3.3 Analysis and design

There is need to develop accurate analytical techniques to account for the effects of connection behaviour. This will lead to more efficient and economical designs. But these aspects are best covered when enough data has been accumulated to accurately define the load-deformation behaviour and proper non-linear mathematical models have been developed.

1.4 Objectives

The objectives of this research are:

1. To develop a mathematical model to be used in the prediction of actual connection behaviour under the following loading conditions:
 - (i) pure shearing load, and
 - (ii) pure rotational load
2. To design and test bolted connections and compare the analytical models and experimental results of the behaviour of steel joints.

In addition to the above main objectives, the research set to establish whether the structural behaviour of bolted connection can be described as either fully pinned or fully rigid as set out in design codes or more appropriately as semi-rigid, i.e. intermediate between fully pinned and fully rigid, in behaviour. The research also set out to investigate the possible application of super position to the experimental data by separation of individual contributions of the connectors and connected material to the overall load-deformation behaviour of bolted connections.

In order to achieve these objectives, this research project has dealt with various but related subjects as follows:

Chapter 2 deals with a brief look at the manufacture steel of and its uses in the Construction Industry.

Chapter 3 deals with a review of related work as done by other researchers.

Chapter 4 examines the subject of mathematical modelling and the basis on which the models used in the research were selected.

Chapter 5 deals with the experimental design and investigation procedures.

Chapter 6 is concerned with the schemes of analysis of data between the experimental data and that predicted by the mathematical model.

Chapter 7 is the discussion of the experimental results in relation to the objectives and literature review.

Chapter 8 carries the conclusions and recommendations of the research work.

1.5 Relevances of Research to structural Engineering

Basically this research was carried out with the ultimate aim of describing as well as predicting the structural behaviour of bolted connections under various loading conditions. But due to time and financial constraints, the research limited the parameters affecting connection behaviour as set out in section 1.2. The experimental data obtained from the investigation would serve as a basis for further research work, that will progressively incorporate other parameters on a wider scope of research.

With time, the researcher envisages a stage when enough data would have been accumulated and accurate predictive models developed to have some kind of standard to which structural design engineers can refer to in the analysis and design of bolted connections given all the necessary parameters.

1.6 Summary of Results

This research was carried out in line with the objectives as set out in section 1.4 and the experimental design and investigation in chapter 5.0. From the experimental results, it was concluded that these connections under pure shearing and pure rotational loading behave in a non-linear manner. The load-deformation characteristics as derived in chapter 7.0 are best described as semi-rigid, being intermediate between the fully pinned and fully rigid cases. The two non-linear mathematical models adopted in predicting the load-deformation characteristics of the bolted connections were ranked and the Inverse Ramberg-Osgood model was found to give better results as compared to the polynomial model.

Overall, the load deformation characteristics as obtained were substantially affected by the residual stresses as a result of the manufacturing process.

CHAPTER 2
STEEL AS A CONSTRUCTION MATERIAL

2.1. INTRODUCTION

The large number of materials which are described as materials of construction includes:

- i) Structural materials which must resist external loads or forces when they are incorporated into a structure e.g. reinforcing steel, steel beams, steel columns, steel plates, trusses, concrete, masonry, wooden elements etc.;, and
- ii) another group of materials which are employed principally for non-structural purposes such as preservation, decoration, insulation and other building purposes. These include rubber, marble, wood products, paint etc.

The engineer engaged in any activity pertaining to construction is more interested in the uses of materials, their properties and their behaviour in service. The design engineer needs to know the properties of the materials and the conditions under which the materials will be used in order to be able to design structural systems. Also a comprehensive knowledge of the production and fabrication of some materials is necessary in order to provide for safe economical design.

2.2. Choice of material

The choice of a suitable material is frequently one of the most difficult tasks facing the design engineer, since only by careful consideration of all the aspects involved in the production and fabrication of material can the most suitable be selected. The main factors involved in selecting a material are:-

- i) mechanical and chemical properties
- ii) method of manufacturing and/or fabrication
- iii) cost
- iv) availability
- v) construction programme

Each of these factors is briefly discussed below:

2.2.1. Mechanical properties

Engineering design is primarily concerned with the development of machines, structural systems and various other products. These elements are usually subjected to internal forces and deformations. The description of the behaviour of these systems under these forces constitute the mechanical properties of the materials of the components used. The most important definition of the mechanical properties of materials is the stress-strain curve. Although there may be a large variation of the shapes of the stress-strain diagrams for different materials, the majority of engineering materials exhibit a reasonably linear variation of stress with strain during the initial loading period upto the limit of proportionality (point A, Fig 2.1).

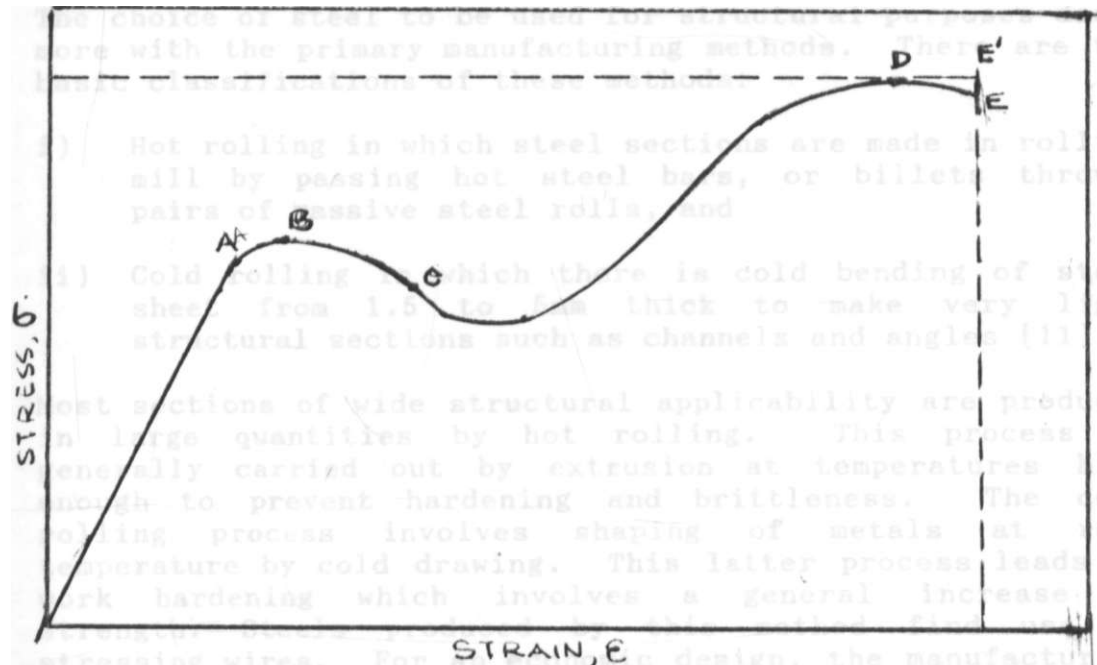


Fig. 2.1 Typical stress-strain diagram for a ductile material e.g steel (9).

Point B is the elastic limit, point C the yield point and point D the ultimate strength. (10). After point D, extension continues with an apparent decrease in stress until fracture eventually occurs at E. The ultimate and yield strengths are two factors that are most commonly referred to in design of structural systems. The latter is often of more use since only rarely is it intended to stress a component beyond the yield point because of the danger of permanent set. The only problem being that the yield strength is difficult to locate, since some materials such as cast iron do not exhibit definite yield points. From the stress-strain curve relevant design properties like modulus of elasticity, E , and plasticity can be defined. [9,10,11].

2.2.2. Manufacturing process

Apart from a material satisfying the mechanical, physical and other required processes, the technological and economical aspects of production are also important. The methods of manufacture are divided into two main groups: [8].

- i) Primary manufacturing method which gives the basic form of the component from the ore, and
- ii) secondary manufacturing methods which include all the machining process.

The choice of steel to be used for structural purposes deals more with the primary manufacturing methods. There are two basic classifications of these methods:

- i) Hot rolling in which steel sections are made in rolling mill by passing hot steel bars, or billets through pairs of massive steel rolls, and
- ii) Cold rolling in which there is cold bending of steel sheet from 1.5 to 5mm thick to make very light structural sections such as channels and angles [11].

Most sections of wide structural applicability are produced in large quantities by hot rolling. This process is generally carried out by extrusion at temperatures high enough to prevent hardening and brittleness. The cold rolling process involves shaping of metals at room temperature by cold drawing. This latter process leads to work hardening which involves a general increase in strength". Steels produced by this method find use as stressing wires. For an economic design, the manufacturing process by which a component is produced should have an end product which, apart from satisfying all the mechanical properties specified, also be easy to work in order to minimise the cost of labour.

2.2.3. Cost and Availability

With the advent of the concept of optimization, cost has become one of the main criteria in the selection of materials, their design and fabrication of structural systems. The economy of the structure, while being dependent on the design approach used, is also affected by the cost of the material. This cost in turn depends on the manufacturing process, sources of the material, and the material availability.

Whereas other materials can be found locally in Kenya, steel has to be imported from producer countries. This means that the controlling factor is not the cost of the material, but the material price which depends on the levels of inflation.

2.2.4. The construction programme

The economy of any construction project revolves around the duration of the working schedules. The longer the project takes, the more costly it is likely to become in terms of both fixed and variable overheads. Thus it is important when choosing construction materials to consider the overall time taken to complete the project.

2.3. Factors affecting mechanical properties of steel

The deformation and fracture of material under loads are the principle phenomena associated with the mechanical behaviour of materials. Other interactive phenomena are the thermal, electrical, magnetic, chemical and optical effects. These interactions and effects depend on several factors which can be traced to manufacturing process and fabrication methods, functional design and detail design of the structural systems and elements. These factors are briefly discussed in the following subsections.

2.3.1. Chemical composition

The chemical composition is one of the most important factors in determining the properties of steel. The properties of the common structural steels are greatly influenced by the amount of manganese and carbon present. These two elements control strength, ductility and weldability. [15].

High carbon content increases strength but affects ductility and weldability. Phosphorous and sulphur affect the impact strength of steels. Generally some ductility is sacrificed to obtain increased strength.

2.3.2. Geometry, Temperature and Strain

In the usual rolling process, the cooling rates, finishing temperature and reduction in cross-sectional area affect the final yield and tensile strength of steel. Differential cooling rates and cold-working produce residual stresses whose effects on structural behaviour are discussed in chapter 3.0. Residual stress is defined as the stress that remains in a material from the manufacturing process. [11]. The final size and shape of the structural element produced influences the stress distribution and the structural

behaviour. Generally, smaller elements tend to give higher failure stresses than large elements, especially in fatigue failure and brittle fracture cases. The temperature and strain rates to which an element is subjected to tend to affect the yield and tensile strength, and possibly the ductility. [15].

2.3.3. Fabrication Effects

Fabrication of structural steelwork includes the production of the sections ready for erection from the component or parent parts as they come from the rolling mill. The principal operation involved in the fabrication process are:-

- i) cutting to length, and
- ii) drilling and welding.

Cutting to length is usually affected by the equipment used. Rough cutting is done by friction saws, whereas accurate cutting is done by high speed cold saws which cut to exact length. The same process can be accomplished by use of blowpipe or flame cutting. With more superior equipment hole drilling has been automated and is of considerable accuracy. The other fabrication technique used is welding. These fabrication processes do affect the behaviour of the final product. The cutting process involves rough handling of the structural steel both in the workshops and in the field.

The drilling process may lead to holes which are not perfectly lined, and during bolting there will be need to pull them into line forcibly in a process known as "drifting". Welding may cause warping and buckling of the section leaving high levels of residual stresses. Thus the fabrication processes will lead to a structure having the elastic limit over small areas. This makes the structure unsafe, considering the high ductility of steel. [17].

2.3.4. Erection effects

One of the great advantages of steel construction lies in the speed with which the structure can be erected. The erection process normally proceeds in planned sequence based on working schedules. The process involves:-

- i) delivery of steelworks
- ii) cramage and hoisting, and
- iii) setting out**

Delivered steelwork is normally inspected for completeness with the delivery schedule and weight verification. The members with accidental damage are then discarded. Also the steelworks are clearly marked according to the working plan. This is to avoid misplacement of members by the contractor which would affect the behaviour of the finished structure. Setting out is done precisely also to avoid cases where foundation bases are neither level nor in line. Cranage involves the method of hoisting sections to higher level. Low-rise frameworks use mobile hydraulic cranes, whereas large structures use tall mobile cranes and tower cranes. The hoisting method is important because some methods may introduce torsional bucking or cambering in the steel sections. The erection process itself involves use of fully braced "box" which ensures greater safety against accidental collapse. Additional bracing is also required to obviate torsional instability and to ensure the structural stability of the partly completed structure. [19]. The precautions mentioned are important because with the fabrication-induced stresses, failure can occur during erection if there is no adherence.

2.3.5. Imperfection effect

One of the major disadvantages with structural steelwork is the imperfection that occurs during each of the following processes:-

- i) manufacture
- ii) fabrication, and
- iii) erection

The overall accuracy of construction depends on mill rolling tolerances, fabrication tolerance and the tolerance of erection. For each of these processes there are acceptable limits from the stated dimensions or straightness. [8]. Temperature variations during erection must also be accounted for as they also cause imperfections. One of the most notable imperfections is introduction of lack of fit which may cause changes in the assumed behaviour. Imperfections may also cause distortions of the structure during erection. For example, differential shortening of internal columns may occur in a highrise structure due to the fact that internal columns carry higher axial load than the external columns. This shortening could cause connecting beams to be fixed in position out of level. Such changes in structure alignment may turn out to be disastrous. Thus it is necessary to use methods of manufacture, fabrication and erection that are precise.

2.4. Steel construction in developing countries

The population of developing countries currently represents three-quarters of the world population. In order to satisfy the enormous requirements of the population, especially in the provision of shelter and other infrastructures, these developing countries need to create a proper construction industry. Steel construction is one of the well known technologies in a number of developing countries e.g Venezuela, Iran, Mexico and China. [19]. Although some countries have not had much in terms of steel construction, the development of this technology in such countries can only take place in conjunction with the production of structural components. Thus there is a need to exploit the effectiveness of steel construction and the associated techniques through co-operation and innovation.

Developing countries which are in the process of industrialization need mass construction techniques. Since the population is growing rapidly, urbanization is proceeding at unprecedented rates and the rise in living standards creates a need for a new type of construction technique at community level. Thus speed of construction is a prime consideration in any construction techniques to be adopted. Steel construction is itself an offshoot of industry, forming a necessary link between industry and providing an area for experiment in individual construction.

Most of developing countries may tend toward steel construction as a complement or an alternative to concrete construction. There are advantages associated with the use of steel in construction namely:-

- i) " ease of fabrication as this process can be industrialised
- ii) ease of erection
- iii) enormous savings in construction time, and
- iv) lighter and taller structure.

2.5. Structural components

The structural components of any system may be grouped into basic types which contribute to the serviceability of the structure by satisfying some functional requirements. These may include:-

- i) buildings
- ii) bridges
- iii) special structures.

These structural forms share some components while others have only specific components associated with them. Generally, these components are classified into the following:-

- i) structural framework
- ii) floor systems
- iii) roof systems
- iv) walls and partitions
- v) operational facilities

Each of these components has a unique function which it contributes in the overall performances of the unified structural system. The continuity in performance is achieved only when there exists a link that effectively transmits the service loads, redistributing them in the desired proportions as per design. This functional requirements is the onus of connections.

2.5.1. Structural requirements

Structural frameworks may be fabricated from rolled shapes or built up sections with bolted or welded connections. Over the years, construction using steel has tended towards the rigid frame. The various components are rigidly fixed to one another to form a continuous system which supports loads in shear, bending and thrust. In case of high rise buildings the structural framework is a system of beams, girders or trusses and columns designed to carry all gravity loads of the structure and to resist wind and earthquake forces. The planning of structural framework caters for special facilities to be incorporated into the building.

The American Institute of steel Construction [A.I.S.C.] specification allows three types of construction in steel frames based on the types and behaviour of the connections. [20].

- (i) Type 1: Commonly referred to as rigid frame or continuous frame. It assumes that beam to column connection have sufficient rigidity to hold virtually unchanged the original angles between intersecting members.
- (ii) Type 2: Commonly designed as simple framing (unrestrained, free-ended) which assumes that in so far as gravity loading is concerned, the end of the beams and girders are connected for shear only and are free to rotate.
- (iii) Type 3: Designated semi-rigid framing (partially restrained), which assumes that connections of the beams and girders possess a dependent and known moment capacity intermediate in degree between complete rigidity of type 1 and the complete flexibility of type 2.

The behaviour of the types connections is presented in chapter 3.0. The type of structure framing chosen depends on the analytical methods at the disposal of the designer and also on the intended use of the structure, whether industrial, residential, recreational etc. The structural framework chosen should satisfy the cardinal requirements of equilibrium, strength, and stability.

2.5.2. Floor systems

The floor systems like the structural framework depends on the intended use of the structure. For a one storeyed industrial or residential building, the floor is usually a concrete slab laid directly on the ground. The construction of such a system pays particular attention to construction detail to avoid cracking due to freezing, shrinkage, expansion or excessive loading. [15] The floor system in high rise buildings is more elaborate and includes a framing of girders and beams which support the floor deck. Several types of floor decks are available with varying durability, fire resistance, weight and adaptability to the application of finished floors and ceilings and to the installation of utilities. The selection of a suitable type of floor deck depends on the occupancy requirements, structural adequacy and cost considerations.

2.5.3. Roof systems

The roof system includes the roof framing, the roof deck and the roof covering (cladding). The roof itself might be pitched or flat. A pitched roof is composed of trusses or rafters which form the main roof framing. The purlins act as secondary framing system spanning the distance between the trusses or rafters. Purlin sections are usually channels, junior beams or cold formed sections.

The roof deck is the structural assembly directly resting on the purlins and providing the enclosing element to the top surface of the building. A roof covering (cladding) may be of the single unit type or made up of factory-processed multiple units. The type of roof cladding chosen should be effective in as far as being leak-proof. Thus it is necessary to take special care in making the joint water-proof. Flat roof systems are commonly used in multi-storey structures although their application is now to be discouraged due to the high maintenance cost and leakage problems.

Apart from the functional planning and overall structure design of the structural members, other details which require attention are fire protection, service shafts, fabrication and erection plans for future expansion etc. In most cases large structural members are provided with field splicing at several points to facilitate handling during fabrication. The manner of erection does influence the design of the members and the type of connections to be used.

2.5.4 Bridges

Bridges can be classified either according to the service they perform or according to their structural arrangements. The majority of them are either highway or railway bridges. There are also bridges carrying a combination of traffic such as highway bridges with pedestrian sidewalks, or railway bridges with highway traffic at the same time. The most important of these bridge classifications are:-

- i) Span type (simple span, rigid frame, cantilever, continuous, arch, suspension, movable)
- ii) cross-section (deck, half-through, through)
- iii) functional (vehicular, pedestrian, material handling)
- iv) span length (short, intermediate, long)

- v) degree of redundancy (determinate, indeterminate)

The most significant of these is classified by span type, though exception ought to be made for multi-span bridges which contain several different types. Also the type of floor system might also be a bridge sub-classification, as this controls the manner in which loads are transmitted to the longitudinal elements and the location and function of bracing. [21.22].

2.5.5. Special structures

These are structural systems, which though finding everyday application, employ special techniques in their analysis, design and construction. There are many structural systems answering to the definition and only a few of them are discussed in the following subsections.

2.5.5.1. Towers and pylons

Transmission line pylons and other tower systems are examples of these special structures. These are three dimensional space structures and are analyzed as such. The design loads on transmission line towers or pylons are, in addition to normal dead loads, wind on the cables and towers, imbalanced cable tension resulting from horizontal changes of direction of a line. Large lateral forces acting on the relatively light towers may cause uplift at the supports, which requires that the superstructure be securely tied to heavy foundations. The combined effect of these forces makes the analysis and design of towers and pylons a special branch of structural engineering [22].

2.5.5.2. Stressed-skin structure

Although most of the structural systems discussed above may be grouped together as framed structures, that is structures made up of discrete elements, there exists another large group of structures in which the load carrying elements are continuous. These may be continuous sheets or plates, reinforced as necessary for strength and stiffness. This category includes storage tanks, boilers, wind tunnels, pipelines and penstocks (pressure vessels) as well as ship hulls, aircraft etc. These are stressed skin structures. Recent developments in stressed skin design have enabled application of the same principle in the design of industrial portal frames and roofing systems. In such cases the cladding strength is taken into account in the overall frame design and deflection of such systems are appreciably reduced by the cladding due to stressed skin effects. The chief reason for the structural efficiency of stressed skin

systems lies in their curved shapes which enables them to resist distributed loads normal to the surface primarily by membrane action. [23,24]. In their analysis bending effects are neglected and specialised mathematical techniques are utilised.

2.5.5.3. Cranes

Craneways represent special design problems related to crane girders and crane columns. [21]. For a crane of a given capacity which includes hoist, trolley and crane bridges or a roller truck, the type of crane girders and column arrangement may be selected from the following consideration:- magnitude of vertical, lateral and longitudinal forces for which the structure is to be designed, girder span between columns, clearance heights above the floor and below the roof. The behaviour of the crane rails is treated as beams on elastic foundations in their analysis, a specialised engineering analytical technique.

2.5.6. Connections

In order to obtain a structure that will function properly, all the four-mentioned structural components have to act in complementary roles. This role is attained only when there is continuity in the structural system to enable it act as a coherent unit. To achieve this, connections of a suitable type are employed. The connections thus act as links in the structure and do affect the overall behaviour of the structural systems and the stress in the main members.

These connections might either be of the welded type or those employing mechanical fasteners such as nails, bolts, rivets etc. In order to understand the behaviour of structural systems, an understanding of the connections under various loading conditions is vital and a review of this aspect of connections forms the basis of the next chapter. The connection types are broadly classified as:- .

- i) fully pinned
- ii) semi-rigid, and
- iii) fully rigid

The fully pinned connection assumes no joint moment transfer, though it undergoes relative member rotation at the joint, in it's behaviour under load. The fully rigid connection is assumed to have full joint moment transfer without relative member rotation at a joint. The semi-rigid

connection is assumed intermediate in behaviour, between the two types in that, it will transfer the full joint moment with relative rotation of the members at a joint. In reality, fully pinned connections do possess some rotational stiffness due to friction of members either from the use of friction grip type of connectors or overtightening of ordinary bolts. Also the fully rigid connections have some degree of flexibility possibly due to lack of tight fitting of the members as a joint during fabrication. Thus the tendency in structural analysis and design is towards an assumed semi-rigid connection behaviour. [24].

CHAPTER 3.0
LITERATURE REVIEW

3.1. Introduction

Research into connection behaviour started as early as the 1900's [26] and the results obtained coupled with other latter research findings have provided cumulative knowledge aimed at an attempt to explain actual connection behaviour.

Rigid connection design, which might include the use of welded end plates, calls for fabrication methods of members to be in close contact. This is to ensure that both force and stiffness are adequately transferred from member to member. Such design assumes full continuity in the system. Similar assumptions of full continuity have been made in reinforced concrete design with tragic consequences. Cases in point are the Bedford County Hall and Ronan point disasters. [27,28]. This is an indication of weakness in appreciating the fundamental properties of the material. Structural steelwork is in itself discontinuous and changes in assumed behaviour such as displacements occurring due to lack of fit may provide a hindrance to rigid design which assumes full continuity of the structural system. In spite of such shortcomings, fully-rigid designs have found application in portal frame and multi-storey buildings with satisfactory results. [28] The design recommendations for fully rigid frameworks have been found to be based on mathematical analysis rather than experimental evidence.

Pinned connections are approximated to joints with top and bottom angle cleats between beam flanges and columns. They have been adopted by designers in preference to fully rigid designs mainly due to their simplicity. In reality the savings in material by weight are minimised. This is mainly because in fully pinned design, the beams are for the most part laterally restrained by the floors they support. This introduces continuity and there is transfer of moments from beam to columns. This transfer relieves moments in the beams and increases moments in the columns which are usually unrestrained. This leads to heavier column and lighter beam sections, whereas in rigid design the two components are of intermediate size.

In reality, fully pinned connections do offer some degree of moment restraint and fully rigid connections do have some flexibility. These factors deserve consideration in design. With this realization and the fact that most practical connections are the field bolted type, there is an increasing tendency towards a connection intermediate in behaviour between the two, namely the semi-rigid joint.

The adoption of semi-rigid connection design means there is need to examine past design methods and come up with more

acceptable ones. There are several factors which need consideration, some of which are:-

- (i) the need to develop methods of assessing semi-rigid connection behaviour acceptable to designers. Despite the complexity of the problem, the solution must be in the form of simple expressions readily usable in design.
- (ii) the evaluation, by tests, of all column types of joints to make possible rationalization of those type capable of developing sufficient moment to be considered viable in the semi-rigid ranges, and the establishment of upper and lower bounds of such ranges.
- (iii) the consideration of material costs, which include labour and fabrication costs. As labour costs continue to increase, automation and standardization of fabrication methods are necessary for economic production. Such a trend leads to the following benefits:-
 - (a) Assists fabricators, and
 - (b) Reduces the parameters to be dealt with in research.

Another need for semi-rigid design is based on the rotational characteristics. Fully pinned connections undergo large angles of rotation, transmitting negligible moments, [fig. 3.1]. Deformations and moments in beams with fully pinned (flexible) connections are taken as for an ideally 'simply supported case. Semi-rigid connections permit some end-rotation but in so doing transmit appreciable end moment. [fig. 3.2]. A fully rigid connection permits redistribution of moments in the framework, which often results in reduction of maximum moments values and use of lighter sections for the beams, [fig. 3.2 and 3.3]. But two problems arise in the analysis and design of structural frameworks with semi-rigid connections. [21]. One problem is the determination of moments for a given structural system with known loads and the other deals with the determination of moment-rotation characteristic of a particular connection. These problems of analysis are treated in chapter four.

3.2. Loading effects on semi-rigidly connected systems

In order to perform the intended functions, all mechanically fastened connections undergo deformation under load. Thus

to understand the behaviour of semi-rigidly connected systems, information concerning deformation characteristics of the connections is a pre-requisite.

Semi-rigid connections possess some properties, as pertain to stiffness and flexibility, intermediate between those of equivalent fully pinned and fully rigid cases. The behaviour of these connections is often complex and with the exception of fully pinned joints, all mechanically fastened joints are highly statically indeterminate. This is because distribution of forces and stresses depends upon the relative deformation of the component part and the fasteners. The situation is further complicated by stress concentrations. [15,29]. Also the entire moment distribution is affected by changes in moments at any points in the structure.

The moments cause some rotation in the connection, which permits redistribution of member end moments due to the load-slip phenomenon. [30] Moment resistance builds on as the joint rotation proceeds while the member end moments decrease as the member tries to relieve itself of the moment build up due to the applied loading. The member end moments eventually balance resisting moment, when the structure has deformed to a state of static equilibrium. A hypothetical visualization of the moment distribution is treated by Mutuku et al [30] as shown in figure 3.4. Curve I in figure 3.4 represents the moment-rotation relationship of a member end 1 framed into a rigid connection in space, [figure 3.4 (a)]. Curve II represents the moment-rotation relationship of the same member end if this is framed into a semi-rigid joint in space, [figure 3.4 (b)]. If initially the member is loaded along curve I until point A, the rotation θ_j , is due to an applied end moment M_j . If the connection is now made semi-rigid, member end moment redistribution would occur along curve III to a point B on curve II thereby reducing member end moment to M_j' and increasing rotation to θ_j'' . Increasing moment leads to a moment-rotation curve following curve II from point B. The moment values on this curve represent the equilibrium of member end moments (resisting moments in semi-rigid joints) due to moment redistribution from curve I.

3.2.1 Moments-rotation characteristics of semi-rigid connections.

Moment-rotation relationships are the basic description of flexural connection behaviour. This relationship expresses the moment transmitted by a connection as a function of the relative rotation of the two or more members framing into a joint. [3,4,5,29]. The moment-rotation characteristics of connections are best depicted as moment- rotation (M- θ)

curves ("connection" curves) as shown in figure 3.5. with rotation, θ as the abscissa and moment, M as the ordinate. In this graphical format, the vertical (M) and the horizontal (θ) axis represents the perfectly rigid and perfectly pinned (flexible) connection respectively. Real or practical connections fall within the quadrant between the two axes. The moment rotation relationships are needed in the following situation involving bolted moment resisting connections in structural systems:-

- (i) in the design of semi-rigid connections with limiting deflection, drift or rotation considerations, and
- (ii) in the analysis of "rigid" frames with non-rigid connections. [29].

For structural adequacy of a framework in accordance with acceptable limit states for both ultimate and serviceability conditions, the connection should have suitable strength ductility characteristics. Bridge et al [31] did some research on a high rise building and plotted the moment-rotation curves shown in figure 3.6(a). The frame was analysed for a range of joint flexibilities and moment capacities. This was achieved by varying the values of moment of inertia of joints, I_j and the theoretical ultimate moment capacity at joint $M \cdot$. The model used was such that the moment capacity of the joint was less than that of either the column or the beam framing into that particular joint. The models are shown in figure 3.6(b).

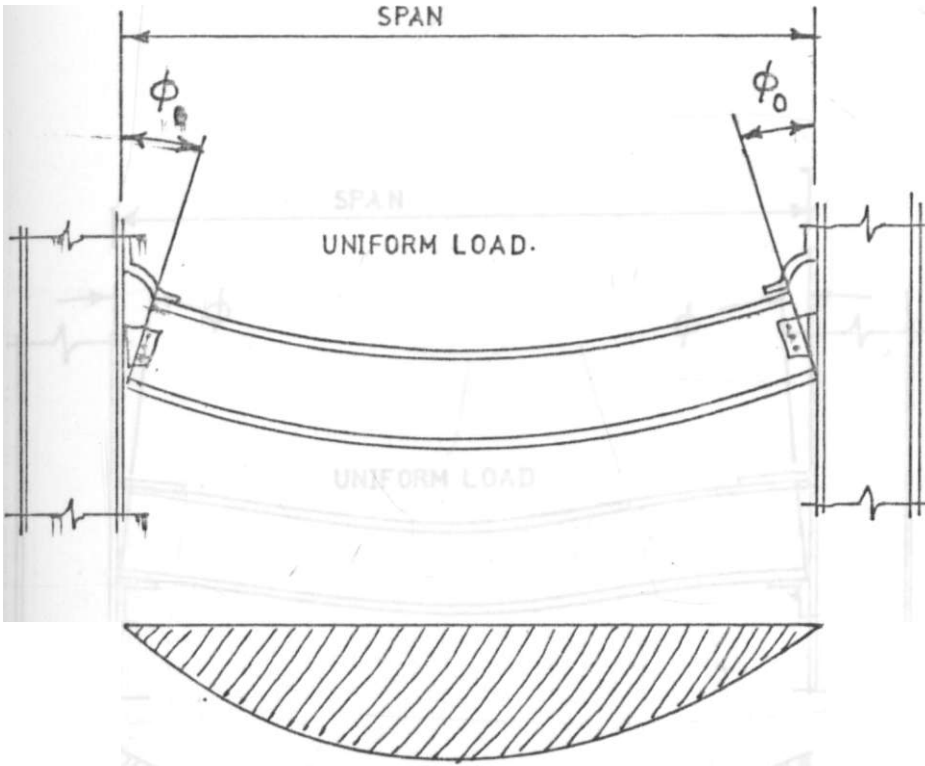


Figure 3.1 Fully pinned connection

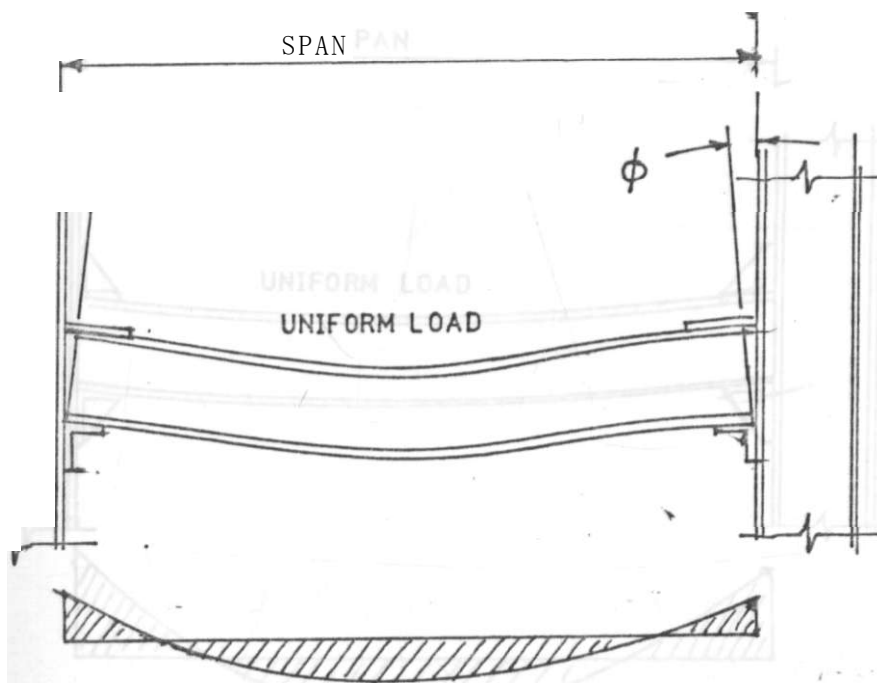


figure 3.2 Semi-rigid connection

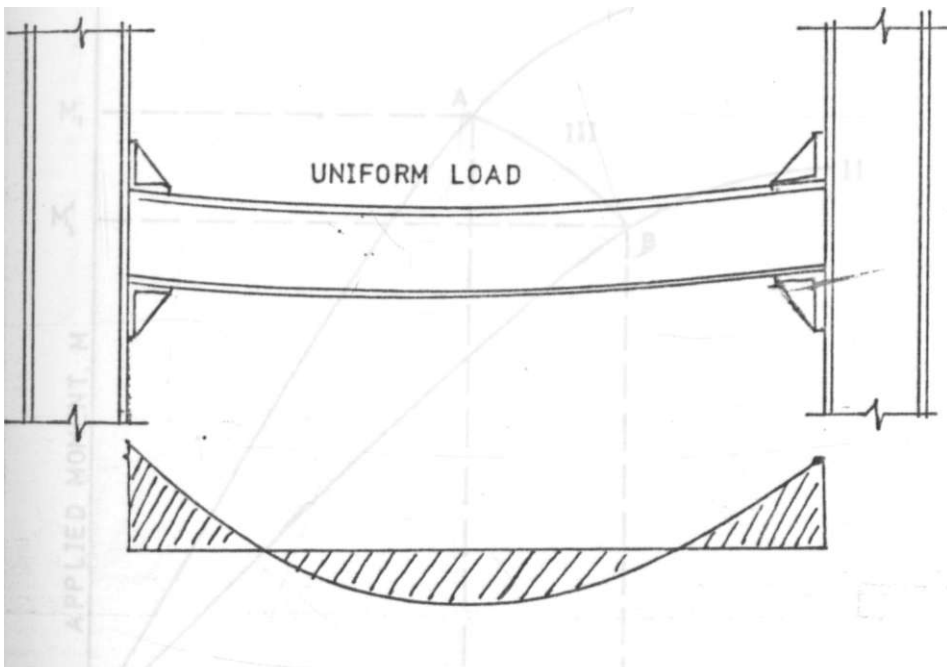
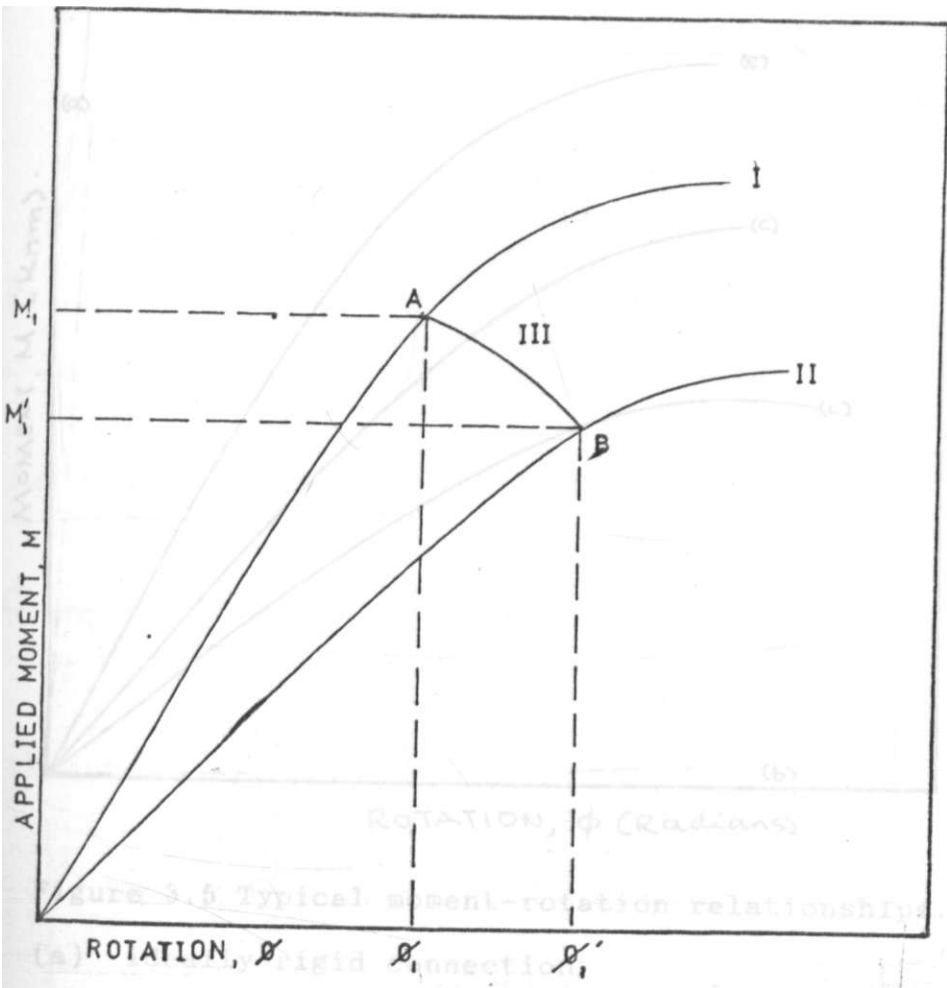
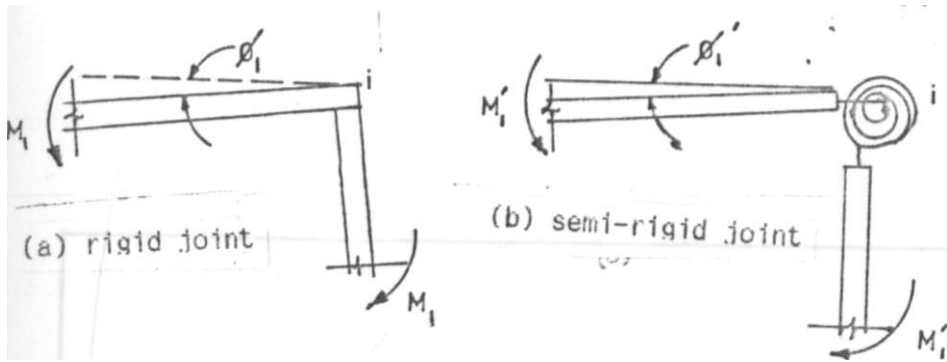
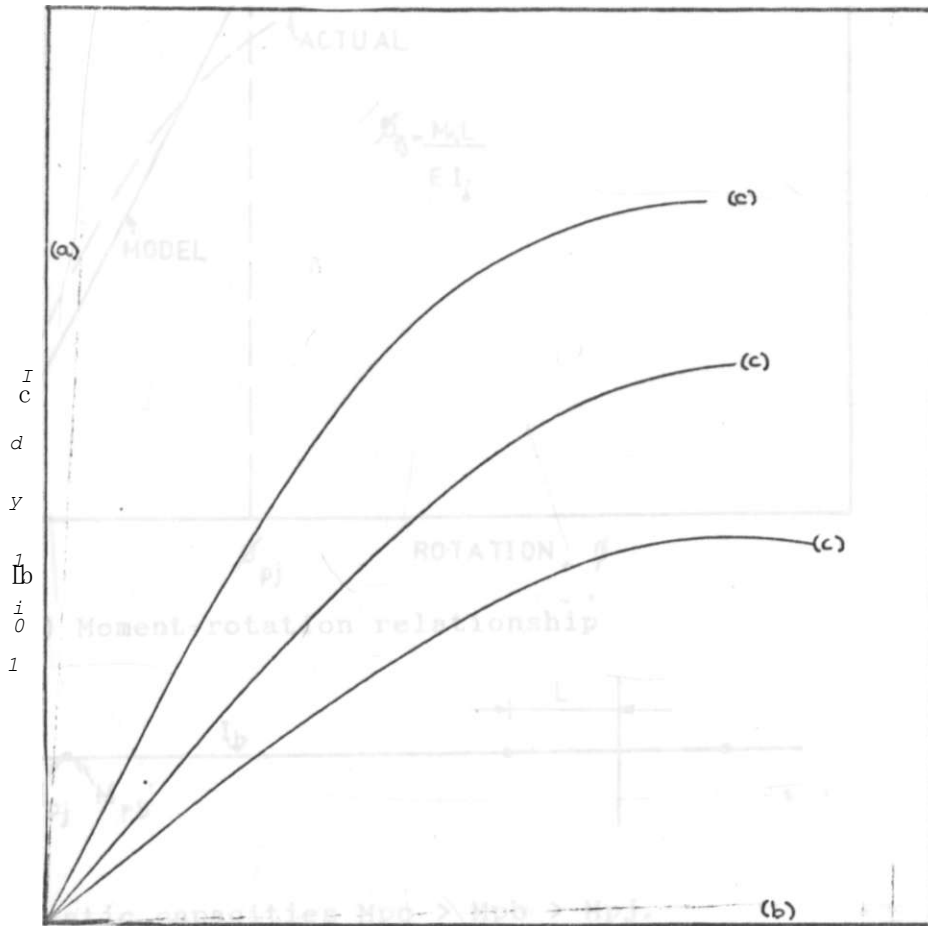


Figure 3.3 Fully rigid connection



(c) Redistribution curve

Figure 3.4 Moment-redistribution in semi-rigid joints



RotA-TVDWj cfi

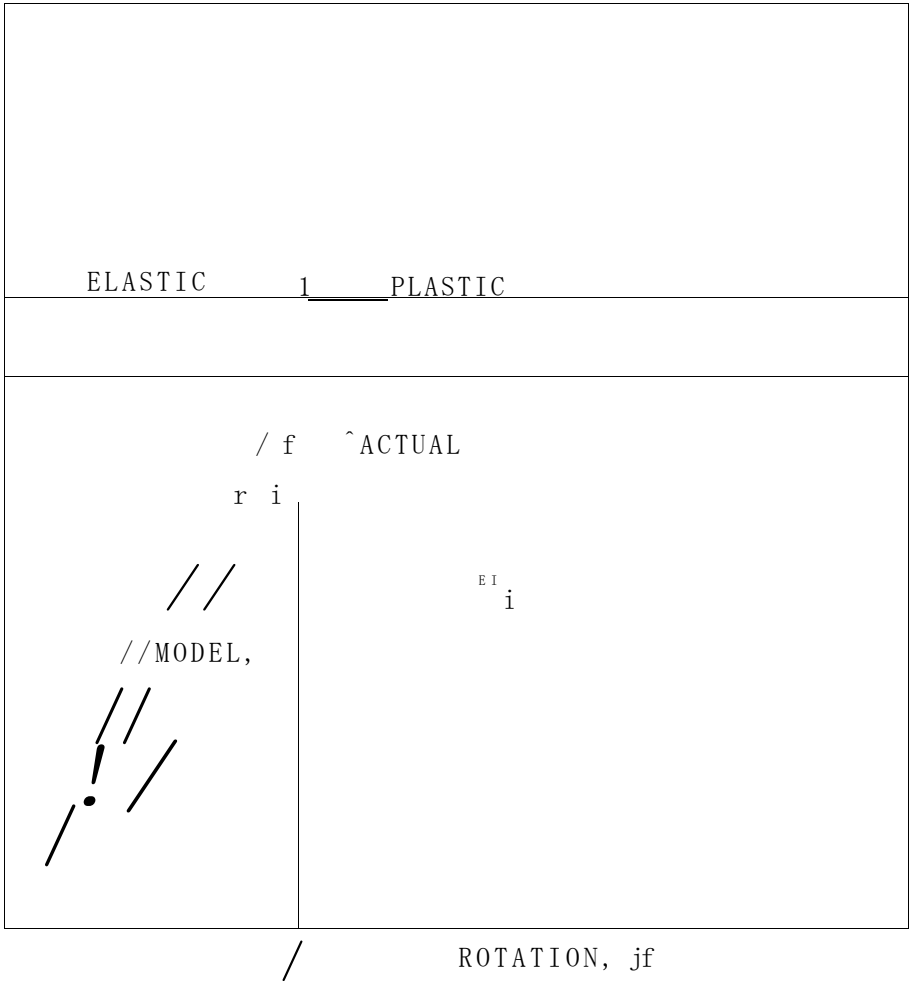
Figure 3.5 Typical moment-rotation relationships.

(a) ideally rigid connection

(b) fully pinned connection

(c) varying degree of partial connection rigidity.

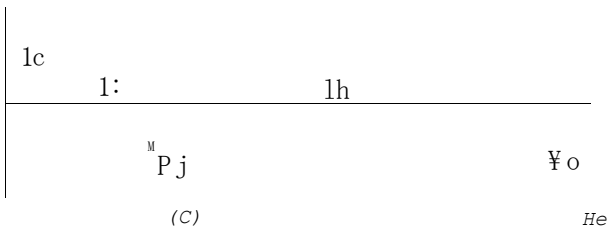
[13, 4, 5, 29]



(a) Moment-rotation relationship



Plastic capacities $M_{pc} > M_{pb} > M_{pj}$.



(b) Model for stiffness and strength

Figure 3.6 Computer model for semi-rigid joints. [31]

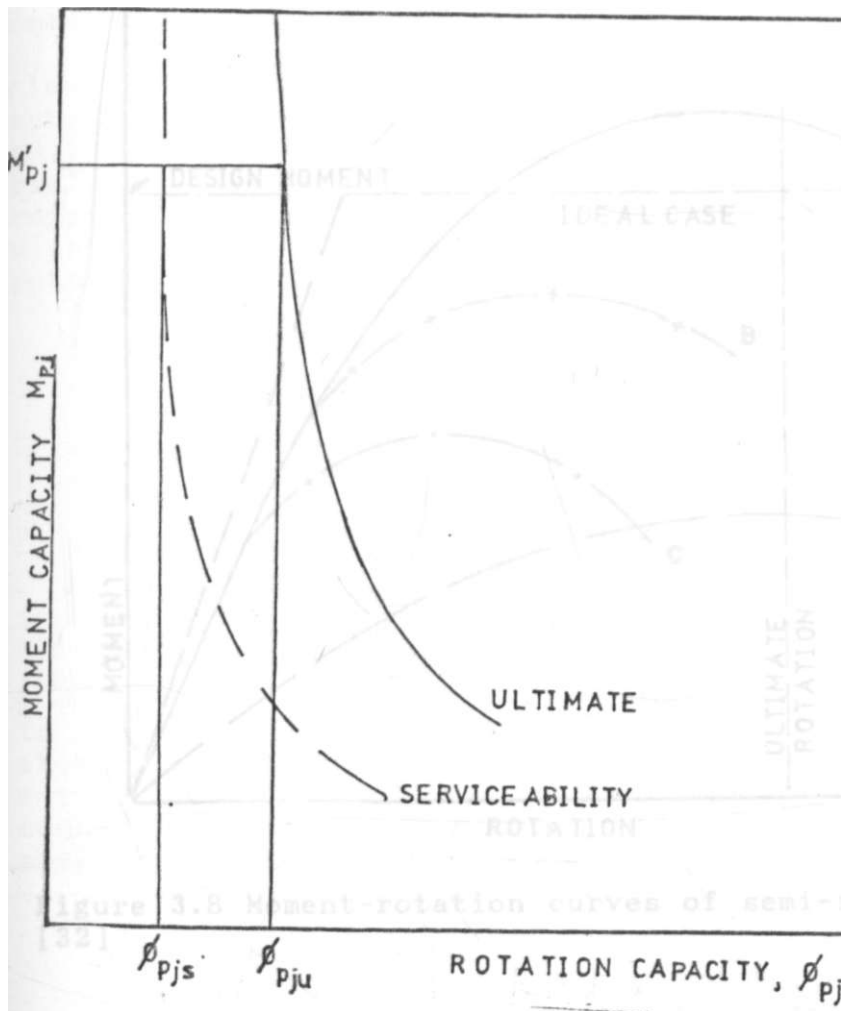


Figure 3.7 Moment-rotation demand [31]

M_{pj} = theoretical ultimate moment capacity

ϕ_{pjs} = rotation capacity at serviceability

ϕ_{pju} = rotation capacity at ultimate.

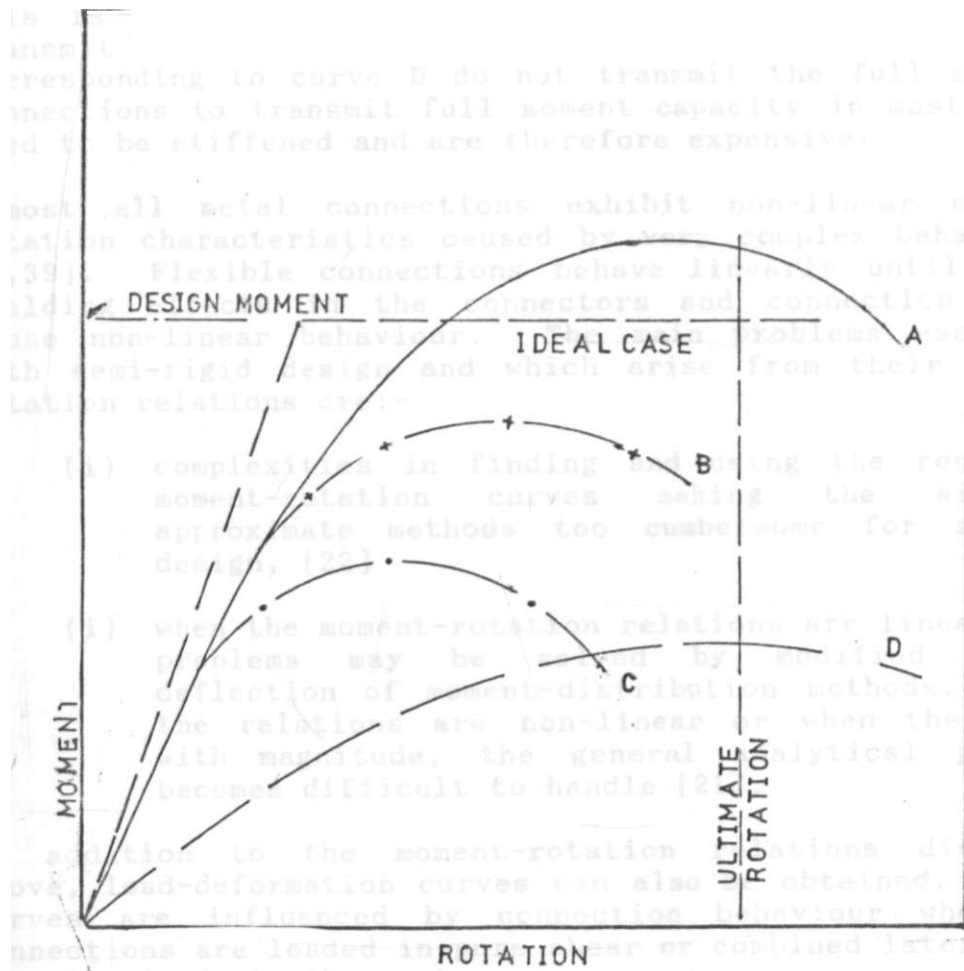


Figure 3.8 Moment-rotation curves of semi-rigid connections [32]

The maximum rotation of the joints in the frame was computed for each semi-rigid model used at both ultimate and serviceability limit states. They found out that for any given value of moment capacity M_j , the total maximum capacity (summation of columns, beams, and joints) required to satisfy the ultimate limit state was independent of the elastic stiffness of the connections. Figure 3.7 shows the acceptable criteria for both the ultimate and serviceability limit states. In a related research, Bijlaard [32] came up with the curves shown in figure 3.8. He found out that when redistribution of moments is required, the connections

corresponding to case B and C have to be rejected because of lack of sufficient rotational capacity. Those corresponding to curves A and D possess sufficient rotational capacity. Whereas curve A is acceptable, curve D is not.

This is because connections corresponding to curve A can transmit full design moment whereas connections corresponding to curve D do not transmit the full moment. Connections to transmit full moment capacity in most cases need to be stiffened and are therefore expensive.

Almost all metal connections exhibit non-linear moment-rotation characteristics caused by very complex behaviour. [3,39], Flexible connections behave linearly until local yielding effects in the connectors and connection parts cause non-linear behaviour. The main problems associated with semi-rigid design and which arise from their moment rotation relations are:-

- (i) complexities in finding and using the requisite moment-rotation curves asking the simplest approximate methods too cumbersome for routine design, [22]
- (ii) when the moment-rotation relations are linear, the problems may be solved by modified slope-deflection of moment-distribution methods. When the relations are non-linear or when they vary with magnitude, the general analytical problem becomes difficult to handle [21].

In addition to the moment-rotation relations discussed above, load-deformation curves can also be obtained. These curves are influenced by connection behaviour when the connections are loaded in pure shear or combined lateral and shearing loads in three stages:-

- (i) elastic
- (ii) elasto-plastic, and
- (iii) a stage where plastic hinge formation has occurred in sufficient locations to define the load carrying capacity of the structure.

Load deformation curves, like moment-rotation relations may either be linear or non-linear [figure 3.9]. The non-linear behaviour may be due to one of the following reasons:-

- (i) local yielding of the metal components in the joint which might cause end-action redistributions
- (ii) the materials may possess non-linear stress-strain behaviour

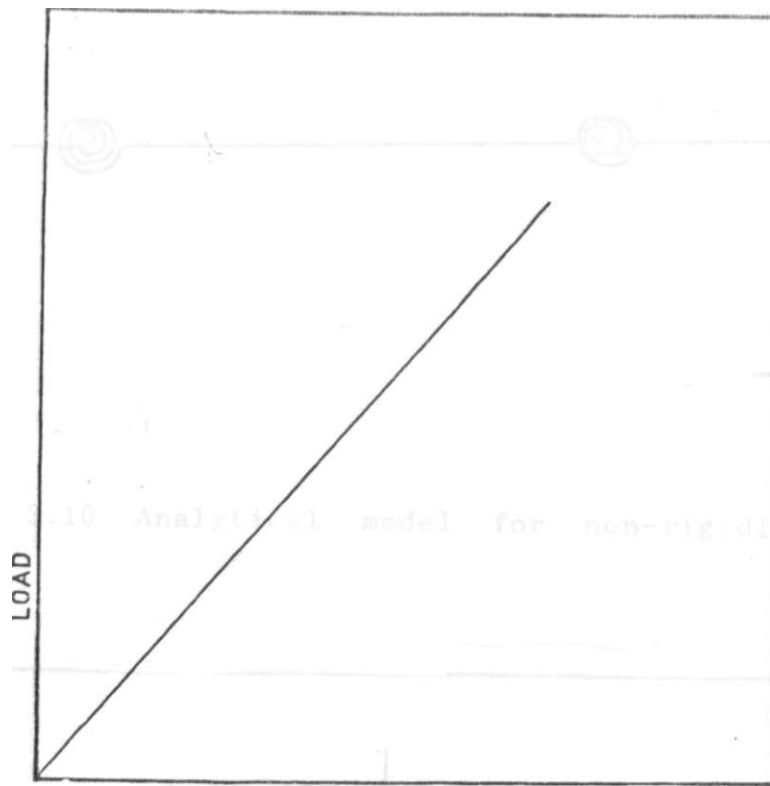
- (iii) the residual stress effects in the components, and
- (iv) progressive deformation due to redistribution of forces in the structure.

Load-deformation curves for rigid, semi-rigid and pinned (flexible) connections are similar in shape to the moment rotation curves, [see figures 3.9 (b) and 3.5] [30]. Thus the main task is to establish whether the connection behaviour nearly approaches either the rigid or the pinned types, [see figure 3.5]. If this is so, then either of them can be used as a basis for linear semi-rigid connection behaviour, [figure 3.9 (a)] [28]. It is essential that non-linear behaviour of any given joint or connection type be modelled correctly and hence analysed for a more definite description of semi-rigid connection behaviour.

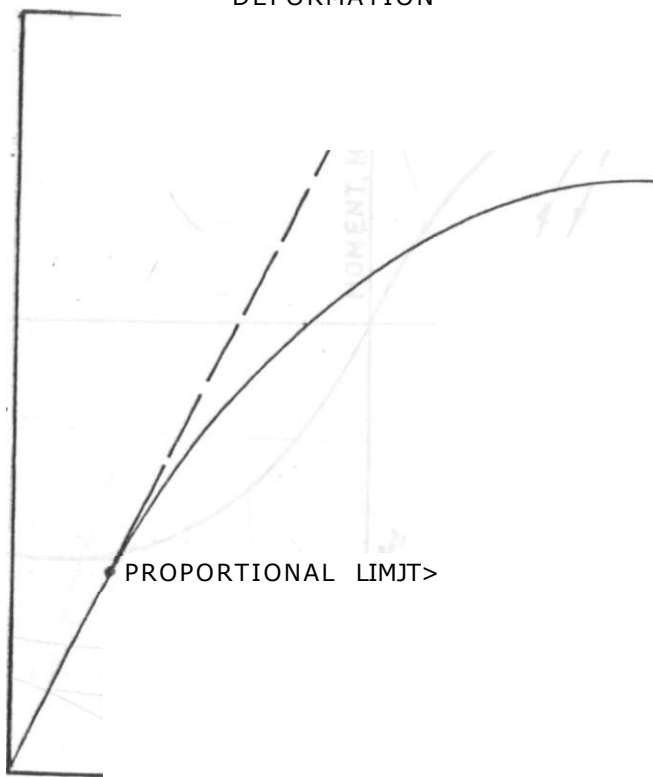
3.2.2 Moment-rotation relations for dynamic loading

Dynamic analysis of framed structures usually involve the assumption of rigid connections but in reality the connections exhibit some flexibility. In non-rigidly connected frames the ability to resist loads may be determined more exactly by the properties of the members themselves. In dynamic analysis the non-rigid connections are modelled as rotational springs [see figure 3.10] and the moment-rotation relationship obtained has a general form of figure 3.11. [33]. From the moment-rotation curves [figure 3.11] it is seen that at low values of moment, the M- θ relationship is approximately linear, but at higher moments the relationship is non-linear. Unloading of the structural system is traced by the dotted lines on figure 3.11 just as in the case of static loading, the moment capacity of the joint M'' is not exceeded in the M- θ relation of figure 3.11 [see also fig. 3.6a]. Weaver et al [33] did some work on dynamic response of a 10-storey frame with non-rigid connections and concluded that:-

- (i) connection stiffness can influence both lateral and end moments
- (ii) the amount of permanent deformation sustained in columns of a frame subjected to dynamic loading can be significantly affected by the properties of the connections. Thus special attention ought to be paid to connection behaviour of structural systems in areas where dynamic loading such as earthquakes and typhoons occur.



LINEAR



(NON LINEAR)

DEFORMATION

Figure 3.9 Typical load-deformation curves in semi-rigid connections [30].

Figure 3.10 Analytical model for non-rigidly connected frames.

S

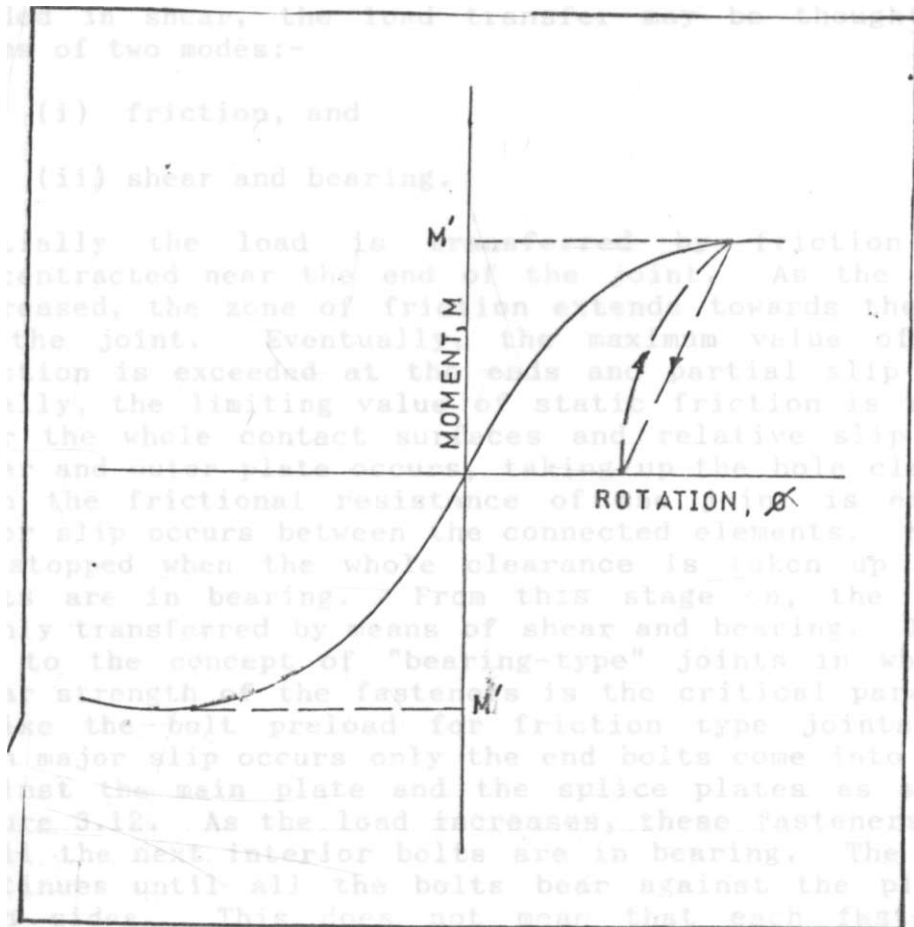


Figure 3.11 Actual M- θ curve for non-rigid connections.

3.3 Load transfer modes

One important aspect in the design of bolted (semi-rigid) connections is the load distribution in the bolts. This load distribution depends on the loading conditions, i.e. whether the connection is loaded in tension, shear, combined tension and shear, bending or several other combinations. Since most connections are statically indeterminate, the distribution of forces and stresses depends upon the relative deformations of the component parts and the fasteners. [21,25] The mode of load transfer or distribution also helps to identify the type of connections to deal with in design. Connections loaded in a manner that tends to shear the fasteners are shear connections and those connections loaded in a manner in which fasteners tend to fail in rotation are moment connections. For connections loaded in shear, the load transfer may be thought of in terms of two modes:-

- (i) friction, and
- (ii) shear and bearing.

Initially the load is transferred by friction forces concentrated near the end of the joint. As the load is increased, the zone of friction extends towards the centre of the joint. Eventually, the maximum value of static friction is exceeded at the ends and partial slip occurs. Finally, the limiting value of static friction is exceeded over the whole contact surfaces and relative slip of the inner and outer plate occurs, taking up the hole clearance. When the frictional resistance of the joint is exceeded, major slip occurs between the connected elements. Movement is stopped when the whole clearance is taken up and the bolts are in bearing. From this stage on, the load is mainly transferred by means of shear and bearing. This has led to the concept of "bearing-type" joints in which the shear strength of the fasteners is the critical parameter, unlike the bolt preload for friction type joints. [21]. When major slip occurs only the end bolts come into bearing against the main plate and the splice plates as shown in figure 3.12. As the load increases, these fasteners deform until the next interior bolts are in bearing. The process continues until all the bolts bear against the plates on both sides. This does not mean that each fastener is carrying an equal share of the total load. As load is increased, the fastener forces change as shown diagrammatically by the height of the bars in figure 3.12 and finally an end fastener fails because of overstraining. [5,21].

Apart from hanger connections and some specific beam to column connections, joints loaded in tension are rarely used. This is mainly due to the concern attached to additive effects of bolt tension pre-stress and applied tensile stress. These factors combined with the complex nature of load transmission make the analysis of tension connections difficult. [21].

For moment connection, it is generally accepted that the most realistic bolt load distribution at low moment in the joint is that depicted in figure 3.13 (a), as the moment increases towards its design value, the distribution changes to that of figure 3.13 (b). [34]. Experimental evidence [34] indicates that the latter distribution gives a good estimate of bolt force at design load. This mode is compatible with true structural appreciation of connection behaviour. Figure 3.13 (c) shows plastic load distribution, though generally the distributions used frequently assume elastic connection behaviour.

3.3.1 Failure modes

The strength of a mechanically fastened connection is related to the type of failure that occurs under loading. The failure mode is in itself, a direct reflection of the loading mode to which the connection is subjected. The overall design of bolted joints is based on the consideration of the failure modes that are likely to occur, these might be one or more of the following: [15].

- (i) tension failure in the side plates
- (ii) shearing failure in the fastener
- (iii) bearing failure between the plate and the fastener
- (iv) shear tear-out failure in the plate

These failure modes are illustrated in figure 3.14

Apart from the loading mode, the failure mode of a connection depends upon several other factors. These are mainly due to material and geometrical properties of the connection.

Joint length is an important parameter influencing the ultimate strength of the joint. Depending on the length and other factors such as material type and fastener deformation capacity, a connection may fail by simultaneous shearing of all the bolts. The fastener length is dependent upon the fastener spacing (pitch).

The minimum spacing to avoid joint failure is not an important variable when it comes to connection failure modes but the material type is. This is because the yield stress of the connection material influences the ultimate strength of the joint. For a given loading and number of bolts, the material properties influence the net area, A_n , and the gross area, A_g , of the bolt hole patterns. Often simple rectangular patterns are used, though staggered hole patterns may be adopted, [see figure 3.15] Such patterns, while satisfying the recommended A_n/A_g ratio requirements, may still fail either at the net or gross section.

J J _ N X I n

_] _ d _ • _ a

o

a . (a) End bolts in bearing

(b) 2nd bolts in bearing

(c) Middle bolt in bearing

(d) All bolts in bearing. End bolts carrying increasing proportion of load and end regions of plate.

(e) End bolts yield 2nd carry. Increasing proportion of load.

(f) 2nd bolts yield middle bolt carries increasing proportion of load

Figure 3.12 Bolt forces for butt splice joints [51]

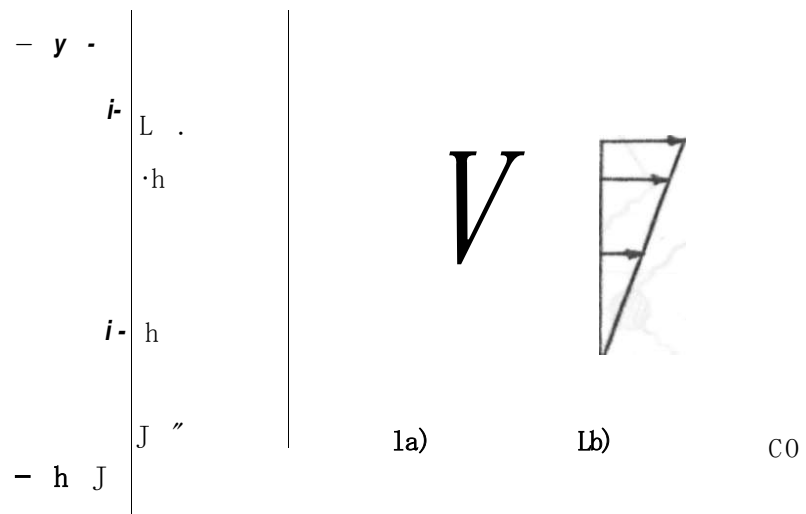


Figure 3.13 Bolt load distribution model in bending [34]

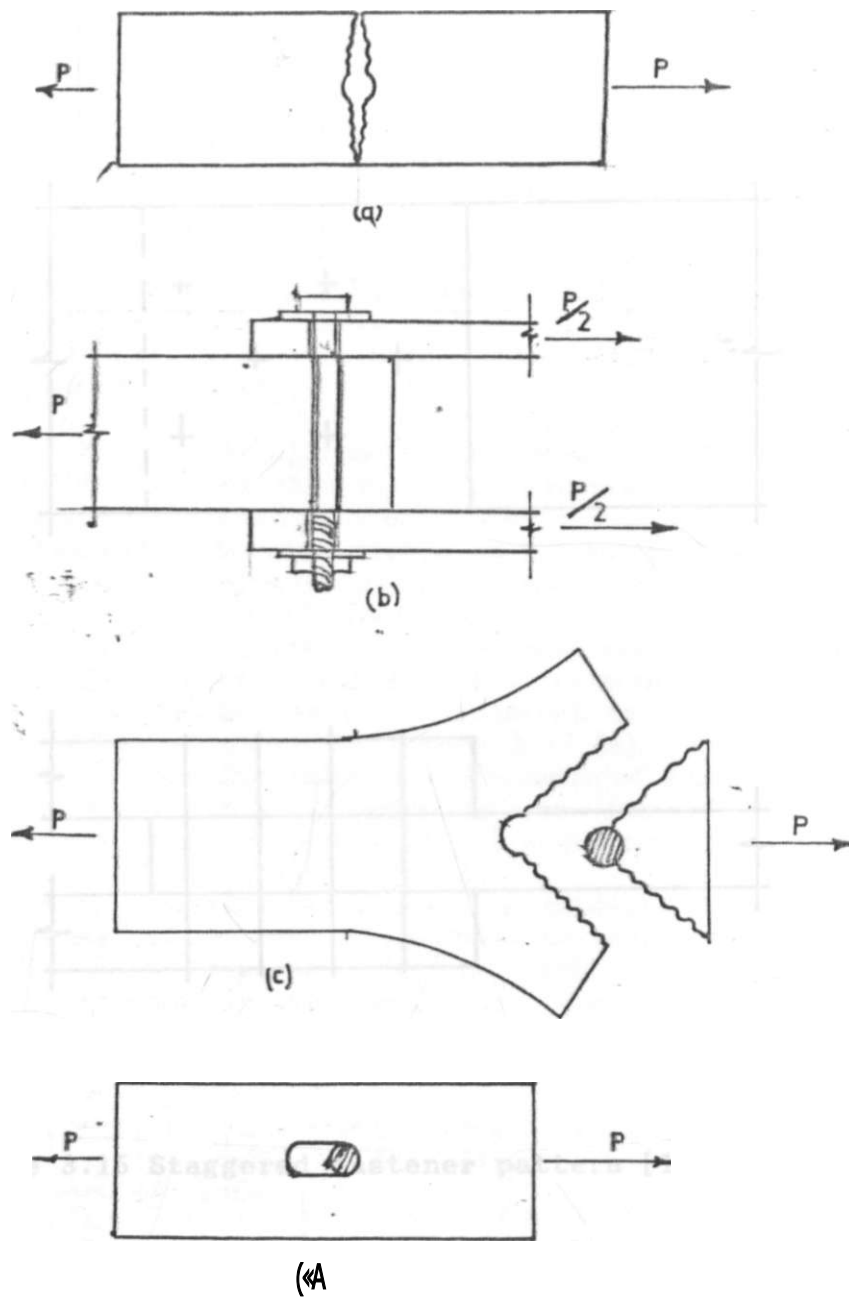


Figure 3.14 Types of connection failure

- (a) tension failure in plate
- (b) shearing failure in fastener
- (c) shear tear-out failure in the plates
- (d) bearing failure in plate [15]

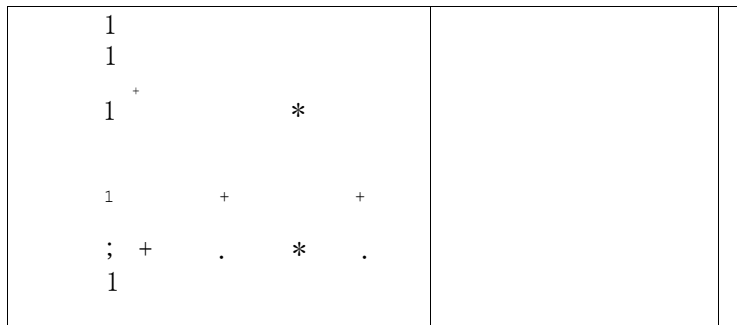


Figure 3.15 Staggered fastener pattern [15]

For the rectangular bolt hole patterns [figure 3.15] failure is likely to occur along A-A. If the pattern is staggered [figure 3.16] failure may occur along C-C, figure 3.15 (b) is intermediate between the patterns shown in figure 3.16 (a) and figure 3.15 (c) as far as reduction in joint capacity is concerned. The reduction in area hence capacity of the connected components is a function of the stagger, S and the gauge, g . [see figure 3.16]

Most of the empirical relation development between g and s hold for a given fastener type. This is because any change in fastener type may increase or decrease the joint length for a given design load, which in turn affects both the pitch and ultimate load as well as the failure mode.

3.3.2 Stress distribution in bolted connections

Though the design of bolted connections is based on postulated failure modes, design codes and specifications use stresses as design guides. The actual stresses in connections subjected to service loads, depends on the amount of friction between the plate, the mechanical properties of the fasteners and the connected parts, fastener sizes, connected part thickness, fastener hole patterns, extent of hole filling by the fasteners and the type of loading.

If the applied load on a connection is less than the frictional resistance, it is transmitted entirely through friction between the connected parts, and there exists no shearing or bearing stress on the bolts. When the load just exceeds the frictional resistance, an initial slip occurs. Any further load increment will be resisted partly by friction and partly by shearing and bearing stresses on bolts. After slippage has occurred, bearing stresses develop in the material adjacent to the hole and in the fastener as shown in figure 3.17 (a). An increase in load causes yielding and the embedment of the bolt on a larger area of contact resulting in larger area of stress distribution [figure 3.17 (b) and figure 3.17 (c)].

Nominal bearing stresses are computed based on half the circumferences of the punched or drilled hole. But since the bolt does not fill the hole completely, the actual stress distribution and hence the maximum bearing stress may be different from the assumed nominal values. [figure 3.17 (c)]. [21]

The actual failure mode depends on such geometrical factors as the end-distance, bolt diameter and the thickness of the connected parts.

In bearing failure, either:-

- (i) the fastener splits out through the end of the plate because of insufficient end distance, or
- (ii) excessive deformations are developed in the material adjacent to a fastener hole [1, 34] [see figure 3-18(a) and figure 3.18 (c)].

Failure may also occur as a combination of (i) and (ii) above.

3.3.3 Residual stresses.

Residual stresses might be due to deliberate introduction of stresses to improve the stress distribution of possibly as a consequences of a manufacturing or fabrication process. When rolled or welded elements are cooled, the areas that cool first become stiffer, resist contraction and develop compressive stresses, while the remaining regions continue to cool and contract in the plastic condition and develop tensile stresses. These stresses are referred to as residual stresses and vary approximately as shown in figure 3.19. Other effects that lead to residual stresses are force fitting of individual components, lifting and transportation and machining to particular geometry. In any structural system, there are two kinds of residual stresses:-

- (i) large scale residual stresses, and
- (ii) small scale residual stresses.

The latter are stresses which are approximately self-balancing in regions of infinitesimal dimensions compared to that of the member, and the former are those which are not self-balancing. [21, 35, 36, 37, 38]. The presence of residual stresses in structural components and systems might either be beneficial or detrimental. These effects are illustrated below in the discussion of residual stress effects on stress-strain curves, moment-curvature, buckling, load-capacity and plastic moment.

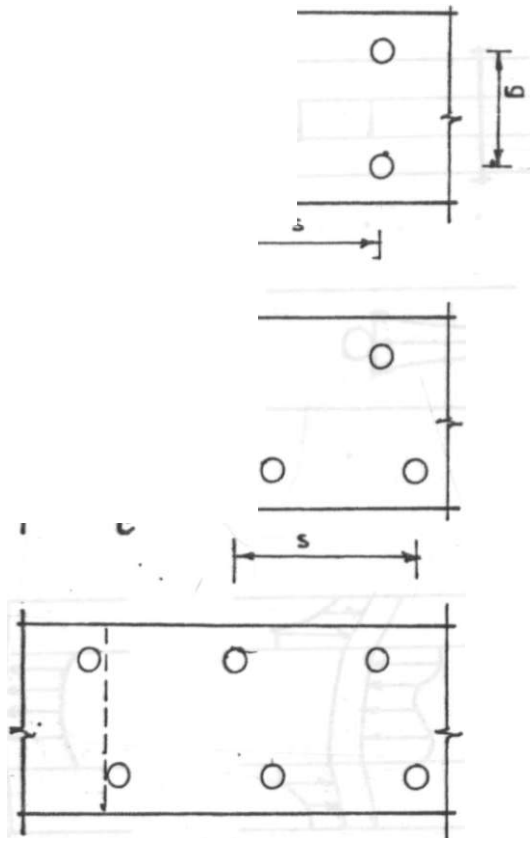
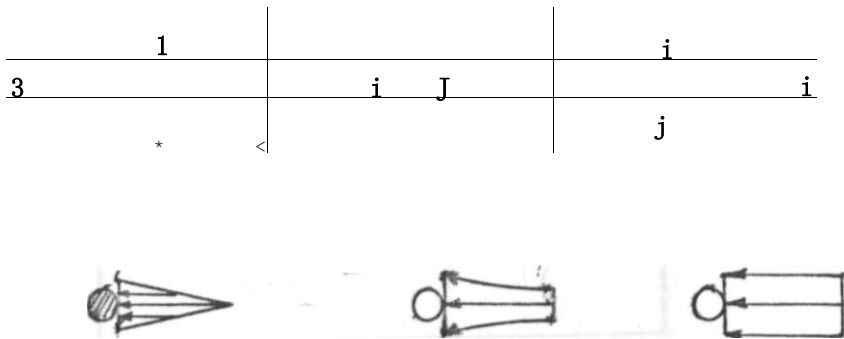


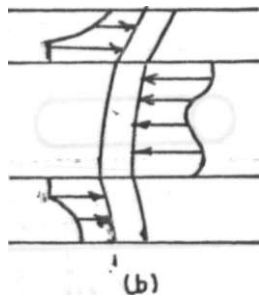
Figure 3.16 Possible failure paths for different holes patterns

(a) rectangular pattern

(b) and (c) staggered



SI
£ I
(c)

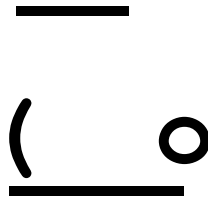


(b)

Figure 3.17 Bearing stresses

- (a) elastic
- (b) elasto-plastic
- (c) nominal

f)



(W

Figure 3.18 Failure modes in bearing

(a) bolt splits out through end zone

(b) large hole deformation

E[^] THICK SECTION-

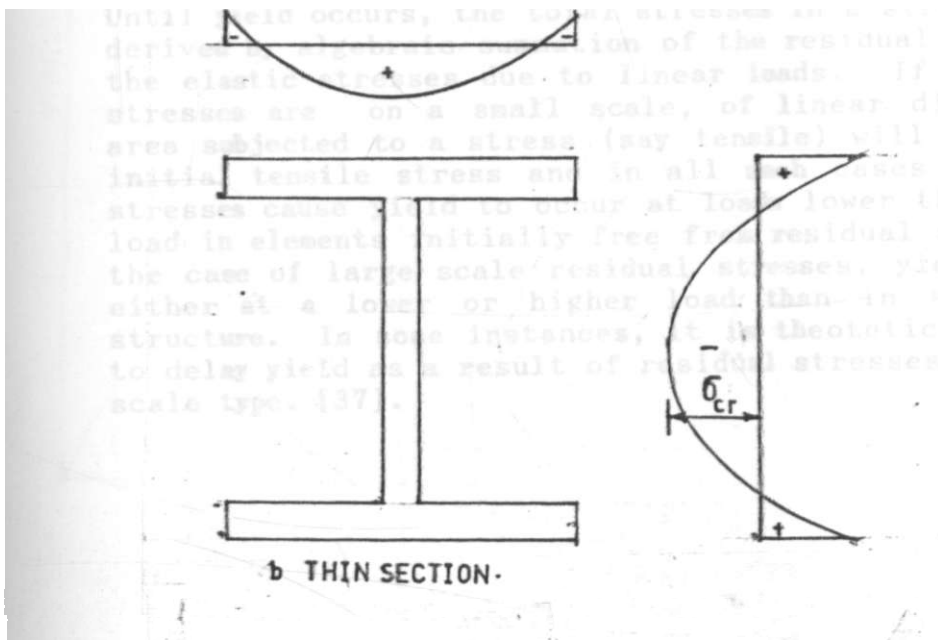


Figure 3.19 Typical residual stress patterns [21, 35, 36, 37, 38]

3.3.3.1. Residual stress effects on stress-strain relations

The net effects of residual stresses is to alter the stress-strain diagram for the shape as compared to ideal material specimens [see figure 3.20]. An alteration in the stress-strain curves also affects important parameters like the yield strengths, f_y and young's modulus (modulus of elasticity), E . Since most of the design values are results of test on ideal specimens knowledge of the residual stress effects on other important design variables is an added advantage in the design of steel structural systems. [21, 36, 37].

3.3.3.2. Effects on load capacity and yield

Equilibrium requires that the summation of residual forces produced by the residual stresses be zero at any section along the length of the loaded member. [35]. This means that residual stresses have no detrimental effects on load-capacity for reasons of equilibrium. This is because the residual stresses have zero resultant force and zero resultant moment. Therefore their total effect neither adds nor subtracts from that of the external loads.

Until yield occurs, the total stresses in a structure may be derived by algebraic summation of the residual stresses and the elastic stresses due to linear loads. If the residual stresses are on a small scale, of linear dimension, any area subjected to a stress (say tensile) will also have an initial tensile stress and in all such cases the residual stresses cause yield to occur at loads lower than the yield load in elements initially free from residual stresses. In the case of large scale residual stresses, yield may occur either at a lower or higher load than in a stress-free structure. In some instances, it is theoretically possible to delay yield as a result of residual stresses of the large scale type. [37].

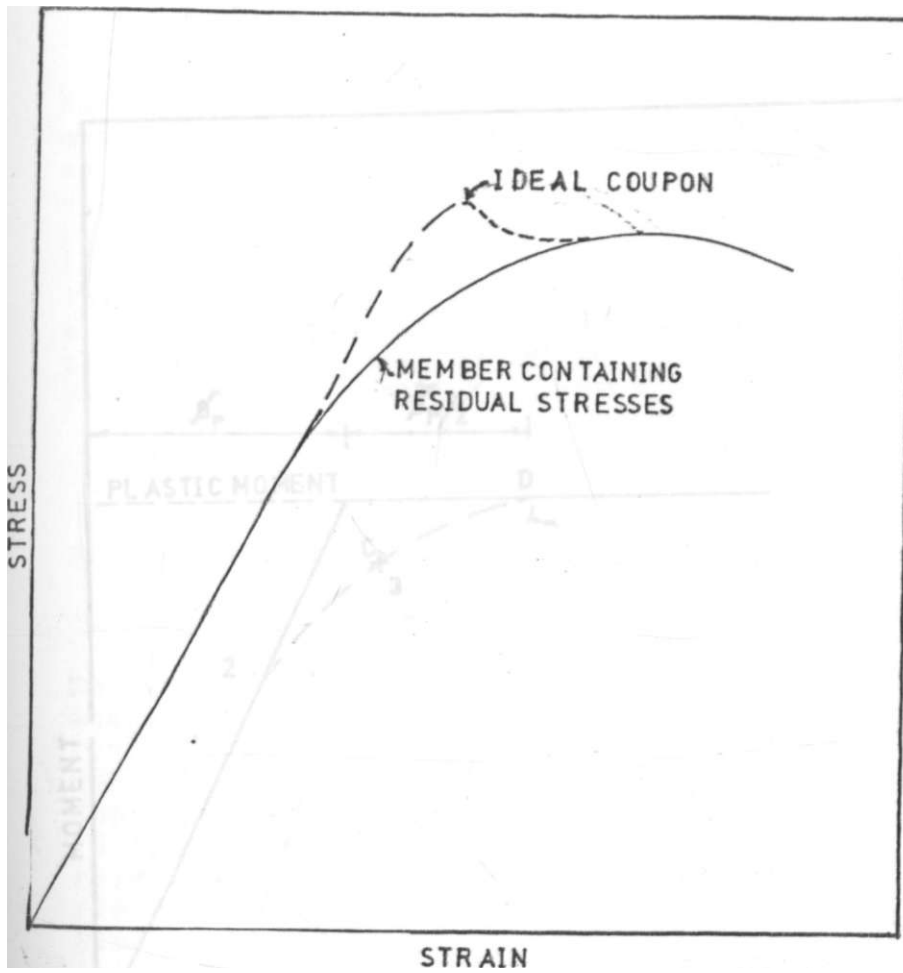
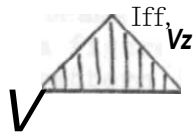
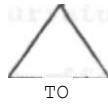


Figure 3.20 Influence of residual stresses on the stress-strain curve [21,36]



(b)

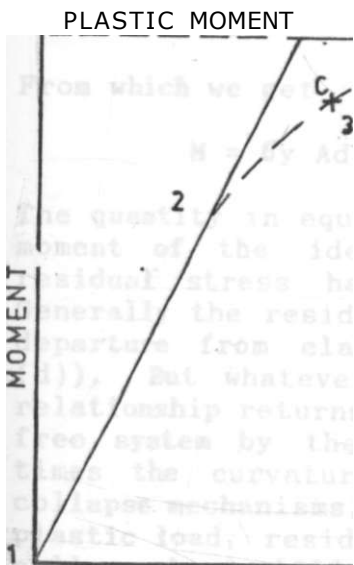


y

to

*

K/i



J .

CURVATURE,

Representation of residual stress effects upon the $M-\theta$ relationship of a beam.

3.3.3.3. Effects on moment-curvature

To examine the residual stress effect on moment-curvature in rolled beams, an idealization of a wide flange shape as shown in figure 3.21 (a) is used. [35], Assume the residual stress pattern in the flange tips of $-T_y/2$ and tension at the flange centres of $+T_y/2$. The total force in one flange at one stage is given by:-

$$P = \int \sigma dA \quad \text{[3.1]}$$

For equilibrium, $P = 0$ before application of any external moment. When uniform strain is applied across the flanges as the member is bent by pure moment, the stress distribution will change from (1) $[M=0]$ to (2) at which point extreme fibre stress reaches the yield stress level, [figure 3.21 (c)]. Beyond stage (2) the behaviour is inelastic as shown in figure 3.21 (d). Stage (3) represents a partially plastic case. The flange being yielded half-way to the centerline. At stage (4) the entire flange has yielded and the moment is given by:-

$$M = \int \sigma dA = P d \quad \text{[3.2]}$$

From which we get

$$M = \int \sigma dA \quad \text{[3.3]}$$

The quantity in equation [3.3] is equal to the full plastic moment of the idealised wide flange shape. Thus the residual stress has no effect on the moment capacity. Generally the residual stress effect is to cause an earlier departure from elastic linearity (OCD) (see figure 3.22 (d)). But whatever the initial state of stress, the $M=0$ relationship returns close to that for an initially stress-free system by the time the curvature reaches about 2.5 times the curvature at first yield. Since in plastic collapse mechanisms, such curvatures are reached at and near plastic load, residual stresses normally have no effect on collapse load. [35].

3.3.3.4. Effects on deflections

Small scale residual stresses always lead to a decrease in the load at which a structure begins to yield. This consequently leads to an increase in the deflections above the load at which yield first occurs. Large scale residual stresses can cause either a decrease or an increase in the load at which yield first occurs,

depending on the stress distribution. Consequently they can lead to either an increase or decrease in deflections as compared with structural systems which are initially free from residual stress. The residual stress distribution giving the highest bending moment at yield for a beam is presented in figure 3.22.

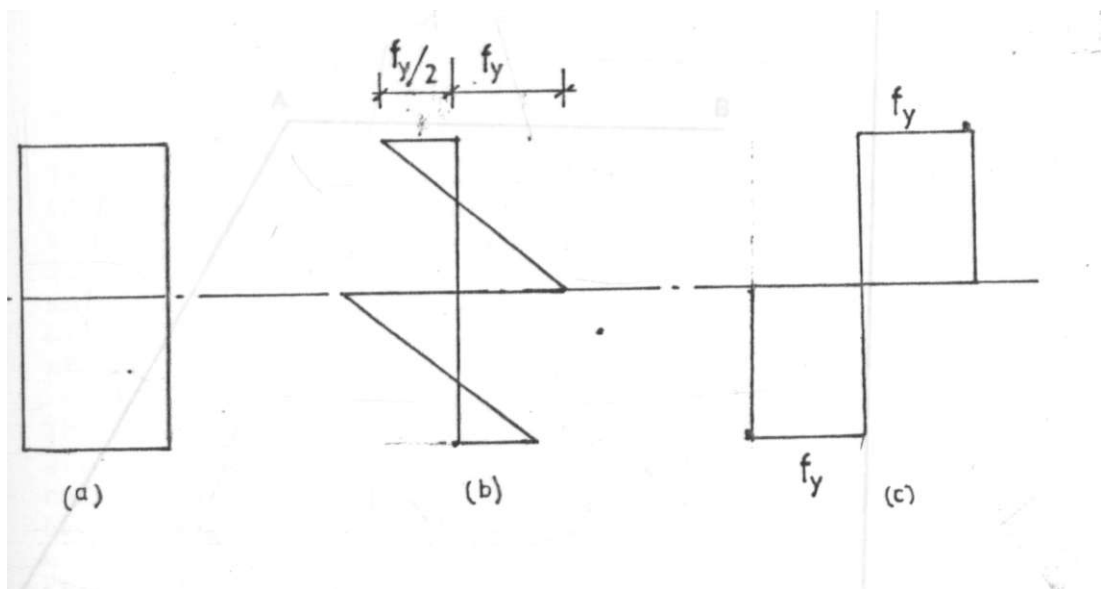


Figure 3.22 Residual stress distribution giving greatest elastic range in bending for a rectangular beam [37].



A

B

·4

STRAIN-

Figure 3.23 Idealised stress-strain curve for mild steel

The same stress distribution would also give the least curvature under any applied moment upto the full plastic moment, M_p .

Similar residual stress distribution giving reduced curvature under applied moments as compared with initially stress-free members can be derived for beams of any cross-section, the minimum attainable curvature at any moment being that corresponding to the elastic bending of a similar beam with a higher yield stress. [37],

3.3.3.5. Effects on plastic collapse load

For materials which can undergo pure plastic deformation after yield, it is possible to calculate the ultimate collapse load of a structure. The plastic theory is thus applicable to mild steel structures with an idealised stress-strain curve as shown in figure 3.23, which describes with sufficient accuracy the behaviour of steel upto a strain from 8 to 20 times the yield strain. If a state can be found for a structure under load satisfying the conditions of yield and the equilibrium, the structure would support the given loads, even though the application of such loads to the actual structure would act produce the state of stress stipulated.

The plastic collapse load is the highest for which such a state of stress can be derived. It follows then that residual stresses can have no effect on plastic collapse loads, be they small or large scale residual stresses. The main reason being that residual stresses have a negligible effect on the useful life of such structural systems under static loads. [37].

The insensitivity of ductile structural systems to residual stresses as far as ultimate load is concerned may be explained by reference to the redistribution of stress which occur when loads sufficient to cause local yielding are applied. To explain the phenomenon, let us consider a theoretical case of an I-beam with an initial residual stress, [figure 3.24]. The flanges, which each have an equal area to that of the web, have an initial tensile stress of $0.35y$, where y , is the material yield stress. The web has a uniform initial compressive stress of $0.66y$. As a bending moment is applied about an axis perpendicular to the web, yield first occurs in compression in the web. [figure 3.24 (b)], then in one of the flanges [figure 3.24 (c)], then in tension in the web [figure 3.24 (d)], and finally in compression in the remaining flange [figure 3.25 (e)]. At this stage, the stress distribution becomes

symmetrical and the beam goes on to develop the full plastic moment of resistance, [figure 3.25 (f)].

Thus residual stress have no effect on the plastic moment of the structure. This is exemplified by considering the stress-strain curves due to residual stress effects, [figure 3.21]. Both curves converge at the same value of yield stress, σ_y and this means that the plastic moment value, M_p is maintained. This is essentially because the theoretical build up is within the plane sections remain plane limits.

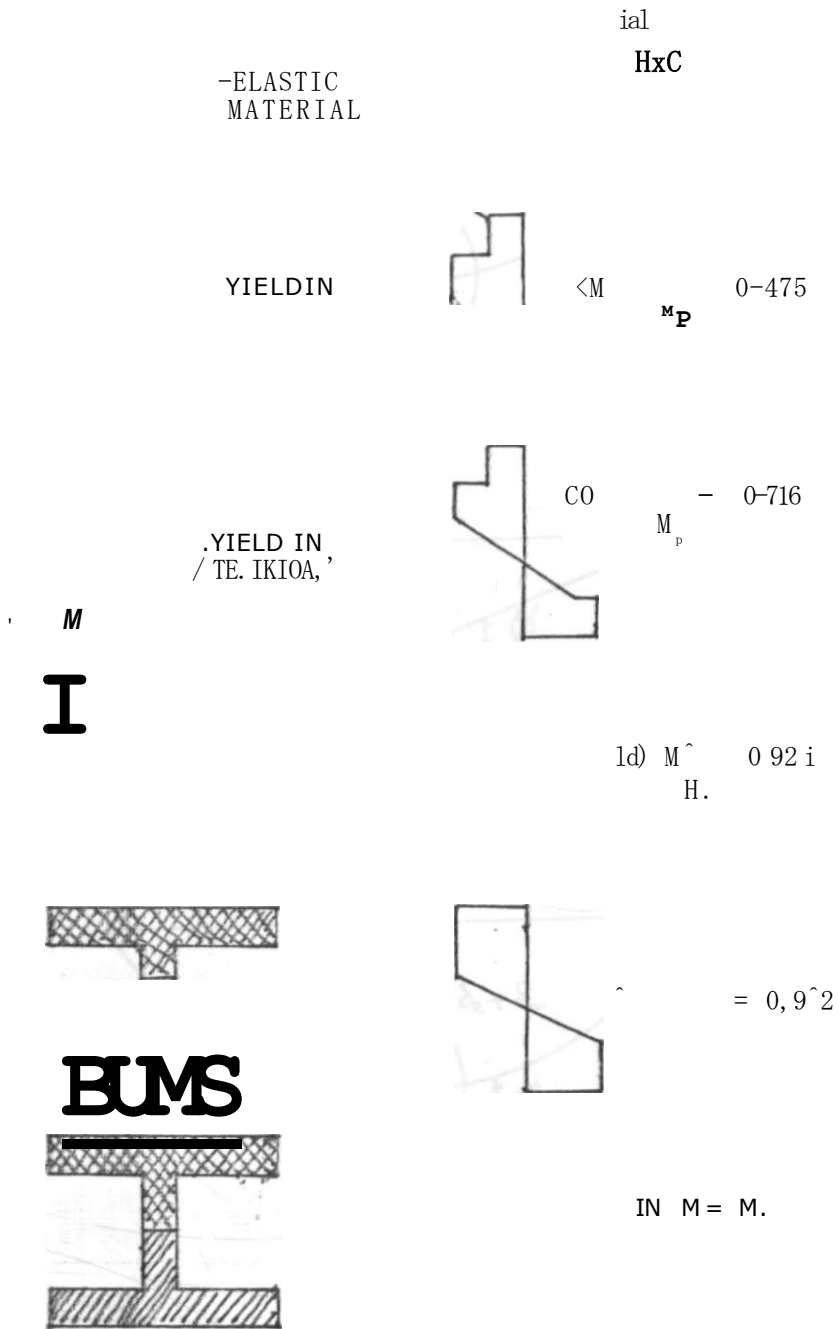


Figure 3.24 Development of plastic zones during the bending of an I beam with residual stresses [37]

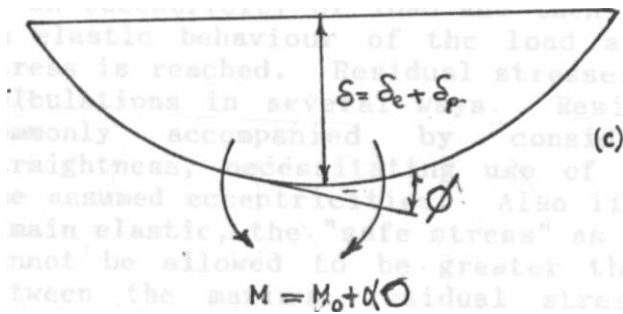
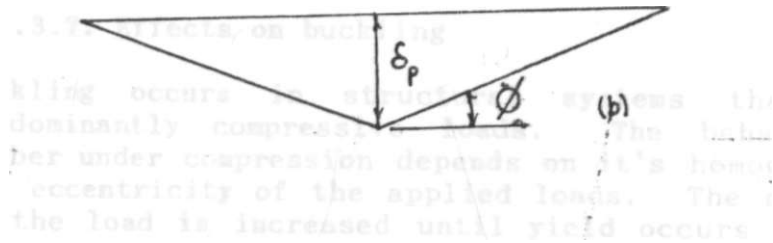
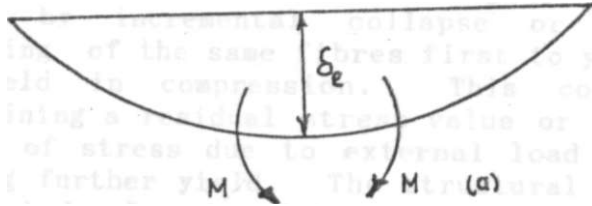


Figure 3.25 Total deformation of a simply supported beam.

- (a) elastic deformation
- (b) plastic deformation
- (c) total deformation

3.3.3.6. Effects on shake down loads

Complications do arise in structural systems when various load distributions are applied successively to the same structure. The alterations of load may not be sufficiently numerous to cause failure by fatigue, but may cause trouble either by incremental collapse or by the alteranate straining of the same fibres first to yield in tension then to yield in compression. This could be avoided by determining a residual stress value or state such that such change of stress due to external load could occur without causing further yield. The structural system is then said to "shakedown" under "shakedown loads". It is immaterial whether or not the stress state postulated could be reached in an actual structure, hence residual stresses have no effect on the theoretical shakedown load of ductile structural systems.[37].

3.3.3.7. Effects on buckling

Buckling occurs in structural systems that are under predominantly compressive loads. The behaviour of any member under compression depends on it's homogeneity and on the eccentricity of the applied loads. The member deforms as the load is increased until yield occurs at a critical section. Design formulae for compression members are derived by use of two basic approaches.[37].

- (i) Assumptions of either an initial lack of straightness or an eccentricity of load and then calculation, based on elastic behaviour of the load at which some safe stress is reached. Residual stresses will affect such calculations in several ways. Residual stresses are commonly accompanied by considerable lack of straightness, necessitating use of higher values for the assumed eccentricities. Also if the member is to remain elastic, the "safe stress" as usually calculated cannot be allowed to be greater than the difference between the maximum residual stress and the yield stress. As soon as the member begins to yield, the material has to be regarded as lacking homogeneity and very high lateral deflections may rapidly develop. Thus it becomes essential to assume a considerably increased eccentricity or initial lack of staightness.
- (ii) By use of the Shanley and Engesser loads. The Shanley load being that at which an initially straight axially loaded strut can first begin to assume an equilibrium deflected position, the deflection increase as the load itself is increased.

The Engesser load is that at which an initially straight axially loaded member could instantly assume a finite deflection without further increase of load. Experimental evidence based on these loads has shown that small scale residual stresses can cause decrease of at least 50% in the Shanley load and 32% in the Engesser load, while potential decrease due to large scale stresses are greater than these figures. [37].

Thus for flanged sections with initial residual stresses carrying compressive loads yielding of some parts earlier than the others, say the flanges, reduces the effective flexural rigidity of the member, which in turn influences the buckling load.

3.3.4. Effects of strain-hardening on behaviour of structural systems

The plastic theory for design and analysis of structural systems estimates the load at which collapse of a system takes place. When the system becomes a mechanism by formation of a sufficient number of hinges at which location rotation takes place without changing the value of the plastic moment, M_p . But this theory does not provide for determination of deflection at the collapse load, hence it was initially considered incomplete. Experimental evidence indicates that the collapse load gives a good estimate of the ultimate carrying capacity of a structural system. [30], But simple plastic theory which neglects strain hardening effects does not give a very good estimate of deflection near the ultimate carrying capacity of the structural system. A good agreement between the theory and experiment can be obtained if strain hardening is included.

The basic assumptions for including strain hardening is to replace the actual load deformation curve by a straight line until a lower plastic moment, M_0 is reached and by a polynomial for the non-linear and strain hardening range. Thus for any value of a moment $M > M_0$, the central deformation of a structural system is made up of two components namely:-

- (i) the elastic deformation, θ_e corresponding to moment M , and
- (ii) the post-elastic or plastic deformation, θ_p corresponding to a rigid body rotation of θ at the plastic hinge, [see figure 3.26]

The moment, M is also made up of two parts:-

- (i) the lower plastic moment M_0 , and

(ii) the strain hardening part which is assumed to be proportional to the relative rotation at the plastic hinge. Thus the moment can be expressed as

$$M = M_0 + \alpha \theta \dots \dots \dots [3.4]$$

where α = strain hardening factor

θ = the angle of rotation in radians, and

M and M_0 and α being in Knm units.

Thus when strain hardening effects are considered the implications on the overall structural system are:-

- (i) concept of plastic hinge is retained
- (ii) spread of plastic hinges along lengths if members is neglected , and
- (iii) the strain hardening factor α has the effect of a spring producing a moment, proportional to the rotation at the hinge. It is possible to use a more general relationship for the moment given by:-

$$M = M_0 + F(\alpha) \theta \dots \dots \dots [3.5]$$

Where $F(\theta)$ is any polynomial . This might be necessary for material such as reinforced concrete or aluminium alloys which do not exhibit definite strain hardening ranges. Home et al [39] and Sawko's [38] experimental investigation led to the conclusion that:-

- (i) the collapse load obtained by using strain-hardening concept did not differ much from that given by the simple plastic theory, however there was a marked difference in deflection.
- (ii) the concept of strain-hardening factors at elastic hinges is not limited to beams of grillages but can be applied equally well to structural frameworks. The concepts limitation to cases where discrete plastic hinges form at ends of members also applies to plastic theory.
- (iii) the strain-hardening theory can be directed toward deflections of the structure in the non-elastic state.

3.4 Design considerations.

The manner in which structural members are to be connected depends upon whether the fastening is to be permanent or detachable.

The connection so designed must be able to withstand service loads as well as ultimate loads. This calls for sufficient strength in the design thereby enabling the sustenance of the moments and shear forces being transferred between the members. The connection should also have adequate rotation capacity to allow redistribution of bending moments assumed in the analysis and stiffness must be such that the relative angles between the connected members is maintained during service. But while trying to satisfy the main design requirements for connections, the cost of fabrications is a criteria equally important as compared to strength, adequate rotation capacity and stiffness. This means the connection designed must be economical. A mechanically fastened connection will generally include the fastener, the connected parts and either components such as plates, angle cleats etc. Generally the size of the fastener will depend upon the space limitations of the connections, design load and the allowable stresses. For economy and compactness, it is general practice to space the fasteners as close as possible. This also reduces the amount of additional connection material required. Minimum spacings are stated in design specifications and they are based on the clearances of the tools required to install the fasteners and avoid local buckling of compressive members respectively.

3.4.1 Bolt types and sizes

Bolts are among the many types of fasteners employed in mechanically fastened connections. A bolt is defined as a metal pin with a head, formed at one end and the shank threaded at the other in order to receive a nut. [11] Structural bolts are used for joining pieces of metal by inserting them through holes and tightening the nut at the threaded ends. The bolts in common use are classified as follows:-

- (i) type of shank - either unfinished or turned.
- (ii) material and strength - ordinary structural bolt or high strength structural bolt.
- (iii) shape of head and nut square or hexagonal, regular or heavy, and
- (iv) pitch and fit of thread - standard, coarse or fine.

The structural bolts usually have square or hexagonal heads and are available in regular or heavy sizes. The nuts are also either square or hexagonal and available in heavy or hexagonal sizes.

Steel washers are used under the bolt head and the nut in order to distribute the clamping pressure on the bolt from bearing on the connected parts. For efficiency, the parts must be clamped tightly between the bolt head and the nut, figure 3.27 shows a typical bolt assembly.

The American and British system of classifying the types of bolts used in connecting structural systems are given below.

3.4.1.1 American classification system

The American classification system is based on the American Standards of Testing Materials [A.S.T.M]. The types of bolts are categorised as follows:- [34]

- (i) low carbon steel bolts and other fasteners ASTM A307, Grade A.
- (ii) high strength medium carbon steel bolts ASTM A325, plain finish, weathering steel finish or galvanised finish.
- (iii) Alloy steel bolts, ASTM A490.
- (iv) special types of high strength bolts, and other interference body bolts, swedge bolts and other externally threaded fasteners of nuts with special locking devices. ASTM 449 and ASTM A 354 Grade BD.

ASTM A307 bolts require no head markings other than the manufacturers identification mark to appear on the head of this bolt. They are also commonly made with both square and hexagonal heads with nuts to match. In application they are tightened to some axial force to prevent movement in the connected members in the axial direction of the bolt and prevent loosening of the nut. Because of small axial forces, little friction resistance is developed and in most cases the bolt will slip into bearing. [34] High strength bolts are heat treated by quenching and tempering. Most widely used are the ASTM A325 high strength medium carbon bolts and A490 alloy steel bolts. Both these bolts are heavy hexagonal structural bolts used with plain hardened washers and heavy hexagonal nuts.

Among the special types of fasteners or fastener components are the interference body bolts, swedge bolts and nuts with locking devices. The interference body bolt meets the strength requirements of the A325 bolt and has an axial ribbed shank that develops an interference fit in the hole and prevents excessive slip [34,21]. A swedge bolt [see figure 3.28] consists of a fastener pin from medium carbon steel and a locking collar of low carbon steel. The pin has a series of annular locking grooves, a break-neck groove and pull-grooves. [34].

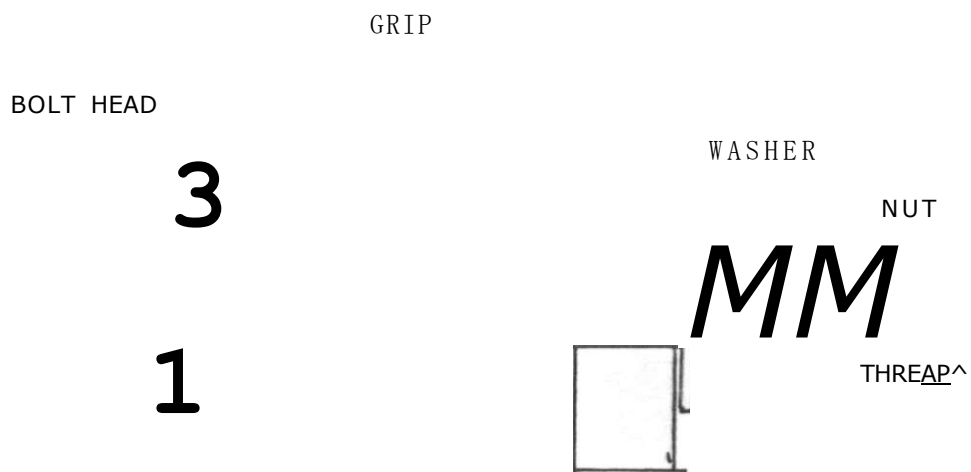


Figure 3.26 Typical bolt assembly. [21]

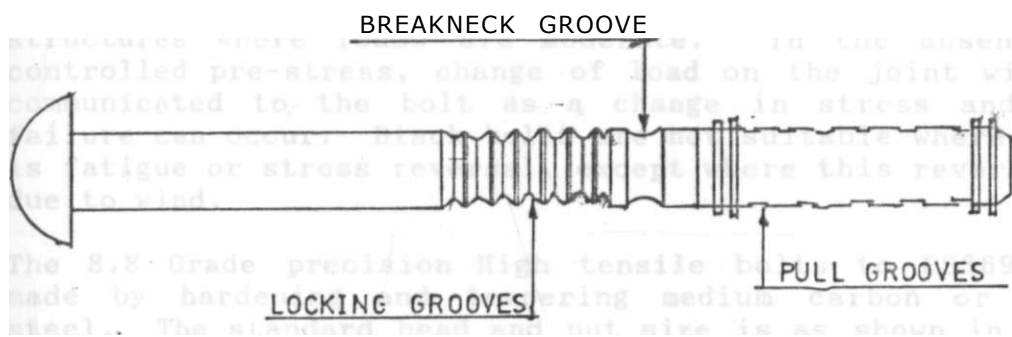


Figure 3.27 High tensile swedge bolt

3.4.1.2 British classification

The British classification system grades structural fasteners by their strength. There are two basic grades:- Grade 4.6 and Grade 8.8. The first figure is one tenth of the ultimate stress in N/mm and the second figure is one tenth of the percentage of the ratio of minimum yield stress to minimum ultimate. Thus "4.6 Grade" means the ultimate stress is 400 N/mm and the yield stress 60% of this. The bolts used in this system, together with the nuts and washers must comply with BS 4395 [40] dealing with high

strength friction grip bolts. Otherwise black bolts are commonly used, conforming to either BS 4190 [41 or BS 3692 [42}. The normal designation of the bolts includes [43]

- (i) general product description, e.g. high tensile or black, headshaped, bolts or nuts as appropriate.
- (ii) the nominal length in millimetre, if applicable.
- (iii) the number of appropriate BS e.g BS3892, BS4190 etc to which the fastener conforms.
- (iv) the strength grade symbol, and
- (v) details of the protective coating if required.

The 4.6 Grade bolts to BS4190 are general purpose mild steel fasteners which may be employed economically in lighter structures where loads are moderate. In the absence of controlled pre-stress, change of load on the joint will be communicated to the bolt as a change in stress and bolt failure can occur. Black bolts are not suitable where there is fatigue or stress reversal, except where this reversal is due to wind.

The 8.8 Grade precision High tensile bolts to BS3692 are made by hardening and tempering medium carbon or alloy steel. The standard head and nut size is as shown in Grade 4.6 bolts. The bolts are used in close tolerance holes. Due to the same reason as for Grade 4.6 bolts, Grade 8.8 bolts in clearance holes may not be used in fatigue or stress reversal conditions.

The High strength friction grip bolts to BS 4395 are applied when the load transfer modes are to be by friction and also to approximate rigid connection highly resistant to movement and fatigue. Some properties of the more commonly used bolts are shown in table 3.1

TABLE 3.1 GRADE 4.6 BLACK MILD STEEL ; AND GRADE 8.8 HIGH BOLTS AND NUTS-MECHANICAL PROPERTIES [43]

SIZE	TENSILE STRESS AREA (MM ²)	GRADE 4.6		GRADE 8.8	
		ULTIMATE LOAD (KN)	PROOF LOAD (KN)	ULTIMATE LOAD (KN)	PROOF LOAD (KN)
M6					
M8					
M10					
M12	84.3	33.1	18.7	66.2	48.1
M16	157	61.6	34.8	123	89.6
M20	245	96.1	54.3	192	140
M22	303	118.3	67.3	238	173
M24	353	138	78.2	277	201
M27	459	180	102	360	262
M30	561	220	124	439	321
M36	817	321	181	641	466
		Allowable stresses: (N/mm ²) Shear: 80 Bearing: 250 Tension: 120		Allowable stresses: (N/mm ²) Shear: 187 Bearing: 250 Tension: 280	

3.4.2 Behaviour of individual fasteners.

Connections are generally classified according to the manner of stressing the fastener, that is, tension, shear, combined tension and shear, rotation, or combinations of all the above stressing modes. The behaviour of a single bolt subjected to typical loading conditions of tension and shear is discussed below:

3.4.2.1 Bolts subjected to tension

Since the behaviour of an axially loaded bolt is governed by the performance of the threaded part, load-elongation

characteristics are more significant than the stress-strain curves of the fastener metal itself. [34,44] To determine the actual mechanical properties of a bolt, direct tensile tests of most sizes and lengths of full size bolts is necessary. There are two versions of these tests, namely:-

- (i) direct tension, and
- (ii) torqued tension test

In the latter test, as the torque is applied to the nut, the portion not resisted by friction between the nut and the gripped material is transmitted to the bolt. That due to friction between the bolt and the nut-threading, induces torsional stresses into the shank. This tightening procedure results in a combined tension-torsional stress condition in the bolt. Thus the load-elongation curves obtained in a torqued test differ from those of a direct tension test. Typical load-elongation curves for direct-tension as well as torqued tension tests are shown in figure 3.29.

A bolt loaded to failure in direct tension has more deformation capacity than that for a bolt failed in torqued tension. To determine whether specified tensile requirements are met, specifications require direct test on full size bolts. [43] Tests have illustrated that the actual tensile strengths of production bolts exceeds the minimum requirements considerably [34].



Figure 3.28 Load-elongation curves for bolts tested in:-
(a) direct tension (b) torqued tension

Loading a bolt in direct tension after pre-stressing by tightening the nut does not significantly decrease the ultimate tensile strength of the bolt, [see figure 3.30]

The torsional stresses induced by torquing the bolt apparently have negligible effect on the tensile strength of the bolt. This means that bolts installed by torquing can withstand or sustain direct tension loads without any apparent reduction in their ultimate tensile strength. Other investigations [34,44] indicate that within the elastic range, the elongation increases slightly with an increase in grip. As the load is increased beyond the elastic limit, the threaded portion which is of approximately uniform length behaves plastically while the shank remains essentially elastic. Hence when there is a specific amount of thread under the nut, grip length has little effect on the load-elongation relationship beyond the elastic limit. [34] For short bolts nearly all deformation occurs in the threaded length and causes a decrease in rotational capacity, since most of the elongation between the thread run out and the face of the nut will affect the load elongation relationship.

3.4.2.2 Bolts subjected to shear

The main objective of testing fasteners in shear is to investigate the effect of a number of variables such as bolt lengths, failure plane, mode of loading, grip and loading spans etc on the shear strength and deformation at ultimate load.



OEFOaWvAfiok-

Figure 3.29 Reserve tensile strength torqued bolts.

- (i) direct tension
- (ii) direct tension after 5/8 turn
- (iii) torqued tension. [34]

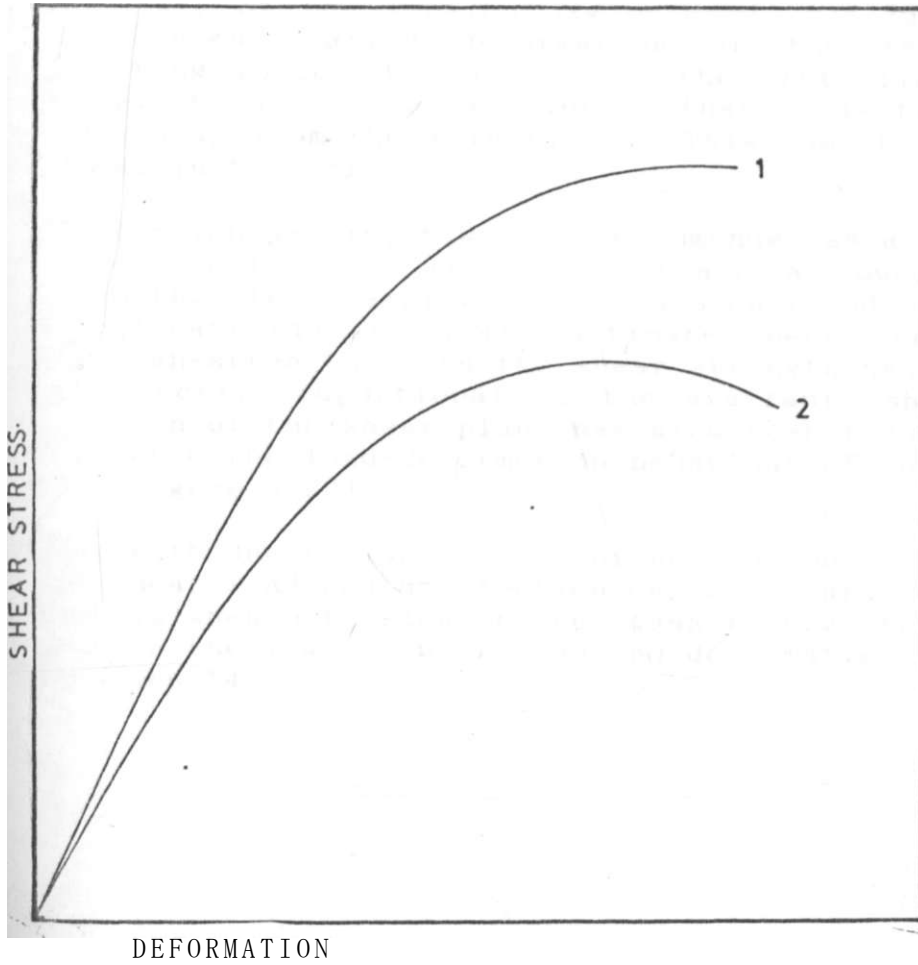


Figure 3.30 Typical shear deformation curves for bolts

(i) High strength bolts (ii) Mild steel bolts [34]

The second objective is to establishment of the complete load-deformation relationship of the fasteners. [34,45] deformation relationships are obtained by subjecting fasteners to shear induced by plates either in tension or compression. Figure 3.31 shows typical load-deformation curves for shear loading.

Generally an increase in tensile strength increases the shear strength with a slight decrease in deformation capacity [figure 3.30] The shear strength is also influenced by type of test. There are two basic tests, i.e. compressive and tensile. The tensile type of shear test exhibit lower shear strength values than the compressive type of tests, [see figure 3.31] The lower shear strength of a bolt observed in a tensile type test is as a result of lap plate prying action, a phenomenon that tends to bend the lap plate of the tension jig outward. [34,45] Because of the uneven bearing deformation of the test bolt, the resisting forces do not act at the centerline of the lap plate, which produces a movement that tends to bend the lap plate away from the main plate. This moment causes tensile forces in the bolt.

The tension jig is, however, recommended as a better testing device to be used so as to obtain a lower bound shear strength. The clamping force has been found [45] to have no significant effect on the ultimate shear strength, though for high-strength bolts the shear strength has been found to be directly proportional to the available shear area. The location of the shear plane has also been found to influence the load-deformation behaviour of the bolts, [see figure 3.32].

When both shear planes pass through the bolt shank the shear load and deformation capacity are maximised whereas when both shear planes pass through the threaded portion, the lowest shear load and deformation capacity are obtained. [45]

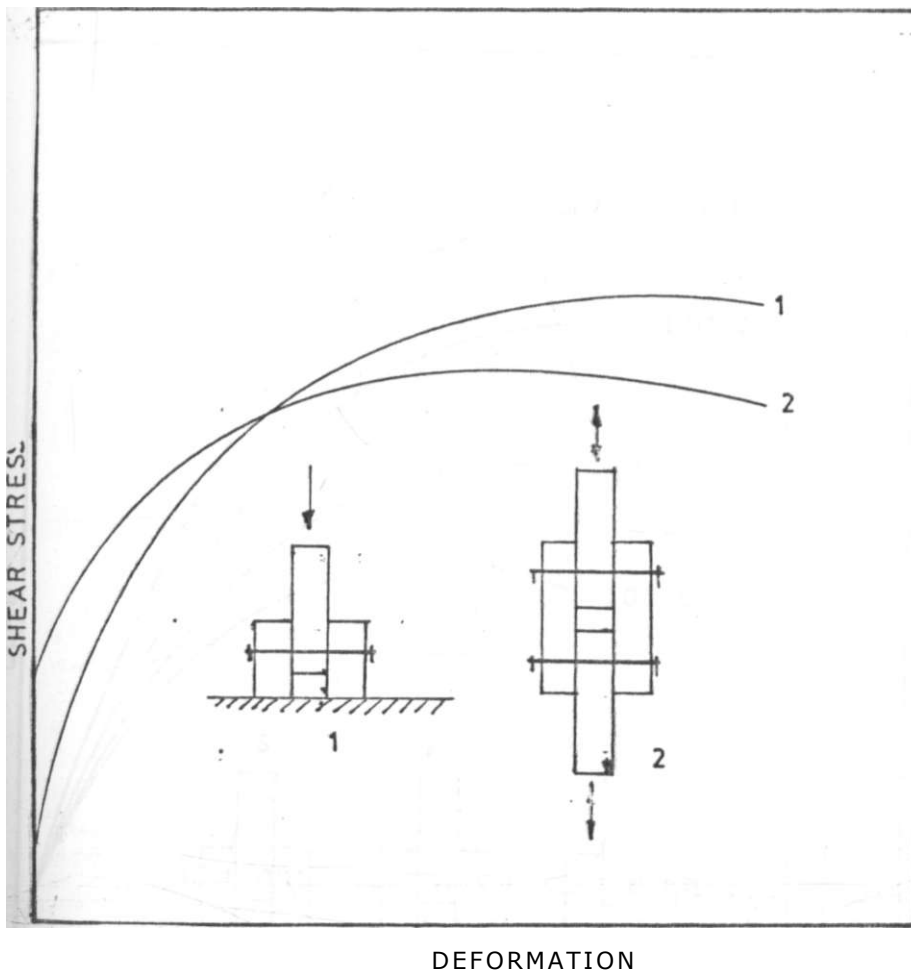


Figure 3.31 Typical shear deformation curves for
 (a) compression, and (b) tensile jigs. [34,45]

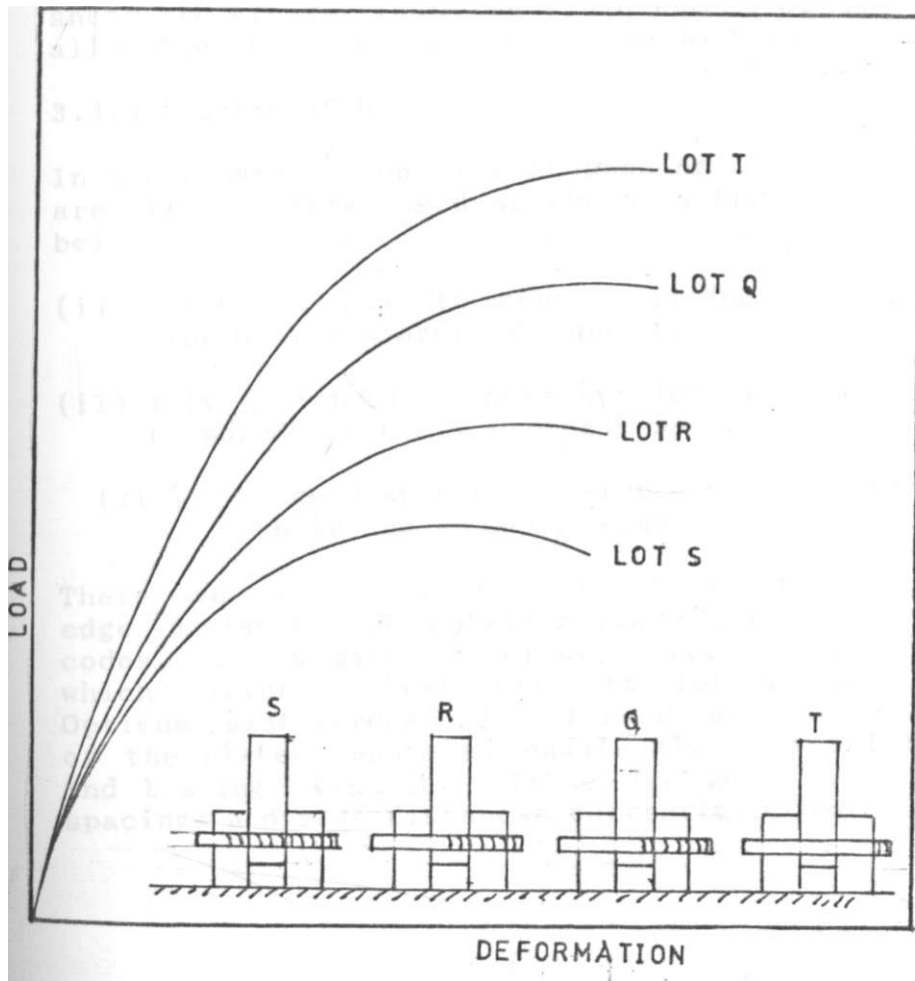


Figure 3.32 Shear deformation curves for different failure Planes [34,45]

3.4.2.3 Bearing properties

Bolts subjected to shear forces develop enclosed bearing stresses between the bolt and the plate as shown in figure 3.18. The real distribution of bearing stresses is non-uniform for a bolt in double shear [figure 3.18 (b)], but this is too complicated for design and the uniform distribution of figure 3.18 (c) is assumed.

Bahia and Martin [45] determined an experimental relationship between average bearing stress and deformation for a bolt failing in single shear. The schematic representation is shown in figure 3.33. The higher the bearing stresses, the greater the elongation of the bolt hole. The bearing stresses at failure of the bolt in single shear are greater than the yield stress of the plate, hence allowable stresses normally are of high values.

3.4.3 Spacing of bolts

In the consideration of bolt spacing in a connection, there are standard terms used as shown in figure 3.34 and defined below.

- (i) pitch:- centre to centre spacing of fasteners along length of a member of connection.
- (ii) bolt distance:- centre spacing of staggered fasteners measured obliquely on the member.
- (iii) edge distance:- distance between centre of bolt hole and adjacent edge of plate.

There are some limitations based on net section area, A_n , edge distance and construction clearance in the design codes. For a given material, there is an optimum spacing which yields highest strength for a particular joint. Optimum joint strength is achieved when the tensile strength of the plates connected equals the combined bolt shearing and bearing strength. Table 3.2 shows the standard bolt spacings and edge distances currently in use.

TABLE 3.2 STANDARD END-DISTANCE FOR VARIOUS HOLE SIZES

DISTANCE TO SHEARED END OR HAND FLAME CUT EDGE			DISTANCE TO ROLLED MACHINE FLAME CUT. SAWN OR PLNED EDGE (MM)	
DIAMETER OF HOLE	(a)	(b)	(a)	(b)
39	68	117	62	117
36	62	108	56	108
33	56	99	50	99
30	50	90	44	90
26	42	78	36	78
24	38	72	32	72
22	34	66	30	66
20	30	60	28	60
18	28	54	26	54
16	26	48	24	48
14	24	42	22	42
12 or less	22	36	20	36

(a) British

(b) American

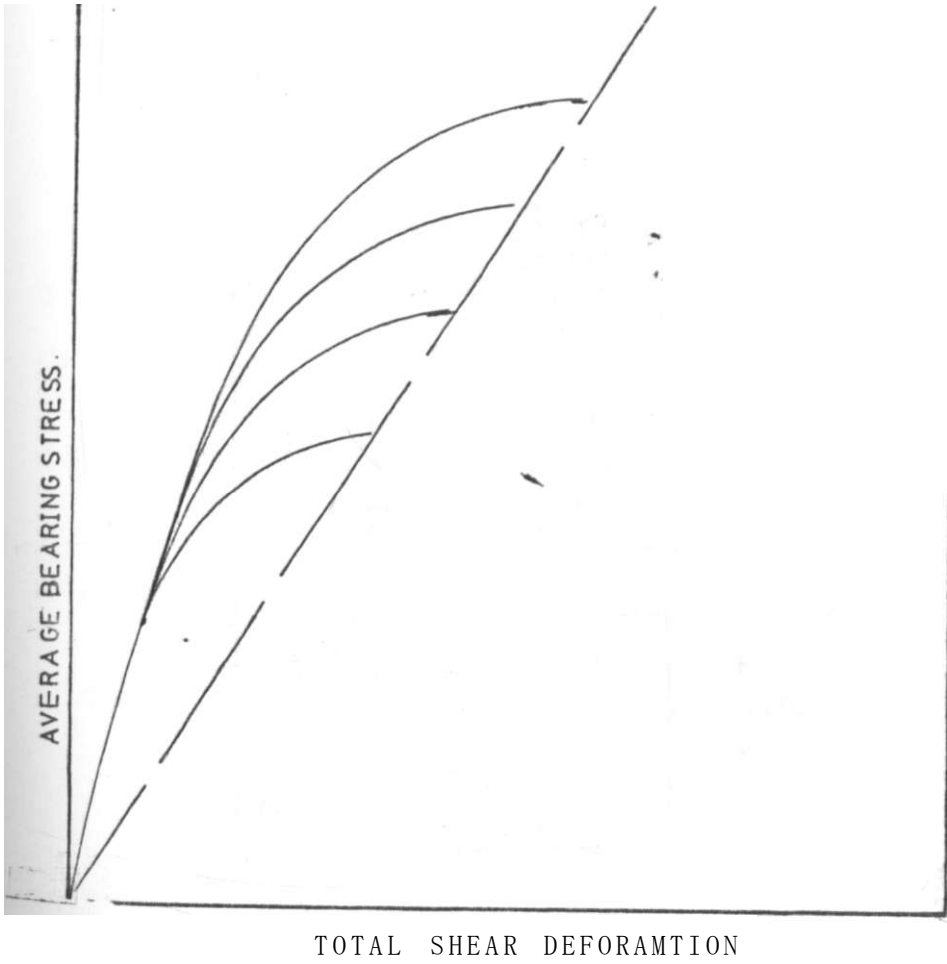
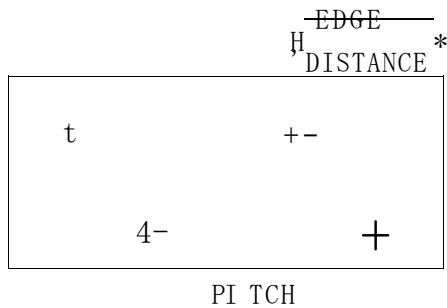
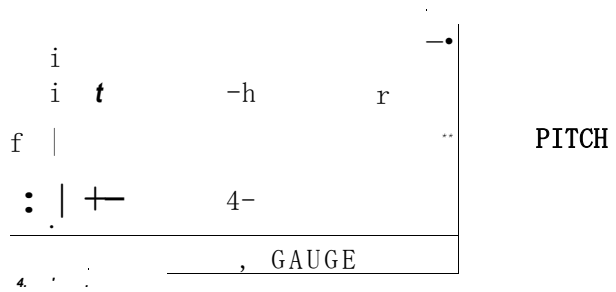


Figure 3.33 Relationship between bearing stress and deformation for tensile type shear.



17

GAUGE



t.

Figure 3.34 Bolt spacing (a) staggered (b) rectangular hole pattern [21,34]

There are two edge distances considered in bolted connections namely:-

- (i) perpendicular to line of stress, i.e unloaded edge distance, e_1 , and
- (ii) loaded edge distance, e_2 . [see figure 3.35]
 The edge distances e_1 , is needed to prevent premature yielding at the unloaded edge B. Under load and with e_2 inadequate shearing and normal stress will be induced in the plates [21]. If e_2 is inadequate, yielding may develop along lines at an angle diameter to the line of loading. This causes excessive distortion in the hole and premature failure. A value of e_2 needed to prevent tear-out when edge off plate fails is normally taken as: [8]

$$e = 2D \dots \dots \dots [3.6]$$

Where D is the bolt hole diameter.

3.4.4. Use of washers.

Originally, washers were thought necessary to bolting practice to serve the following purposes:- [34]

- (i) to protect the outer surface of the connected material from damage or galling as the bolt or nut was torqued or turned,
- (ii) provide surfaces of consistent hardness so that corrosion in the torque-tension relationship could be maintained.

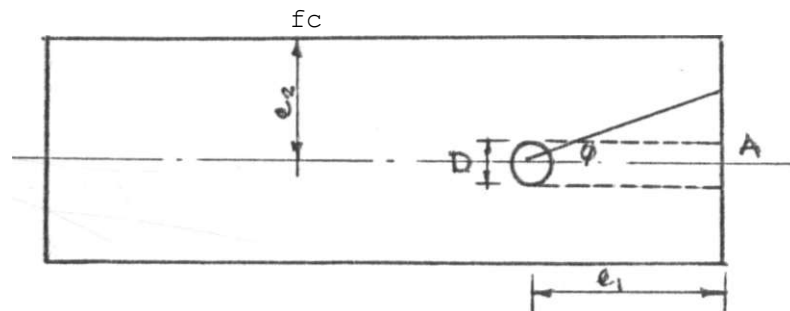


Figure 3.36 Edge distance to prevent shear out failures. [34]

When the turn-of nut method of tightening bolts was adopted reliance upon torque-tension to determine required bolt tension was reduced. Investigations [34] showed that hardness washers were not required, though they are still used mainly to off-set lack of parrallelism especially for sloping members and distribute clamping forces uniformly.

CHAPTER FOUR
MATHEMATICAL MODELLING OF SEMI-RIGID
CONNECTIONS.

INTRODUCTION.

Since the realization that fully pinned connections do possess some rotational stiffness and that fully rigid connections have some degree of flexibility, the concept of semi-rigid restraints in structural systems has been increasingly researched upon. The total study has been divided into two separate but related areas:- analytical and experimental. The main emphasis has been on the analytical effort with the results of the experimental portions being used for verification of the analytical results. In order for the knowledge derived from such studies to be useful to structural analysts, there is need to have fairly accurate methods of mathematically describing the connection behaviour, namely mathematical modelling.

The use of mathematical modelling though convenient, presents some limitations in describing natural phenomena. There will always be errors between the predicted results and the experimentally measured results. This is mainly because mathematical models are idealisations using the techniques of constructed logic, not necessarily natural and certainly not complete. In addition, in order to properly analyse the experimental results, there is need to employ specific mathematical techniques. This enables the presentation of logical comparative conclusions. Such special techniques exist for structural systems as well as for structural components.

4.2 Behaviour of structural systems

Structural systems respond to loads in their own unique ways. These responses may be linear with respect to geometry and elastic or inelastic with respect to the material-properties. The ability to predict this response of behaviour enables proper analysis of the structural systems and hence proper design. Most structural engineering analysis is based on linear elastic mechanics. The concepts involved are straight forward and enable prediction of behaviour of even highly indeterminate systems. Before analysis of structural systems is made, there is need to formulate appropriate mathematical models. Such models ought to be in line with true structural behaviour as concerns material properties, Loading modes and envisaged displacements. Real life physical aspects of any structure are important when it comes to proper matching of the mathematical model and actual structural system behaviour.

Most aspects of structural behaviour are related to experimental evidence. Analysis, and in particular comparison of analytical results with experimental evidence is an important tool of understanding structural behaviour at all functional levels. Overall the structural behaviour of any system is dependent on the behaviour of the components. These behaviour modes have been found to be more dependent on the type of structural connections used than on the individual members.[35].

4.2.1 Behaviour of bolted connections

The behaviour of connections in structural steelworks is a function of the geometric configurations of the connected members, the type of fasteners used, and the ductility of the steel. Two major classes of fasteners are utilised in modern steel construction:- welds and bolts. Bolted connections depend on the transfer of load from one part to another through the fastener, which passes through holes drilled or punched in the individual parts or by friction across the clamped surface. In welded connections the parts are fused together by acetylene or arc welding, normally with the addition of some weld metal in the connection.

Actual design of the connection is a specialised operation making considerable use of empirical rules derived from extensive testing programmes. Some of these empirical relations have been discussed in chapter 3.

This research deals with bolted connections whose behaviour has been described as complex and is not well understood. The complex nature of their structural behaviour makes their structural analysis even more difficult. This arises mainly due to the following reasons:-{29]

- (i) the connection is made up of a number of small components e.g. bolts, nuts, washers etc
- (ii) the bending spans between the fasteners and the connected parts are of the same order of magnitude as, and often smaller than the thickness of the connected parts.
- (iii) details such as bolt heads have a great stiffening influence on the total deformation pattern.
- (iv) the forces and reactions on the connected parts or building elements disperse out through it's thicknesses considerably smoothing cut the moment and stress variations.

- (v) the forces are applied and the reactions are developed in more than one plane, introducing biaxial bending.
- (vi) pre-tensioned bolts compress the plate around them and tend to curl surrounding regions away from the support and
- (vii) the contact regions between the plates and their supports vary with changing load conditions and cannot be precisely predicted.

The factors mentioned above make the connections response basically and intrinsically non-linear. This happens even when all the components remain stressed within their elastic limits. Also the large number of variables to be dealt with make a quantitative description of the behaviour of the connections even more difficult. But with idealisations, an attempt at describing the behaviour can be made and the results obtained would be applied in the analysis of structural systems.

4.3. Analysis of structural systems

Structural analysis is normally carried out in order to determine the internal forces and often the failure loads of a system. Knowledge of these quantities and the properties of the material in the structure can be used to make designs with sensible margins of safety. Like good design, good analysis is based on the accurate predictions of the behaviour of the structure under service conditions. Accuracy also comes up when idealising structural systems for purposes of analysis. The large number of assumptions made in structural idealization erodes the true accuracy achieved in subsequent calculations. Even then, not all structure's can be analysed accurately because some are so complex and render available analytical methods inadequate. Though the evolution of complex structural systems seemed to have been overtaking the analytical capabilities, introduction of computer-aided analysis has made possible the analysis of highly non-linear structural systems.

4.3.1 Analysis of elastic framed structures

Joints of framed structures are usually idealised as either fully pinned or fully rigid. However, the connections themselves may have significant degree of stiffness and flexibility which is important in the analysis of the frameworks. Such connections may be assumed to be either linearly elastic or non-linearly elastic in behaviour. The connections used are chosen according to the relative translations and rotations which can occur at the joints of the structure.

Such connections which may either be welded or bolted are assumed to be elastic. Early attempts at analysing semi-rigidly connected frames were useful in only a few simple cases. [49]

Later on matrix methods, assuming linear connections behaviour were employed. Essentially the method is used in the determination of the structural displacements, $\{6\}$, and the forces, $\{F\}$, under loads causing fixed-end forces $\{FEM\}$. In linear elastic frames, the analysis is accompanied by solving the following equation.

$$\{F\} = \{FEM\} + [KE] \{6\} \quad .. \quad [4.1]$$

and

$$\{F\} = \{ks\} \{6s\} \quad [4.2]$$

Where

$\{F\}$ is the applied load vector

$\{FEM\}$ is the fixed end member force vector

$[KE]$ is the plane beam member stiffness matrix

[see fig. 4.1 (b)]

$\{6E\}$ is the member end displacement vector without elastic end restraints.

$\{ks\}$ is the elastic member end spring stiffness matrix [see fig. 4.2]

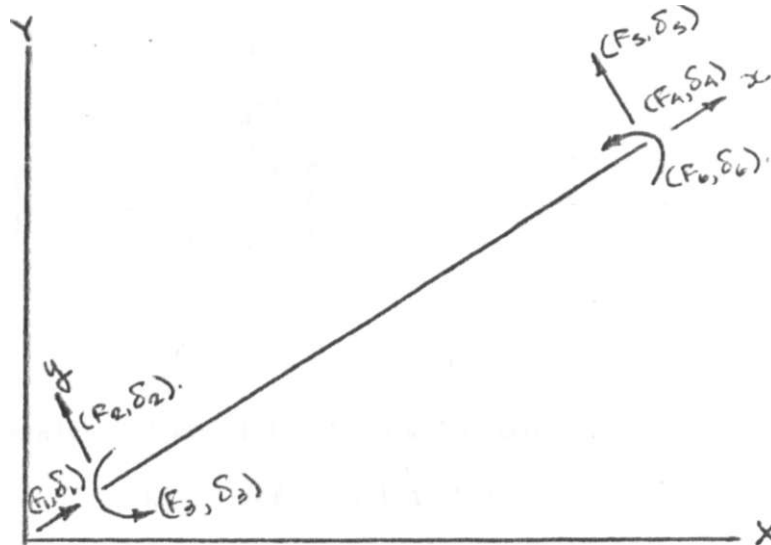
$\{6s\}$ is the member end displacement vector due to the presence of elastic member end connections.

The total member end displacement $\{a^{\wedge}\}$ are obtained thus:-

$$\{6_t\} = \{6_e\} + \{6_s\} \dots \dots \dots [4.3]$$

A typical beam element modelling is shown in figure 4.1 (a) with the ends subjected to axial, shearing and bending forces. These forces correspond to three degrees of freedom. The relationship between member end forces, $\{F\}$, as a function of fixed-end member forces, $\{FEM\}$ and end displacements $\{6E\}$ is indicated in equation 4.1. The corresponding stiffness matrix, $[KE]$ is presented in figure 4.1 (b) as a 6x6 matrix. If the nodes on the beam element are modelled as flexible matrix connections using linear elastic springs, a stiffness matrix $\{ks\}$, can be represented as in figure 4.2 (b). [30]

In non-linear analysis, element stiffness matrices, $[KE]$ and structure stiffness matrix $[k]$ may vary as functions of load and loading history. These variations may be analysed by the use of iterative techniques, the non-linear can be incorporated into already existing linear techniques in order to evaluate systems subjected to specific design loads. There are a wide range of such iterative techniques some of which are readily adopted to computer analysis [49] and are considered in section 4.4

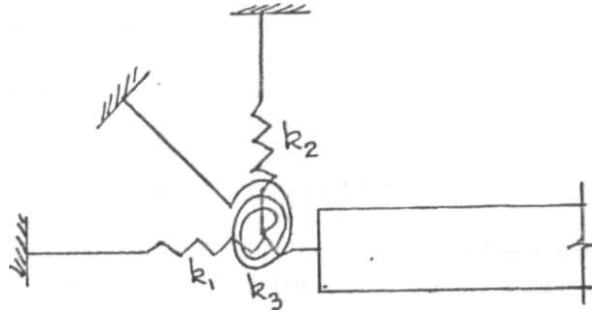


(a) Bar element in load and global co-ordinate systems.

$$kE = \begin{bmatrix} sa & 0 & 0 & -Sa & 0 & 0 \\ 0 & 12S_w/L^* & 6S_b/L & 0 & -12S_w/r & 6S_w/L \\ 0 & 6S_w/L & 4S_b & 0 & -6S_w'L & 2S_k \\ -Sa & 0 & 0 & Sa & 0 & 0 \\ 0 & -12S_b/L^* & -6S_b/L & 0 & 12S_w/L^* & -6S_b/L \\ 0 & 6S_b/L & 2S_v & 0 & -6S_b/L & 4S_v \end{bmatrix}$$

(b) stiffness matrix $I_b^b = EI/L$ $S_a = EA/L$

Figure 4.1 Member stiffness matrix for beam element [30]



(a) Analytical model for beam with semi-rigid connection

k_1 - axial spring stiffness

k_2 - transverse spring stiffness

k_3 - rotational spring stiffness

$$\begin{pmatrix}
 k_1 & 0 & 0 & -k_1 & 0 & 0 \\
 0 & k_2 & 0 & 0 & -k_2 & 0 \\
 0 & 0 & k_3 & 0 & 0 & -k_3 \\
 -k_1 & 0 & 0 & k_1 & 0 & 0 \\
 0 & -k_2 & 0 & 0 & k_2 & 0 \\
 0 & 0 & -k_3 & 0 & 0 & k_3
 \end{pmatrix}$$

(b) Joint element spring stiffness

Figure 4.2 Semi-rigid joint element [30]

4.3.2 Analysis of semi-rigid connections,

The analysis of semi-rigidly connected or bolted members is analogous to that of a haunched beam with rigid connections. [50.51] Despite the problems associated with the analysis of bolted connections., two analytical methods are commonly used namely:-

- (i) the slope deflection method, and
- (ii) the cross method

4.3.2.1 The slope deflection method

The application of the slope deflection method requires use of a factor, Z in conjunction with given values of modulus of Elasticity, E and moment of Inertia, I . [51] The factor, Z is normally referred to as the semi-rigid connection factor. Under load, semi-rigid connections undergo rotation and when yielding of some part occurs, there is additional angle change denoted by θ . For a beam to column connection this is defined as the additional rotation of the end of the beam over that of the column. The value of θ is a function of end moment, M increasing with it. The rate of change depends upon the stiffness or rigidity of the semi-rigid connection and is a unique value for every connection. Thus Z is defined in terms of θ and M as [52]:-

$$Z = \theta/M \dots \dots \dots [4.4]$$

The functional relationship between Z , θ and M is shown in figure 4.3. The connection factor, varies inversely with the rigidity of the semi-rigid connections becoming zero for a rigid connection and infinity for a pinned connection. The reciprocal of this factor is the slope of the moment rotation curve, [see figure 4.4.]

Before analysis of any connection can take place, Z must be determined either by moment-rotation relationship or computed by standard formulae. From figure 4.4 it is seen that the value of Z varies, and for a given moment capacity which a connection can withstand, there is an unique value of Z . This relation is shown in curve (a) of figure 4.4 curves (b) and (c) show the region of variation in which there exists acceptable values of Z . It is between these limiting curves that the design range of the connection

The permissible variation of Z is normally tabulated in design standards [50.52]. Curve (d) is for rigid connections. By definition there is no rotation at a rigid connection when a moment is applied. This implies that the intersection lines of the connected members do not undergo any change in their orientation. Curve (e) is for the fully pinned connection which by definition undergoes infinite rotation under infinitesimally small moments. In the application of the slope deflection method, the sign convention adopted is such that when the column connection twists in a clockwise direction on the end of the beam, the moment at the end of the beam is positive and vice versa.

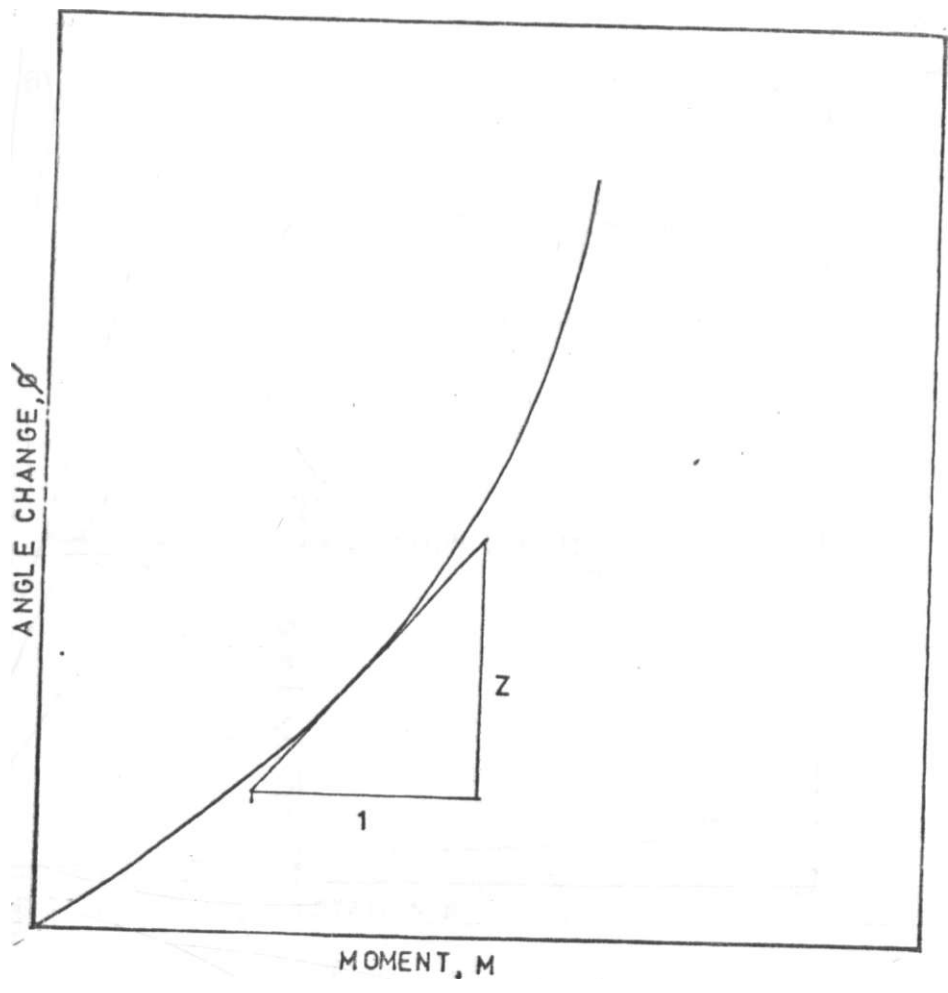


Figure 4.3 Functional relationship for connection factor Z

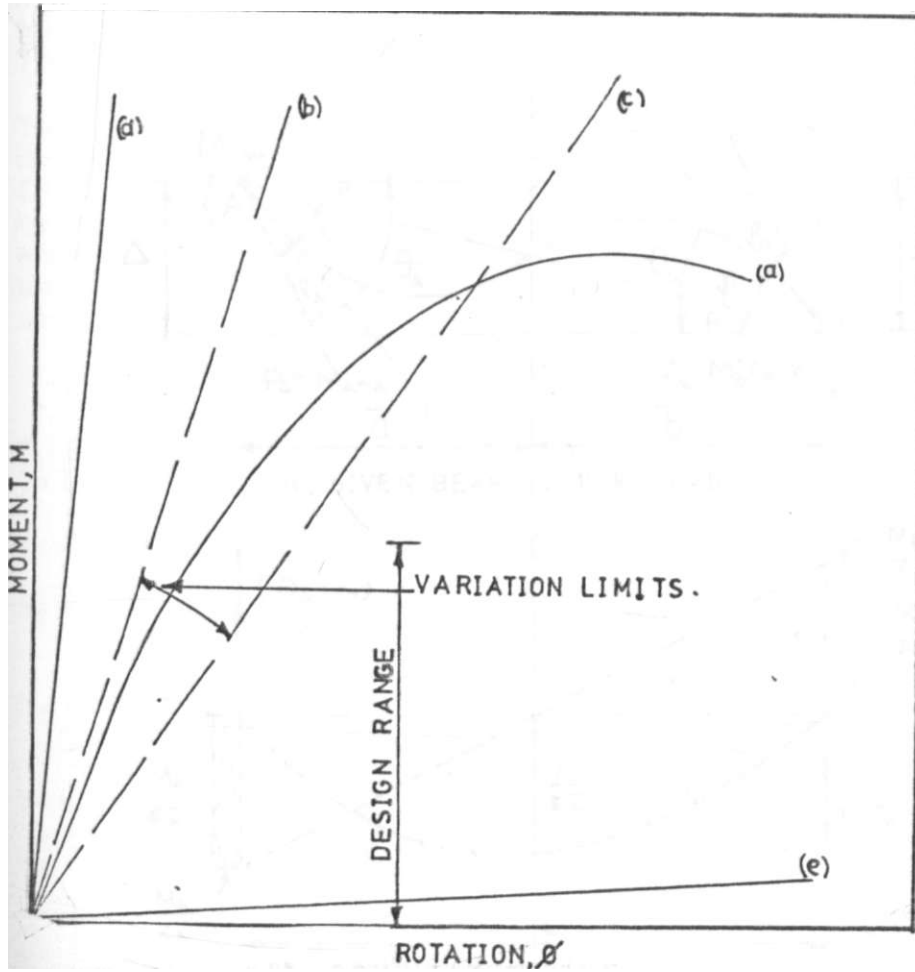


Figure 4.4 M- θ curves for semi-rigid connections (a) test behaviour of specimen, (b) tangent slope at origin = $1/Z$, (c) minimum permissible slope, (d) M- θ for rigid connection, $Z = \infty$, (e) M- θ for pinned connection, $Z = 0$ [52]

LOADING

^ t t t T T T T T J I T T T T T N

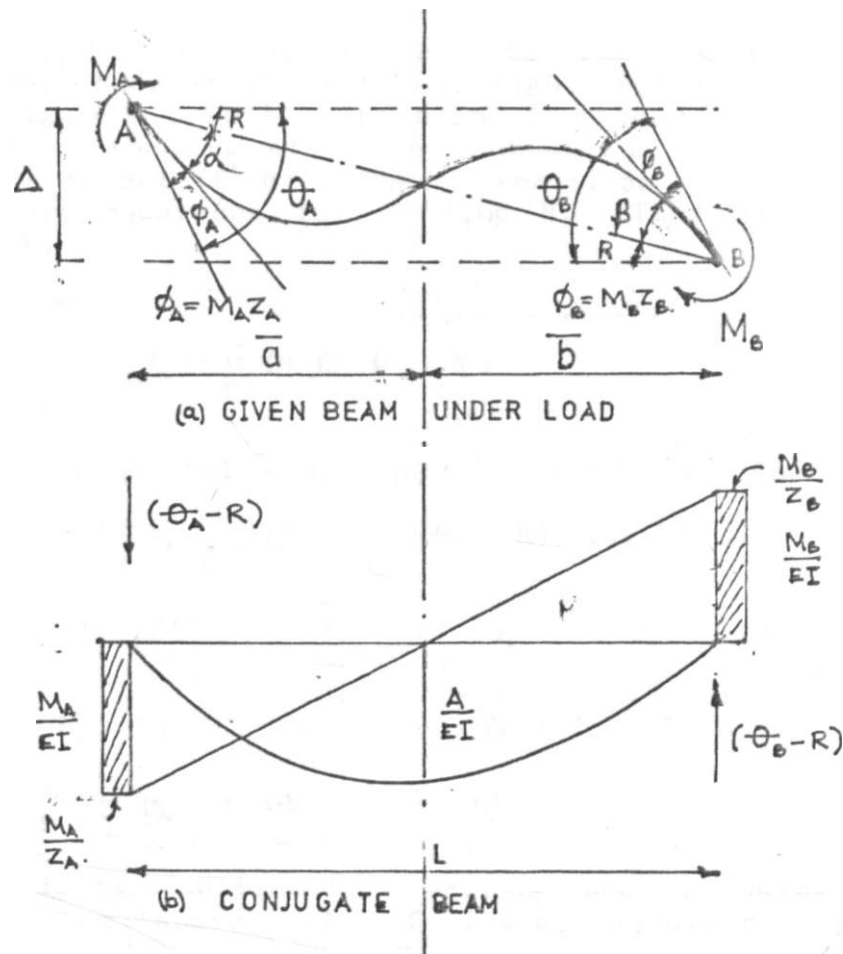


Figure 4.5 Conjugate beam method for semi-rigid connections [3, 5, 2]

The conjugate beam method is utilised in order to obtain the required relationship between moment, M , rotation, θ , the span of connected members, L and the angle of relative deflections, R . [see figure 4.5], Based on the sign convention mentioned above and referring to figure 4.5 (a), it is seen that moment at both ends of the beam are positive. Figure 4.5 (a), represents the total angle between the tangent to the end of the loaded beam and its original direction (before loading). Included in θ is the relative angle of deflection, R which is as a result of the relative deflections of the two ends of the beam. Also included are θ_A, θ_B and θ . θ represents the deviation of the tangent from the origin to the relative deflection line. The net end slope of the loaded beam, therefore is $(\theta - R)$.

Thus $(OJ - R)$ and $(6\theta - R)$ are the end reactions of the conjugate beam at the left and right supports respectively, [see figure 4.5 (b)]. These end reactions can be evaluated by taking the sum of moments about B to get $(G\theta - R)$ and about A to get $(Q\theta - R)$. These summations give rise to two necessary equations for finding M . Thus taking moments about B :-

$$M_B = 0 \dots \dots \dots [4.5]$$

$$M_B = 2M_A + 6EI \frac{M_A Z}{L} - \frac{6AB}{L} - \frac{6EI}{L} (\theta - R) \dots \dots [4.7]$$

From which the following equations can be obtained.

$$M_B = 2M_A + 6EI \frac{M_A Z}{L} - \frac{6AB}{L} - \frac{6EI}{L} (\theta - R) \dots \dots [4.7]$$

$$M_A = 2M_B \cdot \frac{(L+3EIZ)}{L} - 6Aj - \frac{6EI}{L} (\theta - R) \dots \dots [4.7] (b)$$

Setting $L_a = L+3EIZ_a$, we obtain from Eq 4.7 (b)

$$M_B = \frac{2M_A L_a}{L} - \frac{6EI}{L} (\theta - R) \dots \dots [4.8]$$

Similarly by setting $L_b = L+3EIZ_b$, and following the same process as above, the following equation for M_A is obtained:-

$$M_A = 2M_B \frac{L_b}{L} - \frac{6EI}{L} (\theta - R) + M_i \frac{\dots}{L} [4.9]$$

In equations [4.8] and [4.9], A represents the area of the M/EI diagram, whereas a and b are the centroids of

the M/EI diagram from the left and right hand sides respectively. [52, 53].

Equations [4.8] and [4.9] may be solved simultaneously by the method of substitution to obtain the required slope deflection equation, i.e

$$M_h = \frac{6EI}{4L_a L_e - 1} \left[\frac{2L_e}{L} (\xi_e - R) + L \left(\frac{6}{L} \xi_a - R \right) - \frac{6A}{L} \frac{2bL}{4L_a L_e - 1} \right] \dots [4.10]$$

and

$$M_b = 6EI \left[\frac{2L_e}{L} (\xi_e - R) + L \left(\frac{6}{L} \xi_a - R \right) + \frac{6A}{L} \frac{2aL - bL}{4L_a L_e - 1} \right] \dots (4, 31)$$

The equations derived above show that a change of end connection behaviour from rigid to semi-rigid is equivalent to lengthening the member span by 3EIZ. The effects at the restrained ends consists of the following contributory sources: [3]

- (i) fixed end moments
- (ii) rotation at member ends, and
- (iii) relative displacement at member ends, R

The semi-rigid connection factor, Z also contributes to the end moment effects. This last element is interdependent on the preceding three sources. For this reason, it is not possible to apply the method of superposition in deriving the force and displacement relationships which is the customary procedure for the case of rigid connections. [3].

4.3.2.2 The cross method

The application of this method to semi-rigidly connected systems is similar to that for rigidly connected systems with corrections in:- [52]

- (i) the fixed end moments
- (ii) the stiffness or redistribution factors, and
- (iii) the carryover factor.

All these factors can be determined by the slope deflection method. In case of rigid connections, nothing yields under load and the true fixed end moment is distributed about the end joints. In the fixed end for semi-rigid joints, nothing yields except the connection itself. As a result, the fixed

end moment is reduced somewhat below that of a rigid connection with the same loading, [see figures 3.2, 3.3 and 3.4]. Thus for any beam AB [see figure 4.6] connected at the ends in a semi-rigid manner, the fixed moments are given as:-

$$FEM_a = \pm \frac{6A (2b''L_j - a\tilde{L})}{L(4L_a L_b - L)} \quad [4.12]$$

and

$$FEM_b = + \frac{-6A(2a'L_j - bL)}{L(4L_a L_b - L)} \quad [4.13]$$

Where FEM denotes fixed end moments and the other symbols have the same meaning as in section 4.3.2.1.

The stiffness or distribution factor is a function of the properties of the connection as well as of the connected members in a semi-rigidly connected element or member. In practice some of the connections may be rigid and others semi-rigid as shown in figure 4.6. By statics and by referring to figure 4.6.

$$M_{ab} + MAC = 0 \quad [4.14]$$

For the given conditions of loading and restraints, we obtain:-

$$4EI_{AC} \frac{\Delta}{L_{ac}} = r6EI_{Afc} \frac{\Delta}{4L_a L_b - L} \quad [4.15]$$

$$(4E-9) \frac{I_{AC}}{L_{ac}} = \frac{-(4E3t) 3L}{4L_a L_b - L} \frac{I_{ae}}{L_{AB}} \quad [4.16]$$

Dividing through by the common term, $\left(\frac{\Delta}{L_{ac}} \right)$, it is evident that, since $\frac{I_{ae}}{L_{AB}}$ is the relative distribution factor for the A end of the rigidly connected member AC, then the distribution factor for the semi-rigidly connected AB is $\frac{3L I_{ae}}{4L_a L_b - L} \frac{I_{ae}}{L_{AB}}$. As mentioned in section 4.3.2.1 $LA = E + zj$ and $LB = L + Z$

thus for a given member AB,, the distribution factors (D.F) are given by:-

$$D.F_{ab} = \frac{3L I_{ae}}{4L_a L_b - L} \frac{I_{ae}}{L_{AB}} \quad [4.17]$$

and

$$D.F_{AE} = -A \frac{zj}{4L_a L_{fi} - L}$$

The carry over factors for member AB, semi-rigidly connected are given as:-

$$\text{Carryover factor A to B} = L/2L_g \quad [4.19]$$

$$\text{Carryover factor B to A} = L/2L^{\wedge} \quad [4.10]$$

But $L_A = L + 3EI Z_s$, and $L_B = L + 3EI Z_E$, thus for rigidly connected members $Z = 0$, and equations [4.19] and [4.20] reduce to 1/2. [52]

4.4 Analysis of load-deformation curves.

4.4.1 Linear elastic analysis

This technique is applied to structural systems subjected to proportionally increasing quasistatic loading. Loading patterns which may cause cyclic or incremental collapse phenomena are not considered. This assumption is widely used in performing analysis of structural systems and may thus be appropriate for the loading carried by semi-rigid connections, exhibiting non-linear loading deformation responses.

Linear elastic tangent techniques in which the load increments are proportional to the observed deformation can be employed. These techniques become inappropriate when the behaviour of the structural system is non-linear. This arises due to under-estimation of deformation under finite applied loads, (see figure 4.7). This makes the technique inappropriate to non-linear elastic analysis[53].

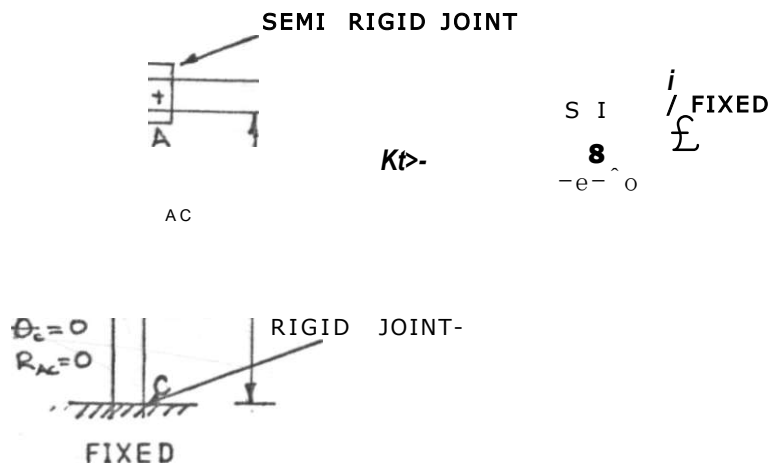


Figure 4.6 Relative distribution for rigid and semi-rigid connections.

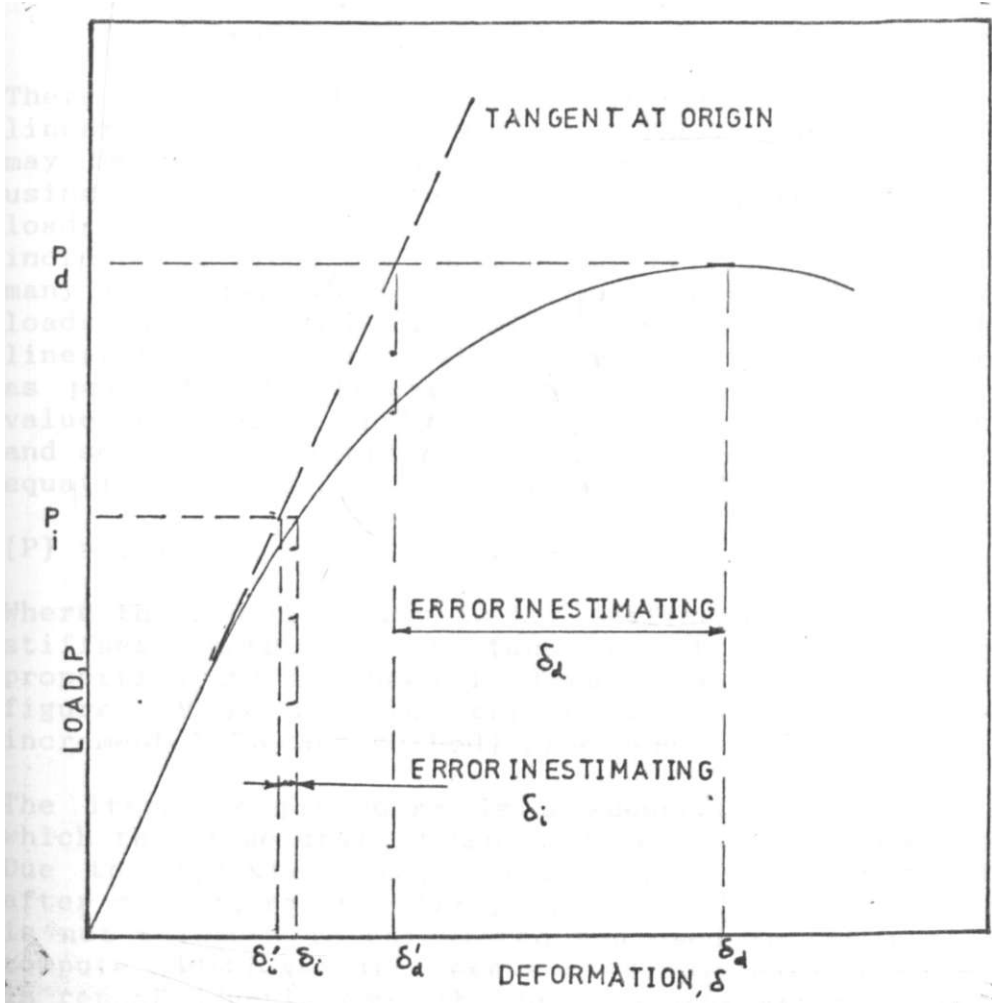


Figure 4.7 Non-linear deformation and it's approximation by tangent [30]

4.4.2. Non-linear elastic analysis.

Though linear formulations of problems are used to obtain engineering solutions, most of the phenomena dealt with are non-linear. These non-linearities may be due to:- [54, 55]

- (i) non-linear elastic and plastic or visco-elastic behaviour of the structural material referred to as material non-linearity, and
- (ii) large deformation and geometrical changes in the structure and the elements referred to as geometric non-linearity.

There are possibilities of combinations of these non-linearities in any one system. These non-linear problems may be solved by carrying out successive linear analysis using either incremental deformation approaches at desired load-levels e.g Newton-Raphson methods. The basis of the incremental procedure is the subdivision of the load into many small partial loads or increments. These incremental loads are applied one at a time, during which time, linearity is assumed. The deformation δ_1 , (see figure 4.8), as predicted by linear analysis initially is used as the value in a second analysis to predict a new deformation, δ_2 and so on. For simplicity, only the non-linear equilibrium equation for a single element is considered, i.e

$$\{P\} = \{K\} \{5\} \dots \dots \dots [4.21]$$

Where the non-linearity is the stiffness matrix, $\{K\}$. This stiffness matrix is a function of non-linear material properties and is shown in figure 4.8. The flow chart in figure 4.9 is used in computer applications of the basic incremental (secant method) procedure.

The iterative procedure is a sequence of calculations in which the structural system is fully loaded in each section. Due to approximations, equilibrium is not satisfied and after each iteration, the portion of the total loading that is not balanced is calculated and used in the next step to compute additional increments of displacement. This process is repeated until equilibrium is approximated to acceptable degree. [see 4.10], This process can be adopted for computer analysis and the flow chart is shown in figure 4.11.

The choice of analytical method to be used depends on the desired accuracy. Desai et al [59] has presented a comparative analysis of the two methods used in solving non-linear problems.

The incremental (secant) method is of general applicability and provides relatively complete description of the load-deformation behaviour of the material. Its disadvantage is that it is more time consuming and it is difficult to know in advance the increment of loads necessary to give a good approximation of the exact solution.

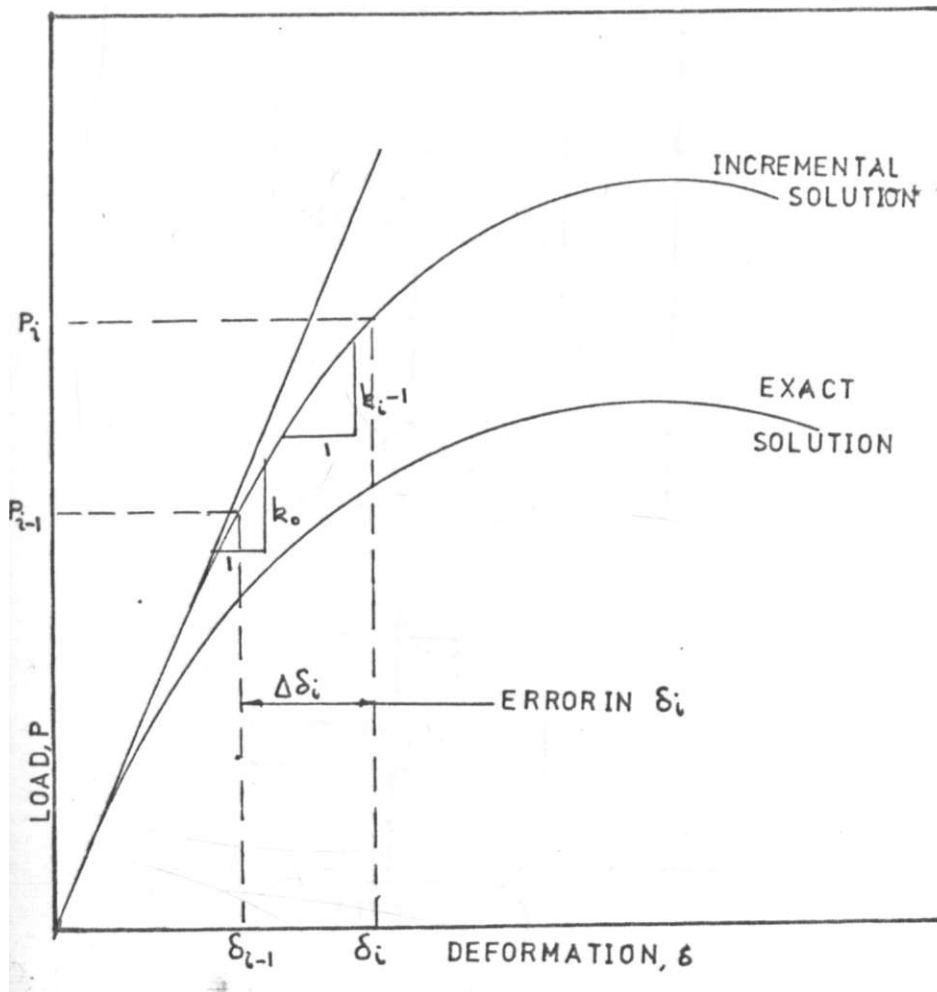


Figure 4.8 Incremental [secant] method for non-linear analysis 130, 56

INITIALIZE, s
COMPUTE $y_{b,1}$

CALCULATE f_e USING
CURRENT VALUE OF
 b

SOLVE
 $p - M W$
FOR s

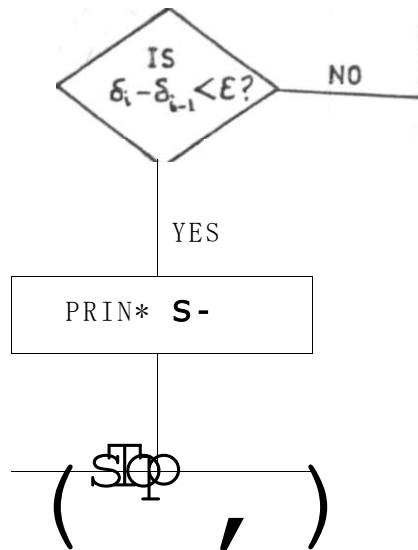


Figure 4.9 Flow chart for incremental [secant] method [30, 56]

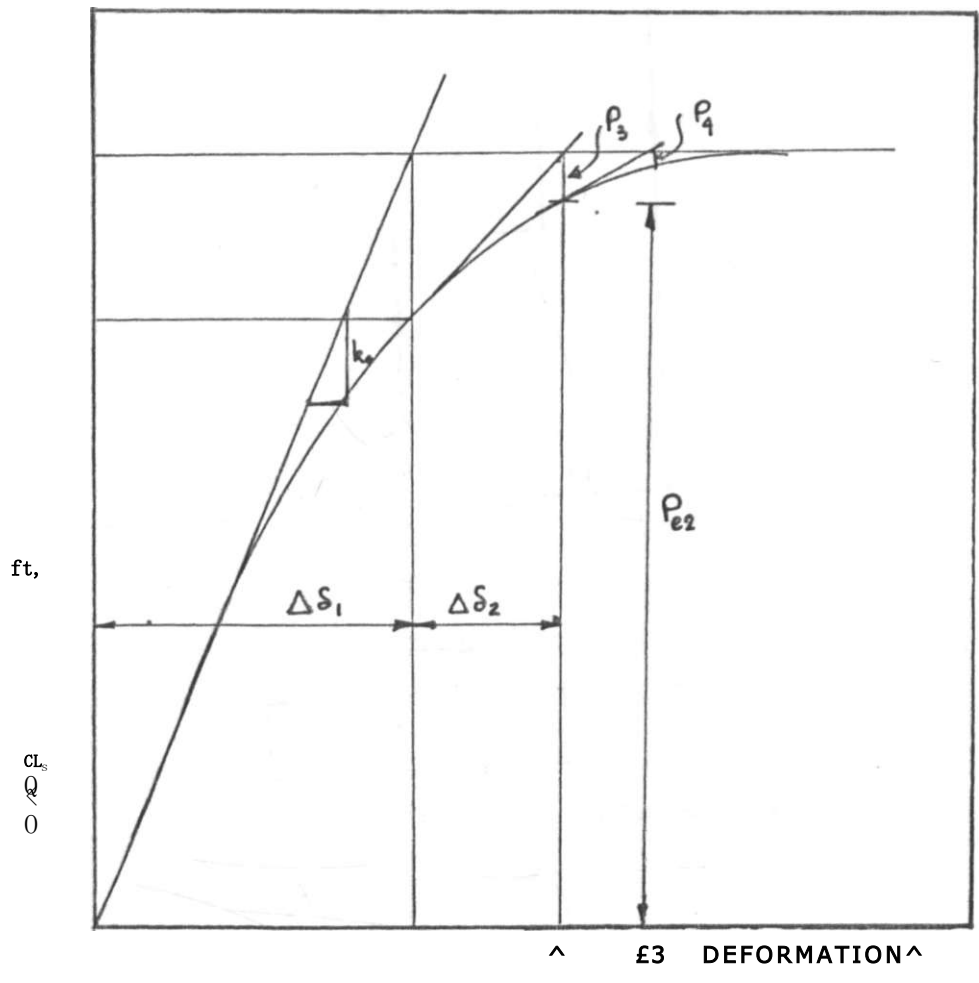


Figure 4.10 Newton-Raphson method [30, 56]

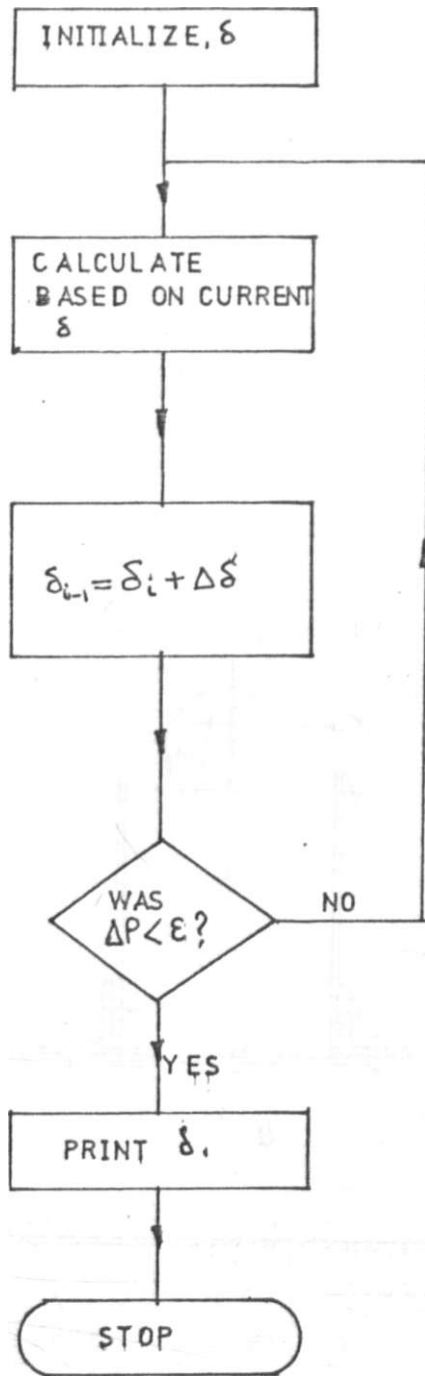


Figure 4.11 Newton-Raphson method flow chart [30,56]

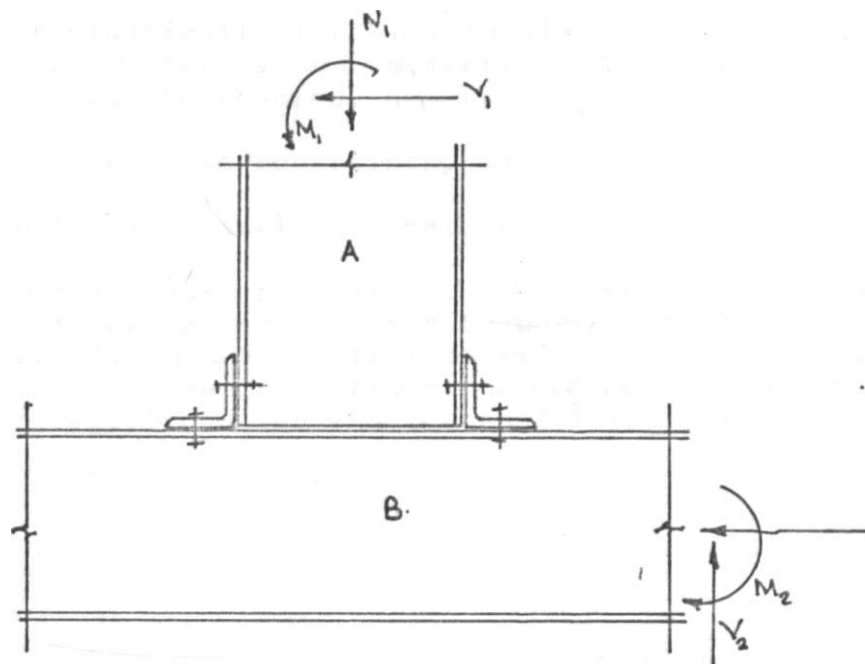


Figure 4.12 Mechanically fastened steel joints under actions.

The iterative (tangent) method is easier to use and program and it is also faster, when dealing with a few different loadings. The main disadvantage of the method lies in the uncertainty of convergence to the exact solution. The technique is also not applicable to dynamic problems. In order to offset the disadvantages of either method and combine their advantages, use is increasingly being made of step-iterative methods.

4.5 Modelling of semi-rigid bolted connections

Though conventional design methods assume linear connection behaviour, the actual behaviour is non-linear due to reasons outlined in sections 4.2.1 and 4.4. Thus in modelling semi-rigid connections, the non-linear deformation characteristics are taken into account in addition to the effects of partial rigidity at the joint.

A mechanically fastened joint is shown in figure 4.12 subjected to internal forces and moments. The non-linear and partial rigidity effects can be modelled by introduction of elastic restraints as shown in figure 4.13. The springs constrain elastically the ends of the members against axial forces, shear forces and moments. Two types of elastic restraints can be assumed, namely:-

- (i) linear elastic restraints, and
- (ii) Non-linear elastic restraints.

In linear elastic restraints, the axial, transverse and rotational springs are assumed to possess constant elastic stiffness k_1 , k_2 and k_3 respectively. The load-deformation relations are linear as shown in figure 3.9 (a) hence the governing equations for end forces deformation are:-

$$N_j = K_1 U_j$$

$$V_j = K_2 V_j$$

$$M_j = K_3 \theta_j$$

Where U_j , V_j are the member end displacements components with respect to the member end local co-ordinates due to the presence of the axial and transverse springs and θ_j is the member end rotation due to the presence of the rotational springs.

Non-linear elastic restraints do possess non-linear load-deformation characteristics. For small displacements, the relationships are linear, but the deformation become larger for the same relative increase of load as the loading

progresses, [see figure 3.10 (b)]. These relationships can be approximated by iterative methods, assuming linearities during each iteration. But due to high deviations in deformation with corresponding load increases, there are errors in the approximations.

These deviations are mainly due to the fact that the spring stiffness is not constant at all load levels within the elastic limit but changes with increasing load.

This non-linear behaviour of the connection under load may be expressed in several ways.

(i) polynomial approximation (Maclaurins series)

$$\begin{aligned}
 N_j &= k_j U_j + a_j U_j^2 + a_2 U_j^3 + \dots \\
 V_j &= k_2 V_j + b_j V_j^2 + b_2 V_j^3 + \dots \dots \dots [4.23] \\
 M_j &= k_3 \theta_j + c_j \theta_j^2 + c_2 \theta_j^3 + \dots
 \end{aligned}$$

Where a_i, b_i, c_i ($i = 1, 2, 3, \dots, n$) are unknown polynomial K_j, K_2, K_j are axial, transverse and rotational spring stiffness at small deformation respectively [i.e initial tangent values to the force-deformation curves in figure 3.10 (b)].

U_j, V_j and θ_j are the axial, transverse and rotational spring deformation at member-ends respectively.

(ii) Trigonometric (or Fourier) series

$$\begin{aligned}
 N_j &= \sum_{n=1}^{\infty} a_n \cos \frac{n\pi}{L} U_j \\
 V_j &= \sum_{n=1}^{\infty} b_n \cos \frac{n\pi}{L} V_j \\
 M_j &= \sum_{n=1}^{\infty} \frac{2EI_s}{n^3} \cos \frac{n\pi}{L} \theta_j
 \end{aligned}$$

Where $a_n, b_n, c_n, L, k_n,$ and m_n are unknown parameters to be determined experimentally.

The use of the above approximation for each of the three non-linear elastic restraints would theoretically require the experimental determination of an infinite number of parameters. However, it may be possible to experimentally determine a sufficient number of the above equations in the prediction of the load-deformation and moment-rotation response curves.

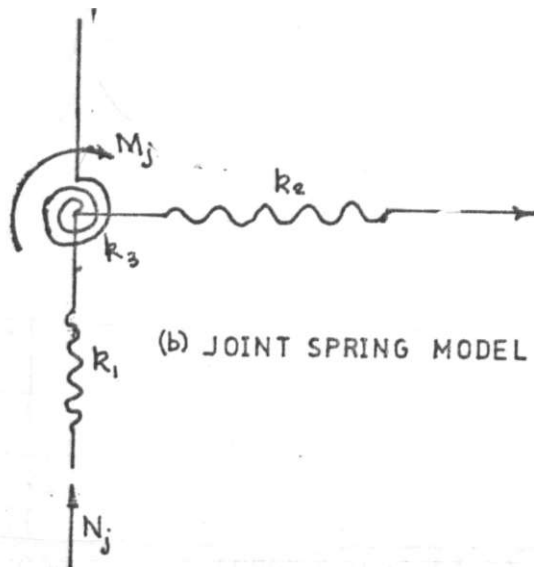
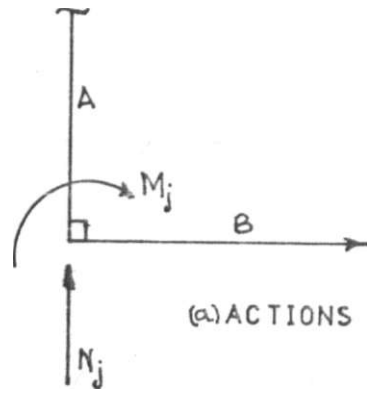


Figure 4.13 Idealised elastic restraint modelling of a joint [30]

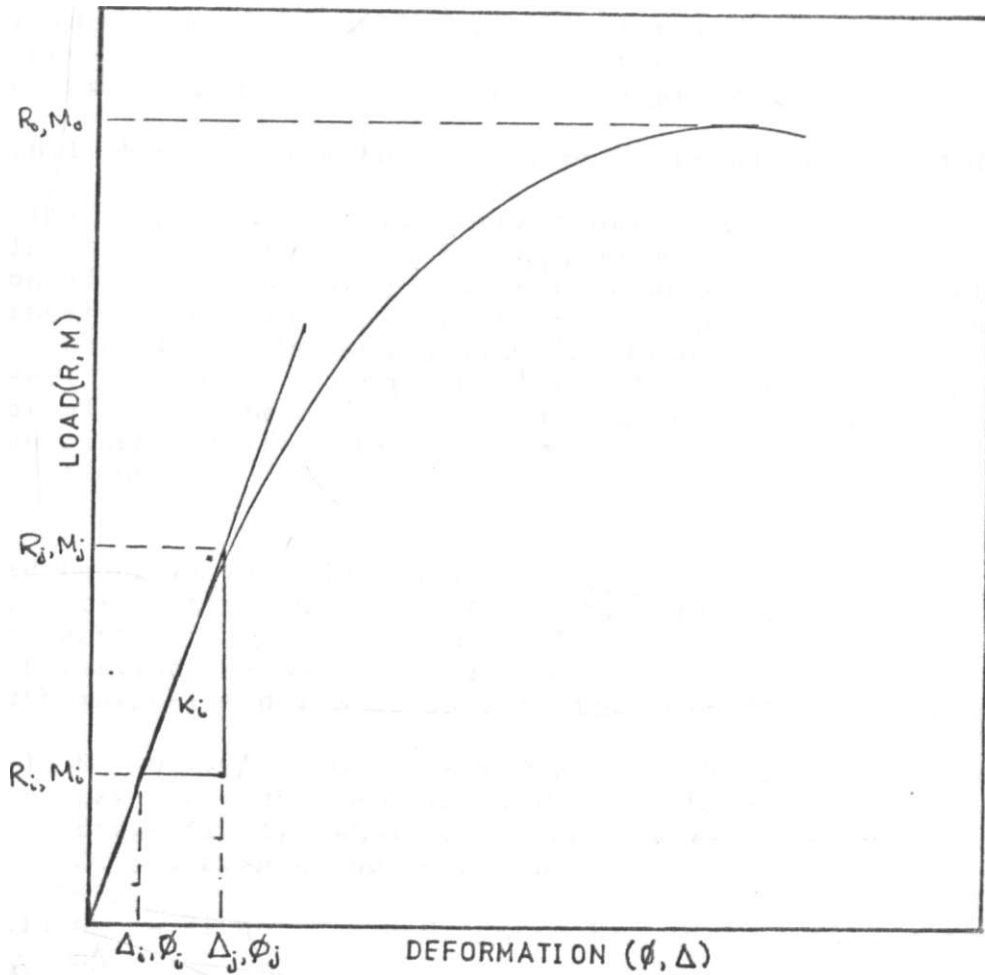


Figure 4.14 Graphical determination of model parameters.

4.6 Development of a non-linear mathematical model for bolted connections

For an accurate analytical form of the load-deformation or moment-rotation curves, mathematical models that are simple to use ought to be adopted. Mathematical models that have been put to use in the past were on the assumption that the load-deformation response of the fasteners was non-elastic and that the yield stress was not exceeded. [57]. However, it has been shown that the load-deformation relationships of individual fasteners is not elastic and that individual fasteners do not have well defined yield stresses. In the development of the mathematical model that is presented herein, it has been assumed that the connected parts remain rigid during load application and that constraints on the members of the connection do not force deformation to occur in any other direction other than that envisaged.

4.6.1 Non-linear mathematical model requirements [lj36]

Difficulty in modelling connection behaviour arises because almost all connections behave inelastically and therefore non-linearly. It is possible to approximate this behaviour linearly, or with bi-, tri- or quadri-linear models. Polynomial models and power function models can also be used. Models based on the aforementioned techniques normally fail because they do not meet the requirements of a non-linear mathematical model for the load-deformation relations.

Yee Leong et al [57] enumerated some of the requirements of moment-rotation curves some of which have been used in this research. By considering the properties of a load-deformation curve, it is evident that a non-linear mathematical model must satisfy the following requirements:-

(i) $R = 0$ at $A = 0$ and $M = 0$ at $\theta = 0$, i.e the curve must pass through the origin. R, M are load and moment values respectively, whereas A and θ are the corresponding displacements and rotations.

(ii) $\frac{dR}{dA} = K_i$ at $A = 0$ or $\frac{dM}{d\theta} = K_i$ at $\theta = 0$, i.e the

slope of the curve at the origin is equal to the initial elastic stiffness of the connections, K_i ,

(iii) $\frac{dR}{dA} = k_p$ as $A \rightarrow \infty$ or $\frac{dM}{d\theta} = k_p$ as $\theta \rightarrow \infty$

i.e as deformation becomes very large, the slope of the curve approaches the strain-hardening stiffness of the connection. If $k_p = 0$, the curves asymptotes to the ultimate load or ultimate moment of the connection.

In addition, the parameters used in the model should be physically meaningful and be determinable easily and accurately. The model should also take a relatively simple form.

4.6.2. Exponential model for load deformation curves

A non-linear mathematical model for load-deformation curves satisfying requirements in section 4.6.1 has the general form of :-

$$T = a_j \{1 - \exp[-(a_2 \frac{-a_1 + a_1 A}{a_1} A)]\} + A \dots \dots [4.25]$$

In which a_j , a_1 , a_2 and a_3 are model parameters. T is the action and A is the resultant reaction or displacement.

Substitution of $A = 0$, yields $T = 0$ which means the curve passes through the origin. When A is large, the curve approaches the straight line defined by the following equation:-

$$T = a_j + a_4 A \dots \dots [4.26]$$

The parameter a_1 represents the strain hardening stiffness, K_p . When no strain-hardening is assumed ($k_p = 0$), as the case is in the research, the curve asymptotes to the horizontal line given by:-

$$T = a_j \dots \dots [4.27]$$

Hence a_j represents the ultimate load or moment (action) capacity of the connector or the connection, T_{fi} .

Differentiating Eq[4.25] and setting $\frac{dT}{dA} = 0$ yields:-

$$\frac{dT}{dA} = a_2 \dots \dots [4.28]$$

Thus the parameter a_j represents the initial stiffness, K_i of the curve.

The parameter a, is introduced to control the rate of decay of the slope of the expression. This parameter was replaced by C, in this research and the model expressed as:-

$$T = T_0 \{1 - \exp[-k_p \frac{t C A}{A_1}] \} + k_p A \dots \dots \dots [4.29]$$

In order to use the model, parameters T₀, K_i and K_p must be evaluated. The value of C was determined empirically from experimental data since the research assumed no strain-hardening in the load-deformation curves, (K_p = 0) the model adopted for use was the general form:-

$$T = T_0 \{ 1 - \exp[-\frac{(k_j + C A)}{A_1} t] \} \dots \dots \dots [4.30]$$

4.6.2.1 Evaluation of model parameters

The model expressed in equation [4.30] was adopted for both pure shear load-deformation curves as well as the pure-rotation moment-rotation curves.

The model for the pure-shear was of the form:-

$$R = R_0 \{1 - \exp[-\frac{(k_i + C A)}{R_0} t] \} \dots \dots \dots [4.31]$$

In which

R = fastener load at any given deformation

R₀ = Ultimate shear load attainable by fastener or connection

A = Shearing, and bearing deformation of fastener and local bearing deformation of the connection plates.

k- = initial tangent of the load-deformation curve at origin

C = factor controlling rate of decay of the slope of the curve.

In case of pure rotation, the model was of the form:-

$$M = M_0 \{1 - \exp[-\frac{(k_i + C_0)}{M_0} t] \} \dots \dots \dots [4.32]$$

In which M = fastener or connection moment at any rotation.

M₀ = Ultimate moment attainable by fastener or connection

$\theta_0 = \text{Effective rotation due to joint or fastener deformation}$
 C and k_j same as defined for E [4.31]

4.6.2.1.1 Evaluation of R_q and M_q

The ultimate load capacity is given as the ultimate load or moment (R_q or M_q) that can be transmitted by connection or fastener without strain hardening occurring. This also assumes that the axial forces acting in the members under consideration is small. Figure 4.14 shows the location of R_q or M_q on a load-deformation curve.

4.6.2.1.2 Evaluation of K_j

The rotational or deformation stiffness of the connection is directly related to the deformation of the individual connection elements. In formulating the initial stiffness, it is assumed that the material behaviour is linearly elastic, the displacements are small, and the beam bending formulae are applicable to describe the deformation of the connection elements where appropriate. For simple connections like those dealt with in this research, the value of initial stiffness is given as:-

$$K_i = \frac{M_j - M_0}{\theta_j - \theta_0} = M \quad \text{or} \quad [4.33]$$

$$K_i = \frac{R_j - R_0}{A_j - A_0} = R \quad , \quad A \quad J$$

This holds for a tangent that starts from the origin and touching at least one point of the initial curve. Figure 4.14 shows the evaluation of K_p graphically.

4.6.2.1.3 Evaluation of C .

Parameter C which controls the rate of decay of the curve could be determined by a trial and error approach. But this was found a laborious exercise. Instead, equation [4.30] was re-arranged making C the subject:-

$$C I = - I_2 [T_j t_n (1 - T/T_q) + K I A^2 J] \dots \dots \dots [4.343]$$

Where

C_j is the value for a given set of data (A ; and T ,)

n is the sets of data on a given curve.

Based on the experiment data obtained, the value of $A \gg T_p$, T and K ; were substituted into E [4.54] to obtain value of C for each set of load and deformation (A and T) data. Then the value of C used in the modelling was obtained as:-

$$C = \left(\sum_{i=1}^n C_i \right) / n \quad [4.35]$$

4.6.3 Inverse Ramberg-Osgood model for load-deformation curves,

This mathematical model was initially developed for analysis of non-linear structural systems using the method of displacements. [58] The model for most flexural members comprises of a beam of any intermediate loading that is linearly elastic in behaviour everywhere except at the connections. The non-linear behaviour of the structural system can then be assumed to be at the centre of the connection because most of the non-linearities occur here, [see section 4.2.1]. Based on this assumption this model was adopted for the bolted connection under investigation. The basic formulae used for the modelling was of the form:-

$$\frac{KA}{[1 + \frac{(KA)^n}{T_0^n}]^{1/n}} \quad [4.36]$$

In which.

T is the action (force or moment)

A is the strain (displacement or rotation)

K is the initial linear relation between T and A

T_0 is the maximum force or moment attainable by the connection and

n is the parameter defining general non-linear relationship between T and A - By choosing an appropriate value of n , Eq [4.36] may be used to represent analytically a wide range of load-deformation curves with acceptable degree of accuracy.

The model equation [4.36] corresponds essentially to the inverse of the Ramberg-Osgood function of the form:-

$$\sigma = E \epsilon + k \epsilon^n \quad [4.37]$$

In which σ is the stress, ϵ the strain, E Young's modulus, k the stress at secant modulus $0.7E$ and n the parameter defining the shape of the stress-strain curve.

Equation [4.36] also meets the basic requirements set out for non-linear models in section 4.6

4.6.3.1 Evaluation of model parameters

The model expressed in Eq [4.36] was also adopted for use in both the pure shear and pure rotation cases of the joints under investigation.

For the connections that were axially loaded (pure shear Equation

[4.38] took the form:-

$$R = \frac{KA}{1 + \left(\frac{KA}{R_0}\right)^{1/n}} \quad (4.38)$$

In which R is the axial load in connection.

K is the initial linear relation between R and

A is the deformation of the connection

R_0 is the maximum axial (shear) load capacity of the connection

n is the parameter defining the shape of the load-deformation curve.

For the connection under rotational loading, Eq [4.36] becomes:-

$$M = \frac{k_m \theta}{1 + \left(\frac{k_m \theta}{M_0}\right)^{1/n}} \quad [4.39]$$

In which M is the moment at connection

k_m is the initial linear relation between M and θ

θ is the effective rotation of the joint

M_0 is the maximum moment capacity of the connection, and
 n is the parameter defining the shape of the $M - \theta$ curve.

The evaluation of parameters R_0 and M_0 was similar to that in section 4.6.2.1.1. and evaluation of parameter k_s and k_m as similar to the evaluation of k_i in section 4.6.2.1.2., as indicated in figure 4.14. Parameter n was evaluated by a trial and error procedure. The value giving the best fit curve being taken for use in the model.

CHAPTER FIVE

EXPERIMENTAL DESIGN AND INVESTIGATION.

5.1 INTRODUCTION

The extensive use of experimental studies preliminary to the analysis, design and construction of new works and the testing procedure for control of established processes of manufacture and construction are well recognised and significant features of technical development. Practically all branches of engineering, especially those dealing with structural systems and machinery are ultimately concerned with the construction material, the properties of which are determined by experimental investigation. Engineering research and development function largely on an experimental basis and call for carefully planned and well devised testing procedures.

Construction materials are functionally required to develop strength, rigidity and adequate durability in service. Serviceability, is broadly the ultimate criterion in the choice of the material for use. In actual selection of materials, the problem of quality, design and application are interrelated. The major sources of information in material selection are:-[10]

- (i) knowledge of record of performance of materials in service, and
- (ii) results of tests made to supply data on material performance.

The data used in this research was based on the first source of information. The experimental work undertaken was mainly to verify the mathematical models developed in chapter 4.0 sections 4.6.2 and 4.6.3 as per objectives in section 3.5 of chapter 3.0.

The investigations were divided into two categories namely:-

- (i) material property tests
- (ii) bolted joint behaviour tests

5.2 Material testing

These tests basically involved tensile testing of the material used in the fabrication of test joints to be used in the second stage of the research work. The main objectives of the tests were:-

- (i) to supply routine information on the material properties, and

- (ii) to obtain accurate measure of fundamental properties of physical constants.

These objectives are broadly classified into commercial or control testing, material research and development, and scientific testing respectively. This research project fell within the last category whose major aim was the accumulation of orderly and reliable fund of information on the fundamental and useful properties of the materials to be used in the investigation, namely the bolts, steel plates and rectangular hollow sections (RHS). This was done with the ultimate aim of supplying data for accurate analysis of structural behaviour and efficient design.

5.2.1 Scope and applicability of material tests

The static tensile test was aimed at furnishing static characteristics of the material. Prepared specimens were subjected to gradually increasing static loads until failure occurred. The tensile test is one of the most commonly made and simplest of all mechanical behaviour tests. Properly conducted tests on the specimen of representative parts can be valuable in indicating directly the performance of such parts under loads in service.

The tensile test was chosen because of the large range of uses to which a stress-strain curve thus obtained can be put to in terms of explaining overall structural behaviour. In choosing the tensile test, factors that were considered included:-

- (i) suitability to the material to perform under the tensile load applied,
- (ii) relative difficulties and complications induced by the gripping or end bearings on the test specimens.

Although most static tensile test are on prepared specimens, their application can be extended to full size manufactured specimens, fabrication parts and structural components.

The tests used specimen from:-

- (i) machined bolts, and
- (ii) machined joint material.

In both cases the test specimens were subjected to axial tensile forces by means of a UTS machine (see plate 5.1 and 5.2)

5.3 Loaded joint behaviour tests.

These experimental investigations were carried out with the ultimate aim of verifying functional relationships between load and deformation for both the connections and the joints as predicted by the mathematical models in chapter 4.0. The experimental procedure was based on the loading modes namely:-

- (i) pure shearing load, and
- (ii) pure rotational load

The tests were designed with the aim of providing data on the connector properties as well as the joint properties (connector and connected parts combined). With information from both these tests and using the principle of superposition, the behaviour of the bolts and the joint material were derived separately.

5.3.1 Scope and applicability of the tests

The importance of bolted connections in the determination of the load-deformation behaviour of steel structural systems was recognised about 75 years ago and research has been done on a varying range of connections, [59].

Yet steel design specifications still treat connections as either fully pinned or fully rigid and prescribe approximate design assumptions. Even from the load-deformation data available, it is not possible to adequately define connection behaviour without resorting to some mathematical formulations.

These experiments aimed at providing data necessary to choose a mathematical model that could best describe such connection behaviour in real structural systems. Identification of such a model would save the costs involved in the rather expensive experimental procedures undertaken to determine connection behaviour under load. These data could also be used in conjunction with the principle of superposition in predicting bolt and joint properties at various load levels, R-, bolt diameters, material thickness, t- and material type. The relationships thus obtained could serve a wide range of practical cases in terms of predicting behaviour for standardised connections based on these parameters.

5.3.2 Pure shearing tests

The objectives of these tests was to study the behaviour of

- (i) single bolt in pure shear, and
- (ii) two member single bolt joints laterally loaded in pure shear.

The concept of pure shear is in itself a misnomer, because it is difficult to accomplish under experimental conditions without the introduction of moments. The moments arise due to joint load eccentricities. But a pure shear case was still assumed based on the premise that resultant joint loads acting in opposite directions at connected member interfaces provide a theoretical case of pure shear. Based on this principle, a pure shear testing rig was designed for use in this research, [see section 5.4] Mutuku et al [30] used a rig design based on the same principle of operation to provide pure shear.

On loading the joint axially, load-deformation curves were obtained and parameters in the non-linear models of chapter 4.0 [see E^{4.31}] evaluated. The predicted joint behaviour curves were then obtained using these equations with the derived parameters.

Thus essentially these tests were aimed at:-

- (i) determining actual load-deformation curves for the connectors and joints.
- (ii) predicting load-deformation curves for the same using the non-linear models of equations [4.31] and [4.38]
- (iii) comparison of actual load-deformation curves to the predicted load-deformation curves at the actual load levels, R_t and the predicted loads, R_p and selected a model describing the joint behaviour with the best degree of accuracy.

5.3.3 Pure rotation test

The main objective of these tests was to determine the moment-rotation characteristics of both the connectors and joint. The joints tested comprised of two members fastened with two bolts. The pure rotational load was obtained by torquing the test specimens by application of a tensile load through a system of pulleys. The rotational load-deformation characteristics were obtained as the loading progressed and latter on analysed to provide the required moment-rotation curve. The tests aimed at:-

- (i) obtaining rotational load-deformation curves for the connectors and the joints.

- (ii) converting the data in (i) above into the required moment-rotation curves.
- (iii) prediction of the moment-rotation curves using the models of E^* [4.32] and [4.39] with parameters obtained from (ii) above.
- (iv) comparison of actual moment values, M_f and the predicted, M at specific rotation values and select a model describing this behaviour with the best accuracy.

5.4 MATERIALS

5.4.1. Bolts and washers

The bolts used in the determination of the material, connector as well as joint behaviour were high tensile black hexagon head bolts Grade 8.8. They were two lengths:-

- (i) M (6,8,10) X 75 to BS 3692, grade 8.8 for the connector properties
- (ii) M (6,8,10) X 125 to BS 3692, grade 8.8 for the joint properties.

All the bolts and nuts were zinc plated to BS 1706: class B. [60, 61].

The bolt holes for the 6,8, and 10mm bolts were of such dimensions that when the bolts were inserted they fitted snugly. The bolt lengths were chosen such that the threads were always outside the connected parts. The washers used in conjunction with the bolts were in accordance to BS 4320 [62].

5.4.2 Steel plates and rectangular hollow sections

Since the behaviour of a given connection is a function of several geometric and material parameters, the connected parts were chosen with the aim of minimising the effects of some of these parameters on the final results.

The steel plates that were used in the determination of connector properties, had the thickness chosen such that the effect due to plate failure in bearing were minimised. The test pieces were obtained from a grade 43,1800 X 25mm Pj (steel plate).

For the RHS that were used in the determination of joint properties, the sections were chosen depending on availability in the market and the fact that they did not undergo distortion or warping on loading. This limited the

wall thickness of the RHS. Those used were grade 43, 150 X 50 X 4mm RHS.

5.5. CONDUCT OF TESTS

5.5.1. Material tests

The major aim of these tests as was pointed out in section 5.2 was the accumulation of an orderly and reliable fund of information on the fundamental and useful properties of the bolts, plates and RHS. The tests carried out were destructive in nature, and the cost involved necessitated use of sampling techniques. Before commencement of the tests, the specimens were visually inspected to determine correctness of dimensions, examination for surface defects, and the presence or absence of undesirable conditions such as excessive moisture or temperature.

5.5.1.1. Tensile tests

In these tests, specimen were subjected to an axial tensile force by means of a Ruell +Korthaus KG UTM machine [see plate 5.1] At various increments of the axial load, R changes in length, A_l of the specimen for an initial gauge length L_p were measured and recorded. The data thus obtained was used to plot stress-strain diagrams for the determination of the material properties such as elastic strength, elastic limit, modulus of elasticity etc.

5.5.1.2. Requirements for specimens

The most commonly used specimens are either of round, square or rectangular cross-sections. The central portion of the specimen is thinned out in order to cause failure to occur at a section where the stresses are not affected by the gripping device employed. The ends are required to be plain, shouldered or threaded depending on the gripping device. Figure 5.1 shows the general features of a typical tensile specimen. The transition from the ends to the central position are made by an adequate fillet in order to reduce the stress concentration caused by the abrupt change in section. The length of the central portion was made sufficient to allow a normal break, i.e drawing out or necking down was inhibited by the mass ends. The specimen dimensions were adopted from the British standards specifications. [63].

Generally, the shape and dimension of the test piece depend on the form and dimension of the material of which the tensile properties are to be determined. The bolts that

were used had circular cross-section, and though not machined, were treated as proportional specimens.

Based on specifications [63] the various parameters shown in figure 5.1 were calculated as follows:-

(i) initial gauge length, L_j

$$L_q = 5.65/A \dots \dots \dots [5.1]$$

Where A is the cross-sectional area of the machined part, alternatively,

$$L_0 = 5D \dots \dots \dots [5.2]$$

Where D is diameter of machined part [gauge diameter]

(ii) minimum parallel length, L_c

$$L_c = L_0 + 2D \dots \dots \dots [5.3]$$

(iii) Gauge diameter or width of strip, D

$$D > = 6\text{mm} \dots \dots \dots [5.4]$$

The test pieces were prepared in a manner meant to cause minimum deformation and heating of the test piece. This was by electric machining with a coolant liquid being used to keep the temperatures down. This was to avoid errors in proof stress or yield stress values.

5.5.1.3 Testing procedure

Before the testing commenced there was the important aspect of familiarising with the machine and its controls. This included graduations on the load indicator. There was also need to certify that the gripping device was fully functional. The speed of the testing machine was not greater than that at which load and other readings can be made with the desired degree of accuracy.

Prior to fixing the specimen into the grips, the dimensions were taken and inspected. The specimen was then fixed and the necessary machine adjustments made before loading commenced. The stress-strain plot was obtained from the inbuilt X-Y plotter as well as a computer output of the ultimate load, and the extension.

5.5.2. Loaded joint behaviour tests

Functional aspects of structural elements are best illustrated when the systems are loaded. The experimental work carried out was aimed at verifying the actual functional relationships of load-deformation characteristics under an actual load as compared to the results predicted using the non-linear models developed in chapter 4.0. The experimental procedures were based on two loading modes, namely:-

- (i) pure shear, and
- (ii) pure rotation.

5.5.2.1 Pure shear tests

The objectives of these tests was to study the behaviour of two member single bolts laterally loaded in shear. Though the concept of pure shear is difficult to accomplish under experimental conditions, the assumptions of section 5.5.2 were adopted in approximating a pure shear case using the testing rig described in the next section.

The test were carried out in two stages: one involved provision of load-deformation data for the connectors alone, whereas the other involved provision of the same data for joint assemblies.

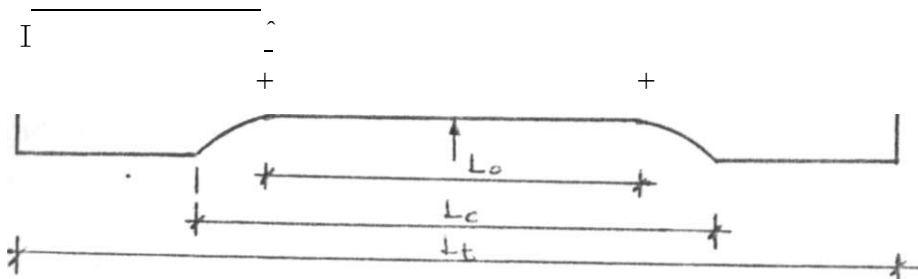


Figure 5.1 Typical tension specimen

D = gauge diameter or breadth

L_0 = initial gauge length

L_c = total parallel gauge length

L = total specimen length

r = transition fillet radius

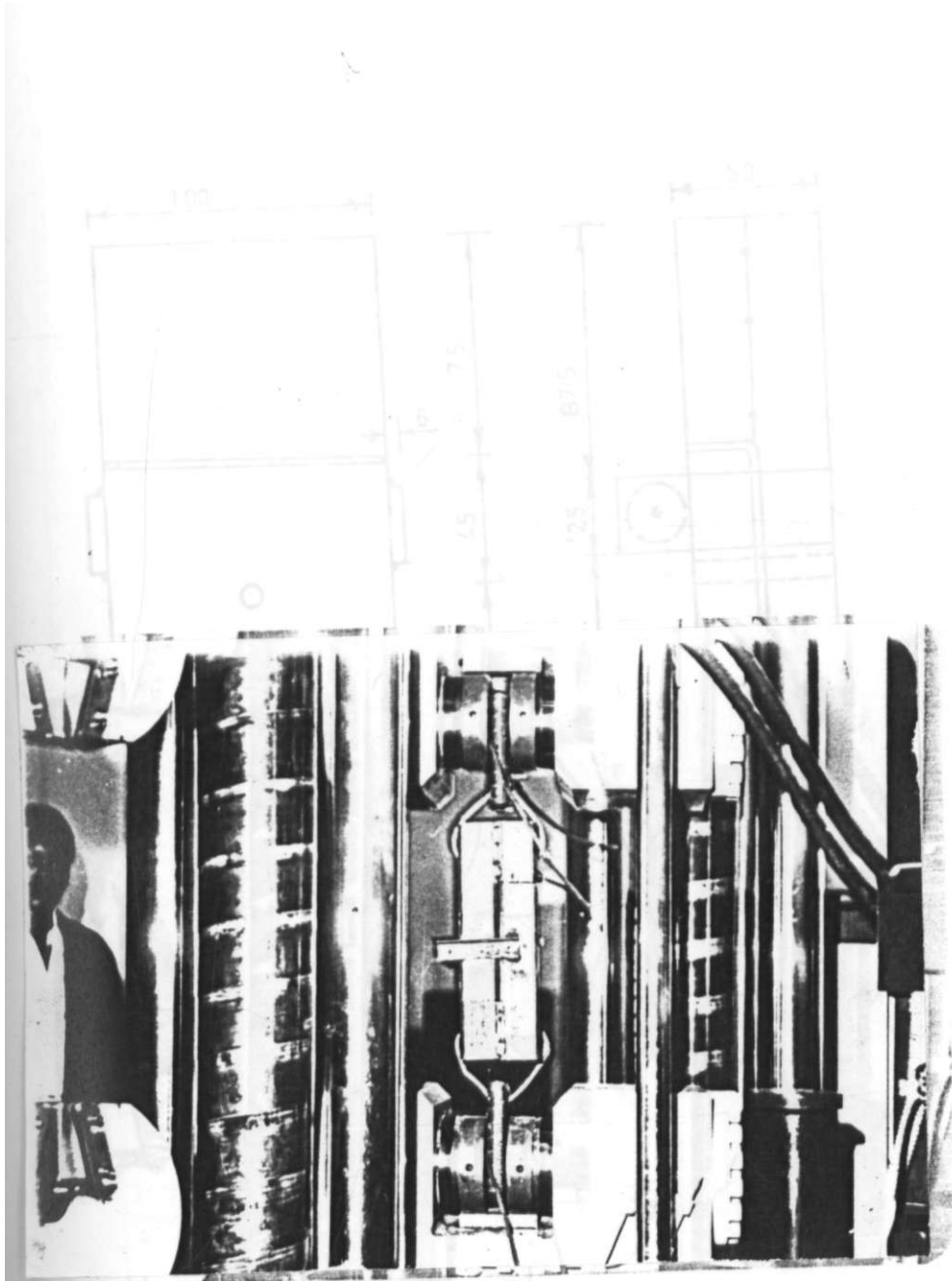
5.5.2.1.1 Specimen dimensions and test joint assembly

The pure shear test specimen also doubled up as the testing rig. [see figure 5.2 and 5.3] The specimen sizes were arrived at after consideration of the connector end and edge distances and spacing. [50] To save on material costs, one testing rig was designed to carry out three tests using different bolt sizes for the connector property test. For the joint property tests, five replications of the same rig for each bolt diameter were fabricated.

In both cases the connector holes were spaced in accordance with the minimum stipulated diameter requirements based on the largest hole diameter. For each test, one bolt (complete with nut and washer) was used.

5.5.2.1.2. Pure shear testing rig

Figures 5.2 , 5.3 and 5.4 show the assembly and general features and the application of shear respectively. As it was mentioned in section 5.3.2 pure shear conditions are extremely difficult to accomplish under experimental conditions. Even the assumptions made during the design of the pure shear rig are not easy to realise in practice. An additional assumption was that the joint loads are applied very close to the interface of the joint members and hence the resultant deformation due to the joint load eccentricity is negligible when compared to shear deformation. Based on principles of operation of shear testing equipment designed and used by Mutuku et al [30] the testing rigs of figure 5.2 and 5.3 were designed.



Wat. 5.!

showing part of the Roell
5Sⁱ : «hln.

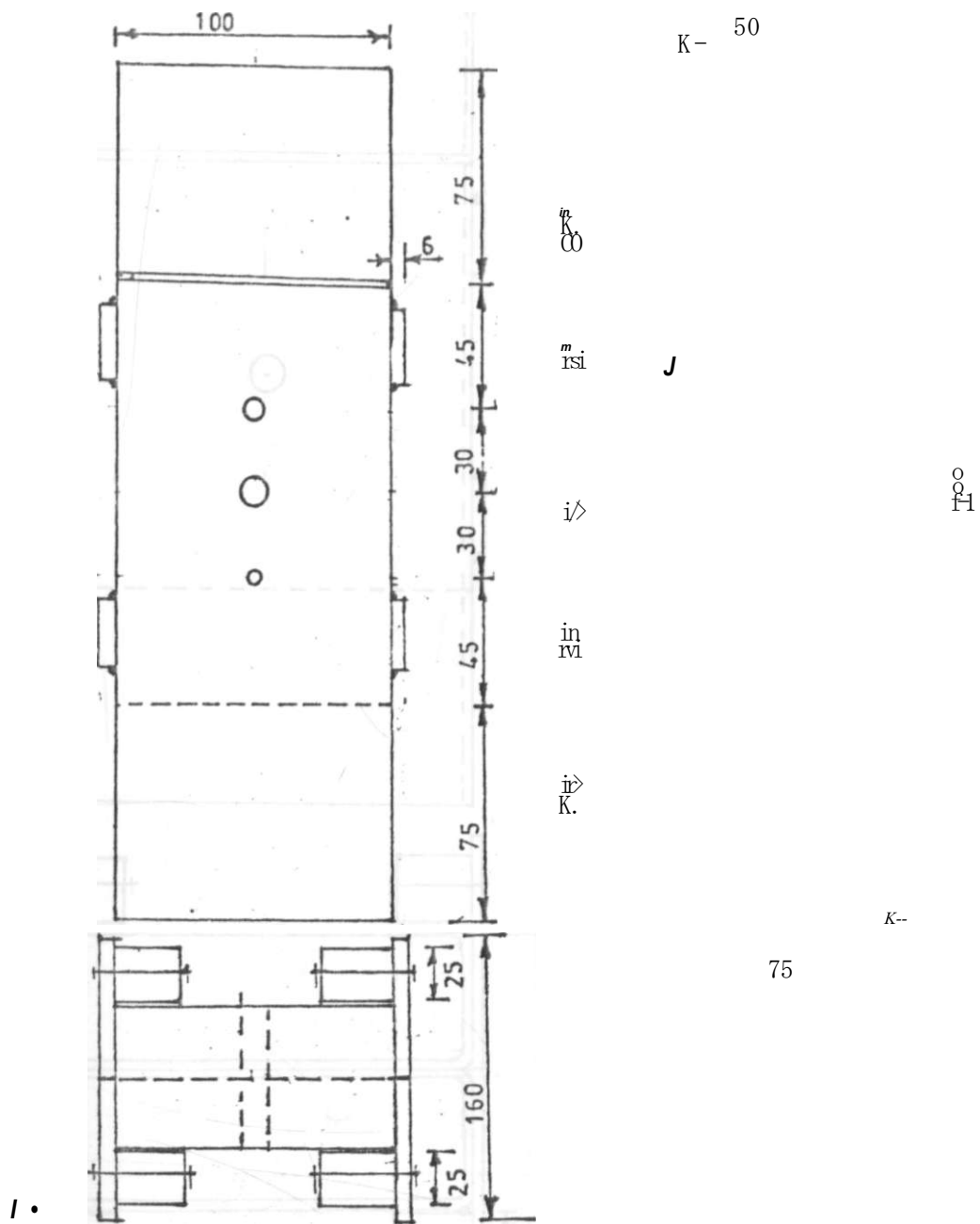
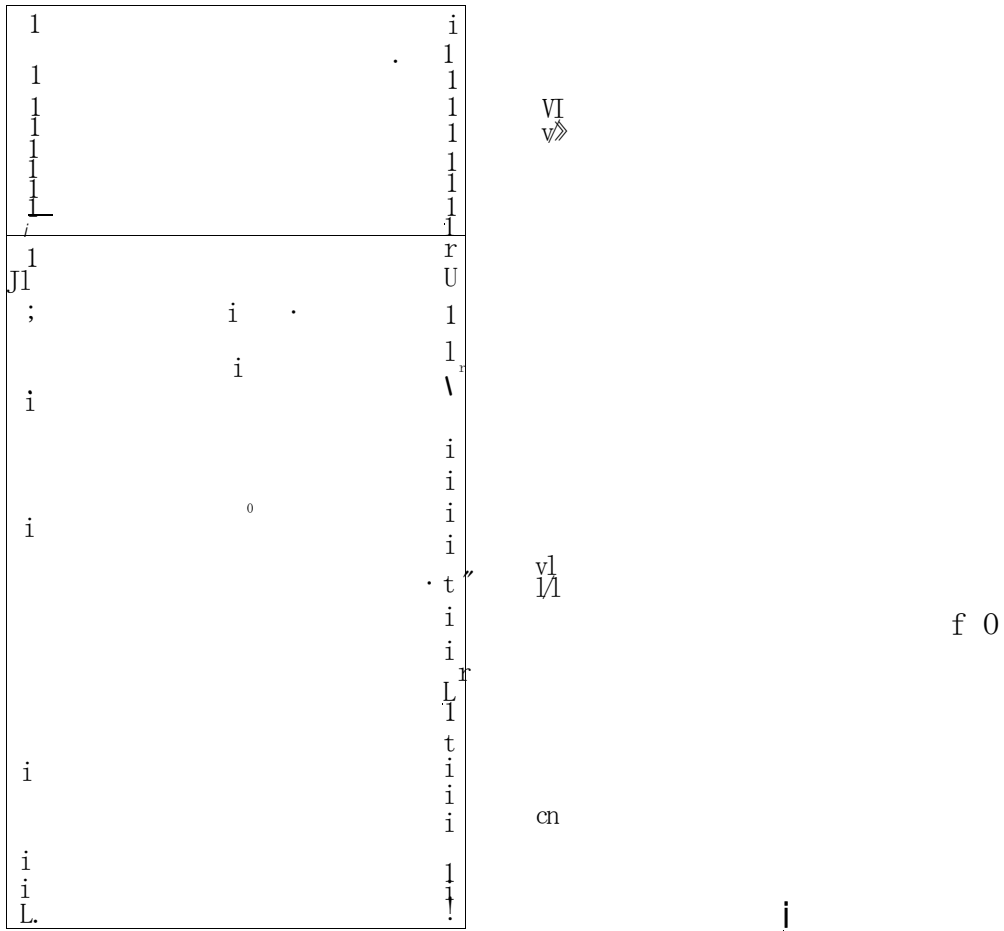
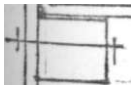


Figure 5.2 Dimensions and configuration of pure shear rig for connector property test.



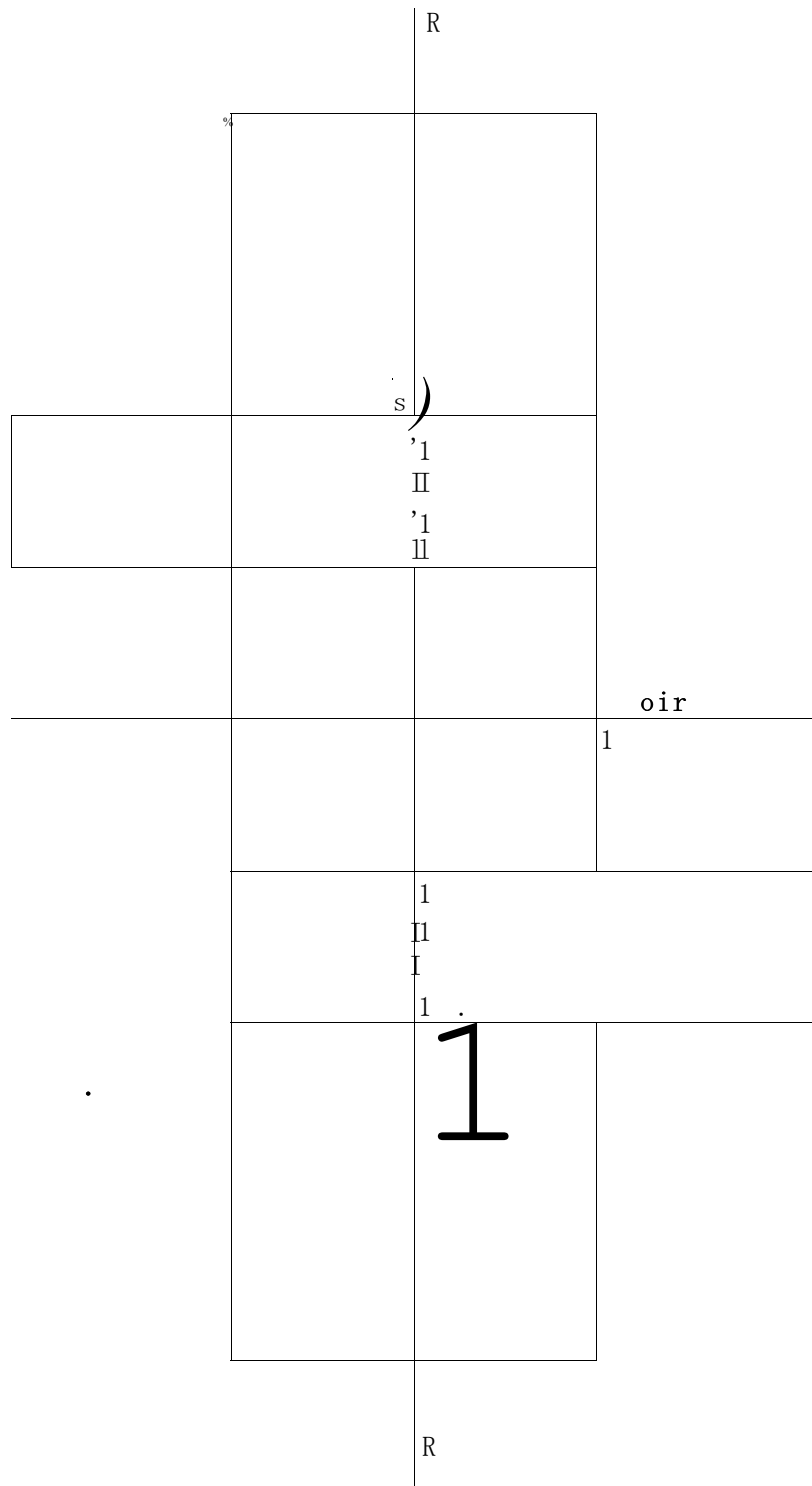
E_kf

σ^n



i

Figure 5.3 Dimension and features of pure shear rig for joint property.



I

Figure 5.4 Load application to pure shear specimen

The rig comprises two halves. By applying the load, R at the midpoint of the specimen as shown in figure 5.4 using a 600KN load capacity universal testing machine (UTM) (see plate 5.4) pure shearing force was transmitted to the interface of the joint members. The average joint deformation was obtained from a plot on the inbuilt X-Y plotter and computer output. Each half of the specimen had roller wheels fixed on it to act as a guide and prevent either half from bending outwards during loading. The material requirements for the testing rig fabrications are shown in Appendix A.

5.5.2.2. Pure rotation tests

Unlike the case of shear, pure rotation conditions are easily accomplished by use of a couple of forces. Figure 5.5 shows how a couple of pure rotational forces can be applied to a bolted connection. Member A was clamped rigidly at the ends shown in figure 5.5, while a couple was applied to member B by use of a system of cables and pulleys. The two major problems associated with load application were:-

- (i) difficulty in rigidly clamping A to make it free of any lateral or rotational movements, and
- (ii) proper alignment of couple forces in terms of distance from the centerline.

Since the rotation or movement of member B is measured relative to member A, movement in A will not affect the movement of B. The couple of forces applied to the test specimen constituted true rotational joint behaviour

5.5.2.2.1 Measurement of joint rotation

The objective of the pure rotation tests was to generate data for a plot of moment-rotation curves. The moment applied to the joint was easily obtained by using the following relation:-

$$M = R \times L, \dots \dots \dots [5.5]$$

In which M = moment acting at the joint

R = load level at a given deformation

L_x = lever arm separating the couple of forces,
[see figure 5.5]

Figure 5.6 shows the schematic outline a b o e f o for the under formed state of member B and a' b' o e' f' o for the deformed state relative to the centraline 0-0 of member A. The horizontal movements a-a', b-b', e-e' and f-f' of member B at a, b, e, and f respectively were recorded as vertical movements of the upper machine cross-head. Before the testing commenced, checks were made to ensure that the joints were tight and the cables taut, implying that recorded movements could only be due to joint deformation as a result of applied load.

To explain determination of joint rotation, let us consider the deformed state of oaa' on a larger scale as shown in figure 5.7. The deformation recorded on the X-Y plotter and computer is indicated as in figure 5.7. It is actually an arc subtended at centre o, by a circle of radius L. The angle subtended is the rotation that occurs in the joint. Based on standard formulae as derived in Appendix C, the angle throug which the joint rotates under load was calculated as follows:

$$\theta = \frac{A}{L} \quad [5.6]$$

Where θ is angle of rotation in radians

A is the deformation recorded at a given load level

L- is the distance from joint centerline to point of couple application.

In the above calculation it is assumed that:-

- (i) the rotational angle is small such that $\tan \theta = \sin \theta = \theta$ in radians
- (ii) member A is fixed and hence the joint rotation is a consequence of movements in member B and the possible yielding in both member A and B at bolt holes, as well as bolt deformation.
- (iii) shear deformation, if any are negligible compared to rotations measured.

Hence the rotation calculated for member B relative to member A may be assumed to be equal to the joint rotations of members about the joint centerline.

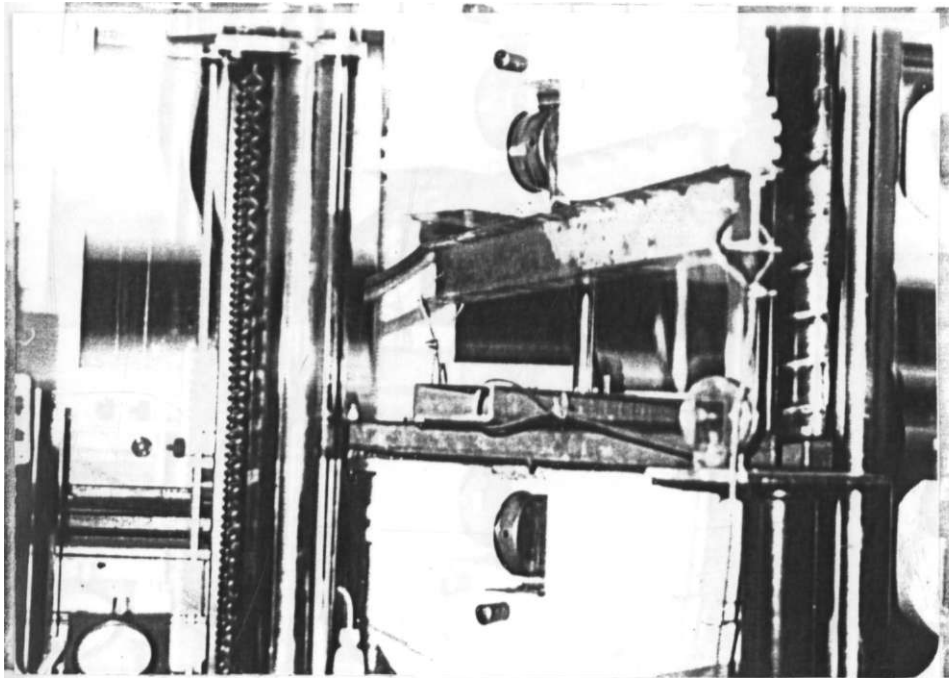


Plate 5.2 Pure rotation test setup showing loading beam
and test specimen

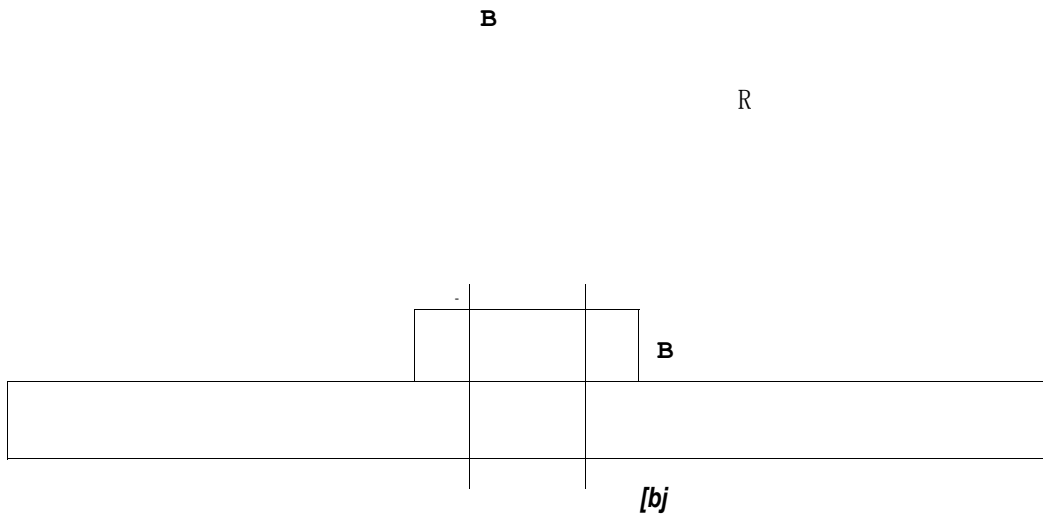


Figure 5.5 Application of a pure couple of forces to bolted connection (a) front view (b) side view

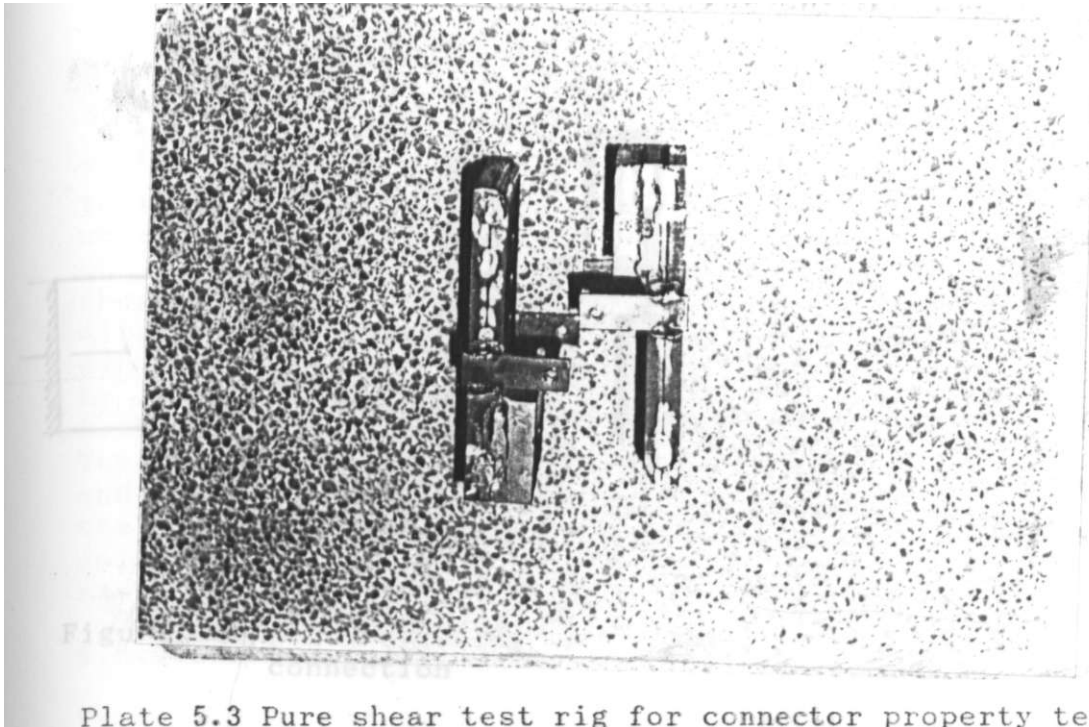


Plate 5.3 Pure shear test rig for connector property tests

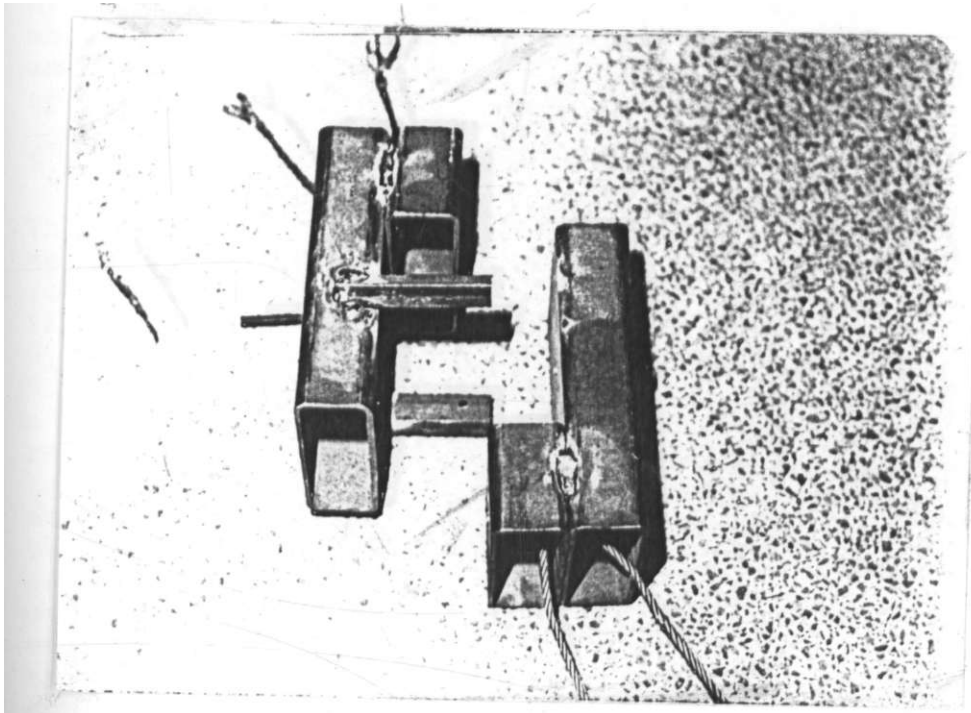


Plate 5.4 Pure shear test rig for joint property tests

i f t a

Figure 5.6 Measurement of joint rotation in bolted connection

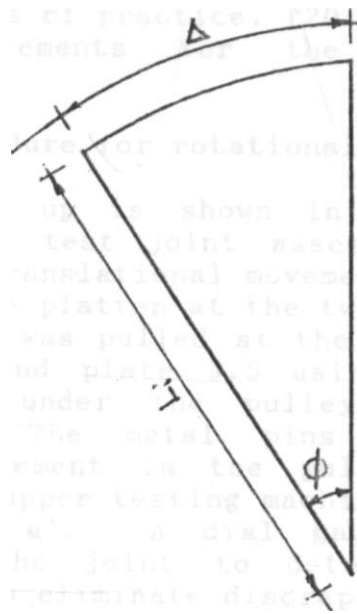


Figure 5.7 Geometric construction showing measurement.

The arrangements of the bolts on the test specimen meant that each bolt size resisted the rotational effects in a unique manner, but generally along similar principles with one another. The bolts were arranged on the specimen as shown in figure 5.8 in such a way that they were on the circumference of a circle of radius 50mm about the joint centerline. The rotational effect is resisted by each bolt by a couple acting on the bolts as shown in figures 5.9, 5.10 and 5.11 for the 6mm, 8mm and 10mm bolts respectively. The forces acting on the bolts can be resolved into vertical and horizontal components by considering the equilibrium of the force, i.e $\sum V = 0$ and moments $\sum M = 0$ in the joint. The joint rotation may then be calculated using these components as shown in Appendix E.

5.5.2.2.2. Specimen dimensions

Figures 5.12 and 5.13 show the diagrammatic representation of the test joint assemblies used in pure rotation tests. The specimen dimensions were arrived at after consideration of the specifications governing the design in standard manuals and codes of practice. [20.50] Appendix B gives the material requirements for the pure rotational test specimens.

5.5.2.3.3. Procedure for rotational tests

The general set up is shown in figures 5.12 and 5.13. Member A of the test joint assembly was clamped against rotational and translational movements by bolting it down on the lower machine platten at the two ends as shown in figure 5.14. Member B was pulled at the ends as shown in figure 5.14 and 5.15 and plate 5.5 using steel cables abc and a'b'c' passing under the pulley systems at b and b' respectively. The metal pins (c and d') prevented translational movement in the pulleys. The cables were attached to the upper testing machine cross-head and loading beam at a and a'. A dial gauge was mounted at the centerline of the joint to determine whether any slip occurred so as to eliminate discrepancies in calculating the actual rotations. The predicted rotations were calculated by applying the non-linear models developed in chapter 4.0 as applied to the forces acting on the bolts. Appendix E gives the detailed analysis of the pure rotation test performance.

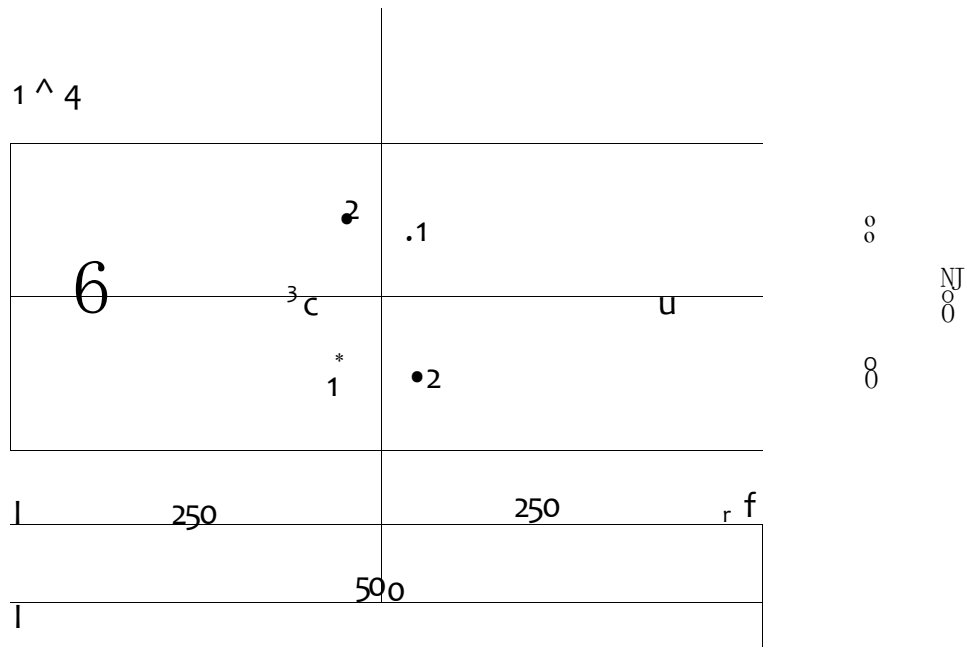


Figure 5.8 Bolt arrangement on test specimen

- (i) 6mm bolt,
- (ii) 8mm bolts,
- (iii) 10mm bolt
- (iv) 25mm diameter hole

?????????? V????????*

X

Figure 5.9 Forces acting on 6mm diameter bolts.

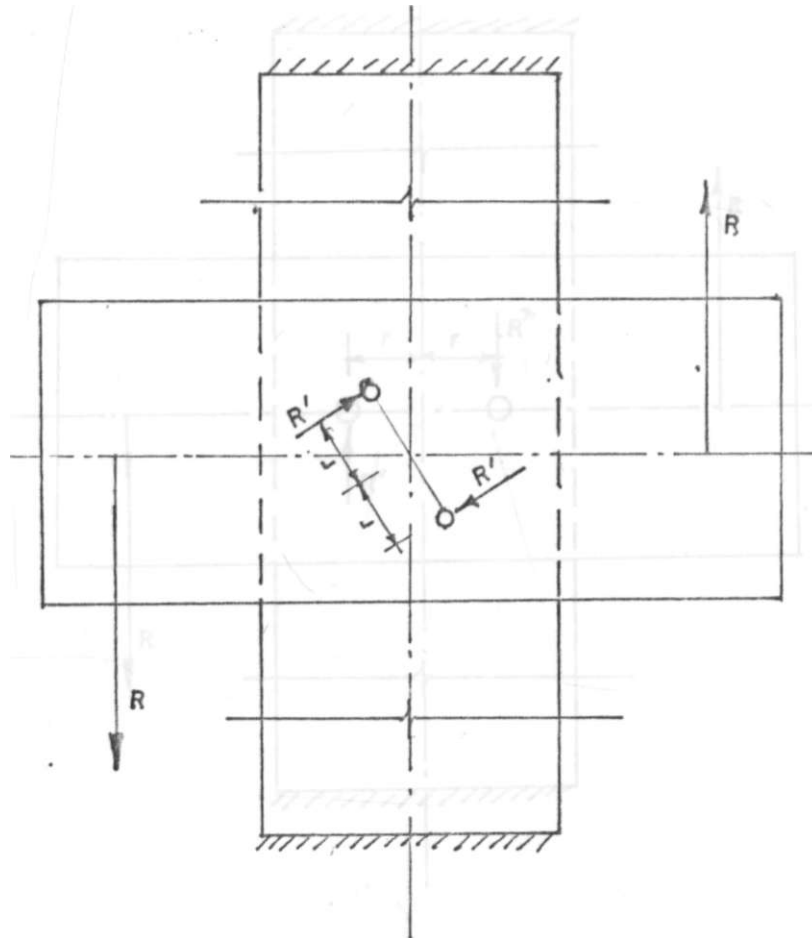


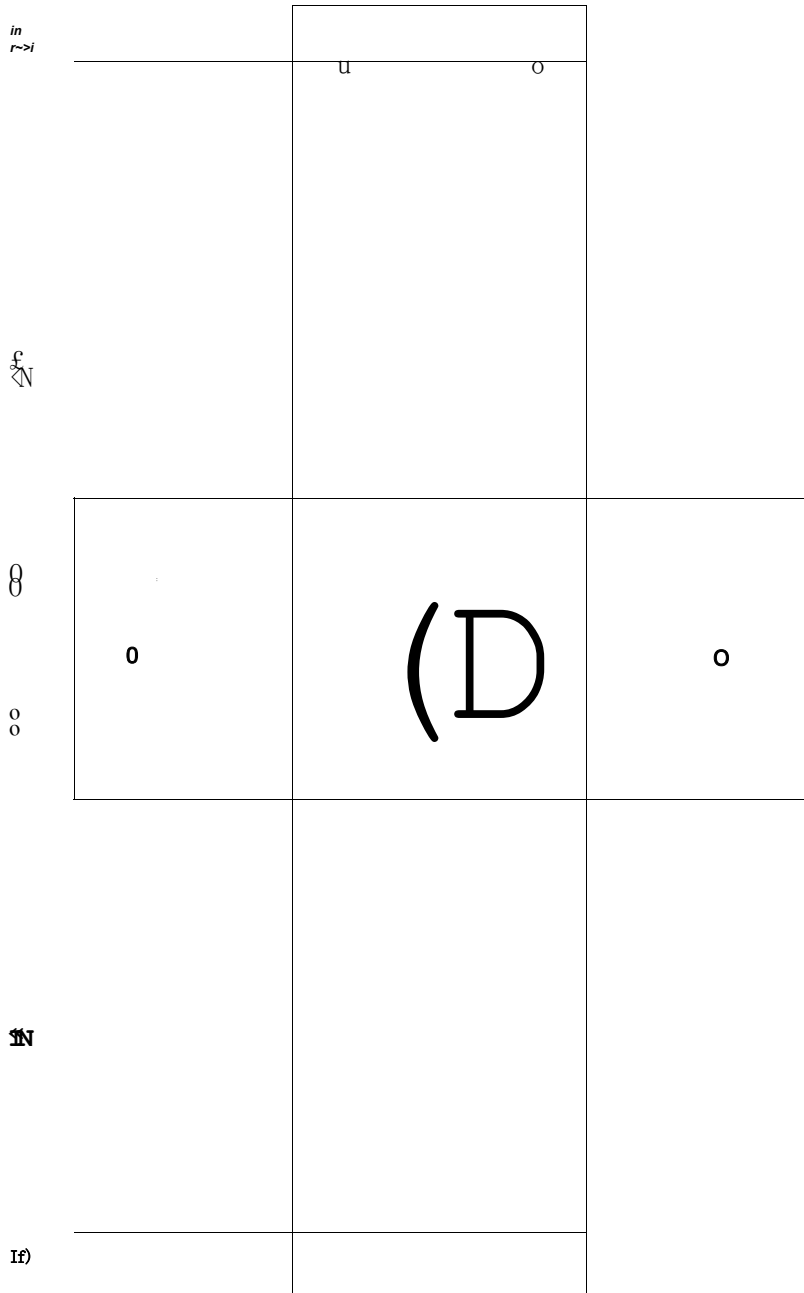
Figure 5.10 Forces acting on 8mm diameter bolts.

-G- -Q-
R'

77777777. 77777777

Figure 5.11 Forces acting on 10mm diameter bolts

130



Lb)

500

-2M-

200

H -
50.

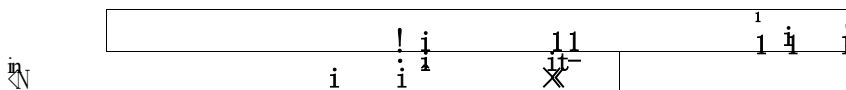
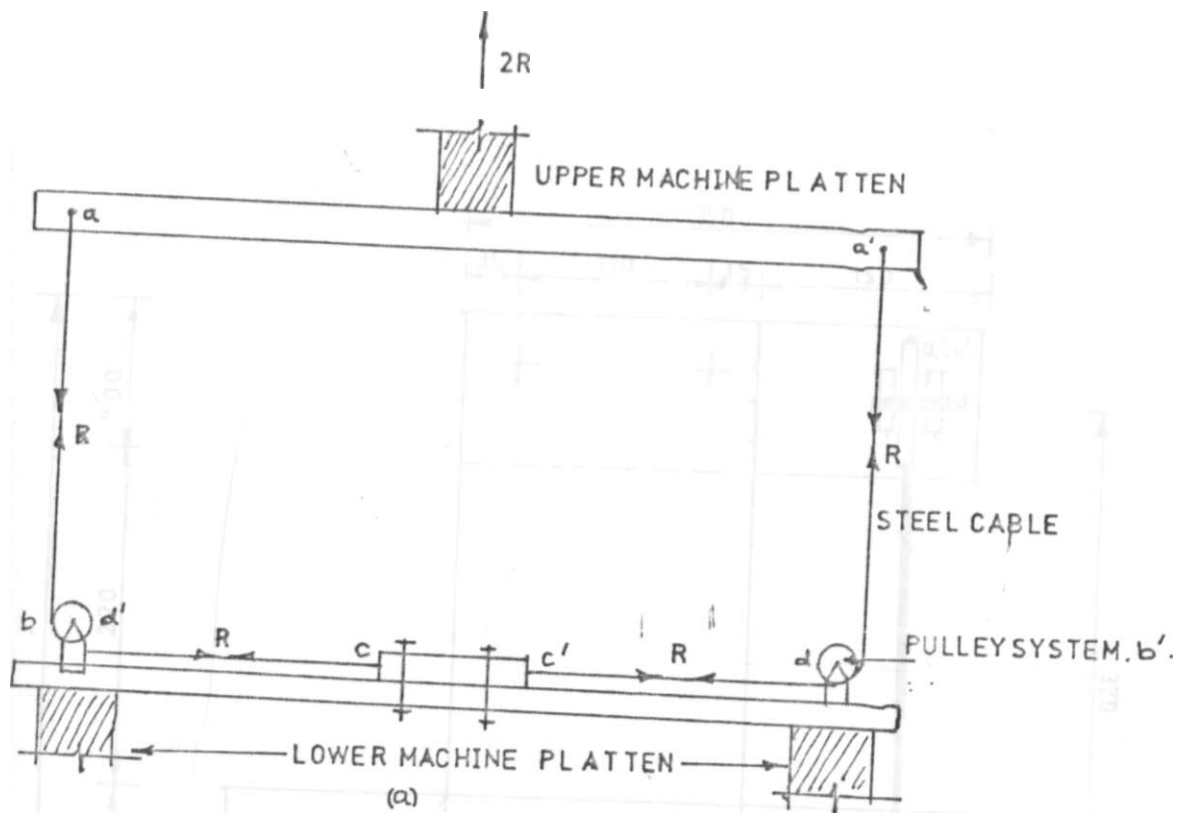


Figure 5.12 Multiple bolt specimen for connector properties.

(a) front view (b) side view. scale: 1:5



8 (X)

G ft J

77J7m

Figure 5.13 General test set up for pure rotational tests

- (a) Front view of test set up;
- (b) Top view of test joint assembly (excluding testing machine)

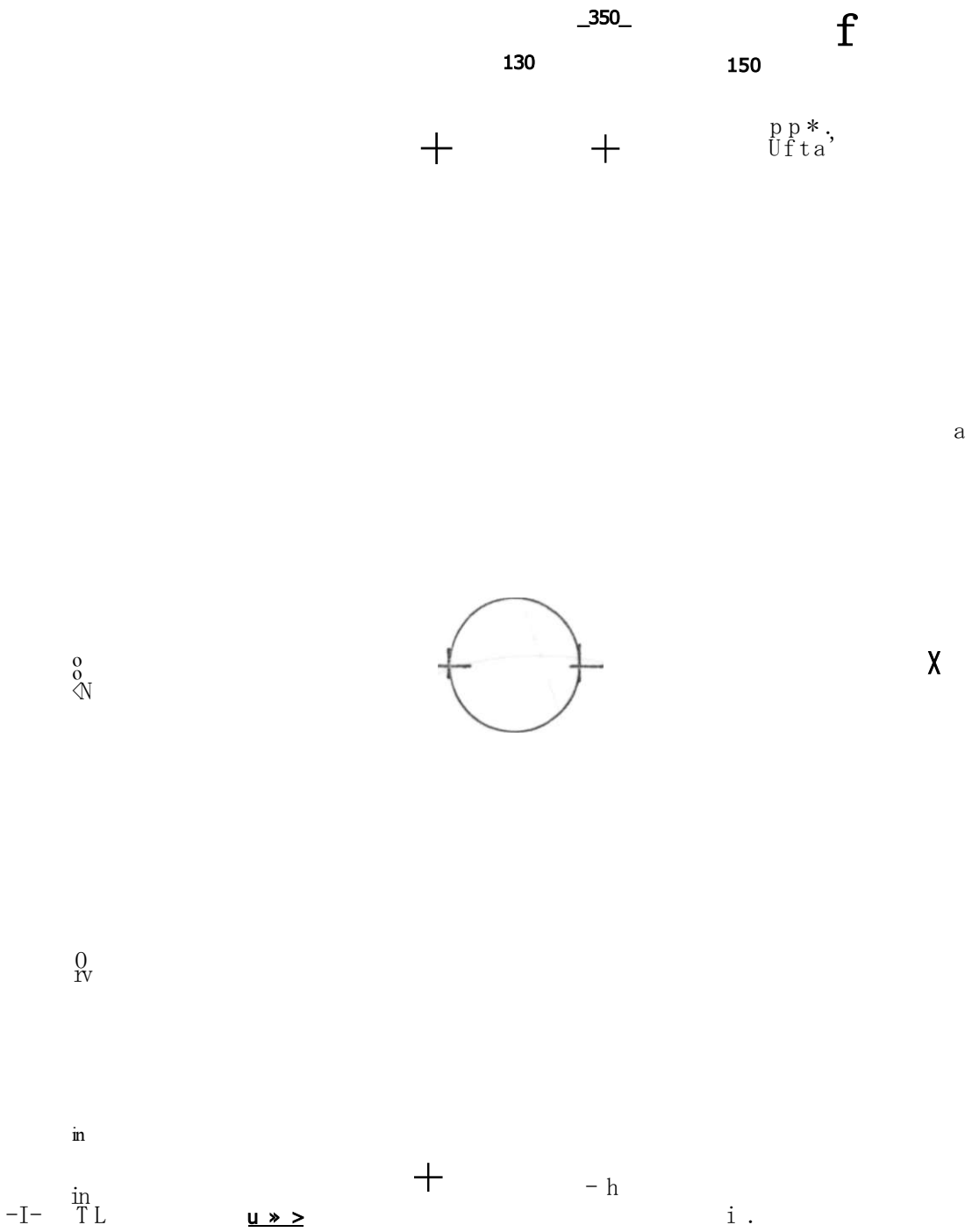


Figure 5.14 Detailed testing set up for rotational tests
Top view

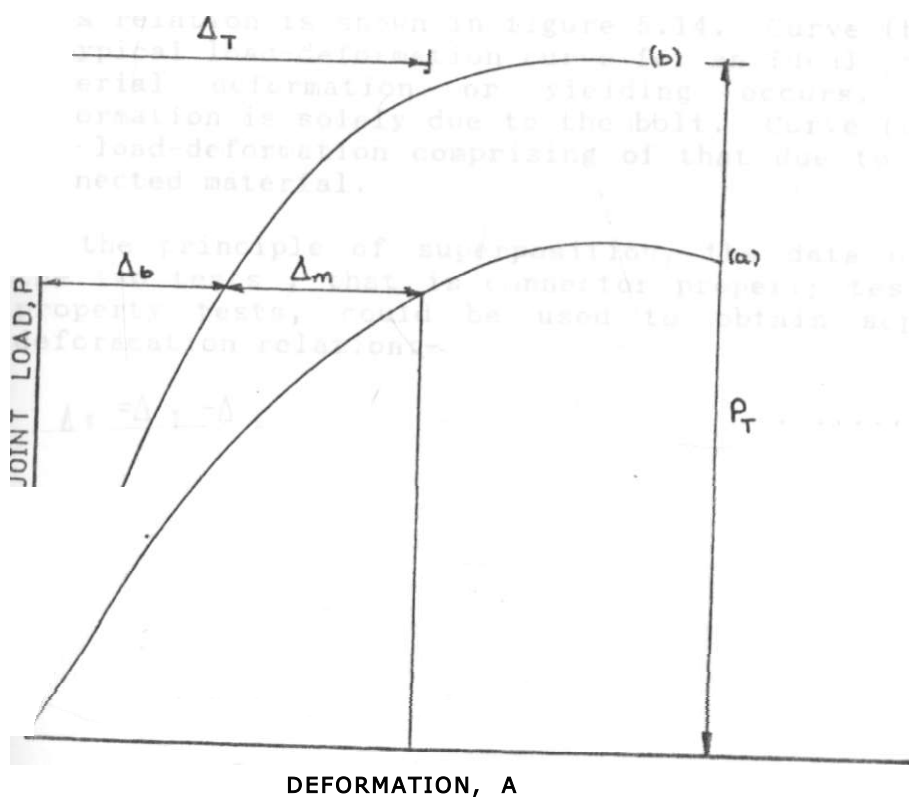


Figure 5.15 Load-deformation curve component'

5.6 Load-deformation curve components

During the testing of the joints in both pure shear and pure rotation, the load deformation curves obtained had several contributory components to the deformation and even the loads. These components were:-

- (i) deformation in the connection material of the test joint. This occurs despite the assumption that the connected parts were rigid
- (ii) the deformation in the bolt $\hat{\quad}$ thus the total deformation, as recorded can be aptly presented as:-

$$A_t = A_b + A_b$$

This relation is shown in figure 5.14. Curve (b) represents a typical load-deformation curve for an ideal joint where no material deformation or yielding occurs. Thus the deformation is solely due to the bolt. Curve (a) represents the load-deformation comprising of that due to the bolt and connected material.

By the principle of superposition, the data obtained from the two tests, that is connector property tests and joint property tests, could be used to obtain separate load-deformation relation:-

$$A_t = A_b + A_b \quad \dots \dots \dots [5.8]$$

CHAPTER SIX
ANALYSIS OF EXPERIMENTAL DATA.

6.1 INTRODUCTION.

Analysis of experimental data provides a basis by which the success or failure of an experimental programme may be evaluated. The knowledge derived from such an analysis helps in making proper decisions as concerns the problem being investigated. The credibility of the basic design of the experiment and reliability of the measured data comes to the fore during such analysis. This also provides force for critical review of basic assumptions made during the original design and execution of the programme.

Competent experimental data analysis makes use of certain mathematical tools whose development leads to application of specific techniques to data, and errors accompanying such measurements.

A major goal of this chapter is to compare the experimental data with that predicted using the non-linear mathematical models of chapter 4.0. This will involve the following aspects of data analysis:-

- (i) utilization of methods, logic and tools of data analysis.
- (ii) determination of the relationship between the measured data and the predicted data vis-avis the experimental program design and execution.
- (iii) evaluation of the validity of the assumptions made at both the experimental and predictive stage.

6.2 Schemes of analysis of experimental data

The scheme of analysis of experimental data for pure shear test joints is outlined in Appendix D. This appendix also contains the analyzed test data and corresponding graphical plots of these data for each of the five test joints as well as the averaged data.

A scheme of analysis of data obtained from pure rotation test joints is given in Appendix E. Also included are the graphical plots of the individual joints tested as well as the averaged data.

Appendix F contains the absolute error comparison by averaging technique as outlined in section 6.4. Appendix G contains the analysis using the principle of superposition as applied to the data obtained from

connector property tests and joint property tests, as outlined in Equation 5.4 of chapter 5.0.

6.3 Failure modes in the test joints

The experimental work carried out was at two levels of investigation:-

- (i) connector property tests, and
- (ii) joint property tests.

In the former, yielding was allowed to take place, only in the connectors, thus failure occurred in the bolts by bending of the bolt shafts as a result of the shearing action of the applied joint load. Plate 6.1 shows typical failure modes of the connectors in both loading cases.

In the latter case, joint specimen failed primarily due to the combined action of :

- (i) crushing of the connected material in the vicinity of the bolt hole as a result of the bearing action of the bolt; and
- (ii) bending of the bolt shafts as a result of shearing action of the applied joint load.

Typical joint failure are shown in plate 6.2 to 6.7. These joint failure patterns and the conditions leading to their occurrence are discussed in the next chapter.

6.4 Comparisons of predictive model data and experimental data.

In the analysis of the load-deformation and or moment-rotation experimental data for the connectors and joints tested under pure shear and pure rotation, two non-linear mathematical models were used to predict the experimentally obtained data. The models were:-

- (i) exponential non-linear model, and
- (ii) inverse Ramberg-Osgood non-linear model. Comparison of the experimental data and model predicted data was done according to a scheme used by Mutuku et al [30].

The closeness of the predictive model data and experimentally generated data was analyzed by use of an error function, $E_j(\%)$. This function may be defined for each model as shown in figure 6.1.

The error $E^{\wedge}(\%)$, is the absolute deviation of the predicted joint load, " P_j (load or moment), from the experimentally measured load, P_{mi} , at a given joint deformation (displacement or rotation). i.e

$$E^{\wedge}(\%) = 100 \text{ ABS} \left(P_j - \frac{P_{mi}}{P_j} \right) \quad [6.1]$$

The error, E_j , associated with the fitting of each model to the entire experimental data may be calculated by averaging absolute errors.

$$E_j(\%) = \frac{\sum E_i(\%)}{N} \quad [6.2]$$

Where $E^{\wedge}(\%)$ is the summation of absolute error at displacement.

N is the number of displacement levels in the entirety of the experimental data.

The non-linear models used had the errors associated with them at each deformation level calculated and compared.

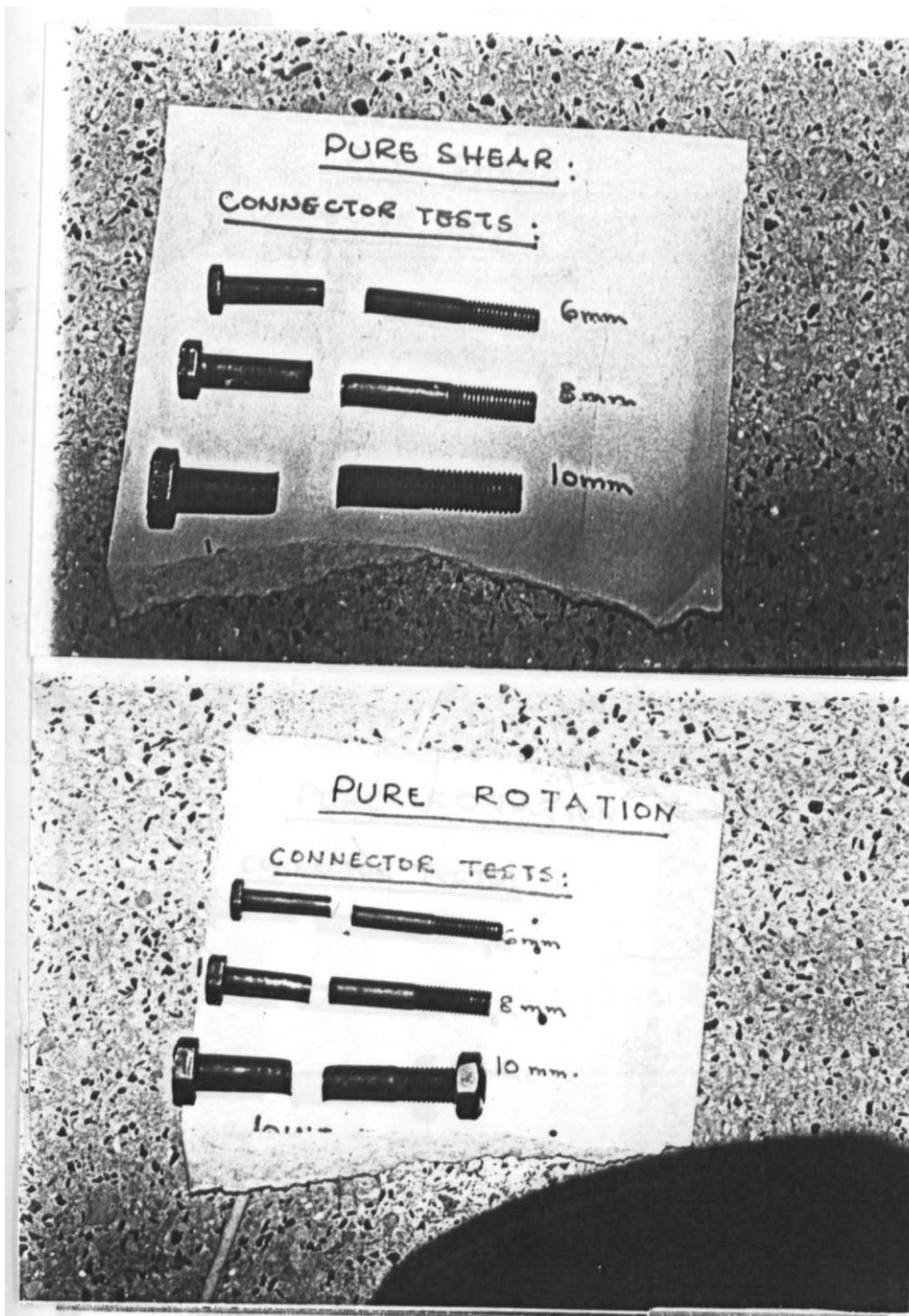


Plate 6.1 Bolt failure in tests on connectors

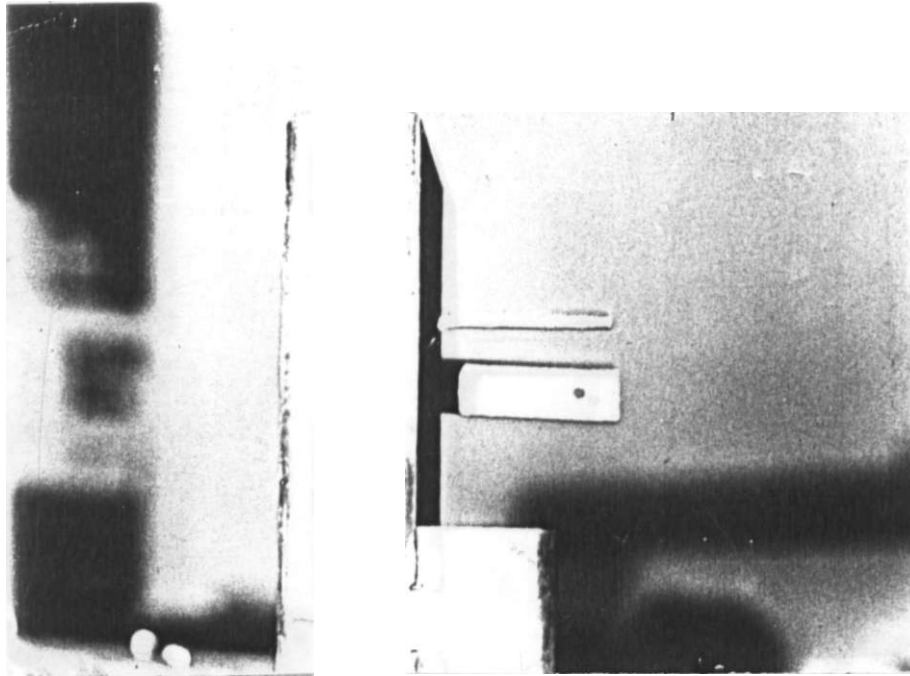


Plate 6.2 Typical bolt deformation for joints in pure shear.

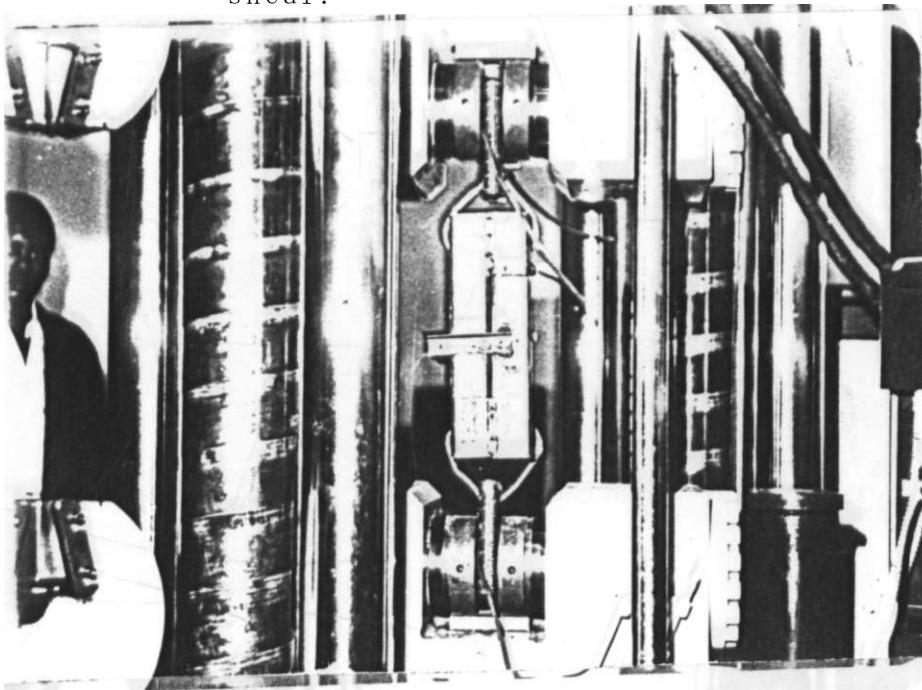


Plate 6.3 Side view of pure shear. " . t ri« showing iocatlon of shear planes and roller guides.

put. 6.4 Pure shear test rig showing locations of test bolt

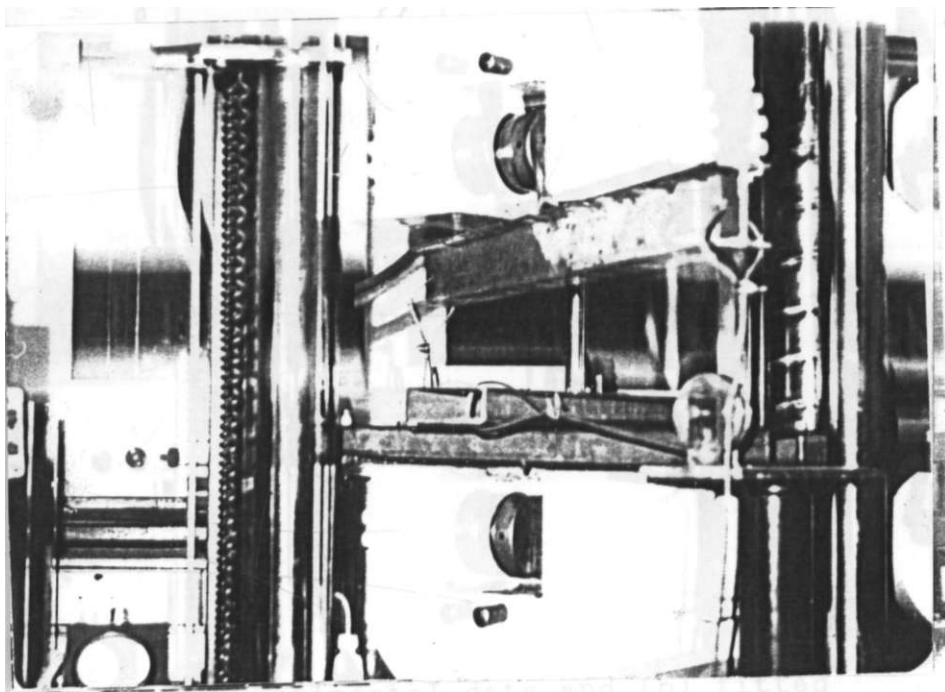


Plate 6.5 **Pure**-rotation test rig showing pulley and cable system.

\ AJ DEFORMATION, A '

Figure 6.1 Schematic representation of errors between:

(a) experimental data and (b) fitted
mathematical model [30]

The comparison of the error analysis in fitting the mathematical models to experimental data are shown in Appendix F.

The load percentage errors calculated using equation [6.1] and [6.2] may exaggerate the actual joint load errors in relative percentage ratio, especially at low joint displacement levels as shown in figure 6.1.

Consider errors E_i and E_j which are absolute deviations of the predicted joint loads, P_{ij} from experimentally measured joint loads, P_i and P_j at two deformations i and j i.e

$$E_i(\%) = 100 \text{ ABS} \left(P_i - \frac{P_{ij}}{V} \right) \quad [6.3]$$

$$E_j(\%) = 100 \text{ ABS} \left(P_j - \frac{P_{ij}}{V} \right) \quad [6.4]$$

If it is assumed that the absolute joint loads, $\text{ABS}(P_{Bi} - p_i)$ and $\text{ABS}(P_{Bj} - p_j)$ at these two displacement's are equal and further that V_j is greater than V_i , then the experimental load level P_{ij} will be greater than P_i . It follows from equations [6.3] and [6.4] that the percentage error E_i for the same relative joint load magnitude $\text{ABS}(P_{Bi} - p_i)$ and $\text{ABS}(P_{Bj} - p_j)$ respectively.

In order to afford an alternative technique for comparing the errors between the predictive models and the experimentally generated data, the following algorithm was used to calculate the absolute errors in fig. 6.1.

$$E(\%) = \text{ABS} \left(P_{ti} - \frac{P_{pi}}{V} \right) \quad [6-5]$$

$$E_{cc} = \frac{1}{n} \sum_{i=1}^n (2 E_i) \quad [6-6]$$

The term in equations 6.5 and 6.6 have the same meanings as in equations 6.1 and 6.2. The results obtained using equations 6.5 and 6.6 are presented in tables 6.1 to 6.4.

Plate 6.6 Pure shear set up showing pulling system
attachement.

Table 6.1 Load errors, Kn, in fitting models to data for connectors loaded in shear.

BOLT DIAMETER (MM)	MODEL	
	EXPONENTIAL MODEL	INVERSE RAMBERG-OSGOOD
6	0.64	0.92
8	0.47	0.45
10	0.95	0.46

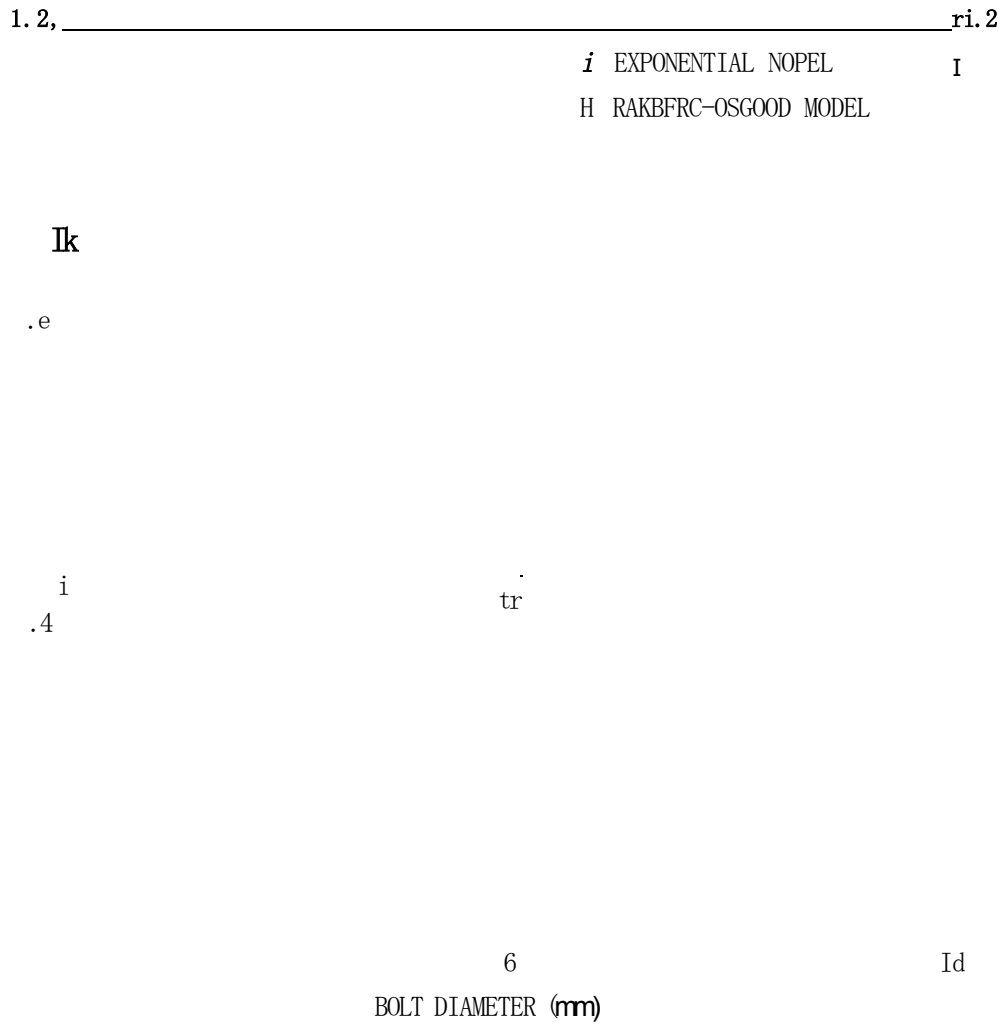


Figure 6.2 Average cumulative load errors, E'' , for connectors loaded in pure shear.

Table 6.2 Moment errors, E , K^{NI} in fitting models to data for connectors loaded in pure rotation.

BOLT DIAMETER (MM)	MODEL	
	EXPONENTIAL MODEL	INVERSE RAMBERG-OSGOOD
6	0.141	0.100
8	0.632	0.54
10	0.369	0.179

i exponential model
D KAMBERC-OSGOOD model

u

$\frac{n}{vCK}$

I 4
i

at

19
10

BOLT CI ft METER (hk)

Average cumulative moment errors, E^v
for connectors loaded in pure rotation,

Table 6.3 Load errors, $K\%$ in fitting models to data for connections loaded in pure shear

BOLT DIAMETER (MM)	MODEL	
	EXPONENTIAL MODEL	INVERSE RAMBERG-OSGOOD
6	0.520	0.160
8	0.830	0.276
10	0.872	0.373

1 EXPONENTIAL MODEL
D RAMBERG-OSGOOD MODEL

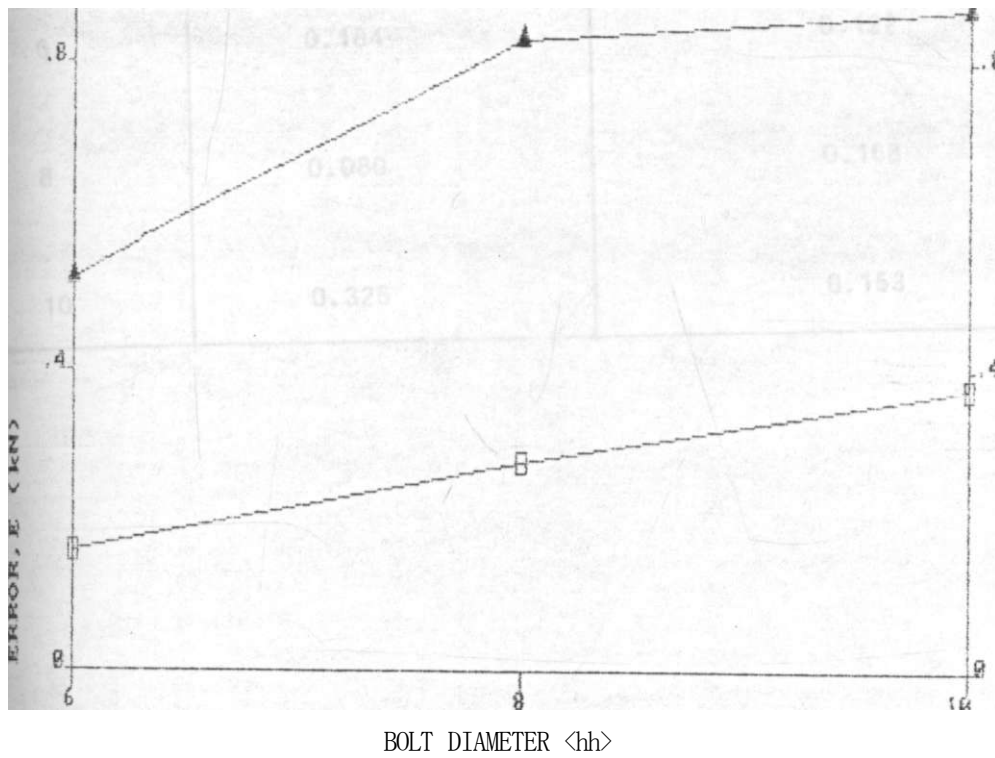


Figure 6.4 Average cumulative load error, E_c , for connection loaded in pure shear,

Table 6.4 Moment errors, $E_c K^{N1}$ for fitting models
to data for connections loaded in pure rotation

BOLT DIAMETER (MM)	MODEL	
	EXPONENTIAL MODEL	INVERSE RAMBERG-OSGOOD
6	0.184	0.122
8	0.080	0.168
10	0.325	0.153

1.2,

k IWONENTJAL KOIDEI
Q RAMBERG-OSGOOD MODEL

A
f
l

a
o
f
t
hi

fl-

16

BOL1 DIAMETER (hh)

Figure 6.5 Average cumulative moment errors, E^c ,
loaded in pure rotation,

The graphical plots of these absolute error values as shown in figures 6.2 to 6.5 were then used, in conjunction with the percentage error values obtained by use of equation 6.1, to rank the non-linear models in terms of their suitability to predict the load-deformation/moment-rotation curves for the 6mm, 8mm and 10mm bolts.

CHAPTER SEVEN

DISCUSSION

7.1 INTRODUCTION

Despite the importance of bolted connections in the overall economy of structural systems, their application has been constrained by lack of knowledge on their real behaviour and of data relating to connection strength and stiffness. Structural analysis will only adequately describe real structural behaviour when there is an incorporation of actual behaviour of the structural systems in terms of the connections employed. Against this background, this research aimed at initiating a consistent accumulation of data on the real behaviour of bolted connections which could be latter incorporated into structural analysis. This was done by use of non-linear mathematical models to predict the connection behaviour and then compare the results with experimentally obtained data for connectors and joints under pure shearing and pure rotational loading.

7.2 Basis for selecting mathematical models

The basic characteristic describing the structural behaviour of bolted connections is the load-deformation curve. In the process of determining the load deformation characteristics of bolted connections two mathematical models could have been used. The first of these is normally carried out in conjunction with an experimental investigation of a particular connection type. An elastic or plastic analysis of the typical connection needs to be conducted, often incorporating phenomena observed during the experimental investigation. This could have led to one or more expressions involving factors specific to the connections tested being derived as approximate representations of the curves depicting the load-deformation relationships.

The second approach is a more general one which finds application to any connection type for which appropriate experimental load-deformation data are available. The geometric factors that most strongly affect the load-deformation behaviour are first identified, and then comparative experimental data used to isolate the effect of each parameter in turn. A convenient form of non-linear mathematical function is then chosen to model the actual load-deformation behaviour and a regression analysis performed to fit the function to the available experimental data. This latter modelling approach was used during this research. But the model for use was only chosen after it had been proved that it satisfied the non-linear model requirements as set out in section 5.4.1.

The mathematical models chosen had only three parameters to be investigated. These parameters were found to be dependent on:

- (i) fastener type and size, and
- (ii) type of material.

For the exponential model (Equation 4-30),

$$T = T_0 \{1 - \exp[-(K_i + CA)A] / T_0\} \dots \dots \dots [7.1]$$

the parameter T_0 is dependent on the material in the joint, steel plate or (RHS). Parameters K_j and C are also dependent on the same. For the Ramberg-Osgood model (equation 4.36),

$$T = KA / [1 + (KA / T_0)^n] T(1/n) \dots \dots \dots [7.2]$$

parameters T , K , and n are dependent on the material type. Thus the mathematical models chosen had only two parameters to be investigated, namely material type and material size. As indicated in section 4.6.2.1 and 4.6.3.1 these model parameters were easily obtained from the experimental data.

This aspect made the models easy to apply during the research.

7.3 Material stress-strain characteristics.

Before evaluating the behaviour of bolted structural connections, the behaviour of the component parts ought to be determined. The static strengths of both the bolts and connected material were determined by coupon tests of material obtained from the same stock as those used during the research.

7.3.1 Bolts

Figures 7.1, 7.2 and 7.3 are graphical plots of the averaged stress-strain data for the 6,8 and 10mm bolts respectively. Table 7.1 gives the important material properties which have been derived from the graphical plots according to procedures of section 2.2.1. Appendix G contains the averaged data from which these plots have been made. Compared to the theoretical plots of ideal coupons of mild steel stress-strain curve, the three curves (fig. 7.1, 7.2 and 7.3) exhibit no definite yield point. This means that the residual stress effects due to either the manufacturing Process or the specimen fabrication process have affected the final stress-strain curve by removing the humped Portion. This can be seen by comparing figures 2.1, 7.1, 7.2 and 7.3.

Table 7.1 Characteristic values from stress-strain curves.

TEST	TENSILE		
	BOLT DIAMETER (MM)		
	6	8	10
young's modulus E (kN/sq.mm)	205	193.3	197.0
Tensile strength (N/sq.mm)	490	541	550
0.2% proof stress (N/sq.mm)	325	375	455
% elongation	21.5	21.5	22.5

The elastic modulus values obtained compare favourably with the average values in codes of practice. The low values for the 8 and 10mm bolts can be attributed to the imperfection effects due to manufacturing processes on the stress-strain curve.

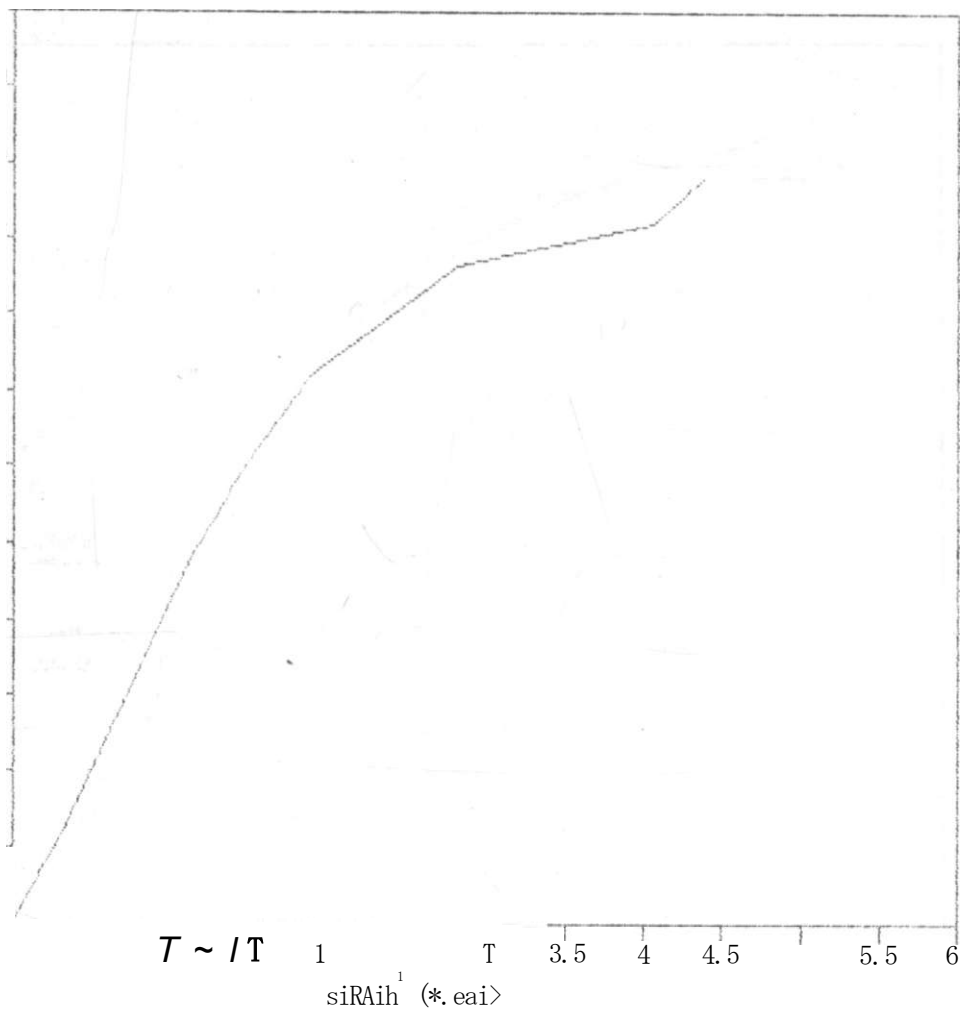


Figure 7.1 Stress-strain curve for 6mm bolt, (data app. G, Tab. G.1)

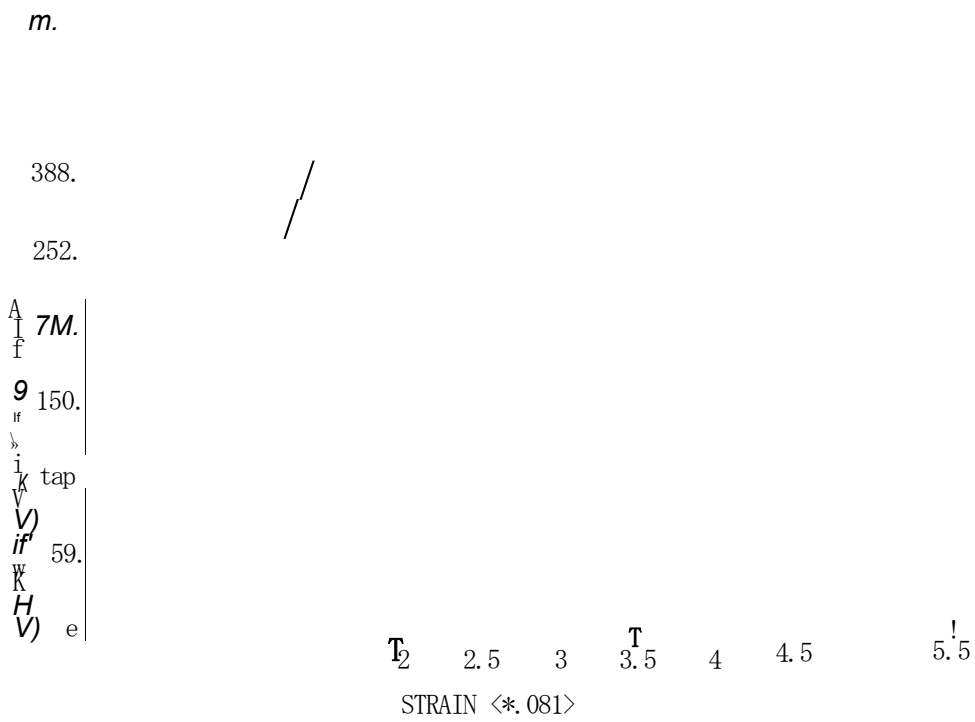
tee

//

/

SIRKIN (*, 831)

Figure 7.2 Stress-strain curve for 8mm bolt (data app. G,
Tab. G.2)



Fig(jgure 7.3 Stress-strain curve for 10mm bolt, (data G, Tab. G.3)

7.3.2 Joint material (RHS)

Figure 7.4 shows the stress-strain curve for the test coupon obtained from the the RHS used during the research. Table G.4 gives the experimental data obtained during the tests. From figure 7.4, the elastic modulus of the RHS coupon is 204 KN/sq.mm which compares well with the given range of this value of 200 - 210 KN/sq.mm in codes of practice. The 0.2% proof stress value of 285 N/sq.mm is slightly higher than the recommended value of 275 N/sq.mm. The ultimate tensile strength value of 485 N/sq.mm is also slightly higher than the recommended value of 430 N/sq.mm. The shape of the curve is such that there is no pronounced yield point, indicating a possible residual stress effect. Generally the strength characteristics of steel depend on the carbon content. Mild steel is expected to have a carbon content of 0.25% and an ultimate tensile strength of 450 N/sq.mm. On the whole, the data obtained from the coupon test indicate that the material is brittle to some extent making it unsuitable for use in the plastic design approach. This is mainly because the stress-strain curves obtained can be idealised to the form generally adopted for plastic design. The results obtained are a reflection of the quality of steel available on the market which is not to B.S.4360 specification, as most of it is recycled.

7.4 Pure shear load-deformation curves.

The main objective of these tests was to establish the load-deformation relationships of both the connectors and joints. The non-linear mathematical models of chapter 4.0 (equation 4.30 and 4.36) were used to predict the load-deformation curves of the same and comparisons made between the experimental and predicted results. The principle of superposition was then applied to the data obtained experimentally to determine the relative contribution of the joint material under load.

7.4.1 Connector load-deformation curves

Figures 7.5, 7.6 and 7.7 show the graphical plots of the experimental and non-linear model load-deformation curves for the 6, 8 and 10mm bolts loaded in pure shear. During the research, there were some related observations for each bolt size which are discussed briefly in the following sections.

7.4.1.1 Initial slip

Each of the five test specimens for the 6, 8 and 10mm bolts underwent some initial slip on application of load to the testing rig. Thus before the experimental data was analysed

and the models fitted, the value of initial slip for each test specimen was corrected for by assuming that actual load resistance by the bolt started after the initial slip had taken place. This phenomena of slip could be traced to the raelignment of the testing rig components on load applications, so that they lie in the same plane as the applied load. Another contributory aspect to this slip is the fact that the bolts were only hand tightened in order to offset the effects of friction in their application. This was so because the models used in the research did not take account of friction in their application. The bolts were also only hand tightened so as not to introduce initial pre-load in them. The tightening was such that there was sufficient clamping force being transmitted by the bolt onto the connected parts. Thus on loading, and with the ensuing alignment, some play was introduced as the system sought an equilibrium state of the clamping force before load resistance by the bolt started.

After this alignment and clamping force, the subsequenat deformation was due to the applied load acting on the bolts. Table 7.2 shows the relative initial slips for each bolt size tested.

Table 7.2 Initial slip values for 6,8 and 10mm bolts tested in pure shear.

BOLT DIAMETER (mm)	SLIP (mm)	LOAD LEVEL (kN)
6	0.2	2
8	0.1	3
10	-	-

The 6 and 8mm bolts underwent appreciable slip. Usually after slip the load in the test speciment starts being transmitted by bothe shear and bearing. This is because initially most of the applied load goes into resisting the frictional forces between the connected parts. Thus lack of initial slip in the 10mm bolt specimen indicates that the bolt went into bearing soon after application of load. The significance of slip and it's importance of failure loads is dealt with in the next section. The magnirudes of the slip values and the loads at which they occurred in the 6 and 8mm bolts were nearly the same signifying that the two bolt sizes were bearing against the test rigs at same load levels.

STRESS-STRAIN CURVE FOR RHS COUPON

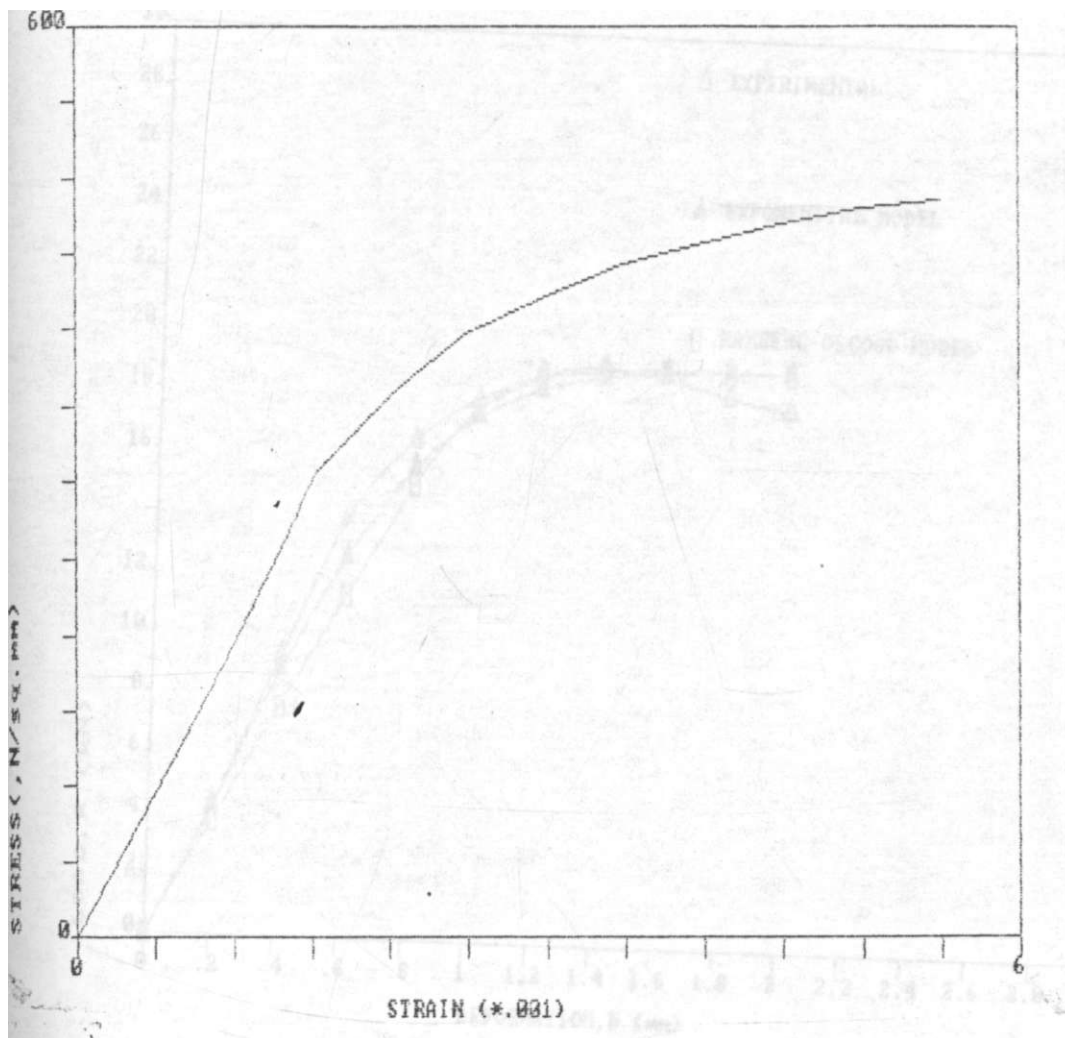


Figure 7.4 Stress strain curves for RHS coupon
(data app. G, Tab G. 4)

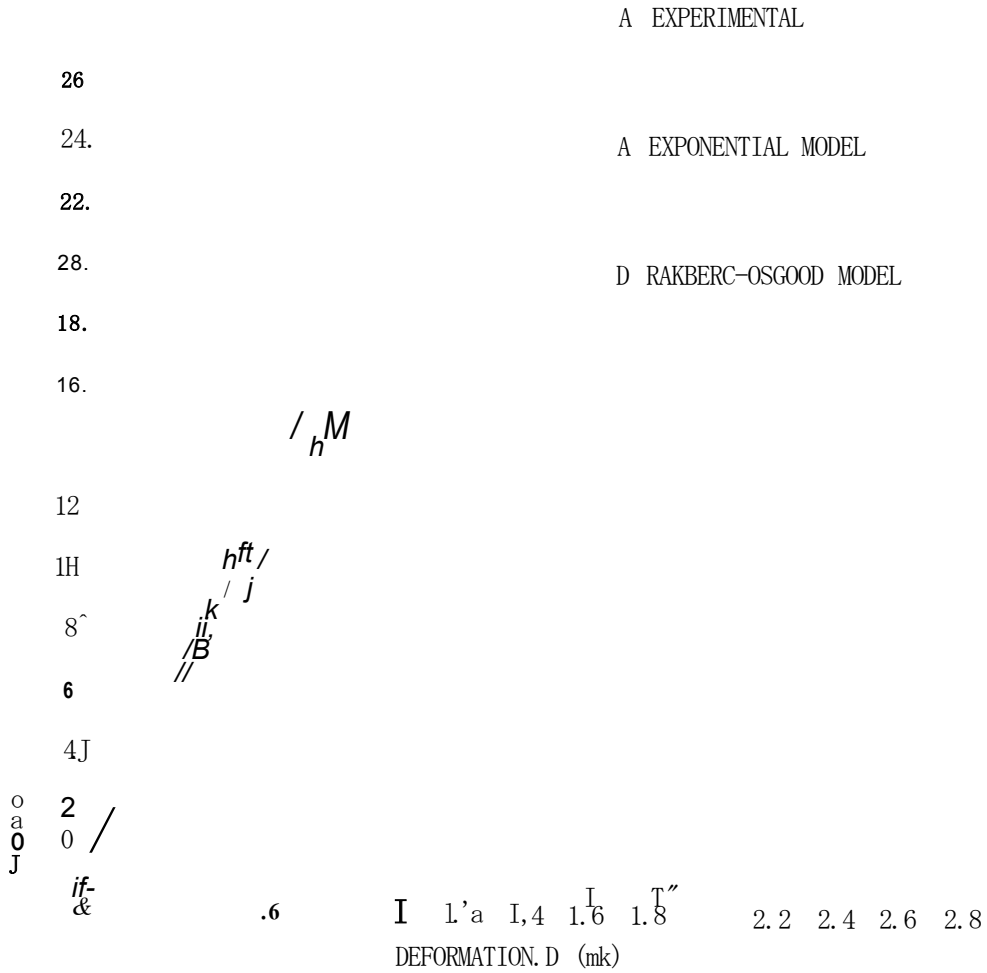
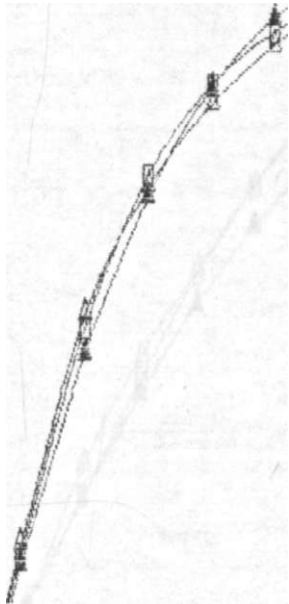


Figure 7.5 Load-deformation curves for 6mm bolts tested in pure shear (data app. D, Tab. D.1)

LOAD-DEFORMATION CURVES FOR 8 mm BOLTS IN SHEAR



▲ EXPERIMENTAL

— EXPONENTIAL MODEL

- - - RAMBERG-OSGOOD MODEL

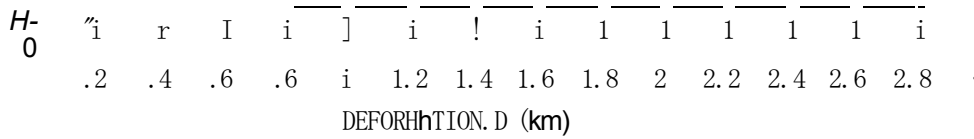
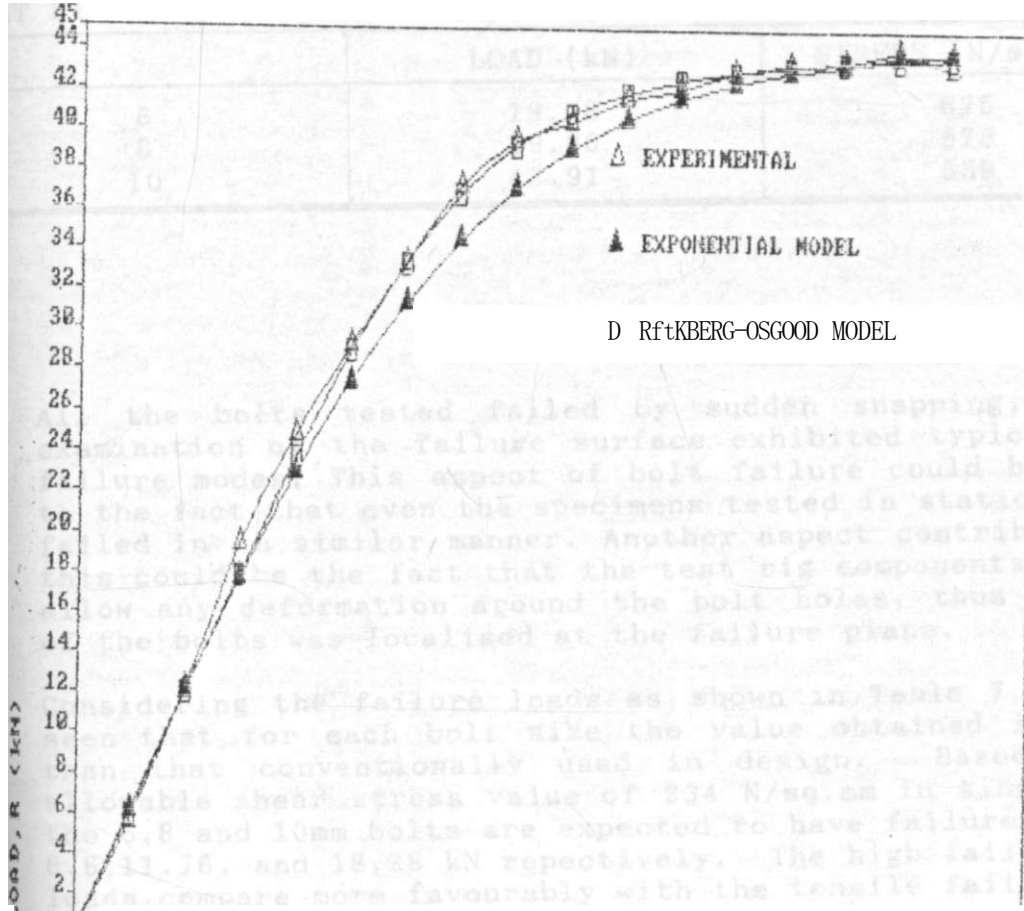


Figure 7.6 Load-deformation curves for 8mm bolts tested in pure shear. (data app. D, Tab. D.2)

LOAD-DEFORMATION CURVES FOR 10 mm BOLTS IN SHIM



f "I .4 ,8 1 1!_ 1VjTTlle i 2'2 2.4 2.6 2.1 3.2 3.45
 DEFORMEILLON ,D (*h)

Figure 7.7 Load-deformation curves for 10mm bolts,
 (data app. D, Tab. D, 3)

7.4.1.2 Failure loads

Table 7.3 shows the failure shear loads and corresponding stresses at which the bolts failed.

Table 7.3 Failure loads/stresses for the bolts

BOLT DIAMETER (mm)	FAILURE	
	LOAD (kN)	STRESS (N/sq. mm)
6	19.08	675
8	29.30	578
10	43.91	559

All the bolts tested failed by sudden snapping, but on examination of the failure surface exhibited typical shear failure modes. This aspect of bolt failure could be traced to the fact that even the specimens tested in static tension failed in a similar manner. Another aspect contributing to this could be the fact that the test rig components did not allow any deformation around the bolt holes, thus yielding of the bolts was localised at the failure plane.

Considering the failure loads as shown in Table 7.3, it is seen that for each bolt size the value obtained is higher than that conventionally used in design. Based on the allowable shear stress value of 234 N/sq.mm in single shear the 6,8 and 10mm bolts are expected to have failure loads of 6.6, 11.76, and 18.38 kN respectively. The high failure shear loads compare more favourably with the tensile failure loads of Table 7.1. These loads (Table 7.3) lead to shear stress values higher than those for single shear of 234 N/sq.mm and closer to the bearing stress value of 701 N/sq.mm. This indicates that bearing failure had a greater contribution than shear in these tests. This is even reflected in mode of load resistance of combined shear and bearing soon after slip occurs. The chances of either of these load resistance modes causing failure depends on both the connector and connected material. In this case no yielding was allowed to take place in the connected parts hence the bolt resisted

the load applied by bearing against the connected parts. This aspect might have contributed significantly to the high failure load. $R_{SCC} = \frac{P}{A} \cdot \frac{d}{d_c}$

Considering figure 7.8 and Table 7.3, it is observed that the failure shear loads increased with bolt diameter. The same trend can be seen from Table 7.1 as pertains to the failure tensile loads. Theoretically an increase in bolt diameter or tensile strength is supposed to cause only a slight increase in failure shear loads with a corresponding decrease in deformation. The bolt deformation at which failure occurred also increased with bolt size, (see Fig. 7.8)

But considering the failure shear load ratios, that for the 10mm bolt is 2.3 times and 1.5 times that of the 6 and 8mm bolts respectively. The corresponding deformation ratios are: 0.46:0.6:1 for the 6, 8 and 10mm bolts respectively. The area ratios of the 10mm bolt to the 6 and 8mm bolts is 2.8 and 1.6 respectively. Thus there is closer correlation between the shear area and the failure load ratios than the tensile load ratios. This implies that the differences in the shear stresses or loads recorded are not as a result of the bolt diameter variation but due to the variation in the shear area ratios.

7.4.1.3 Modelling of experimental data

The two non-linear mathematical models of equations 4.30 and 4.36 were used in the prediction of the experimental load-deformation data from which the predictive data curves were plotted. Using the schemes of error analysis of chapter 6.0, the closeness of fit of the predicted results to the experimental data was evaluated. All the model parameters were determined from the experimental load-deformation curves as outlined in sections 4.6.2.1 and 4.6.3.1 of chapter 4.0.

7.4.1.3.1 Exponential model

The basic relationship used in the application of this model was:

$$R = R_0 \{1 - \exp[-(K_t + CA)A/R_0]\} \dots \dots \dots [7.3]$$

For the 6mm bolt, the empirical form of this equation was (see Tab. D.1) App. D):

$$R = 19.08 \{1 - \exp[-(19 + 26.07 A)A/19.08]\} \dots \dots \dots [7.4]$$

And for the 8mm bolt (see Tab. D.2, App. D)

$$R = 29.3 \{1 - \exp[-(45 + 23.7A)A J/29.3]\} \quad [7.5]$$

\hat{J} f i k P ~ 4-V 1 W~T 4 I rp "n o A^ T>#
 aiiu i x n a x x i u x u n c i . unit u u x t i o c c i a u . j . o j n p p . d ;

$$R = 43.91 \{1 - \exp L-(30 + 13.06A)A^3/43.91\} \dots [7.6]$$

The two important parameters in the description of the load-deformation curves are K_1 and C . Essentially, K_1 , which is the initial tangent stiffness, is an indicator of the resistance offered to the applied load by the bolts. High values of this parameter indicate high resistance to load and less deformation for given load levels. But this only applies to the initial linear portion of the curve. Parameter C encompasses both the linear and non-linear portions of the load-deformation curve. High values of this parameter indicate a more flexible system, whereas low values indicate a stiffer system. This value is seen to increase with bolt diameter as shown by equations 7.4, 7.5 and 7.6 for the 6, 8 and 10mm bolts respectively. Figure 7.8 shows the bolt load resistance, with the 10mm bolts having higher load resistance and less deformation,

From the data on cumulative load error analysis of Table 6.1 and Fig. 6.2, it is seen that this model predicted the 8mm bolt load-deformation curve better with an error of 0.47, followed by 6mm with an error of 0.64, and 10mm with an error of 0.95.

7.4.1.3.2 Inverse Ramberg-Osgood model

The Inverse Ramberg-Osgood model of the form:

$$R = KA / [1 + (KA / R_0)^n]^{1/n} \dots [7.7]$$

was used to model the non-linear load-deformation curves for the bolts tested in pure shear. Based on the methodology of parameter evaluation of section 4.6.3.1, the value of K and n were obtained from the experimental data for each of the bolts. K gave an indication of the load resistance of the bolt. Parameter n showed the rate of decay of the curve. Thus Parameter n was a better indicator of load resistance as it was capable of describing both the linear and non-linear load-deformation curve.

The empirical formulation of this model for the 6mm bolt was (see - D.1, App. D):

$$R = 19A / [1 + (19A / 19.08)^{8.5}]^{1/8.5} \dots [7.8]$$

For the 8mm bolt (see Tab. D.2, App. D):

$$R = 45A / [1 - (45A / 29.3) T^{2.5}]^{1/2.5} \quad [7.9]$$

And for the 10mm bolt (See Tab. D. ii, App. D) :

$$R = 30A / [1 + (30A/43.91)T^{4.5}]^{1/4.5} \dots \dots \dots [7.10]$$

The variation of the value of parameter n, from 8.5 to 2.5 to 4.5 for the 6,8, and 10mm bolts is an indicator to the resistance offered and the deformation undergone by each bolt at given load levels. Basically, the higher the value of n the higher the deformation and the lower the resistance offered at a given load level, whereas the lower the value n, the higher the resistance offered and the lower the deformation. This is reflected in the graphical plots of figure 7.8 for the bolt sizes tested. The break with the general trend for the 10mm bolt is traced to the fact that though the bolts tested failed in shear, there was a hairline split along the bolt axis in three of the test pieces. This signified a weakness in the bolt structure and the total effect was to reduce the average deformation at given load levels as compared to the 8mm bolt (also see section 7.8).

From Table 6.2 and fig. 6.2, the inverse Ramberg-Osgood model predicted the 8mm bolt curve with an error of 0.45, closely followed by the 10mm bolt with 0.46 and the 6mm bolt with an error of 0.92.

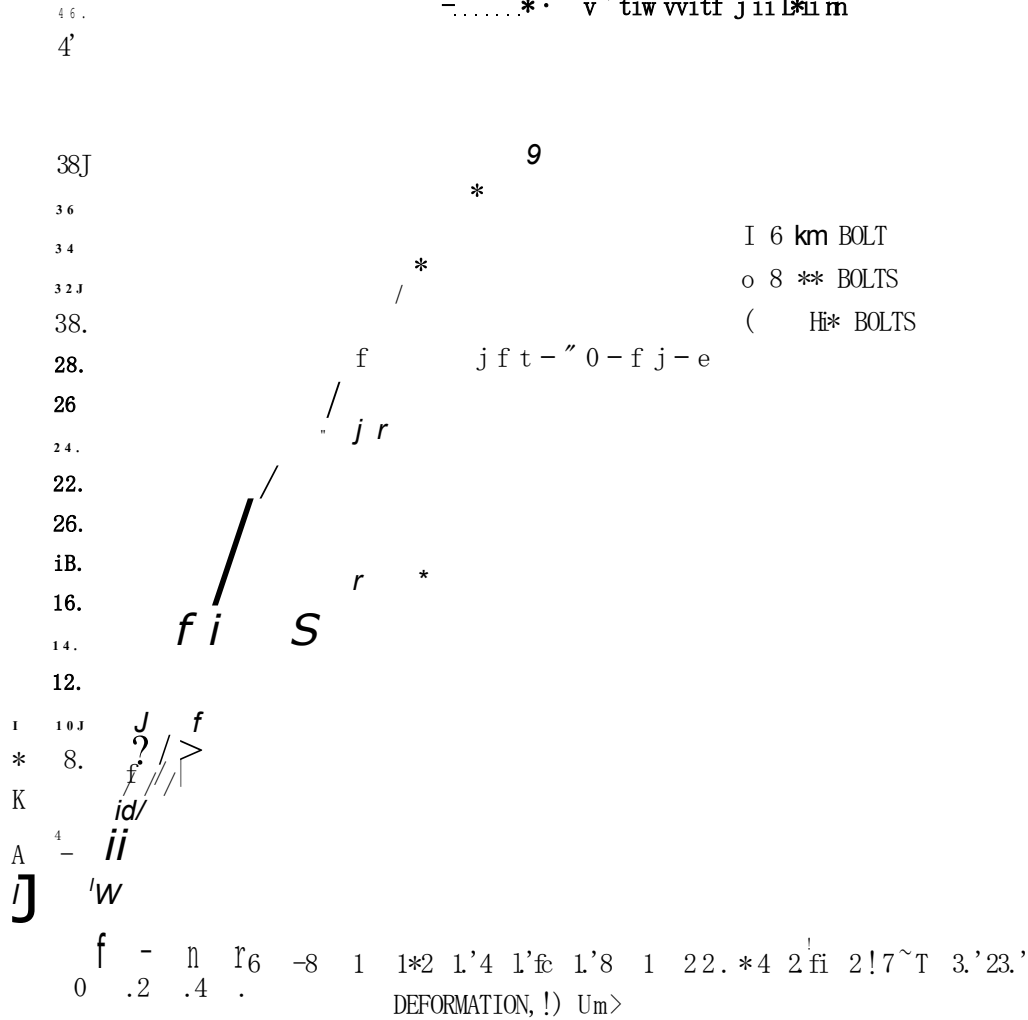


Figure 7.8 Comparative load-deformation curves for bolts tested in pure shear.

7.4.2 Joint load-deformation curves

Figures 7.9, 7.10 and 7.11 show the graphical plots of the experimental and non-linear model predictive data for the 6, 8, and 10mm bolted joint load-deformation curves. Figure 7.12 shows the comparative plots of the data for the three joints together.

7.4.2.1 Initial slip

Unlike in the case of the pure shear tests on the connectors, there was no initial slip recorded during all tests on the joints. The possible reason for this was because of the initial tension applied to the cables that were being used to load the test joints. This initial tension could have realigned the testing rig, and on resetting the loading devices for the actual testing to commence the joint started resisting load immediately. The same mode of load resistance, i.e by shear and bearing as in the case of connector tests was assumed.

7.4.2.2. Failure loads

Table 7.4 shows the loads at which the test joint assemblies failed.

Table 7.4 Joint failure loads in pure shear

BOLT DIAMETER (mm)	FAILURE LOAD (kN)
6	14.2
8	25.14
10	33.4

Compared to the shear failure loads for the connectors (see table 7.3), it is observed that in all cases joint material failure occurred. The corresponding deformations at particular load levels for the connector and the joint are appreciably different. This means that the joint material had a significant contribution to overall joint deformation (see section 7.10). Although the general conclusion is that the joint material failed before the bolt for the test joints, the observations during the testing indicated that the bolts had yielded by the time testing stopped for the 6 and 8mm bolt fastened joints. The 6 and 8mm bolt fastened joint behaviour indicates a combined action of the bolt and joint material in load resistance, as a result of which there was lowering of the joint failure loads below that of the individual fasteners. The failure load of the joints in shear for the 8mm bolt fastened joint was close to that of the individual bolt (29.3 for bolt and 25.14 for the joint), whereas that for the 6mm bolt fastened joint was 14.2 as

compared to 19.08 for the bolt alone. Although the differences in the failure loads for the two cases is the

advanced to explain the reduction in the failure loads for the joint. This is mainly because the interaction between the fasteners and the joint material is so complex that it cannot be explained by the simple principle of the mechanical behaviour of structural elements under load.

In contrast to the 6 and 8mm bolt fastened joints, the 10mm bolt fastened joint failed at a load value close to that for the bolt alone. This indicates that there was failure of the joint material long before the bolt failed. This is borne out by the fact that no appreciable yielding was observed in the 10mm bolts in these joints. It was also observed that the joint material had failed in bearing since there was piling of material around the bolt holes. Considering

Table 7.4 and Fig. 7.12, there was a tendency of increased deformation of the joint with increase in bolt diameter. This can be explained in terms of increased bearing action of the bolt against the joint material given the small wall thickness of the RHS used as joint material (4mm).

7.4.2.3 Modelling of experimental data

The two non-linear mathematical model forms of equations 4.30 and 4.36 were used to model the joint load-deformation curves obtained experimentally. The accuracy of model prediction of the experimental data was assessed by use of the load error analysis techniques of chapter 6.0

7.4.2.3.1 Exponential model

The basic form of this non-linear model as indicated in equation 7.3 was used to predict the experimental load-deformation curves for the 6, 8 and 10mm fastened joints loaded in pure shear.

For the 6mm bolt fastened joint, the empirical form of the model was found to be as (see table D.4, app.D)

$$R = 14.2 \{1 - \exp[1.4 + 0.17A)A/14.2]\} \dots \dots \dots [7.11]$$

From the data of table D.5, App.D, the empirical model for the 8mm bolt fastened joint was taken as:

$$R = 25.14 \{1 - \exp [-(2.25 + 0.259A)A/25.14]\} \dots \dots \dots [7.12]$$

For the 10mm bolt joint the model took the form (see table D. 6, App. D):

$$R = 33.4 \{ 1 - \exp[-(2.35 + 0.194^4)/33.4] \} \quad [7.13]$$

In terms of closeness of fit (see tab. 6.3 and fig.6.4), the model predicted the 6mm bolt joint better with an averaged load error of 0.52, followed by the 8mm bolt joint with an error of 0.830 and the 10mm bolt joint had an error of 0.872. Of importance to the modelling and explanation of joint behaviour are the two model parameters K_j and C . Considering tables in appendix D giving the numerical values of these parameters, it is seen that apart from the discrepancy in the value of K - for the 10mm bolt joint there is an increase of this value with the bolt diameter.

The value of parameter C was found to decrease with bolt diameter for the bolts alone but no consistent pattern could be discerned for the joints. This lack of consistency can be attributed to the fact that the combined action of the bolts and the material in resisting the applied loads was unique and complex as stated in section 7.4.2.1.

The decrease in the absolute values of K_j and C for the connectors and joints respectively can be traced to the increased deformation in the joints at the same load levels as for the fasteners.

7.4.2.3.2. The Inverse Ramberg-Osgood model

Table 6.3 and figure 6.4 show that the Ramberg-Osgood model of the basic form of equation 7.7, predicted the load-deformation behaviour of the 6mm bolt joint better with an averaged cumulative load error of 0.160, followed by 0.276 for the 8mm bolt joint and 0.373 for the 10mm bolt joint.

The empirical formulations of the model for the 6,8, and 10mm bolt joints, based on the parameter values in tables D.4, D.5, and D.6 of appendix D were:

$$R = 1.4A / [1 + (1.4A/14.2)^{13.5}] \quad (1/13.5) \quad [7.14]$$

$$R = 2.25A / [1 + (2.25A/25.14)^{15}] \quad (1/15) \quad \dots \quad [7.15]$$

$$R = 2.35A / [1 + (2.35A/33.4)^{11.5}] \quad (1/11.5) \quad [7.16]$$

Based on the data in the same tables in appendix D for both the connectors and joints, the parameters are seen not to

offer any consistent pattern, especially the value of n which is an indicator of the rate of decay of the curve. Basically the higher the value of n , the lower the rate of decay of the load-deformation curve. Based on this premise and the values in the tables in appendix D, it is seen that the value of n for the 8mm bolt joint was the lowest whereas it is the highest for the same bolt tested alone. But within limits of experimental error the values of parameter n are close enough indicating the same shape of curve for the joints. The reduction in the value of K is due to the increased deformation in the joint, whereas the same factor tends to increase the value of n . It is important to point out now that the values of the model are unique for each bolt size, since the mode of load resistance though generally the same for all bolt sizes, is also unique to each individual bolt (see sections 2.4.2.1 and 7.9).

7.5 Pure rotation Moment-Rotation curves.

The flexural moment-rotation relationships are the most important aspect of connection behaviour and practically all connection tests have concentrated on the determination of these properties. During this research, idealised pure rotation load application modes were assumed in order to reduce the many parameters affecting the moment-rotation curves of bolted connections (see section 1.2). The main objective of these tests was to determine the moment-rotation characteristics of both the connectors (bolts) as well as the joints in pure rotation. The non-linear mathematical models as given by equation 1.32 and 4.39 were used to predict the experimental moment-rotation curves for each bolt size and comparative analysis of accuracy of prediction done as outlined in chapter 6.0. The principle of superposition was applied to the data obtained to assess the relative contributions of both the bolt and joint material to the overall joint rotation.

7.5.1 Connector moment-rotation curves

Figures 7.13, 7.14, and 7.15 show the experimental and non-linear model predictive moment-rotation curves for the 6, 8, and 10mm bolts tested in pure rotation. Figure 7.16 is the plot of the moment-rotation curves of the three bolts sizes together. The general shape of the curves obtained is the same for each bolt size, exhibiting both the linear and non-linear portions, with a well rounded crest at the failure loads.

7.5.1.1. Failure moments

Table 7.5 shows the failure moments and corresponding loads being resisted by the bolts at failure. The moment and bolt resistance loads were calculated based on the schemes of analysis of appendix E.

Table 7.5 Failure moments and bolt load resistance values

BOLT DIAMETER (mm)	MOMENT (kNm)	BOLT LOAD (kN)
6	10.94	109.4
8	14.06	140.6
10	17.2	172.0

The observed trend is that of increasing failure moment with bolt size. The corresponding loads being resisted by the bolts are considerably high compared to those for the bolts loaded in pure shear, as shown in table 7.4. Ideally these two values are supposed to be the same bearing in mind that the mode of load resistance is by shear in both cases. But the load resistance by the bolts in either mode of loading is not linear, hence the principle of superposition cannot be liberally applied here.

The ultimate failure moment values are closely related to the bolt diameters. The bolt diameter ratios for the 6, 8, and 10mm bolts are 1: 1.33: 1.67 respectively, whereas the ultimate moment value ratios are 1: 1.28: 1.57 for the 6, 8,

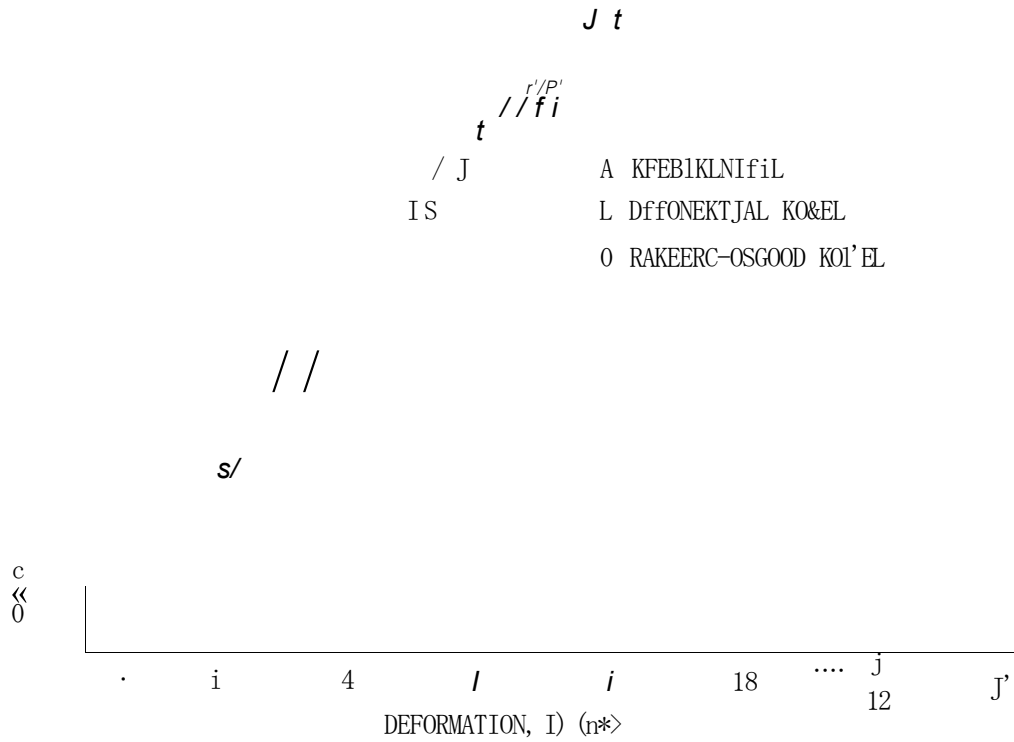


Figure 7.9 Load-deformation curves for the 6mm joints tested in pure shear (data app. D, Tab. D. 4)

LOAD-DEFORMATION CURVES FOR 8 mm JOINTS IN SHEAR

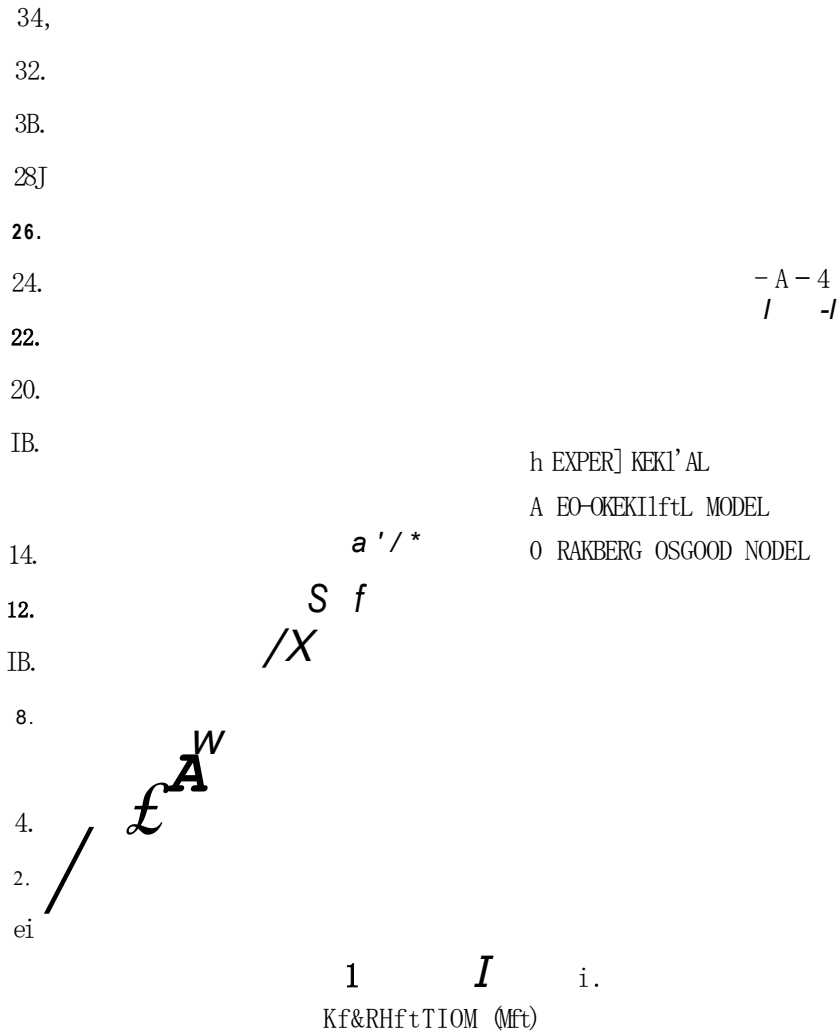


Figure 7.10 Load-deformation curves for 8mm joints tested in pure shear. (data, app D, Tab D.5).

LOAD-DEFORROATION CURVES FOR 10 mm JOINTS TESTED IN PURE SHEAR

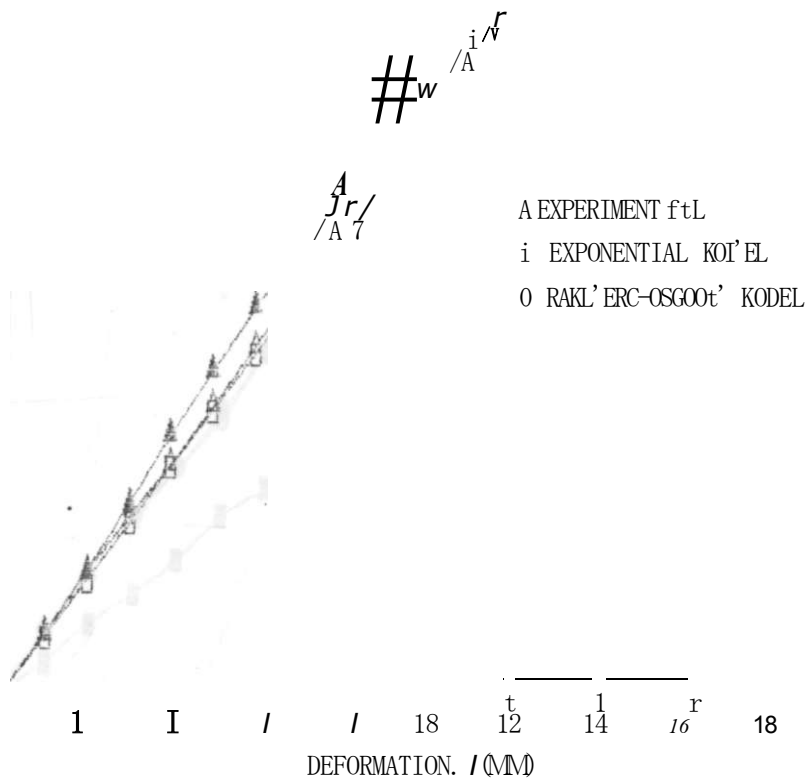


Figure 7.11 Load-deformation curves for 10mm joints tested in pure shear (data app. D, Tab D.6)

COMPARATIVE LOAD-DEFORMATION CURVES JOINTS SHEAR

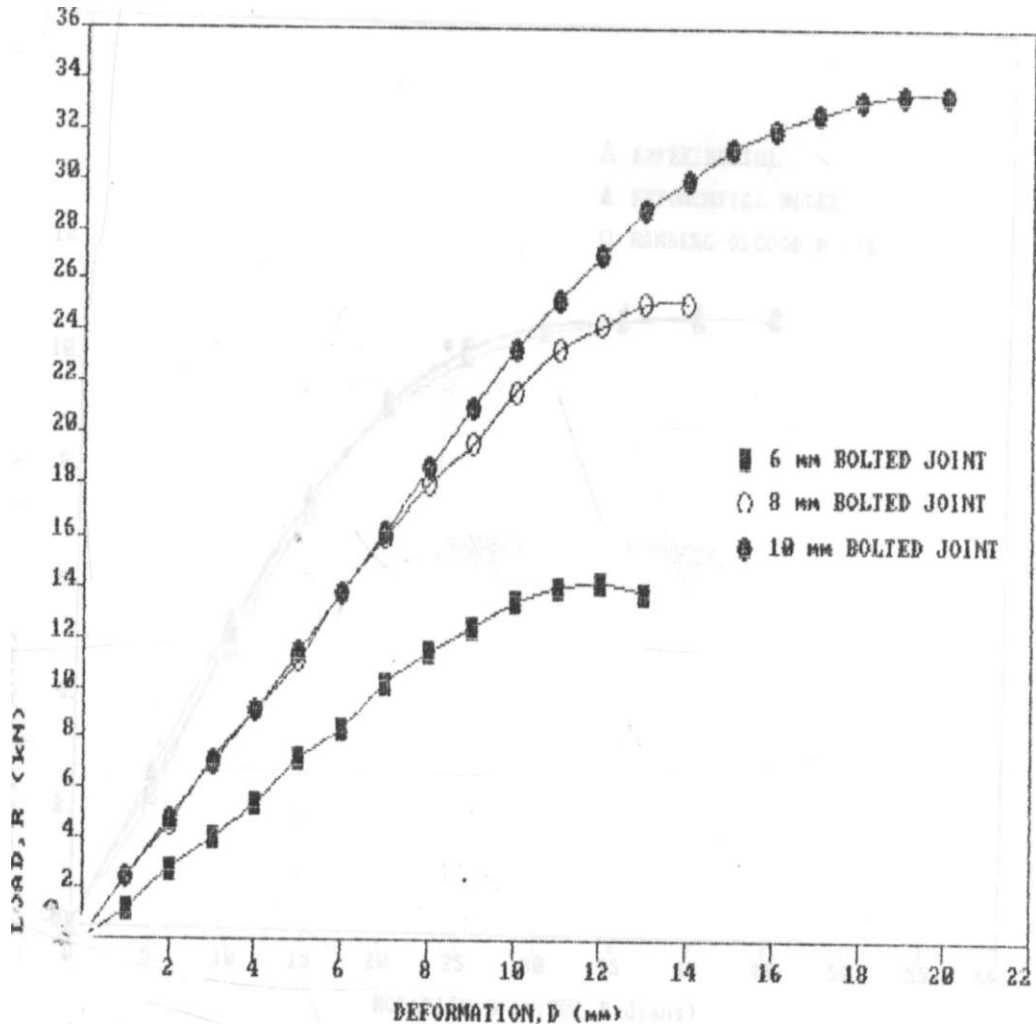


Figure 7.12 Comparative load-deformation curves for joints tested in pure shear.

KOKEMT-ROTAIIOK CURULS FOR 6 HK BOLTS IK ROTATION

If.

14J

A EMIIKEHTA1,
 A EXPONENTIAL HCl'El
 D RftrtBIRG-OSGOOD f. m

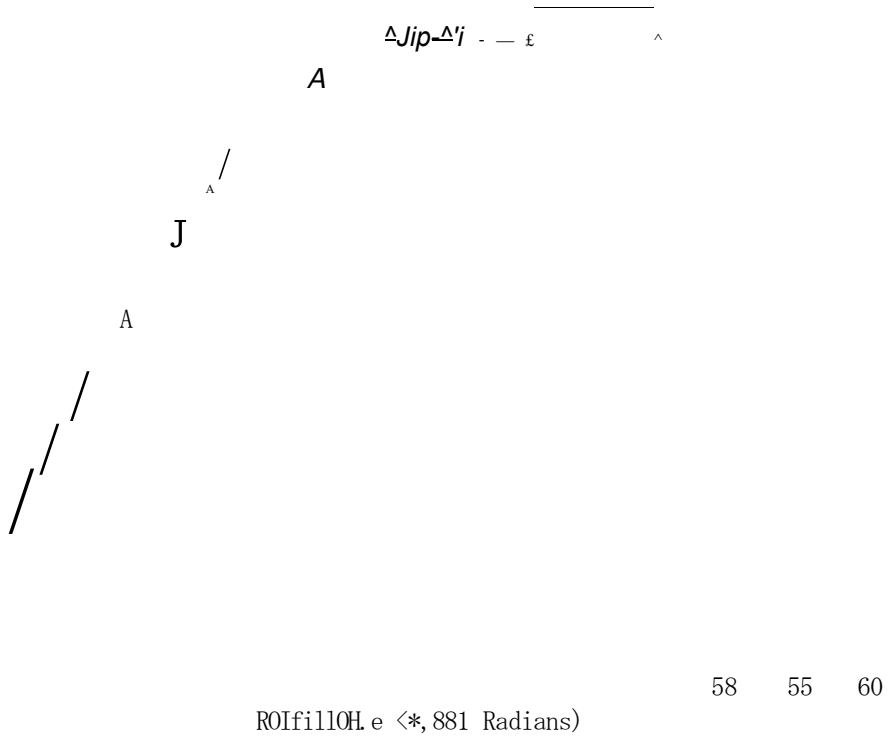


Figure 7.13 Moment-rotation curves for 6mm bolts in pure rotation. (data App. E, Tab. E.1)

KOMEKJ-ROLFTJOH CURVES FOR 8 *m* BOLTS IK ROTATION

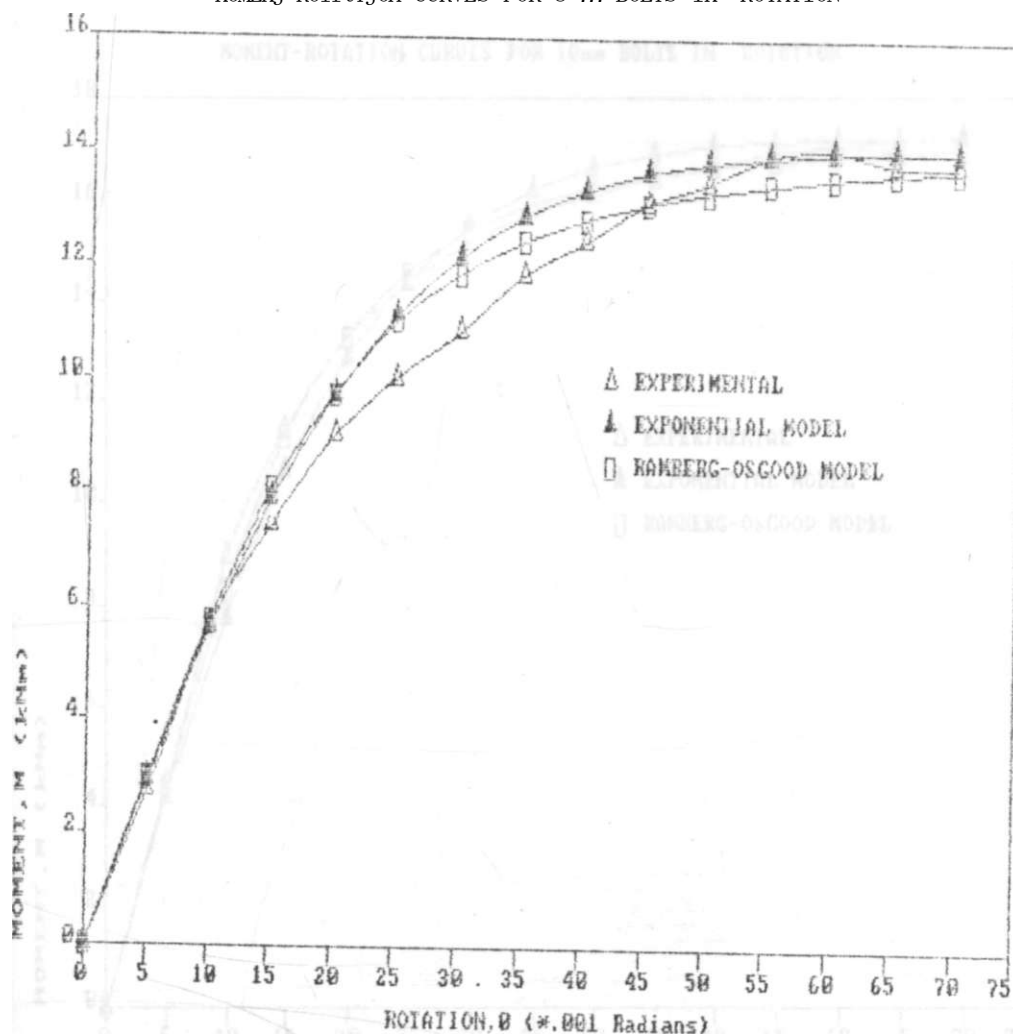


Figure 7.14 Moment-rotation curves for 8mm bolts in pure rotation. (data App. E, Tab. E.2)

and 10mm bolts respectively. Though the ratios are not exactly the same, they are close enough to serve as guidelines as to the kind of ultimate moment values to expect with other bolt sizes, but this is a point that might need further investigation.

The two non-linear mathematical models of equations 4.32 and 4.39 were used to predict the experimental moment-rotation curves after determining the model parameters as outlined in sections 4.6.2.1 and 4.6.3.1. The accuracy of prediction of each model was assessed by the schemes of analysis of chapter 6.0.

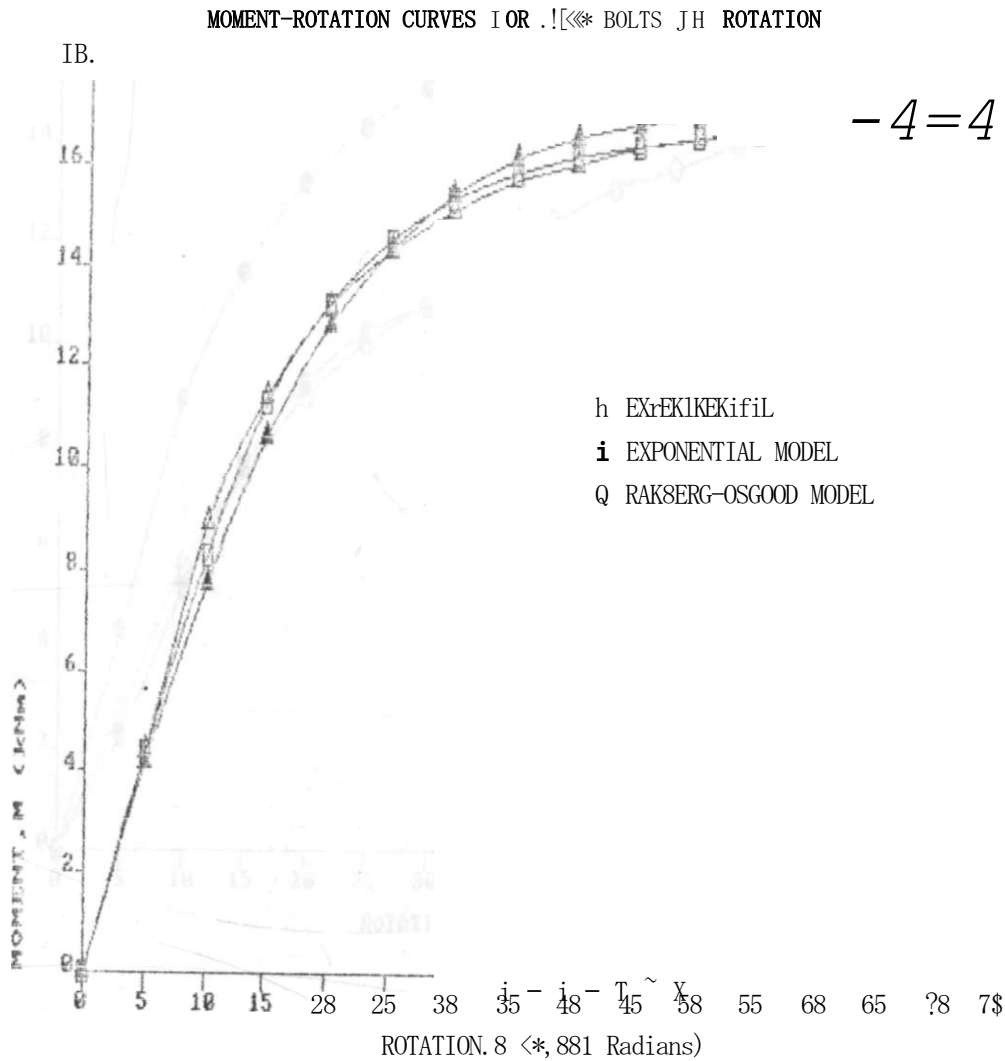


Figure 7.15 Moment-rotation curves for 10mm bolts in pure rotation.

COMPARATIVE MOMENT-ROTATION CURVES 80L1S KOIATJ OH

18_

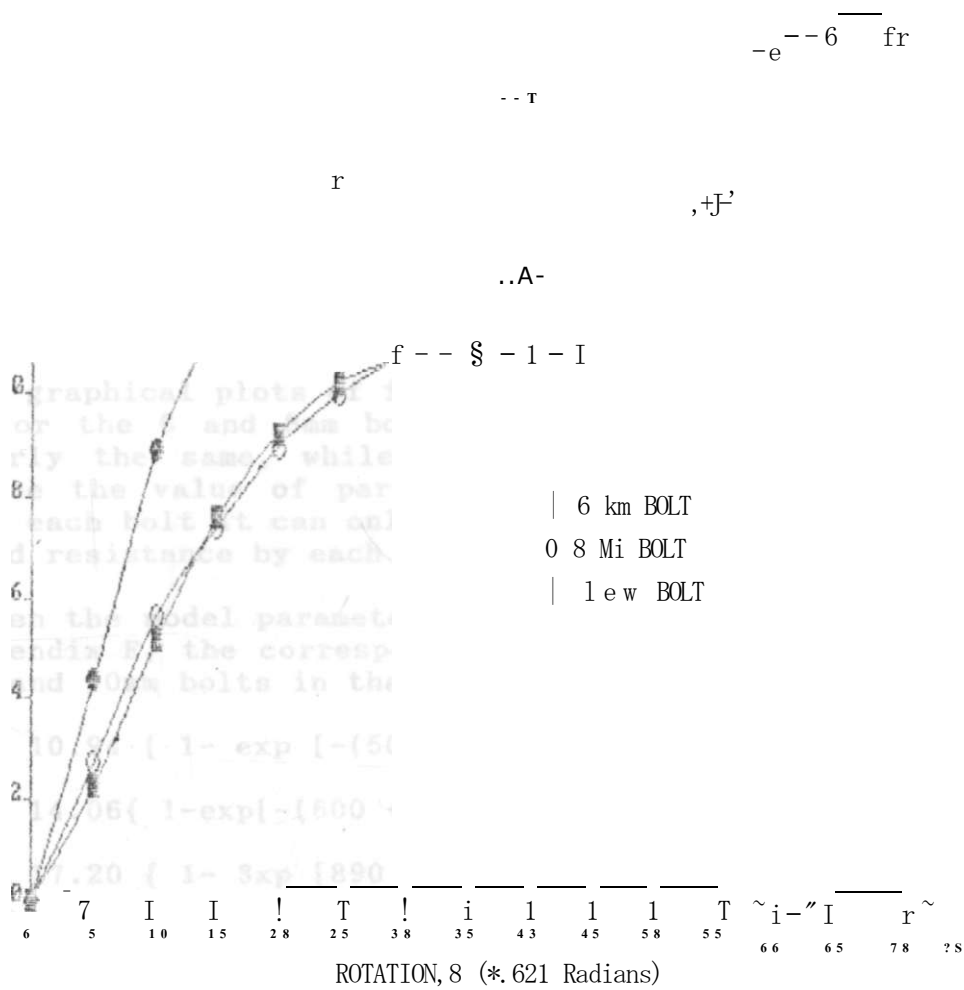


Figure 7.16 Comparative moment-rotation curves for bolts in pure rotation.

7.5.1.2.1. Exponential model

The basic equation used in the prediction of the experimental moment-rotation curves for the connectors loaded in pure rotation was:

$$M = M_0 \{ 1 - \exp [-(K + C\theta) / M_0] \} \dots \dots \dots [7.17]$$

From table 6.1 and figure 6.2, it is seen that this model fitted the data for the 6mm bolt better with an averaged cumulative moment error of 0.141, followed by 0.369 for the 10mm bolt and 0.632 for the 8mm bolt. Figures 7.13 to 7.15 also show graphically the closeness of fit of the models to the experimental data.

The basic model parameters (K and C) varied in such a way that K increased with bolt diameter: 500, 600 and 890 for the 6, 8, and 10mm bolts respectively, whereas the value of C showed no consistent pattern of variation being 24090, 11014, and 13700 for the 6, 8, and 10mm bolts respectively.

The graphical plots of fig. 7.16 indicate that the parameter K for the 6 and 8mm bolts are close, as these slopes are nearly the same, while that for the 10mm bolt is high. Since the value of parameter C cannot relate consistently for each bolt it can only be attributed to the uniqueness of load resistance by each bolt (see section 2.4.2.1 and 7.10).

Given the model parameters as shown in tables E.1 to E.3 in appendix E, the corresponding empirical relations for the 6, 8, and 10mm bolts in that order are:

$$M = 10.94 \{ 1 - \exp [-(500 + 24900 \theta) / 10.94] \} \dots \dots \dots [7.18]$$

$$M = 14.06 \{ 1 - \exp [-(600 + 11014 \theta) / 14.06] \} \dots \dots \dots [7.19]$$

$$M = 17.20 \{ 1 - \exp [-(890 + 13700 \theta) / 17.20] \} \dots \dots \dots [7.20]$$

7.5.1.2.2. Inverse Ramberg-Osgood model

The basic form of this non-linear mathematical model used in the prediction of the experimental moment-rotation curves for the connectors in pure rotation was:

$$M = K \theta^n / [1 + (K\theta / M_{fl})^n] \dots \dots \dots [7.21]$$

Based on the parameters determined from the experimental data and shown in tables E.1 to E.3 of appendix E, the corresponding empirical relations for the model for the 6, 8 and 10mm bolts loaded in pure rotation in that order are:

$$M = 5000 / [I + (5000 / 10.94) T^6] T^{1/6} \dots [7.22]$$

$$M = 6000 / [I + (6000 / 14.06) T^{2.5}]^{1/2.5} \dots [7.23]$$

$$M = 8900 / [I + (8900 / 17.20) T^{2.5}] T^{1/2.5} \dots [7.24]$$

Whereas the initial tangent stiffness value increased with bolt diameter that for parameter n decreased. For the 8 and 10mm bolts, the value of parameter n was the same indicating that the general shape of the moment-rotation curves to be the same. This can be ascertained from fig. 7.16. From table 6.1 and fig. 6.2, the ranking of the model for each bolt size was such that the average cumulative moment error was least for the 6mm bolt at 0.100, followed by 0.179 for the 10mm bolt and 0.540 for the 8mm bolt. This ranking compares well with that for the exponential model. But in absolute terms the Inverse Ramberg-Osgood model had a better fit than the exponential model.

7.5.2 Joint moment-rotation curves.

Figures 7.17, 7.18 and 7.19 show the experimental and non-linear model predictive moment-rotation curves for joints loaded in pure rotation. Comparative plots of the three joints are shown in figure 7.20. The graphical plots exhibit the same general shape for the moment-rotation curves.

MOKEKT-ROTATJON CURVES FOR £hh JOINT IN ROTATION

- A EXPERIMENTAL
- k EXPOfiEKTlfil MODEL
- o RAMBERC-OSGOOD MODEL

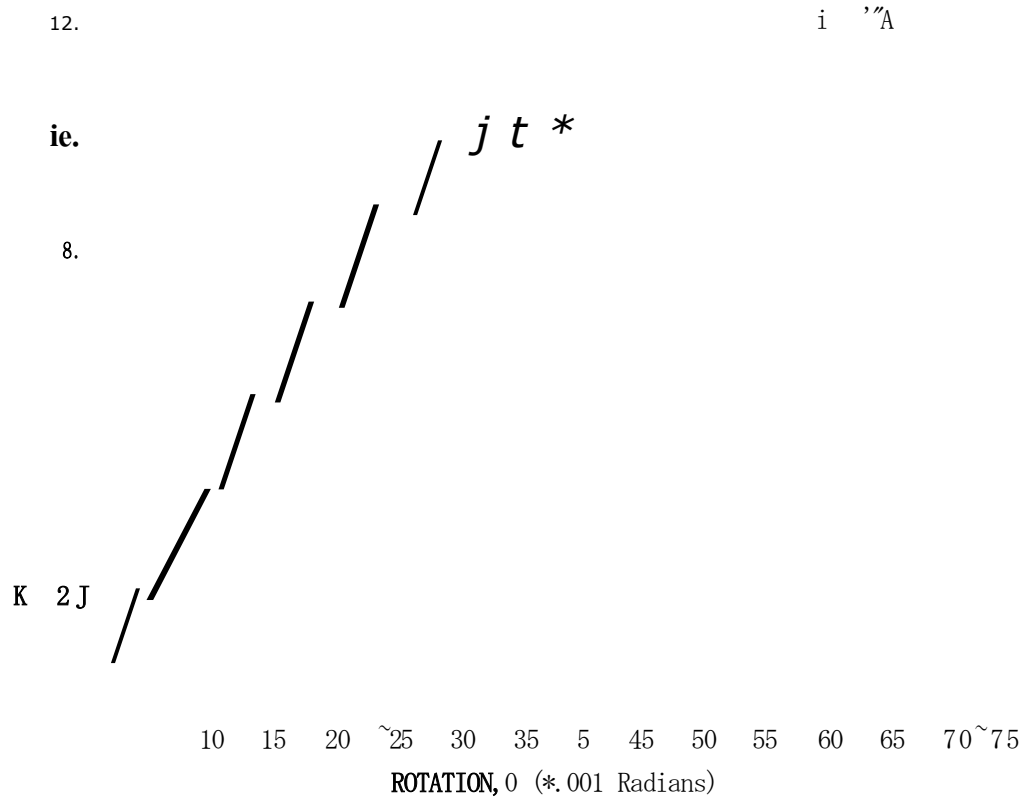


Figure 7.17 Moment-rotation curves for the 6mm bolt joints in pure rotation, (data App. E, Tab. E.4)

MOMENT-ROTATION CURVES FOR 8mm JOINT IN HOT fill OH

t EXPERIMENTAL
 I EXPONENTIAL MODEL
 D RAKBERG-OSGOOD MODEL,

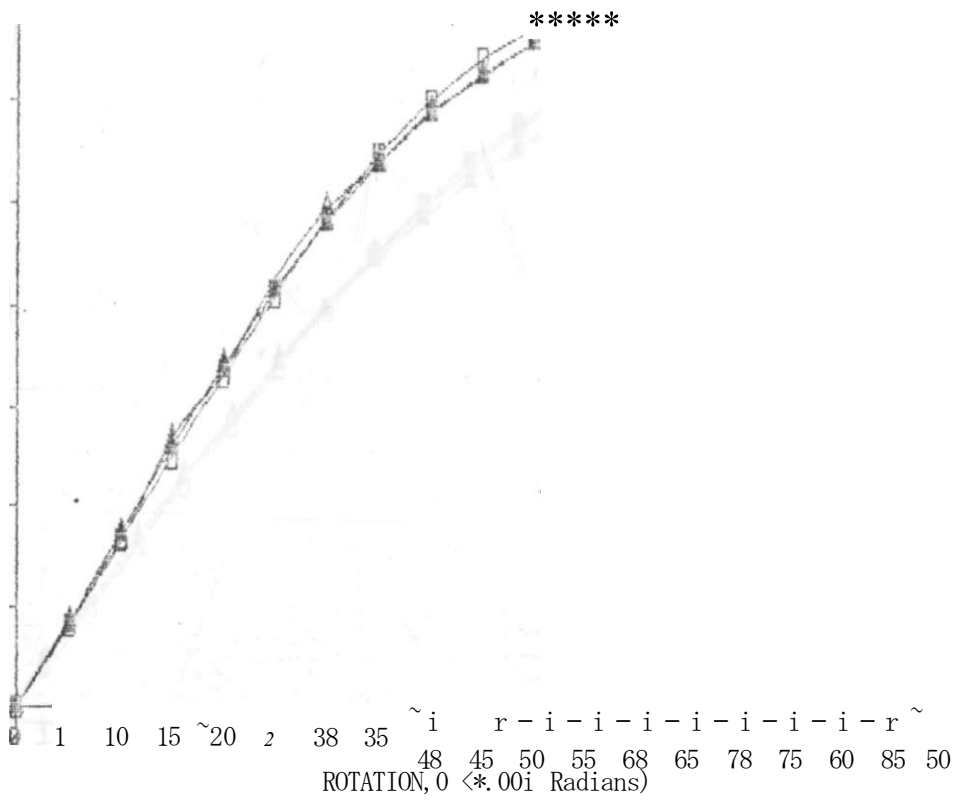


Figure 7.18 Moment-rotation curves for 8mm bolt joints in pure rotation (data App. E, Tab. E.5)

MOMENT-ROTATION CURVES FOR 10mm JOINT IN ROTATION

A EXPERIMENTAL
 A EXPONENTIAL MODEL
 O BAKBERG-OSGOOD HOWL

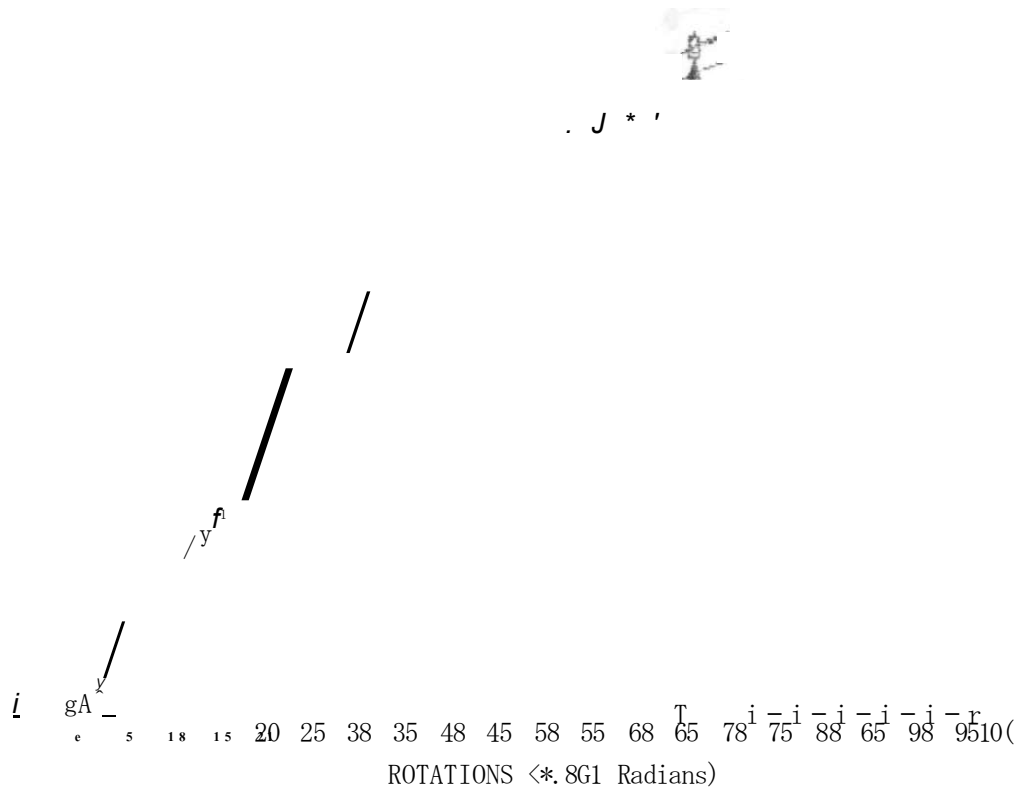


Figure 7.19 Moment-rotation for 10mm bolt joints in pure rotation, (data App. E, Tab. E.5)

COKPARAHVE KOKEKI-FOIATIOH CURVES JOINTS ROTATION

IB.

JOIKI
 o 8 KK JO]HI
 t, 18 MM joim

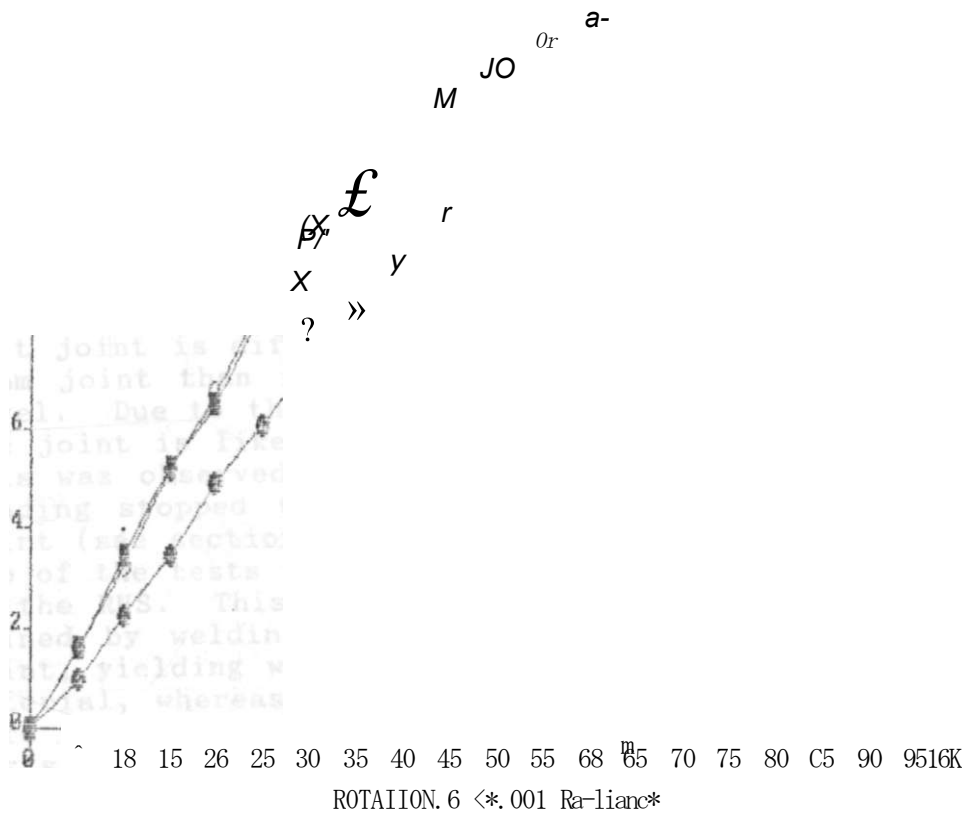


Figure 7.20 Comparative moment-rotation curves for joints in pure rotation.

7.5.2.1 Failure moments

Table 7.6 shows the ultimate moments for the 6, 8 and 10mm bolt joints and the corresponding bolt resistance loads acting on the joint at failure. The values were calculated based on the schemes of analysis of appendix E. Compared to the ultimate moments for the connectors in table 7.7, it is observed that the failure moment for the 6mm bolt joint is higher than that for the individual bolt, the same applies for the 8mm bolt joint.

Table 7.6 Ultimate moment and joint loads

BOLT DIAMETER (mm)	MOMENT (kNm)	LOAD (kN)
6	12.34	123.4
8	14.96	149.6
10	14.50	145.0

The 10mm bolt joint failed at a load lower than that for the individual bolt. Whereas the initial deformation for the 6 and 8mm bolt joint is nearly the same for the 10mm bolt joint is different. There is more deformation in the 10mm joint than in the other two joints for a given load level. Due to the increased deformation in the 10mm joint, the joint is likely to have yielded earlier than the bolt. This was observed during the testing, in that by the time loading stopped there was considerable deformation in the joint (see section 7.6), as compared to the bolt. In fact in two of the tests there was a sizeable split along the centre of the RHS. This was along the point where the section was joined by welding during manufacture. For the 6mm bolt joint, yielding was observed in both the bolt and the joint material, whereas for the 8mm bolt joint, the yielding was more pronounced in the joint material in two of the five tests carried out.

Apart from the failure of the joint material in the 10mm bolt joint, no tangible explanation can be offered for the high magnitudes of failure loads in other joints. The observation here is at variance with that for the pure shear cases where the joints failed at loads lower than those for the individual bolts.

The increased deformation with bolt diameter can be attributed to increased bearing action of the bolts against the joint material, an aspect exemplified by the failure modes as outlined in section 7.6 .

7.5.2.2 Modelling of experimental data

The non-linear mathematical models of chapter 4.0 (equation 4.32 and 4.39), were used to predict the experimental data for the joints loaded in pure rotation. The closeness of fit of these models to the experimental data was done by use of the schemes of analysis of chapter 6.0.

7.5.2.2.1 Exponential model

The same basic form of equation 7.17 was used to predict the experimental moment-rotation curves for the joints. Table 6.4 and figure 6.5 indicate that the 8mm bolt joint experimental data was predicted with least cumulative moment error of 0.080, followed by 0.184 for the 6mm bolt joint, and then the 10mm bolt joint with an error of 0.325. This closeness of fit can also be assessed from figures 7.17 to 7.19, for the joints. Based on the parameters determined from the experimental data and shown in tables E.4 to E.6 in appendix E, the corresponding empirical formulations of this model for the 6, 8 and 10mm bolt in that order were:

$$M = 12.34 \{1 - \exp [-(350 + 77730) \theta / 12.34]\} \dots [7.30]$$

$$M = 14.96 \{1 - \exp [-(333.3 + 60290) \theta / 14.96]\} \dots [7.31]$$

$$M = 14.5 \{1 - \exp [-(240 + 31840) \theta / 14.5]\} \dots [7.32]$$

Considering the parameter values as shown in the tables in appendix E for both the connectors and the joints, it is seen that the initial tangent stiffness value K, increases with the bolt diameter for the connection properties whereas it decreases with the bolt diameter for the joint tests. This indicates that there was increased deformation in the case of joints as compared with the connectors alone. The increased joint deformation offset the bolt diameter effect on this parameter. The absolute values for the joints are less than for the bolts also indicating increased deformation.

For the connectors parameter C showed no consistency whereas for the joint data, there was a decrease with increase in bolt diameter. The closeness in the K and C values for the 6 and 8mm bolt joints can also be seen from figure 7.20 which shows the two joints to have nearly the same profile for most of the moment values.

7.5.2.2.2. Inverse Ramberg-Osgood model

Equation 7.21 gives the basic form of the model as applied to the prediction of the experimental data for the joints in pure rotation. From table 6.4 and figure 6.5, this model predicted the 6mm bolt joint better with an average cumulative moment error of 0.122, followed by 0.153 for the 10mm bolt joint and 0.168 for the 8mm bolt joint. Based on the model parameters of appendix E, tables E.4 to E.6, the corresponding empirical forms of the model for the 6, 8 and 10mm bolt joints respectively were:

$$M = 3500 / [I + (3500 / 12.34)^T 4.5] T (1/4.5) \dots [7.33]$$

$$M = 333.30 / [1 + (333.30 / 14.96)^T 4.5] T (1/4.5) \dots [7.34]$$

$$M = 2400 / [I + (2400 / 14.5)^T 5.0] T (1/5.0) \dots [7.35]$$

The parameter K follows the same trend as for the exponential model. Generally parameter n decreased for the 6mm bolt joint and increased for the 8 and 10mm bolt joint as compared to the values for the individual bolts, as shown in the relevant tables in appendix E. The differences indicate that there was increased deformation in the 8 and 10mm bolt joints as compared to the individual bolts, whereas for the 6mm bolt joint there was decreased deformation for given moment levels. The close numerical values for parameter n for the joints indicates that the rate of decay or load resistance is typically the same for all the joint types tested, more so for the 6 and 8mm bolt joints as shown in figure 7.20.

7.6 Failure of test pieces.

The structural behaviour of bolted connections in cold formed steel construction is somewhat different from that in hot rolled heavy construction mainly because of the thinness of the connected parts in the former. During the conduct of the research, there were three failure modes that were observed with combinations of the three in some instances. These were:

- (i) bearing or pilling up of material in front of the bolt hole,
- (ii) tearing of the sheet in the net section of the joint material, and
- (iii) Shearing of the bolt.

Some of these modes of failure are reviewed in section 3.3, and briefly discussed below as they occurred during the research.

7.6.1 Shearing of the bolts

Figure 3.15(b) shows schematically the shearing process in a bolted joint. This mode of failure was observed during the testing of the connectors and joints in both pure shear and pure rotation. Plate 6.1 shows these failure modes. The joints tested in pure shear failed by shearing of the bolt with little deformation in the joint material for the 6 and 8mm bolt joints. No shear failure of the bolt occurred for the 10mm bolt joint. The same trend was observed for the joints tested in pure rotation.

Although some research work (71) indicates that shear failure in the bolt is expected to occur at a shear load equal to 0.6 times the tensile strength of the bolt, such a relation could not be established during this research work.

As in some instances the ultimate shear loads observed were much higher than the ultimate tensile loads.

7.6.2 Bearing failure

This kind of failure normally occurs when the edge distance is not sufficient, and is accompanied by considerable joint material deformation. This failure was observed in most of the joint property tests, though it was more pronounced in the 10mm bolt joints. Figure 7.21 shows a diagrammatic representation of the failure.

Bearing failure can occur depending on several parameters, including the tensile strength, and thickness of the connected parts, the type of joint, and the rotational capacity of the joints. Generally high tensile strength of the connected parts, thick sheets, and highly flexible bolts prevent bearing failure of the connected material.

In the 10mm bolt joints, bearing failure occurred because of the low deformation capacity of the bolts, the thinness of the connected material (4mm), and the low ultimate tensile strength of the connected material (33.81KN).

7.6.3 Tearing out of connected material

This kind of failure was observed in the 10mm bolt joint loaded in pure rotation. This failure mode is related to the stress concentration caused by:

- (i) presence of 'holes', 'flaws', and 'pipes', in the connected material.
- (ii) the concentrated localised force transmitted by the bolt to the connected sheets.

This failure occurred because of the mode of manufacture of the RHS (see section 7.10) which induces residual stresses, and also because of factor (ii) above. The location of the 10mm bolt holes on the test joint pieces for the pure rotation case was along the centreline of the RHS, and it was along this same line where the RHS was welded during the cold forming manufacturing process. The concentrated stress acting along this weldment from the bolts coupled with the already existing residual stresses in the joint material could have led to the observed failure in the 10mm bolt joint test pieces in pure rotation, as shown in figure 7.22.

7.7 Effects of initial bolt pre-load.

Results from several experimental works carried out indicate that there is consistent pattern of variation of the bolts 'or joints' ultimate strengths with initial bolt pre-load (34). The reasons for this being that:

- (i) when a bolt is torqued to a certain pre-load, most of the inelastic deformation develop in the threaded portion of the bolt. Thus it is expected that the internal bolt tension has less influence on the ultimate strength.
- (ii) at ultimate strength there is little initial clamping force remaining in the bolt.

During this research all the bolts were hand tightened. This was to ensure that no pre-load was introduced, as the non-linear models used did not take account of this aspect as a research parameter. This was aimed at avoiding the introduction of frictional forces in the test pieces. But an aspect observed during the research that could be linked to the absence of initial bolt pre-load was the initial slip. Absence of clamping force against the connected parts because of hand tightening could have had an added effect on the magnitude of the initial slip observed. although after slip, this lack of bolt pre-load became insignificant as the

bolts started to resist the applied loads in modes akin those of joints that had no pre-load.

7.8 Location of shear planes and faying surface condition.

Figure 3.33 shows the effect of shear plane location on the load-deformation curves for bolts and joints in shear. The tests of this research were designed such that the shear planes of the test pieces were through the bolt shank. But the shear stress distribution which is non-uniform has a peak value at the centre of the shank, at which point the bolt bears directly on the connected parts (refer to figure 3.18 and section 3.3.2). When bolted connections are subjected to shear, it is usually assumed in the calculations that there is no friction between the faying surfaces, and that the force applied is resisted by shear alone and bearing of the bolts and connected parts.

Kulak et al (34) report from their research finding that faying surface conditions affect the ultimate loads of the joints. The faying surface of the connected parts during this research were unmilled, hence some of the applied load went into overcoming the friction between them. This could have been the reason why such high ultimate load and moment values were observed. In normal conditions, the faying surface of connected parts are neither cleanmill nor lubricated, but usually unmilled. Thus the failure loads obtained during this research might be indicative of the expected load resistances and failure loads in actual connection types with the same loading conditions.

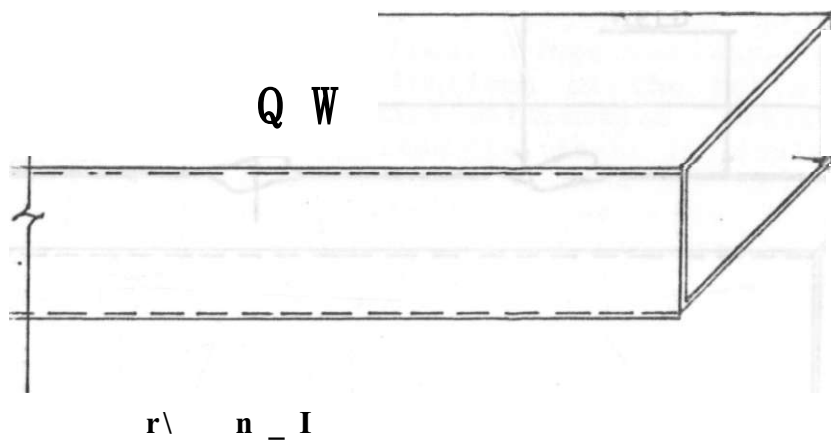


Figure 7.21 Bearing failure connected material

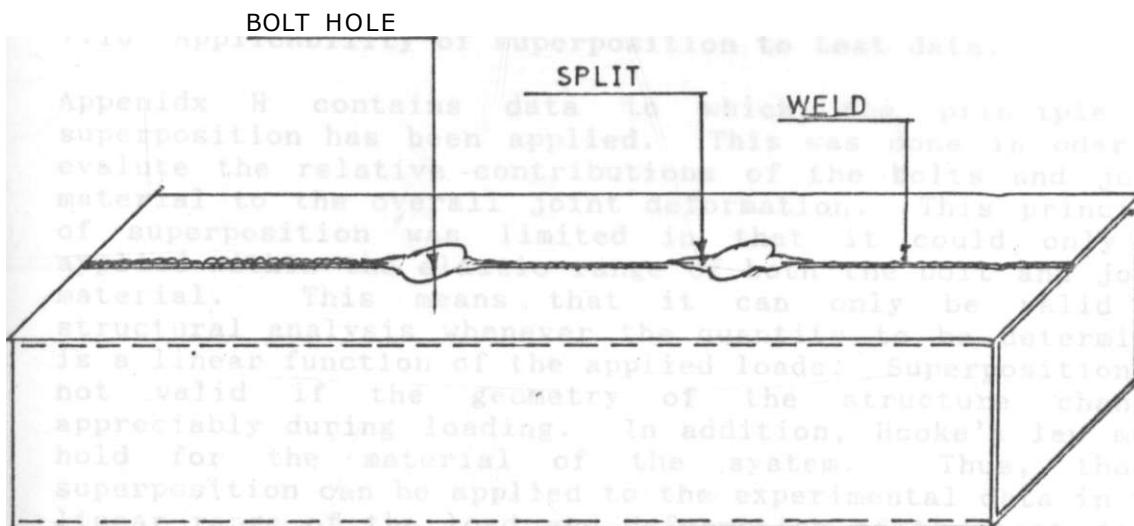


Figure 7.22 Failure by tension tear-out of connected material.

7.9 Imperfection effects.

Section 2.3.5 of chapter 2.0 has a general review of the imperfection effects of the mechanical behaviour of structural materials. The stress-strain curves obtained for the materials used in the research (see figure 7.1 to 7.4).

Section 7.4), indicate that there was considerable residual stress effect on this property (see section 3.3.3.2).

Added to the residual stress effects due to the manufacturing process were those due to the fabrication of the test joint assemblies. Section 3.3.3.2 reviews the residual stress effects on load capacity and yield of ultimate load capacity, indicating that yielding may occur at either a lower or higher load level than in a stress free system for large scale residual stresses. Also the presence of residual stresses of the large scale type may cause actual decay of yield. The observations during the research indicated failure loads that were higher than those initially anticipated, indicating a possible presence of large scale residual stresses in the materials used.

7.10 Applicability of superposition to test data.

Appendix H contains data to which the principle of superposition has been applied. This was done in order to evaluate the relative contributions of the bolts and joint material to the overall joint deformation. This principle of superposition was limited in that it could only be applied within the elastic range of both the bolt and joint material. This means that it can only be valid in structural analysis whenever the quantity to be determined is a linear function of the applied loads. Superposition is not valid if the geometry of the structure changes appreciably during loading. In addition, Hooke's law must hold for the material of the system. Thus, though superposition can be applied to the experimental data in the linear range of the load and deformation of the test joint specimens, the same cannot be said of the non-linear range. The other snag encountered in the application of this principle was the fact that the linear ranges of the bolts and the joint material were not the same, as the two materials yielded at different load levels. Thus a great deal of the work needs to be done on these aspects before any tangible conclusions can be made.

7.11 Ranking of the mathematical models.

The main objective of this research was to identify suitable mathematical models that could best describe the non-linear behaviour of bolted connections loaded in pure shear and pure rotation. Two non-linear mathematical models namely, Exponential model and the Ramberg-Osgood model, were used to predict the experimental load-deformation and moment-rotation data for the loading cases adopted. The models were applied to the connector as well as the joint data. The model ranking was arrived at based on the schemes of analysis as outlined in chapter 6.0. Tables 7.7 and 7.8 show the model ranking for pure shear and pure rotation loading cases for the connectors and joint

Table 7.7 Model ranking for pure shear loading

BOLT DIAMETER (mm)	RANKING			
	BOLT		JOINT	
	1	2	1	2
6	Exp	Ram	Ram	Exp
8	Ram	Exp	Ram	Exp
10	Ram	Exp	Ram	Exp

Key:

Ram = Inverse Ramberg-Osgood model

Exp = Exponential model

Table 7.8 Ranking of models for pure rotation

BOLT DIAMETER (mm)	RANKING			
	BOLT		JOINT	
	1	2	1	2
6	Exp	Ram	Ram	Exp
8	Ram	Exp	Ram	Exp
10	Ram	Exp	Ram	Exp

Thus overall, the Inverse Ramberg-Osgood model was better at predicting the non-linear behaviour of bolted connections in both pure shear and pure rotation, for the materials, loading and experimental conditions of this research.

CHAPTER EIGHT
CONCLUSIONS AND RECCOMENDATIONS

8.1 CONCLUSIONS

This research project set out to investigate the load-deformation and moment-rotation characteristics of bolted connections loaded in pure shear and pure rotation respectively, and to develop mathematical models that could best describe this behaviour.

From this investigation it was concluded that residual stresses of the large scale type were present in the materials used during the research. Some of the residual stresses could be traced to the method of manufacture while others could be traced to the fabrication aspects of the test joint assemblies.

Based of the experimental data obtained during the research, it is concluded that bolted connections loaded in pure shear and pure rotation behave in a non-linear manner and that they are not subject to the simple principles of superposition in terms of load resistance as this is essentially complex. The connection behaviour was also found to be best described as semi-rigid and cannot as such be subject to the conventional assumptions of fully rigid or fully pinned as found in the design codes. The degree of semi-rigidity of these joints could not be assessed owing to the limited amount of experimental work carried out. The Inverse Ramberg-Osgood model was ranked as the best in predicting the behaviour of both the bolts and joints loaded in pure shear and pure rotation, using the materials available and the prevailing research conditions.

As concerns the applicability of the principle of superposition to the experimental data, it is concluded that the results obtained cannot be applied generally until sufficient work has been done on the relationship between the bolt and joint material yield loads, and their deformation in both the linear and non-linear ranges.

Thus the relative contribution of the bolts and joint material to the overall joint deformation as shown in appendix H cannot be recommended for incorporation in the analysis and design of structural systems.

Of importance to the development of structural analysis techniques is the fact that in most bolted connections used in structural systems there may be considerable joint material deformation which are normally overlooked and which could economize the whole design process if they were to be accounted for at the analysis stage. Also such connections should best be treated as semi-rigid, and the non-linear

aspects of their Vload resistance incorporated in their analysis and design.

With more research work relations can be developed for various bolt size and material types and thicknesses to enable more realistic analysis and design incorporating each components contribution to the resulting structural behaviour of a given system. These are aspects that will be of great importance to structural engineers in that they will appreciate real structural behaviour in terms of the type and geometry of the connections employed.

8.2 RECOMMENDATIONS

The scope of research on the behaviour of bolted connections is wide, and it might take along time before substantive conclusions and viable data on the force deformation characteristics are obtained. based on the research findings, the following recommendations are made:

- (i) more research work be done on the material properties of both the bolts and RHS available on the market. This is to give information on the static behaviour of these materials in tension, combined tension and shear, double shear, torsion and combinations of these loading modes. This is because most materials used in structural systems are loaded in various combined modes of these cases.
- (ii) using the same research conditions an investigation of effects of the following factors on the load-deformation curves be done.
 - (a) initial bolt pre-load
 - (b) conditions of the faying surface
 - (c) bolt diameter
 - (d) bolt type and grade
 - (e) connected material size and type
- (iii) investigate the possibility of using other mathematical models in describing the load-deformation curves obtained. Also an assesment of the effect of including the strain-hardening effect factor in the Exponential model to asses the effect on the accuracy of fit to the experimental data.

REFERENCES

1. Home, M.R. and Morris, L.J. "Plastic design of low-rise frames" Granada publishing Ltd, 1981.
2. Karl, M.R. and Chittor, V.S. "Analysis of frames with partial connection rigidity" Journal of structural Engineering, ASCE, ST. II Nov. 1970.
3. Roustard K.M. and Subramanian C.V. "Analysis of frames with partial connection rigidity" Journal of structural Engineering, ASCE Vol. 96, ST II, processings paper 7664, Nov. 1970.
4. Morris, G.A. and Packer J.A. "Beam-to-column connections in steel frames" Canadian journal of Civil Engineering, Vol 14, 1987, pp 68-76.
5. Nethercott, D.A. "Joint action and the design of steel frames" The structural Engineer, Vol, 63A No. 12, Dec. 1985 pp 371-379.
6. Jones, S.W., Kirby, P.A. and Nethercott, D.A. 1981. "Modelling of semi-rigid connections and its influence of steel column behaviour" In joints in structural steel work, Ed. Howlett, Jenkins and Stainsby, pp 5.73-5.87.
7. Jones, S.W., Kirby, P.A. and Nethercott, D.A. "Influence of semi-rigid joints on steel column behaviour" Journal of structural Engineering, A.C.S.E., Vol 108, ST 2, 1982.
8. Duggan, V.T. "Applied engineering design and analysis" London Illife books ltd, pp 32-71.
9. McLinocle, F.A. "Mechanical behaviour of materials" Addison-Wesley publishing company Inc, 1966 pp 32-41.
10. Harmer, E.D, George, E.T. and Clement, T.W. "The testing and Inspection of Engineering materials" McGraw-Hill Company Inc, 1955 pp.
11. Scott, J.S. "The Penguin dictionary of civil engineering" Penguin reference books, 1979.
12. Bateman, J.H. "Materials of construction" Pitman publishing corporation, 1950 pp 300-468.
13. Dieter, G.E. "Mechanical metallurgy" Edward Arnold publishers Ltd pp 493.

- 14 Costrell, A.H. "An introduction to metallurgy" Edward Arnold publishers Ltd pp 132-134.
- 15 Lambert, T. "Structural steel Design" The Ronald Press Company New York 2nd Edition.
- 16 Stanley, F.R. "Strength of materials" McGraw-Hill Book Company Inc, 1957.
- 17 Grinter, L.E. "Design of modern steel structures" The Mcmillan Company, 1960 pp6.
- 18 Clarke, A.B. and Coverman, S.H. "Structural steelwork limit state design" Chapman and Hall 1987 pp 213-220, 77-162.
- 19 Commission of the European countries publication "Construction: A challenge for steel" International Conference, Luxembourg, 24-26 Sept. 1980, pp 110.
- 20 American Institute of steel construction manual "Manual of steel construction" 8th Edition, 1980.
- 21 Bresler, B. Len T.Y and Scalzi, J.B. "Design of steel structures" John Wiley and Sons, 2nd Edition 1968, pp 114-115, 606-607.
- 22 McGuire, W. "Steel structures" Prentice Hall Inc, 1968.
- 23 Ugural, A.C. "Stresses in plates and shells" McGraw-Hill Inc, 1981.
- 24 Timonshenko, S.P. and Woinosky-Krieger, W. "The theory of plates and shells" McGraw-Hill Book Company Inc, 1970.
- 25 Krishnamurthy, N. "A fresh look at bolted end behaviour and design" Engineering Journal American Institute of steel construction Inc, Vol, 15 No. 2 1978.
- 26 Maxwell, S.M., Holeh, S.H. Jenkins, Bose, B. "A realistic approach to the performance and application of semi-rigid joints in steel structures" In joints in structural steelwork Ed. Holwett, Jenkins and Steinsby. Pentech press, 1981, pp 2.71-2.98.
- 27 Feld, J. "Lessons from failure of concrete structures" American Concrete Institute Monograph Series, 1964, pp 61-94.

- 28 Needham, F.H. and Welter A.D. "Philosophy of design in multi-storey frames" In joints in structural steelworks Ed Howlet, Jenkins and Stinsby, Pentech press pp 2.3-2.9.
- 29 Krishnamurthy, N. Huang, H. Jeffrey, P.K. and Avery K.L. "Analytical moment-rotation (M-0) curves for end plate connections" Journal of structural engineering, A.S.C.E. STI, Jan, 1979 pp 133-145.
- 30 Mutuku, R.N., Bodig, J., Pellicane, P.J, Gutowski, R.M. and Shules, E.C. " Applicability of superposition to bolted report No. 60, Colorado University, 1985(Resource reference)
- 31 Bridge, R.Q., Spencer, J.A. and Antarkis, M.K. "Acceptable M-0 capacities for semi-rigid connection" In joints in structural steelworks Ed. Howlet, Jenkins and Stainsby, Pentech press pp 2.26-2.39.
- 32 Bijlaard, F.S. "Requirements for welded and bolted beam-to-column connections in Non-sway frames" In joints in structural steelworks, Ed. Howlet, Jenkins and Stainsby. Pentech press 1981 pp 2.119-2.137.
- 33 Weaver, W. Jr and Lionberger, S.R. "Dynamic response of frames with non-rigid connections" A.S.C.E Journal of mechanics Division, EMI, Feb. 1969, pp 95-144.
- 34 Kulak, G.L., Fischer, J.W. and Struite, J.H. " Guide to design criteria for bolted and rivetted joints" 2nd edition, John Wiley and Sons, 1987.
- 35 White, R.N., Gergley, P. and Sexsmith, R.G. "Behaviour of members and systems" Structural Engineering Vol. 3 John Wiley and Sons, 1972 pp 279-282.
- 36 Beedle, L.S. "Plastic design of steel frames" John Wiley and Sons, 1958.
- 37 Garman Jez-Gala "Residual stresses in rolled I-section" Institute of Civil Engineers Proceeding Nov. 1962, Vol. 23 pp 361-378.
- 38 Home M.R. "The influence of residual stresses on the behaviour of ductile structures" In residual stresses in metals and metal construction, Ed-Osgood W.R. Reinhold Publishing Company, 1954 pp 139-161.

- 39 Sawko, F. "Effects of strain-hardening on the elasto-plastic behaviour of beams and grillages" Institution of Civil Engineers Proceedings, Aug. 1964, Vol, 28 pp 489-504.
- 40 Home, M.R. and Medland, L.C. "Collapse loads of steel frameworks allowing for the effects of strain hardening" Institution of Civil Engineers Proceedings, March, 1966, Vol 33 pp 381-408.
- 41 British Standards Institute: BS 4395 "High strength friction grip bolts and associated nuts and washers" Part 1 1969.
- 42 BSI: BS4190: 1967 "ISO Metric Black bolts, screws and nuts"
- 43 BSI: BS3692: ISO metric precision hexagonal bolts, screws and nuts.
- 44 Boston, R.M. and Parte J.W. "Structural fasteners and their applications" The British Constructional steelwork Association Ltd, July, 1978.
- 45 Sharkir-Khahil, H. and Ho, C.M. "Black bolts under combined tension and shear" The structural Engineer, vol 57B, No. 4 Dec. 1979 pp 69-76.
- 46 Wallaert, J.J. and Fischer, J.W. "Shear strength of high strength bolts" ASCE, journal of the structural Division, ST3 June, 1965 pp 99-125.
- 47 Croxton, P.C.L., Martin, L.H. and Prokiss, J.A. "Elementary structural design of steel work to BS449" Edward Arnold 1984, pp 173-175.
- 48 Bahia, C.S and Martin L.N "Experiments on stressed and unstressed bolt groups subject to torsion and shear". In joints in structural steelwork Ed. Howlett, Jenkins and Stainsby, Pentech press pp 1.17-1.34
- 49 Construction steelwork research and development organisation "Steel designers manual" ELBS and Granada Publishing, 4th Edition, 1983 pp 701
- 50 Weaver, W. "Computer programs for structural analysis" D Van Norstord Company Inc., 1967

- 51 BSI BS 5950. "The structural use of steelwork in building" Part 1:1985
- 52 Lothers J.E "Advanced design in structural steel" Prentice Hall Inc, 1960 pp 367-405
- 53 Przemiencecki J.S, "The theory of matrix structural analysis" Mc-Graw Hill Book Company, 1968
- 54 Zienkiewiz O.C, and Chung Y.K, "The finite element method in structural and continuum mechanics" Mc-Graw Hill book company, 1968 pp192-210
- 55 Ross C.F.T, "Finite element methods in structural mechanics" Ellis Horwood Ltd. 1985 pp 208-312
- 56 Desai C.S, "Introduction to the finite element method" Van Norstrad Reihold company 1972 pp215-242
- 57 Yei L.Y and Melchers R.E , "Moment-rotation curves for bolted connections" .A.S.C.E Structural division journal , vol 113 March 1988 pp 615-635
- 58 Goldberg J.E, and Ralph R.M, "Analysis of non-linear structures" A.S.C.E Structural division journal, vol.89 no. st4, Aug 1963 pp 333-351
- 59 Morris G.A and Packer J.A, "Beam to column connections in steel frames", Canadian journal of civil engineering, No.14 1987, pp 68-76
- 60 BSI BS 4360:1968 "Metal washers for general engineering purposes: Metric series"
- 61 Yu Wen "Cold formed steel design " John Wiley and sons Ltd. 1985 pp41-60
- 62 Egers J. "Faults in design revealed by service failures" In engineering design ed. Rolang T Pergamon series 1964 pp 295-313
- 63 Bodgood E ditto pp 269-393
- 64 Mann A.P and Morris L.J "Significance of lack of fit in flush beam-column connections" In Joints in structural steelwork Ed. Howlett, Jenkins and Stainsby Pentech press pp6.22-6.36

- 65 Elms D.C "Linear elastic analysis" Bartford Ltd.
London 1979 pp 16-18
- 66 Masubuchi K "Analysis of welded structures" Pergamon
press 1st Edition 1980 pp 112-147
- 67 Dhalla A.K, Errera S.J, and Winter G "Connections in
thin low-ductility steels" A.S.C.E Journal of the
structural division proceedings vol.97 Oct.1971
- 68 Winters G " Tests on bolted connections in light
gauge steel" A.S.C.E Journal of the structural
division vol 82 March 19,'6

APPENDICES

APPENDIX A

MATERIAL REQUIREMENT FOR PURE SHEAR TESTS

A.1 BOLT SIZES AND NUMBERS

The bolts used in this research were of two different lengths, those for connector property tests and those for the joint property tests. Three different diameters were used for each set of test. The bolts were high tensile hexagon headed type to BS 3692, Grade 8.8 Zinc plated to BS1706: class B, and supplied by GF Kenya limited. Five tests were conducted for each bolt diameter.

Table A.1 Numbers, sizes and lengths of bolts for pure tests

Bolt diameter mm	connector property tests		joints property test	
	length	number	length	number
6	75	5	125	5
8	75	5	125	5
10	75	5	125	5

Each bolt was provided with two (2) washers to BS 4320.

A.2.1 Connector property tests.

The testing rig utilized steel plates 25mm thick. Only one set of equipment was designed and fabricated, and it was used five times for each bolt size tested.

- (a) Steel plates: (i) 2 Nos 25 by 100 by 225
(ii) 2 Nos 25 by 100 by 75
- (b) Side strips: 4 Nos flat 6 by 25 by 75
- (c) roller guides: 4 Nos 6mm 0 by 75 bolts complete with washers

A.2.2 Joint property tests.

These tests used rectangular hollow sections (RHS) of size 150 by 50 by 4mm. Each bolt size required five (5) numbers testing rigs. The roller guide, side strip, and holding bolt requirements were as in A.2.1, excepting the length of the strips being 125mm. The RHS requirements were as follows:

- (a) 30 Nos 150 by 50 by 4 by 225
- (b) 30 Nos 150 by 50 by 4 75

APPENDIX B
MATERIAL REQUIREMENTS FOR ROTATIONAL TESTING EQUIPMENT

- (a) Pulley system assembly A and B
 - (i) 2 No 0 100 by 75 mm steel wire rope pulleys with 20 mm bore.
 - (ii) 2 No 0 20mm by 100 shafts
 - (iii) 4 No 75 by 50mm support blocks with 20mm bore
 - (iv) 4 No 0 12.5mm by 100 bolts complete with nuts and washers.
 - (v) 2 No 350 by 150 by 12.5mm steel plates.

Half of these components were used for each of the pulley systems A or B in both the connector and joint property tests.

- (b) Cable pulling systems c or c
 - (i) 2 No 10mm 0 by 3 500mm long steel wire ropes.
 - (ii) 1 No 102 by 64 by 7.44kg joist used as loading beam.
- (c) Connector property testing rig.
 - (i) 1 No 840 by 200 by 25mm steel plate drilled with 6, 8, and 10mm 0 holes on a 100mm 0 circle concentric with plate centre.
 - (ii) 1 No 500 by 200 by 25mm steel plate drilled with 6, 8, and 10mm holes on a 100mm 0 circle concentrate with plate centre to match those on plate in (i) above
- (d) Joint property testing rig.
 - (i) 15 No. 150 by 50 by 4 by 840 RHS
 - (ii) 15 No 150 by 50 by 500 RHS

These RHS were drilled with holes as in (c) above indicated in figure 5.8.

APPENDIX C

CALCULATION OF JOINT ROTATION

Length of arc rule.

The length of an arc depends on the angle it subtends at the centre of the circle; the total angle subtended at the centre being 360, this being the angle subtended by the circumference. In general,

$$\text{arc length} = \frac{\text{angle in degree}}{360} \times \text{circumference} \quad (\text{C.1})$$

or

$$\text{arc length} = \frac{2\pi r \times \text{angle in degree}}{360^\circ}$$

$$\text{thus } l_c = r \times \theta / 57.3 \quad (\text{C.2})$$

where l_c is the arc length
 r the radius of the circle
 θ is the angle in degrees

If the arc is exactly equal in length to the radius, the angle then subtended ought to serve as a useful unit of measurement, for one always expresses circumference in terms of the radius. This angle is known as the radian.

If the chord were equal to the radius, the central angle would be 60° , so that when the arc is involved in the same way the angle must be slightly less than 60° .

Actually the radius is contained 2π times in the circumference, hence.

$$2\pi \text{ radians} = 360^\circ \quad (\text{C.3})$$

$$\text{i.e. } 1 \text{ radian} = \frac{360^\circ}{2\pi} = 57.3^\circ \quad (\text{C.4})$$

Thus to convert from degrees to radians divide by 57.3° . Radian as circular measure is the most natural system of angular measurement. A simple rule for the length of an arc now be established.

$$\text{Length of arc} = \frac{2\pi r \times \text{angle in degrees}}{360^\circ}$$

$$= \frac{2\pi r \times \text{angle in degrees}}{360^\circ}$$

$$l_c = r \times \text{angle subtended by the arc expressed in radians}$$

$$l_c = r \times \theta \quad (\text{C. 5})$$

where l_c = arc length
 r = radius
 θ = angle in radians

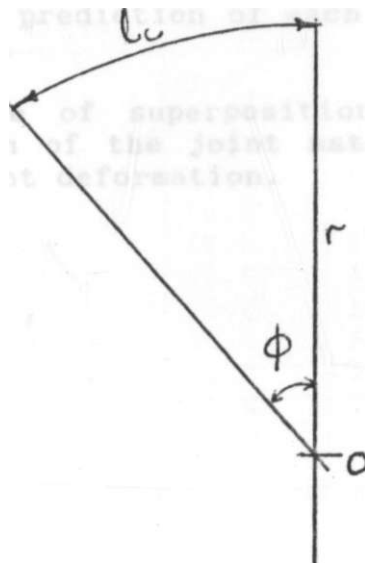


FIGURE C.1 Geometric Determination of angle of arc

APPENDIX D

SCHEME OF ANALYSIS OF PURE SHEAR TEST DATA

D.1 Scheme of analysis

(a) Proposed models

(i) $R = R_0 \{1 - \exp[-(i+C) A / R_0]\}$

(ii) $R = K A / \{1 + (K A / R_0) T^n\} T^{1/n}$

(b) Fit the models to connector property test data for the bolt diameter 6mm, 8mm and hence determine parameters:

(i) K_i and C

(ii) K and n

(c) For each bolt diameter at given deformation D determine the loads from the models above.

(d) Fit the models to the experimental data and the accuracy of prediction of each model as laid down in chapter 6.0.

(f) By principle of superposition obtain the relative contribution of the joint material and bolt to the overall joint deformation.

TABLE D.1 Load - deformation data for 6mm diameter bolt tested in pure shear.

j TEST TYPE		PURE SHEAR			
MATHEMATICAL MODELS	1. $R = KA$ LINEAR 2. $R = R_n \exp[-(i+C_n) A/R_o]$ EXPONENTIAL 3. $R = K_s A / \{1 + (K_f A/R_o)^n\}$ RAMBERG				
CONSTANTS	1. $K = 19 \text{ kN/mrn}$ 2. $R_n = 19.68 \text{ kN}$, $K_s = 19 \text{ kN/mm}$, $C = 26.07$ 3. $R_c = 19.08 \text{ kN}$, $K = 19 \text{ kN/mm}$, $n = 8.1$				
DEFORMATION A mm	LOADS , R kN				
	EXPERIMENTAL	LINEAR	EXPONENTIAL	RAMBERG	
0.0	0.0	0.0	0.0	0.0	
0.2	4.34	3.8	4.28	3.5	
0.4	9.3	7.6	8.78	7.60	
0.6	13.92	11.4	12.66	11.38	
0.8	16.44	15.2	15.49	14.96	
1.0	17.86	19.0	17.28	17.55	
1.2	18.76	22.8	18.27	18.64	
1.4	19.08	26.4	18.75	18.95	
1.6	18.76	30.4	18.96	19.04	
1.8	18.22	34.2	19.04	19.06	
2.0	17.8	38.8	19.07	19.07	
2.2					

TABLE D.2 Load-deformation data for 8mm diameter bolt tested in pure shear

TEST TYPE PURE SHEAR

MATHEMATICAL MODELS 1. $R = K \&$ LINEAR
 2. $R = R_0 \{1 - \exp[-(j+C) A / R^0]\}$ EXPONENTIAL
 3. $R = K A / \{1 + (K A / R_0)^n\}$ RAMBERG

CONSTANTS 1. $K = 45 \text{ kN/mm}$
 2. $R_{f1} = 29.3 \text{ kN}$, $K_j = 45 \text{ kN/mm}$, $C = 23.73$
 3. $R_n = 29.3 \text{ kN}$, $K_n = 45 \text{ kN/mm}$, $n = 2.5$

DEFORMATION A mm	LOADS , R kN			
	EXPERIMENTAL	LINEAR	EXPONENTIAL	RAMBERG
0.0	0.0	0.0	0.0	0.0
0.2	9.14	9.0	8.44	8.82
0.4	16.64	18.0	25.35	16.23
0.6	20.88	27.0	20.59	21.27
0.8	23.63	36.0	24.19	24.29
1.0	25.61	45.0	26.49	26.04
1.2	27.21	54.0	27.85	27.09
1.4	28.49	63.0	28.60	27.7
1.6	29.11	72.0	28.98	28.14
1.8	29.29	81.0	29.17	25.43
20.0	29.02	90.0	29.25	28.62
2.2	29.00	99.0	29.28	28.75
2.4				

TABLE D.3 Load-deformation data for 10mm diameter bolt tested in pure shear

TEST TYPE		PURE SHEAR			
MATHEMATICAL MODELS	1. $R = KA$	LINEAR			
	2. $R = R_0 \{1 - \exp[-(i + C \frac{A}{R_0})^n]\}$	EXPONENTIAL			
	3. $R = K_E A / \{i + (K_s A / R_0)^n\}$	RAMBERG			
CONSTANTS		1. $K = 30 \text{ kN/mm}$			
		2. $R_c = 43.91 \text{ kN}$, $K_j = 30 \text{ kN/mm}$, $C = 13.06$			
		$\frac{3R}{P} = 43.91 \text{ kN}$, $K = 30 \text{ kN/mm}$, $n = 4.5$			
DEFORMATION		LOADS, R kN			
A mm	EXPERIMENTAL	LINEAR	EXPONENTIAL	RAMBERG	
0.0	0.0	0.0	0.0	0.0	
0.2	5.6	6.0	6.06	6.00	
0.4	12.2	12.0	12.05	11.99	
0.6	19.5	18.0	17.73	17.93	
0.8	24.8	24.0	22.9	23.66	
1.0	29	30.0	27.44	28.92	
1.2	33	36.0	31.31	33.36	
1.4	37	42.0	34.49	36.77	
1	39.42	48.0	37.09	39.18	
1	40	54.0	39.01	40.78	
2	41	60.0	40.50	41.82	
2	42,		41.59	42.49	
2	42		42.37	42.92	
2	43		42.91	43.21	
2	43,		43.28	43.40	
3	43.91		43.68	43.53	
3	43.1		43.77	43.63	
3					
3					

TABLE D. 4 Load-doformation data for 6mm diameter bolt fastened joint in pure shear

TEST TYPE PURE SHEAR

MATHEMATICAL MODELS 1. $R = KA,$ LINEAR
 2. $R = R_0 \{1 - \exp[-(i + C \frac{A}{R_0})^n]\}$ EXPONENTIAL
 3. $R = \frac{K_0 A}{\{1 - \frac{K_0 A}{R_0}\}^n}$ RAMBERG

CONSTANTS 1. $K = 1.40 \text{ kN/mm}$
 2. $R = 1.40 \text{ kN}, K_j = 14.2 \text{ kN/mm}, C = 0.170$
 3. $R = 1.40 \text{ kN}, K_0 = 14.2 \text{ kN/mm}, n = 13.5$

DEFORMATION LOADS, R kN

A mm	EXPERIMENTAL	LINEAR	EXPONENTIAL	RAMBERG
0.0	0.0	0.0	0.0	0.0
1.0	1.2	1.4	1.49	1.4
2.0	2.8	2.8	3.09	2.8
3.0	4.0	4.2	4.71	4.2
4.0	5.4	5.6	6.30	5.60
5.0	7.2	7.0	7.80	7.00
6.0	8.4	8.4	9.10	8.40
7.0	10.2	9.8	10.23	9.80
8.0	11.4	11.2	11.20	11.17
9.0	12.4	12.6	11.98	12.43
10.0	13.4	14.0	12.60	13.90
11.0	14.0	15.4	13.07	14.10
12.0	14.2	16.8	13.42	14.20
13.0	13.8	18.2	13.68	
14.0				
15.0				
16.0				

TABLE D.5 Load-deformation data for 8mm diameter bolt fastened joint loaded in pure shear

TEST TYPE	PURE SHEAR				" 1
MATHEMATICAL MODELS	1. $R = KA$	LINEAR			
	2. $R = R_0 \{1 - \exp[-(i + C_n \frac{R_0}{L_0}) \frac{A}{R_0}]\}$	EXPONENTIAL			
	3. $R = K_s A / \{i + (K_s A / R_0)\}$	RAMBERG			
CONSTANTS	1. $K = 2.05 \text{ kN/mm}$				
	2. $R_0 = 2.25 \text{ kN}, K_c = 25.14 \text{ kN/mm}, C = 0.259$				
	3. $R_0 = 2.25 \text{ kN}, K_c = 25.14 \text{ kN/mm}, n = 15.0$				
DEFORMATION A mm	LOADS, R kN				
	EXPERIMENTAL	LINEAR	EXPONENTIAL	RAMBERG	
0.0	0.0	0.0	0.0	0.0	
.0	2.4	2.25	2.38	2.25	
,0	4.6	4.5	4.96	4.50	
.0	7.14	6.75	7.62	6.75	
.0	9.10	9.0	10.29	8.99	
,0	11.08	11.25	10.29	11.25	
.0	13.8	13.5	12.71	13.49	
,0	16.00	15.75	14.99	15.75	
.0	18.90	18.0	17.02	17.99	
.0	19.54	20.25	18.8	20.24	
10.0	21.64	22.5	20.26	23.81	
11.0	23.28	24.75	21.47	24.65	
12.0	24.2	27.0	22.43	24.98	
13.0	25.06	29.25	23.20	25.08	
14.0	25.14	31.5	23.76		
15.0			24.2		
16.0					
17.0					

TABLE D.6 Load-deformation data for 10mm diameter bolt fastened joint loaded in pure shear

TEST TYPE		PURE SHEAR			
MATHEMATICAL MODELS	1. $R = KA$ LINEAR 2. $R = R_c (1 - \exp[-(K_i A/R_c)^{1/n}])$ EXPONENTIAL 3. $R = K_s A / \{1 + (K_i A/R_c)^n\}$ RAMBERG				
CONSTANTS	1. $K = 2.35$ kN/mm 2. $R_c = 2.35$ kN, $K_i = 33.4$ kN/mm, $C = 0.194$ 3. $R_c = 2.35$ kN, $K_s = 33.4$ kN/mm, $n = 11.5$				
DEFORMATION A mm	LOADS , R kN				
	EXPERIMENTAL	LINEAR	EXPONENTIAL	RAMBERG	
0.0	0.0	0.0	0.0	0.0	
1.0	2.4	2.35	2.36	2.25	
2.0	4.8	4.7	4.88	4.50	
3.0	7.0	6.75	7.50	6.75	
4.0	9.1	9.0	10.20	8.99	
5.0	11.4	11.25	12.77	11.25	
6.0	13.8	13.5	15.31	13.49	
7.0	16.2	15.75	17.71	15.74	
8.0	18.6	18.0	19.96	17.99	
9.0	21.0	20.25	22.02	20.24	
10.0	23.3	22.5	25.51	22.49	
11.0	25.2	24.75	27.0	24.71	
12.0	27.0	27.0	28.2	26.80	
13.0	28.8	29.25	29.2	28.75	
14.0	30.0	31.5	30.11	30.39	
15.0	31.2	33.75	30.82	31.60	
16.0	32.0	36.0	31.90	32.39	
17.0	32.6	38.25	32.3	32.85	
18.0	33.1	40.5	32.54	33.10	
19.0	33.4	42.75		33.23	
20.0	33.4	45.0		33.30	
21.0					
22.0					
23.0					

APPENDIX E

SCHEMES OF ANALYSIS FOR PURE ROTATION DATA

- (a) Bolt forces in pure rotational joints.
 Figure E.1 shows the forces acting on the bolts in a joint subjected to pure rotational forces. P. Summing up moments about the joints centre of rotation 0 in figure E.1 (a) external applied couple, M = bolt resisting couple

$$P \times La = Pr \times 2 \times r \quad (E.1)$$

$$\text{or } M = P \times La = 2xr \times Pr \quad (E.2)$$

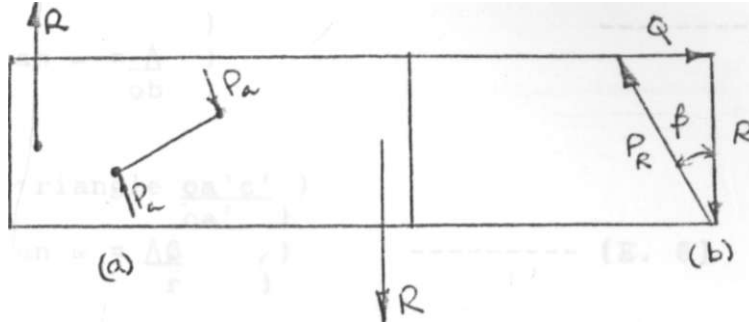


FIGURE E. 1 Forces acting on bolts in a joint in pure rotation (a) bolt resisting couple and force components parallel and perpendicular to direction of applied load (b) force vector components.

\$Q\$ is the force component perpendicular to applied force, \$P\$ is the component parallel to direction of applied force \$P_r\$ is the resultant of the two components to be resisted by the bolt.

From fig E. 1(b)
 $P = Pr \cos \theta$
 $Q = Pr \sin \theta$

$$Pr = \text{SQRT} (P^2 + Q^2)$$

Expressed in terms of the models used:

$$Pr = P_{to} \left\{ \left[\frac{\exp L - (KjB + CBAB)}{r_0} \right] - 1 \right\} \quad - [E.3]$$

for the exponential model where \$P_{to}\$ is the maximum bolt resistance

\$KjB, C/3\$ is the parameter to be determined experimentally
 \$Af3\$ is the bolt deformation in direction of \$Pr\$ and

$$Pr = KP \frac{AP}{\left[1 + \left(\frac{Kf3AP}{Pro}\right)^{1/nP}\right]} \quad [E. 4]$$

For the inverse Ramberg-Osgood model where Pro_n is the maximum bolt resistance KP, P parameters be determined

AP deformation in direction Pr.
From triangle obc,

$$\begin{aligned} \tan \langle x &= \frac{ac}{ob} \\ \text{or } \tan \langle &= \frac{A}{ob} \end{aligned} \quad [E. 5]$$

Consider triangle $oa'c'$

$$\text{or } \tan \langle = \frac{oa'}{r} = \frac{AP}{r} \quad [E. 6]$$

$$\text{Thus } \frac{M}{r} = \frac{A}{ob}$$

$$\text{But } ob = oc - A \sin \langle$$

$$ob = 200 - A \sin \langle$$

$$\cdot \frac{A \mathcal{E}}{r} = \frac{A}{(200 - A \sin \langle)}$$

$$\text{Thus } A = \frac{A \cdot r}{(200 - A \sin \langle)} \quad [E. 7]$$

$$\text{But } \tan \langle = \sin \langle = \langle x \text{ in radius}$$

$$\text{Thus } AP = \frac{A \cdot r}{(200 - A \cdot cc)} \quad [E. 8]$$

Equation E.8 gives the actual bolt deformation from recorded total deformation $A \rangle$ bolt separation r and angle of rotation \langle . In the case of connector properties, AP is due to bolt alone, whereas in the joint property test it might include joint material deformation. This expression for AP could then be substituted into expression [E.3] and [E.4] to determine the values of load resistance of the individual bolts.

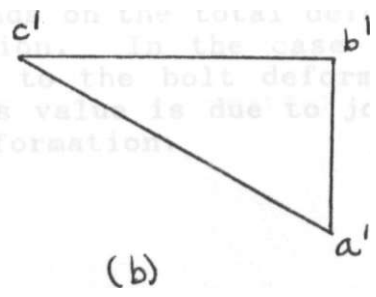
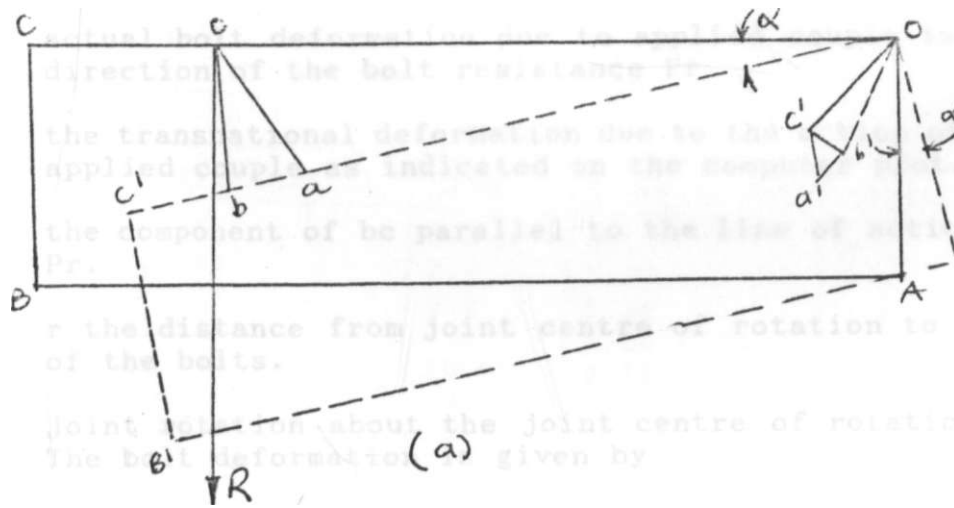


Fig . E.2 Rotational joint deformation (a) member and bolt deformation, (b) bolt deformation properties - this value is due to the bolt deformation alone, whereas in the joint tests this Value is due to joint material deformation.

Fig E.2 shows how the joint member and the bolt in the lower quarter of the joint in figure E.1(a) deforms theoretically about the joint centre of rotation 0, due to the acting external applied couple, M Small displacements theory is assumed to apply. Bolt in the upper quarter of the joint deform in a similar but antisymmetrical manner. The experimental joint deformations were calculated at position c as shown in figure E.2(a). In figure E.2(a) OABC is the underformed lower quarter.

- a'b' = bolt translation parallel to applied load
- b'c' = bolt translation perpendicular to applied load
- a'c* = actual bolt deformation due to applied couple in the direction of the bolt resistance Pr
- b'c' = the transnational deformation due to the action of the applied couple as indicated on the computer plot.
- a'c = the component of be parallel to the line of action of Pr.
- oa' = r the distance from joint centre of rotation to each of the bolts.
- a. = joint rotation about the joint centre of rotation 0. The bolt deformation is given by
- $$a'c' = bc-r / (200-bcc<) \quad (E.3)$$

Thus the bolt deformation depends on the total deformation bolt separation and angle of rotation. In the case of connector properties, this value is due to the bolt deformation alone, whereas in the joint tests this value is due to joint material deformation as well as bolt deformation.

e E.1 Moment-rotation data for 6mm bolt tested in pure rotation.

j TEST TYPE		PURE ROTATION			
MATHEMATICAL MODELS		1. $M = K\theta$ 2. $M = M_0 \{1 - \exp[-\{K_j + C(j)\} \theta / M]\}$ 3. $M = M_0 / [1 - MK_1 \theta / M]^{1/n}$			
CONSTANTS		1. $K = 500$ kNm/Rad 2. $M_0 = 10.94$ kNm, $K_1 = 500$ kNm/Rad, $C=24090$ 3. $M_0 = 10.94$ kNm, $K_1 = 500$ kNm/Rad, $n=0.0$			
ROTATION d) $\times 10^{-3}$ Rad	MOMENTS, M kNm				
	EXPERIMENTAL	LINEAR	EXPONENTIAL	RAMBERG	
0.0	0.0	0.0	0.0	0.0	
5.0	2.27	2.6	2.70	2.5	
10.0	5.17	5.0	5.38	4.99	
20.0	7.6	7.5	7.58	7.38	
25.0	9.22	10.0	9.12	9.26	
30.0	10.23	12.5	10.06	10.28	
J 35.0	10.73	15.0	10.56	10.69	
j 40.0	10.87	17.5	10.79	10.83	
j 45.0	10.94	20.0	10.89	10.89	
	10.88	22.5	10.92	10.92	

Figure E.2 - Rotational joint deformation (a) member and bolt deformation, (b) bolt deformation

Table E.2 Moment-rotation data for 8mm bolt tested in pure rotation.

TEST TYPE PURE ROTATION
 [MATHEMATICAL 1. M K(J)
 ilMODELS 2. M $M_0 \{1 - \exp[-\{K + C(J)\} (J)/M_0]\}$
 3. M $M \quad 1/n$

CONSTANTS 1. K = 600 kNm/Rad
 2. $M_0 = 14.06$ kNm, K: 600 kNm/Rad, C=11014
 3. M = 14.06 kNm, Kj 600 kNm/Rad, n=2.5

ROTATION (°)xl -' " Rad	LOADS, R kN			
	EXPERIMENTAL	LINEAR	EXPONENTIAL	RAMBERG
0.0	0.0	0.0	0.0	0.0
5.0	2.74	3.0	2.92	2.90
10.0	5.65	6.0	5.58	5.74
15.0	7.42	9.0	7.85	8.04
20.0	8.97	12.0	9.68	9.71
25.0	10.00	15.0	11.09	10.99
30.0	10.82	18.0	12.13	11.83
35.0	11.81	21.0	12.85	12.41
40.0	12.43	24.0	13.33	12.81
45.0	13.10	27.0	13.64	13.29
50.0	13.48	30.0	13.83	13.44
55.0	13.96	33.0	13.93	13.56
60.0	14.06	36.0	14.00	13.64
65.0	13.81	36.0	14.03	13.71
70.0	13.78	42.0	14.04	

Table E.3 Moment-rotation data for 10mra bolt tested in pure rotation.

TEST TYPE

PURE ROTATION

MATHEMATICAL MODELS 1. M K(i) LINEAR MODEL
 2. M $M_0 \{1 - \exp[-(K_i C^n) A/M_i]\}$ EXPONENTIAL MODEL
 3. M $K_i / [1 + CK_i^n / M_i^n]$ 1/n RAMBERG

CONSTANTS 1. K = 890 kNm/Rad
 2. $M_{fi} = 890$ kNm, $K_i = 17.2$ kNm/Rad, C=13700
 3. $M_0 = 890$ kNm, $K_i = 17.2$ kNm/Rad, n=2.5

ROTATION I (i)x1- Rad	LOADS, R kN			
	EXPERIMENTAL	LINEAR	EXPONENTIAL	RAMBERG
0.0	0.0	0.0	0.0	0.0
i 5.0	4.4	4.45	4.20	4.39
j 10.0	8.9	8.9	7.73	8.29
15.0	11.4	13.35	10.60	11.26
20.0	13.2	17.8	12.80	13.25
25.0	14.3	22.25	14.33	14.52
30.0	15.1	26.7	15.42	15.33
! 35.0	15.7	31.15	16.14	15.55
! 50.0	16.05	35.6	16.59	16.20
i 45.0	16.4	40.05	16.86	16.43
50.0	16.6	44.5	17.02	16.60
55.0	16.9	48.95	17.11	16.72
! 60.0	17.0	53.4	17.15	16.81
! 65.0	17.15	57.85	17.17	16.88
70.0	17.20	62.3	17.20	16.93
75.0				
80.0				
85.0				
90.0				

Table E.4 **Moment-rotation data for 6mm bolt fastened joint tested in pure shear.**

TEST TYPE		PURE ROTATION			
MATHEMATICAL MODELS	1. $M = K(\theta)$				
	2. $M = M_0 \{1 - \exp[-(K_0 + C\theta) / M_0]\}$				
	3. $M = K_1 / [1 + (K_1 / H_0)^n]^{1/n}$				
CONSTANTS	1. $K = 350 \text{ kNm/Rad}$				
	2. $M_0 = 350 \text{ kNm}, K_j = 12.34 \text{ kNm/Rad}, C = 7773$				
	3. $M_0 = 350 \text{ kNm}, K_j = 17.2 \text{ kNm/Rad}, n = 4.5$				
ROTATION (j) x 10 ⁻³ Rad	LOADS, R kN				
	EXPERIMENTAL	LINEAR	EXPONENTIAL	RAMBERG	
0.0	0.00	0, 0	0.0	0.0	
5.0	1.65	1, 75	1.75	1.74	
10.0	3.50	3, 5	3.61	3.49	
15.0	5.24	5, 25	5.35	5.22	
20.0	6.50	7, 0	6.90	6.88	
25.0	8.32	8 75	8.24	8.28	
30.0	10.46	10.5	9.35	9.62	
35.0	11.14	12.05	10.23	10.54	
40.0	11.66	14.0	10.89	11.17	
45.0	11.96	15.75	11.38	11.58	
50.0	12.24	17.5	11.72	11.83	
55.0	12.34	19.25	11.95	12.00	
60.0	12.2	21.0	12.11	12.10	
65.0		22.75	12.20	12.17	

Table E.6 Moment-rotation data for 10mm bolt fastened joint tested in pure rotation.

TEST TYPE PURE ROTATION

MATHEMATICAL MODELS 1. $M = K\theta$
 2. $M = M_0 \{1 - \exp[-(K + C)\theta / M]\}$
 3. $M = K\theta / [1 + (K\theta / M)^r]^{1/n}$

CONSTANTS 1. $K = 333.3 \text{ kNm/Rad}$
 2. $M_0 = 333.3 \text{ kNm}$, $C = 14.96 \text{ kNm/Rad}$, $C = 6029$
 3. $M_0 = 333.3 \text{ kNm}$, $K = 14.96 \text{ kNm/Rad}$, $n = 4.5$

ROTATION 0x1- Rad	LOADS, R kN			
	EXPERIMENTAL	LINEAR	EXPONENTIAL	RAMBERG
0.0	0.0	0.0	0.0	0.0
5.0	1.62	1.67	1.71	1.66
10.0	3.30	3.33	3.46	3.33
15.0	5.36	5.00	5.18	4.99
20.0	6.70	6.6	6.81	6.62
25.0	8.52	8.25	8.30	8.20
30.0	9.88	10.0	9.62	9.67
35.0	10.80	11.66	10.77	10.95
40.0	11.80	13.32	11.74	12.01
1 45.0	12.48	14.99	12.53	12.54
50.0	13.18	16.65	13.17	13.45
55.0	13.60	18.32	13.66	13.88
60.0	14.04	19.98	14.04	14.18
65.0	13.34	21.65	14.31	14.39
70.0	14.76	23.31	13.52	14.54
75.0	14.90	24.98	14.67	14.65
80.0	14.96	62.69	14.77	14.72
85.0		28.31	14.84	14.79

Table E.6 Moment-rotation data for 10mm bolt fastened joint tested in pure rotation.

TEST TYPE	PURE ROTATION			
MATHEMATICAL MODELS	1. $M = K(\theta)$			
	2. $M = M_0 \{1 - \exp[-\{K_1 + C\theta\} / M_0]\}$			
	3. $M = K_1 \theta / [1 + (K_1 \theta / M_0)^n]$			
CONSTANTS	1. $K = 240 \text{ kNm/Rad}$			
	2. $M_0 = 240 \text{ kNm}, K_1 = 14.5 \text{ kNm/Rad}, C = 3184$			
	3. $M_0 = 240 \text{ kNm}, K_1 = 14.5 \text{ kNm/Rad}, n = 5.0$			
ROTATION A 1 "3D,,.	LOADS, R kN			
	EXPERIMENTAL	LINEAR	EXPONENTIAL	RAMBERG
0.0	0.0	0.0	0.0	0.0
5.0	1.0		1.22	1.19
10.0	2.3		2.48	39
15.0	3.5		3.73	59
20.0	4.9		4.96	79
25.0	6.1		6.14	98
30.0	7.3		7.26	15
35.0	8.4		8.29	8.29
40.0	9.35		9.24	9.37
45.0	10.3		10.09	10.36
50.0	11.1		10.83	11.24
55.0	11.9		11.50	11.98
60.0	12.5		12.06	12.58
65.0	13.5		12.54	13.05
70.0	13.9		12.95	13.41
75.0	14.2		13.30	13.68
80.0	14.4		13.55	13.88
85.0	14.5		13.77	14.02
90.0			13.95	14.13
100.0				

APPENDIX F

ABSOLUTE ERROR COMPARISONS BY THE AVERAGING TECHNIQUE USING
EQUATIONS 6-2 AND 6-6

Table F.1 Comparison of load errors, E_c (kN) and E_c (%) in fitting models to data for bolts in shear

BOLT DIAMETER (mm)	MODEL			
	EXPONENTIAL		RAMBERG OSGOOD	
	E_c (kN)	E_c (X)	E_c (kN)	E_c (X)
6	0.64	4.2	0.92	7.4
8	0.47	2.5	0.45	2.2
10	0.95	5.6	0.46	2.0

ABSOLUTE ERROR COMPARISONS BOLTS IN SHEAR

1.2,

- h EXPONENTIAL MODEL EQU 6-2
- i EXPONENTIAL MODEL EQU 6-3
- o RAMBERG-OSGOOD MODEL EQU 6-2
- | RAMBERG-OSGOOD MODEL EQU 6-3 j

.6.

W
N,
W
V
"-w'X

t
X .4
v

is?
£
0
i
ft

ft

J fi

mn DIAMETER

ii

Table F.2 Comparison of Moment errors, E_c (kN) and E_c (%) in fitting models to data for bolts in rotation.

BOLT DIAMETER (mm)	MODEL			
	EXPONENTIAL		RAMBERG OSGOOD	
	E_c (kN)	E_c (%)	E_c (kN)	E_c (%)
6	0.141	3.2	0.10	2.1
8	0.632	7.3	0.54	6.6
10	0.469	5.2	0.20	2.0

ABSOLUTE EMOS COMPARISONS BOLTS IN ROTATION

J.2,

A EXPONENTIAL MODEL eq 6-3
 B exponential model eq 6-3
 C RAMBERG-OSGOOD MODEL eq 6-2
 D RAMBERG-OSGOOD MODEL eq 6-3

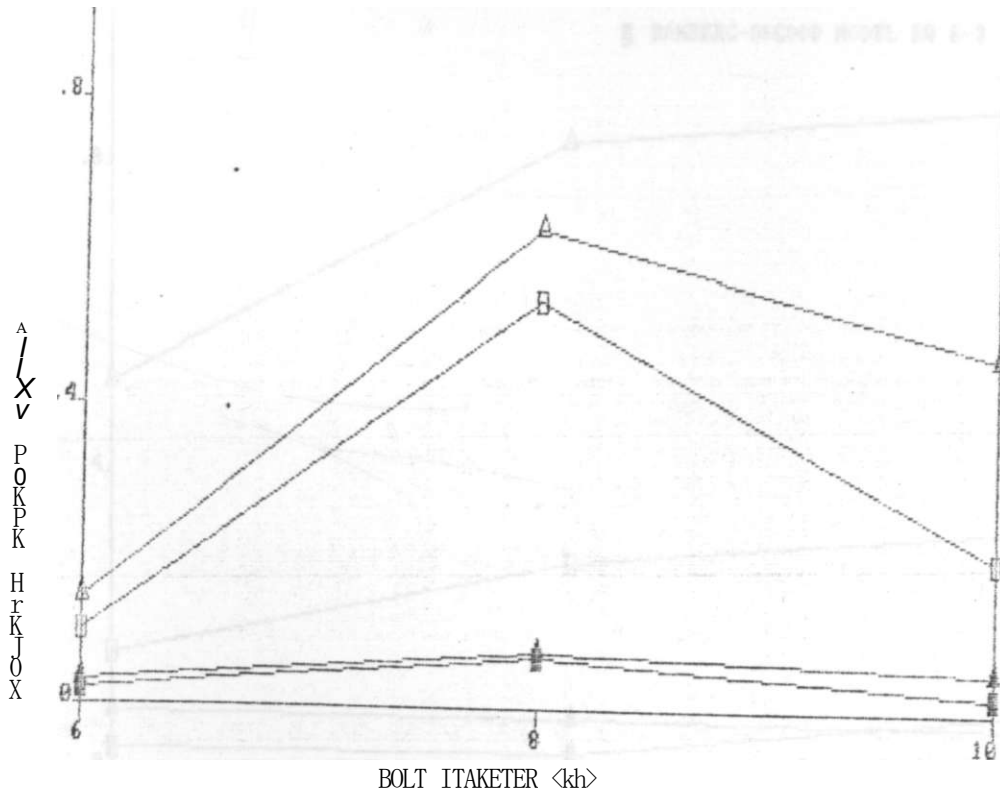


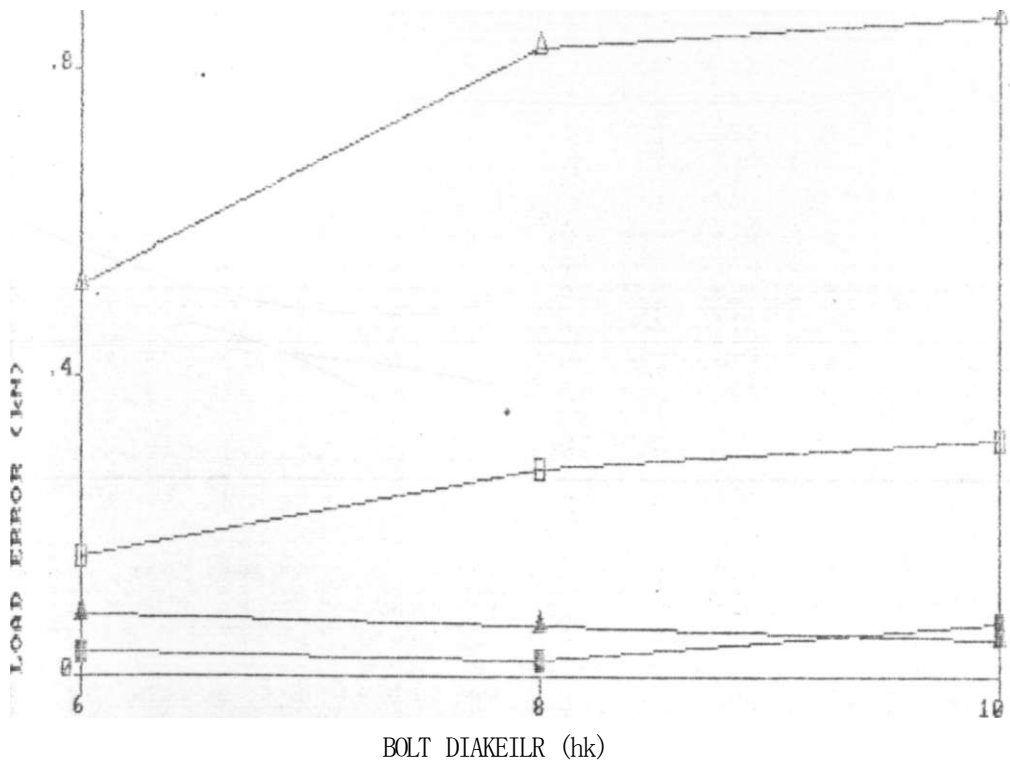
Table F.3 Comparison of Load errors, E_c (kN) and E_c (%) in fitting models to data for joints in shear.

BOLT DIAMETER (mm)	MODEL			
	EXPONENTIAL		RAMBERG	OSGOOD
	E_c (kN)	E_c (%)	E_c (kN)	E_c (%)
6	0.52	8.08	0.160	3.02
8	0.83	6.6	0.276	2.2
10	0.872	4.78	0.313	7.1

ABSOLUTE ERROR COMPARISONS FOR JOINTS IN SHEAR

J. 2_n

- A EXPONENTIAL MODEL EC fc-2
- A EXPONENTIAL MODEL EC fc-3
- D RAMBERG-OSGOOD MODEL EC f-2
- £ RAMBERG-OSGOOD MODEL EC f-3



APPENDIX G

STRESS-STRAIN DATA FOR TEST MATERIALS

Table G.3 Stress-strain data for 10mm Bolt

	STRAIN, ϵ (x.001)	STRESS, σ (N/sq.mm)
	0.0	0.0
	0.31	60.0
	0.75	157.5
	1.13	242.5
I	1.50	306.0
	1.88	360.0
	2.31	394.0
	2.81	432.5
	4.06	460.0
	4.38	490.0

Table G.3 Stress-strain data for 10mm Bolt

STRAIN, ϵ (x.001)	STRESS, σ (N/sq.mm)	
0.0	0.0	
0.31	45.0	
0.75	132.0	
1.13	215.0	
1.50	297.5	
1.88	373.2	
2.31	420.0	j
3.00	467.5	
3.75	502.5	
5.0	541.0	j

Table G.3 Stress-strain data for 10mm Bolt

STRAIN, ϵ (x.001)	STRESS, σ (N/sq. mm)
0.0	0.0
0.36	74.5
0.74	151.0
1.13	226.0
1.47	302.5
1.86	377.4
2.29	453.0
3.00	488.0
3.82	525.0
5.5	550.0

Table G.4 tress-strain data for RHS coupon

STRAIN, ϵ (x.001)	STRESS, σ (N/sq. mm)
0.0	0.0
0.50	95.0
1.00	195.0
1.50	305.0
2.00	362.0
2.50	397.0
3.00	422.5
3.50	442.5
4.00	457.5
4.5	470.0
5.0	480.0
5.5	485.0

APPENDIX H

APPLICABILITY OF SUPERPOSITION TO TEST DATA

There are three principles of superposition concerned respectively with statics, kinematics and with the linking of both in linearly elastic structures. These are principles of superposition of forces, displacement and elasticity (66). The principle of displacement superposition was applied in this case. The principle state that if a Series of small internal deformations is applied to a statically determinate structure, then the displacement at some point **due** to all the internal deformations applied simultaneously is equal to the sum of the displacements at that point **due** to the deformations applied separately. This implies that if small deformation, 61,62, --,6n applied **separately produce deflections A1>A2, An at a** point A in a structural system, where $A_i = b_i \cdot \delta_i$ and where b_i is a constant, then the deflection when all the deformations are applied together is

$$A = b_1 \delta_1 + b_2 \delta_2 + \dots + b_n \delta_n \quad (G.1)$$

This principle only holds for small displacements. In this research there were two contributory sources to the total joint deformation, D_t ; that due to the bolt alone, D_b and that due to the joint material, D_m . Thus Equation (G.1) in this case was of the form:

$$A_t = A_b + A_m \quad (G.1)$$

Since A_b had been determined from the connector property tests, and A from the joint property tests, A_m could be obtained by superposing the two as:

$$A_m = A_t - A \quad (G.3)$$

This was applied within the elastic range of both the connectors **and** joint material.

Table H.1 Superposition of Load-deformation components for joint in pure shear (6mm bolt)

LOAD (kN)	DEFORMATION, D (mm)		
	At (mm)	Ab (mm)	Am (mm)
1.0	0.8	0.06	0.74
2.0	1.6	0.12	1.48
3.0	2.2	0.16	2.84
4.0	3.6	0.20	3.80
5.0	4.3	0.24	4.76
6.0	4.3	0.28	5.72
7.0	5.0	0.32	6.68
8.0	5.7	0.36	7.64
9.0	6.4	0.40	8.60

j

Table H.1 Superposition of Load-deformation components for joint in pure shear (6mm bolt)

LOAD (kN)	DEFORMATION, D (mm)		
	At (mm)	Ab (mm)	Am (mm)
1.0	0.8	0.06	0.74
2.0	1.6	0.12	1.48
3.0	2.2	0.16	2.84
4.0	3.6	0.20	3.80
5.0	4.3	0.24	4.76
6.0	4.3	0.28	5.72
7.0	5.0	0.32	6.68
8.0	5.7	0.36	7.64
9.0	6.4	0.40	8.60

Table H.2 Superposition of Load-deformation data for joint in pure shear (8mm bolt)

LOAD (kN)	DEFORMATION, D (mm)		
	At (mm)	Ab (mm)	Am (mm)
1.0	0.4	0.02	0.38
2.0	1.0	0.05	0.95
3.0	1.2	0.08	1.12
4.0	1.6	0.10	1.50
5.0	2.0	0.11	1.89
6.0	2.4	0.14	2.26
7.0	3.0	0.16	2.89
8.0	3.2	0.18	3.02
9.0	4.0	0.20	3.80
10.0	4.4	0.22	4.18
11.0	4.8	0.24	4.56
12.0	5.4	0.28	5.12
13.0	5.8	0.30	5.50

Table H.3 Superposition of Load-deformation data for joint in pure shear (10mm bolt)

LOAD (kN)	DEFORMATION, D (mm)		
	At (mm)	Ah (mm)	Am (mm)
1.0	0.4	0.04	0.38
2.0	1.0	0.07	0.36
3.0	1.3	0.10	0.39
4.0	1.8	0.14	1.20
5.0	2.2	0.18	1.66
6.0	2.6	0.21	2.02
7.0	3.0	0.24	2.39
8.0	3.6	0.28	2.76
9.0	4.0	0.30	3.70
10.0	4.4	0.33	4.07
11.0	5.0	0.36	4.64

Table H.4 Superposition of Moment - rotation data for joint in pure rotation (6mm bolt)

MOMENT (kNm)	ROTATION, D (x.001 Radians)		
	0t (mm)	0b (mm)	0m (mm)
1.0	3.0	2.0	1.0
2.0	6.0	4.0	2.0
3.0	9.0	6.0	2.0
4.0	12.0	7.5	4.5
5.0	14.0	9.0	5.0
6.0	18.0	12.0	6.0

Table H.4 Superposition of Moment - rotation data for joint in pure rotation (6mm bolt)

MOMENT (kNm)	ROTATION, D (x.001 Radians)		
	0t (rad)	0b (rad)	0m (rad)
1.0	3.0	2.0	1.0
2.0	6.0	3.5	2.5
3.0	9.0	5.5	3.5
4.0	12.0	12.0	4.1
5.0	14.5	14.5	5.5